Defining the roles of endothelial adhesion receptors during mammary gland development, functional differentiation, and cancer

Wesley J. Fowler

A thesis submitted for the degree of Doctor of Philosophy (Ph.D.) in Biomolecular Science.

University of Easy Anglia
School of Biological Sciences

Quadram Institute Bioscience
Gut Microbes and Health

October 2020

Abstract

Angiogenesis is a fundamental process entailing the generation of nascent vasculature from pre-existing blood vessels. Driven by endothelial cells (ECs) in response to pro-angiogenic factors, the angiogenic cascade results in the upregulation of multiple essential proteins in these cells; including integrin-β3, integrin-α5 and neuropilin-1. All three molecules are attractive anti-angiogenic targets. Despite an array of studies supporting their druggability, attempts at targeting them in patients have failed. With breast cancer (BC) being the second most common cancer globally, gaining an understanding of how angiogenesis affects the development of the mammary gland throughout its lifecycle will provide insight into why current anti-angiogenics are ineffective. I hypothesized that the ablation of these three molecules to impede angiogenesis during different stages of the mammary life cycle would offer the opportunity to ascertain how angiogenesis influences mammary epithelial morphogenesis. I developed model systems in which I can deplete the EC expression of integrin-β3, integrin-α5 and neuropilin-1, simultaneously, and then study the effects of this depletion on the mammary gland in vivo, or on mammary ECs in vitro. My findings show that impairing the angiogenesis that is mediated by these three proteins during pubertal development of the gland has minor effects on mammary ductal branching morphogenesis. Similarly, there is little to no effect on mammary alveolar development during gestation and early lactation. However, I uncovered changes in placental development that may help to explain these findings. In contrast to what happens during the physiological life cycle of the mammary gland, I observed a significant reduction in BC growth when all three targets were depleted, suggesting pathological development of the breast is dependent on angiogenesis driven by integrin-β3, integrin-α5 and neuropilin-1. Lastly, the in vitro study of mammary ECs provide insight into potential alternative signalling pathways through which the mammary gland may achieve angiogenesis, specifically, via progesterone.

Contents

List of Figures

List of Tables

Acknowledgments

To personally thank everyone who has helped me in some way, shape or form along this journey would be impossible. Having said that, I must namely thank several people who have greatly contributed to helping me achieve this feat and shaped me into the man I am today.

The first and sincerest thanks goes to Dr. Stephen Robinson. Mentor, gym buddy, boss man and friend, this man granted me the opportunity to undertake a PhD from which I walk away with fond memories and a friendship that will last my lifetime. People radiate towards Stephen for one, predominant, reason. Worn on his sleeve more often than not, his heart; this man wields the most incredible heart. Stephen is eternally seeking what is best for others, extracting their true potential, doing his damnedest to make sure they succeed, all whilst exuberating nothing but care and trust along the way. If not the PhD, the greatest thing to have come from this journey is the opportunity to have worked by your side.

Second to Stephen, I owe thanks to Sarah. My rock. From the beginning of my undergraduate full circle to the end of my PhD, this woman is one in a million, and without her love and support I most definitely would not be where or who I am today. Through my worries, my grumps and my outright despair, she profusely offered me reassurance and encouragement – I cannot express how grateful I am to have you in my life.

Third I thank Dr. Robert Johnson, my scientific partner in crime. This mans unbridled passion for science saw me as a useful asset early on, for which I am grateful (as was he I am sure). Perpetually ensuring my enthusiasm was sated, I owe thanks to Rob for nurturing my scientific learning and ensuring I was ready for the science that lay ahead of me. Next, I cannot spend more word count thanking you all personally, however I shall name everyone who has contributed in some manner to my time in the Robinson lab. Thanks to Aleks, Ben, Kate, Jordi, Sam, Abdu, Tim, Stuart, Sally, Alastair, James, Chris B and Chris P – you have all made this time in my life memorable in more ways than one.

Last, and by no means least, I humbly thank my parents Vanessa and Timothy. Without you both, I would not be where, or who, I am today – thank you.

1   Introduction

1.1   Preface

The mammary gland is an incredible organ. It develops both pre- and post-embryonically, exhibits transient remodelling throughout female adulthood, and can undergo huge waves of proliferation and regression during pregnancy to synthesise milk for the nourishment of offspring. Coinciding with such feats, remodelling of the vasculature through angiogenesis is presumed given the mitogenic demand ensuing epithelial expansion and remodelling. Despite this, sparse research exists exploring the role of angiogenesis throughout the dynamic behaviour of the mammary gland, warranting exploration into whether angiogenesis is a permitting factor in its functionality. Aside from this, given changes in vasculature have been observed through the life cycle of the mammary gland, evidence of the mechanisms by which these changes occur are incomplete. Acknowledged, the plasticity exhibited by the mammary gland although impressive, burdens the mammary gland with many opportunities in which cancer can arise. A plethora of cell lineages to be maintained by mammary stem cells, highly metabolic phases during pregnancy and lactation, signalling cues to instigate involution (controlled cellular regression via apoptosis), all attribute points at which tumorigenesis can occur. This thesis aims to address the fundamentals regarding the role, if any, angiogenesis plays in the life cycle of the mammary gland, how angiogenesis is achieved (in terms of signalling pathway(s)) and the anti-tumorigenic effect of impeding angiogenesis in breast cancer (BC). The introduction proceeding shall aim to describe the canonical processes involved in formation, maturation and remodelling of the vascular system, the roles and targetability of integrins as a means of anti-angiogenic targets, the life cycle of the mammary gland and BC.

1.2 The vascular system

The vascular system is a vital component of many multicellular organisms. Conceptualised during embryogenesis, the rudimentary, and continuing, function of the vascular system is to provide a steady supply of nutrients, oxygen, and removal of metabolic waste, throughout a lifetime. Composed of arteries, arterioles, capillaries, venules and veins, this vessel hierarchy established early in life undergoes allometric growth, maturation, and remodelling, to summate these feats. However, this is not a flawless process. As with most fundamental systems, their continual use, proliferative capacity, or exposure to carcinogens deems them susceptible to disease – the vascular system is no exception. Although beyond the scope of this thesis, it is worth mentioning that the vascular system possesses its own innate potential to give rise to disease, alongside being a perpetrator in perpetuating tumorigenesis.

1.2.1 Vasculogenesis – The primordial vascular network

In prelude to exploring what angiogenesis is and the mechanisms involved, it is important to understand the process which allows angiogenesis to proceed, that is, vasculogenesis. Early on in gestation, embryonic development occurs in an avascular environment where organ and tissue growth is achieved by simple diffusion of oxygen and nutrients [1]. During embryonic growth, however, there reaches a point of critical mass whereby an embryo must regimentally undergo rapid *de novo* vascularisation in order to maintain adequate access to oxygen and nutrients – vasculogenesis. For the human embryo, the point in which simple diffusion becomes insufficient in supplying adequate nutrients and oxygen to perpetuate growth is approximately embryonic day 21 (E21) and the mouse is E7 [2–4]. Broadly speaking, vasculogenesis is the process by which the primordial vasculature is formed, conceptualising gaseous exchange and removal of metabolic waste in embryos too large to exercise these feats via simple diffusion alone [5]. During vasculogenesis, a primitive vascular system is formed through the aggregation of Endothelial Cell (EC) precursors, giving rise ultimately to a vascular plexus. This vascular plexus then undergoes vast maturation through functional and morphological remodelling to enable it to function as a rudimentary vasculature system, permitting exchange of gases and nutrients and paving the way for angiogenesis.

The first sighting of vasculogenesis dates back to the mid 1800's when His Wilhelm documented the *in situ* formation of blood vessels whilst microscopically investigating early chick embryos, with the process being later characterised and coined by Risau *et al*. in 1988 [6,7]. The process of vasculogenesis has been largely discerned, including the cellular mechanisms involved. The cascade of events leading to vasculogenesis begins during gastrulation with the invagination of the ectoderm resulting in the formation of the primitive streak. Pluripotent stem cells then pass through the posterior of the primitive streak, giving rise to the intraembryonic mesoderm (**Figure 1.1**) [8]. A subset of mesodermal cells within these two regions are destined as precursor cells that sequentially migrate, associate, and differentiate into clusters called blood islands (**Figure 1.1**). Within these blood islands, physical location of the mesodermal cells defines their fate. Peripherally located progenitor cells differentiate into angioblasts and later into ECs, defining the blood vessel structure, composition and permeability, whilst those that are centrally situated differentiate first into hematopoietic stem cells (HSCs) and further into both ECs and primitive erythrocytes, hence perfusing the vessel lumen (**Figure 1.1b**) [9–11]. Angioblasts are recognised as EC progenitors as they possess an incomplete set of characteristic markers for ECs, along with haemangioblasts sharing some of these markers and being spatially associated [12–14]. Post formation, blood islands coalesce to form the primary vascular plexus, the subsequent growth and remodelling of which constitutes vasculature maturation through angiogenesis (**Figure 1.1b**) [15,16]. A key driver and regulator of embryonic vasculogenesis is the Vascular Endothelial Growth Factor (VEGF) signalling pathway, comprised of two major binding receptors for VEGF, namely VEGFR1 (Flt-1) and VEGFR2 (Flk-1/KDR) [17,18]. Alongside the VEGF signalling pathway, studies have also shown the indispensable roles of Ephrin signalling, EphB4, and hypoxia during vasculogenesis [19,20].
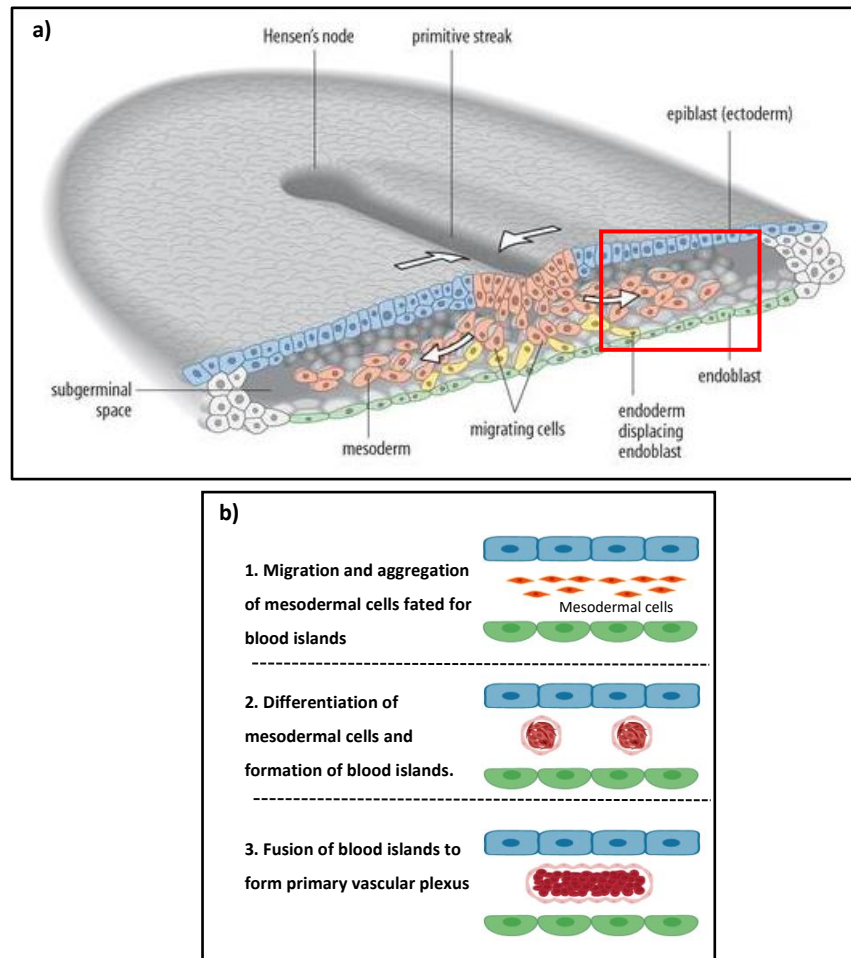
Figure 1.1 Formation of the primitive streak and emergence of mesoderm cells (top). Schematic of mesodermal blood island fate (bottom). a) Gastrulation, formation of the three germ layers, highlighting the formation of the primitive streak and differentiation of ectoderm into mesoderm. Mesodermal cells migrate into the sub-germinal space, a portion of which are fated to become blood island derivatives. **b)** Blood island fated mesodermal cells aggregate (1) and differentiate into blood islands pre-cursors (peripheral cells into angioblasts and centrally located into hematopoietic stem cells) (2), before fusing and forming the primary vascular plexus (3) (adapted from Carsten, 2017 and Wolpert et al., 1998 [21,22]).

1.2.2 Angiogenesis

Angiogenesis broadly describes the process by which new blood vessels are formed from the remodelling and expansion of pre-existing vasculature. The formation of these new blood vessels can occur via two main mechanisms, Sprouting Angiogenesis (SA) or Intussusceptive Angiogenesis (IA); the latter being a much rarer form, however both forms will be covered in section 1.2.2.3. As alluded to, angiogenesis differs from vasculogenesis in that angiogenesis builds upon, and matures, the primordial vascular network generated during early embryogenesis (section 1.2.1). In terms of being a biological process for allometric tissue growth, angiogenesis is crucial in that it enables successful wound healing, execution of the menstrual cycle, morphogenesis to take place in the mammary gland and vascularisation of the placenta and uterus during pregnancy [23–25]. However, as well as being a fundamental part of embryonic and postnatal development, angiogenesis also harbours the ability to promote several ischaemic and inflammatory diseases, including cancer development and its ability to metastasise [26].

1.2.2.1 Angiogenic Factors and Regulators

Angiogenesis is initiated in response to pro-angiogenic stimuli, often factors secreted by nearby tissue entering a hypoxic state. Although a broad range of growth factors and cytokines can initiate angiogenesis, i.e. Fibroblast Growth Factor (FGF), Tumour Necrosis Factor-Alpha (TNF-α), Transforming Growth Factor-Beta (TGF-β) and Angiopoietins (ANG) – a non-exhaustive list, the most renowned factor is VEGF [27]. VEGF is a family of homodimeric glycoproteins which collectively play fundamental roles across vasculogenesis, lymphangiogenesis and angiogenesis – lymphangiogenesis defined as the formation of lymphatic vessels from the pre-existing lymphatic system [28]. Identified members of the VEGF family include: VEGF-A, VEGF-B, VEGF-C, VEGF-D, Placental Growth Factor (PLGF) plus a viral homolog to VEGF, derived from Orf Virus NZ-7, denoted as VEGF-E (**Figure 1.2**) [29,30]. VEGF-A (also known as Vascular Permeability Factor – VPF) is documented as the most important member for angiogenesis. Previous studies investigating VEGF and its family identified VEGF-A as lacking exons 6 and 7, although no differences were observed between the VEGF members with regards to their activity, VEGF-A interestingly is unable to bind heparin [31]. VEGF-A interacts with and binds to both VEGFR1 (Flt-1) and VEGFR2 (Flk-1/KDR), the latter with an affinity approximately 10-fold less [30]. To discuss with evidence, a multitude of studies have demonstrated the importance of VEGF-A in angiogenesis. Disruption of the *VEGF-A* gene, resulting in either *VEGF-A$^{+/-}$* or *VEGF-A$^{-/-}$* mutant mice, results in embryonic death. *VEGF-A$^{+/-}$* animals showed poorly developed and segmented branchial arches in the cranium, an underdeveloped forebrain, mispositioned and un-segmented forelimb buds with the compartments of the heart and its vessels lagging in development [32]. Furthermore, *VEGF-A$^{-/-}$*

embryos showed the most severe developmental defects, including complete lack of aortic development, widespread necrosis and delayed endothelial development [33].

As aforementioned, the receptors through which VEGF signals are members of the VEGFR family. VEGFR1 and VEGFR2 both bind VEGF-A, are highly expressed on vascular endothelium and have been shown as vital propagators of angiogenesis [34]. VEGFR1 and -2 are both transmembrane spanning glycoproteins comprised of an extracellular domain containing 7 immunoglobulin-like domains, a single transmembrane domain and an intracellular domain containing a consensus tyrosine kinase sequence, interrupted by a kinase-insert domain (**Figure 1.2**) [35,36]. However, when it comes to angiogenesis both receptors seem to play rather different yet fundamental roles.

VEGFR1 has been seen to have an essential yet controversial function. Early developmental studies on VEGFR1^{-/-} mice demonstrated its absence to be embryonic lethal, with ECs developing but lacking organisation combined with excessive angioblast proliferation; interestingly this lethality showed the function of VEGFR1 to be a negative regulator of angiogenesis, controlling angioblast proliferation [37]. Further confirmation comes from Kendall and Thomas who identified a vascular EC derived cDNA sequence encoding a truncated, secreted and soluble form of VEGFR1 [38]. This version of VEGFR1 had a high affinity for VEGF and hence negatively regulated VEGF induced mitogenic activity. Furthermore, a study utilising partial gene targeting interrupted the exon encoding the tyrosine kinase domain of VEGFR1, proving non-lethal and non-detrimental to vascular development, plus supporting the notion that VEGFR1 is primarily a "decoy" receptor for VEGF to mitigate its activity [39].

VEGFR2, on the other hand, performs a pro-angiogenic function when in contact with VEGF. The vitality of this receptor during both developmental angiogenesis and haematopoiesis is evident from its embryonic lethality in VEGFR2 null mice; embryonic death $8.5 - 9.5$ consequence of lacking blood island formation and blood vessel organisation [40]. This isoform gains its function via ligand induced homodimerization resulting in autophosphorylation, which in turn induces survival, proliferation, mitogenesis and permeability signals. These signals are transduced through a number of intracellular signalling pathways including: MAPK/ERK, PI3K, IP3/DAG and PLC-γ [41]. Specifically, activation of the mitogenic and proliferative pathways are what enable endothelial cells (ECs) to proliferate and migrate, thus forming new blood vessels. Consequence these pro-angiogenic signals, ECs begin the next phase of the angiogenic cascade – remodelling the extracellular matrix (ECM).
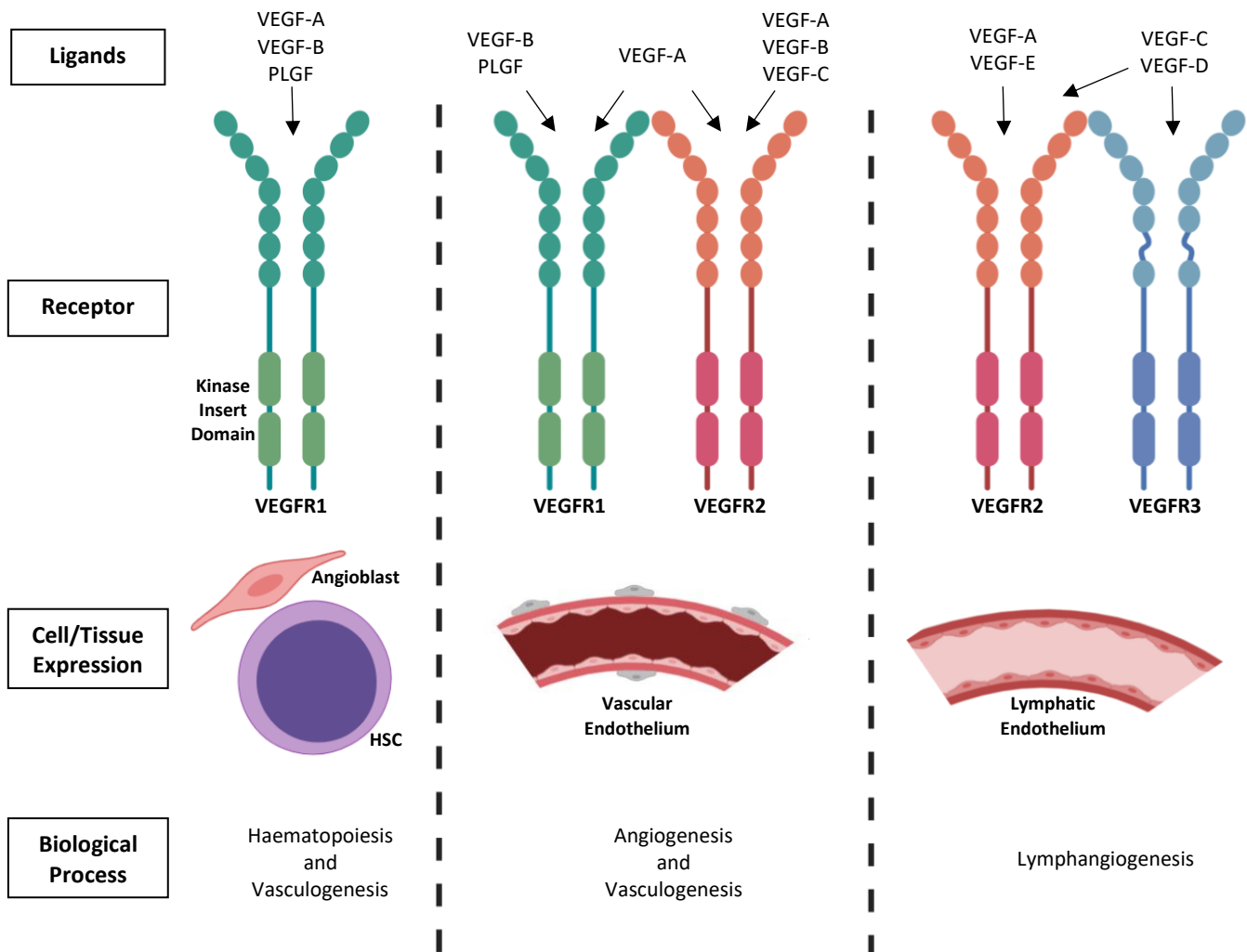
Figure 1.2 The VEGFR and VEGF family members, their predominant tissue expressions sites and the biological activity they contribute towards. VEGF-A binds preferentially to VEGFR2 which is expressed near exclusively on vascular endothelium (adapted from Holmes *et al.*, 2007 [30]).

1.2.2.2 Remodelling the ECM in Prelude to Endothelial Expansion

Prior to the mass mitogenic onslaught that ensues pro-angiogenic stimulation, the ECM that summates the basement membrane of the activating vessel, and path toward the secreted pro-angiogenic stimuli, must be remodelled to enable EC migration. Stimulation of endothelium with pro-angiogenic stimuli results, sequentially, in the detachment of supporting pericytes, loosening of EC junctions and increased EC permeability. In turn, this enables the extravasation of plasma proteins, i.e. fibrinogen and fibronectin, and proteases, specifically matrix metalloproteinases (MMPs) and A disintegrin and metalloproteinases (ADAMs), to remodel the ECM (**Figure 1.3c**) [42]. The combinatorial work of proteases and plasma proteins concludes in an angiogenic-competent matrix, permitting EC migration. Concomitant with this interplay, proteases release a slurry of cytokines and pro-angiogenic factors, previously sequestered in the ECM, exacerbating the mitogenic activity of the ECs and aiding in directional EC motility (**Figure 1.3d**) [43,44]. Key receptors expressed by ECs which bind this remodelled ECM are integrins, discussed in section 1.2.3.
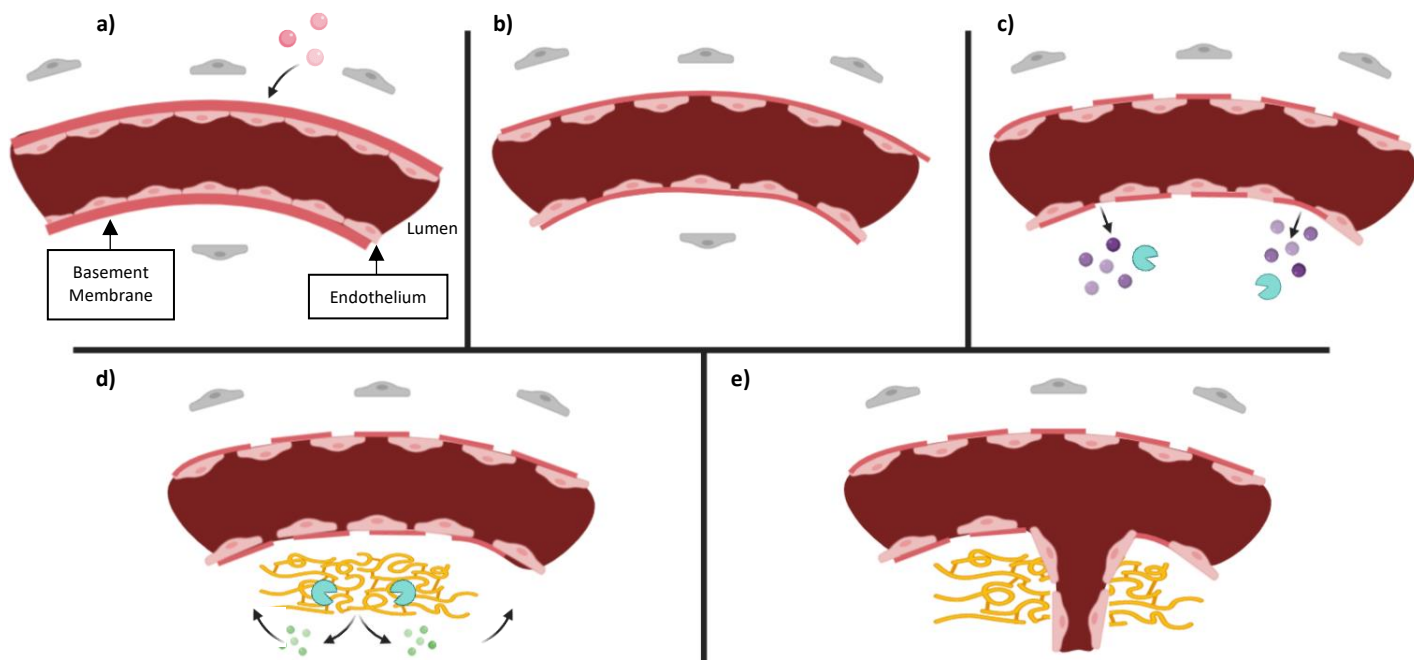
Figure 1.3 Schematic of sprouting angiogenesis. Pro-angiogenic stimuli (pink spheres) induce a cascade of events instigating vascular expansion. Initial stimulation leads to the detachment of pericytes (grey). **b)** Tight junctions between endothelial cells loosen and the supporting basement membrane slackens. **c)** Subsequently, endothelium permeability is increased, resulting in the extravasation of proteases (turquoise) and plasma proteins (purple). **d)** Proteases degrade and remodel the ECM to enable endothelial cell proliferation and migration, whilst simultaneously release sequestered cytokines and pro-angiogenic factors (green spheres) held within the ECM. **e)** Endothelial cells proliferate and migrate towards the pro-angiogenic stimuli.

1.2.2.3 Sprouting Angiogenesis

The physical process of angiogenesis can occur via two mechanisms, SA and IA [45]. IA entails the division of a single blood vessel into two vessels, however is a rare and infrequently observed process, especially in comparison to SA [46]. During SA cells initially receive an aforementioned stimulus, such as hypoxia or inflammation, which triggers the synthesis of pro-angiogenic factors, such as VEGF; aside from VEGF stimulation, ECs possess other oxygen sensing molecules such as oxygen-sensitive NADPH oxidases, endothelial nitric oxide synthase (eNOS) and heme-oxygenases and hypoxia-inducible factor 1 (HIF-1α) [47–49]. Hypoxia induced angiogenesis is primarily driven by HIF-1α. Under normoxic conditions, HIF-1α becomes hydroxylated and subsequently poly-ubiquitinated by an enzyme family known as Prolyl Hydroxylases (PHDs). This leads to the recognition of the ubiquitinated HIF-1α by VHL E3 ubiquitin ligase complex, resulting in its degradation by proteasome 26S. However, in low oxygen conditions HIF-1α is unable to undergo hydroxylation by PHD and translocates to the nucleus where it forms a complex with HIF-1β [50,51]. This HIF-1αβ complex serves as a transcription factor for several pro-angiogenic factors, one of which is VEGF [52]. Following this, these pro-angiogenic factors are secreted into the extracellular environment in a bid to trigger angiogenesis. The secreted factors bind to their respective receptors on the surface of ECs; in the case of VEGF these receptors are VEGFR1 and VEGFR2 [34]. As previously mentioned, the binding of VEGF to its receptors VEGFR1/2 induces, sequentially, receptor dimerization, autophosphorylation and intracellular signalling via the MAPK/ERK signalling pathway, among others. The consequential MAPK/ERK signalling results in the upregulation of genes responsible for cell proliferation and migration, such as MMPs, and survival (**Figure 1.4**) [53,54]. In order to drive the expansion of a new blood vessel, a tip cell is selected through delta-like ligand 4 (DLL4)/Notch-mediated lateral inhibition. Exposure of ECs to VEGF induces the expression of DLL4 on their surface. Binding of DLL4 to notch on neighbouring ECs triggers the notch signalling cascade. Sequentially, ligand engagement induces proteolytic cleavage of Notch intracellular domain (NICD) from the Notch extracellular domain (NECD), primarily by ADAM-17 (TACE) and ultimately by γ-secretase [55]. Cleaved NCID is then able to translocate to the nucleus where it recognises and binds Recombination Signal Binding Protein for Immunoglobulin Kappa J Region (RBPJ) followed by recruitment of transcriptional coactivator mastermind-like (MAML) [56]. This transcriptional complex (NCID-RBPJ-MAML) upregulates genes from the Hairy enhancer of split (HES) and Hes-related with YRPW motif families (HEY1), down regulating the expression of VEGFR-2 as well as dampening pathways for migration and proliferation, rendering the fate of these ECs as stalk cells (**Figure 1.5**) [57–59]. In response to VEGF, tip cells guide the direction of the sprouting vessel, whilst stalk cells proliferate in response, physically elongating the sprouting vessel [60].

Genes coding for integrins are one of many to be upregulated via the MAPK/ERK signalling pathway in response to VEGFR1/2 activation. These cell surface proteins aid in migration through the formation of focal adhesions with the ECM, and intracellular signalling via Focal Adhesion Kinase (FAK) [61–63]. To emphasise, the angiogenic process is rigorous, each step being an essential pre-requisite for the next in order for angiogenesis to occur successfully [64]. Given this, integrins provide a key role in facilitating the migration of ECs, and hence offer an exploitable potential in which to prevent angiogenesis and investigate the subsequent effects. Integrins are discussed detail in section 1.2.3.

The ultimate stage in SA is the fusion and integration of the nascent vascular sprouts into the existing vascular system, achieved through a process called anastomosis [65]. Proximity of tip-cells leads to an accumulation of macrophages which orchestrate the interaction, and fusion, of two nascent vessels [66]. Consolidation of the newly integrated vessels is established through the formation of tight junctions comprised of VE-cadherin, resulting in vessel perfusion. Consequence perfusion, VEGF expression is reduced in response to the influx of oxygen and nutrients, shifting the phenotypic state of the vessel to quiescence and instigating maturation [67]. PDGFB and TGF-β are secreted by ECs triggering the recruitment and differentiation of mural cells to pericytes, enabling physical stabilisation of the newly fused vessel, and the synthesis of collagen (types IV, XV and XVIII) for basement formation [68]. Concomitantly, vessel permeability is reduced through the expression of Ang-1, enhancing pericyte-EC interaction and tightening EC-EC junctions, whilst protease activity is inhibited through expression of tissue inhibitors of MMPs (TIMPs) [69–71].

To ensure anastomosis is successful and a functioning vascular system is formed, one final factor must be considered – vessel identification. Specifically, new vessels need to be identified as either artery or vein to permit directional perfusion concomitant with the current vascular system. The system involved in enabling such a feat is the Ephrin/Eph system, namely the receptors Ephrin-B2 and EphB4 [72]. Several studies have highlighted the importance of these two molecules in successful angiogenesis, demonstrating perturbation of either to result in highly disorganised vasculature, no boundaries between arteries and veins, and consequently embryonic lethality by E11 [73–75]. One factor which contributes towards arterio-venous identity via Ephrin-B2 and EphB4 are haemodynamic forces. Haemodynamic forces (arterial/venous blood flow) results in the expression of Ephrin-B2 in arterial ECs and EphB4 in venous ECs [76]. Aside these forces, the Notch signalling pathway has also been implicated in defining arterio-venous boundaries. Mutation in the gene encoding for Dll4 ligand proved embryonic lethal whilst resulting in vascular defects. Furthermore, mutations in a primary transcription factor for Notch signalling demonstrated arterio-venous malformation and embryonic lethality [77]. These findings all suggest that the absence of

either Ephrin-B2 and/or EphB4, be it directly or indirectly, manifests in arterio-venous malformation and lethality.
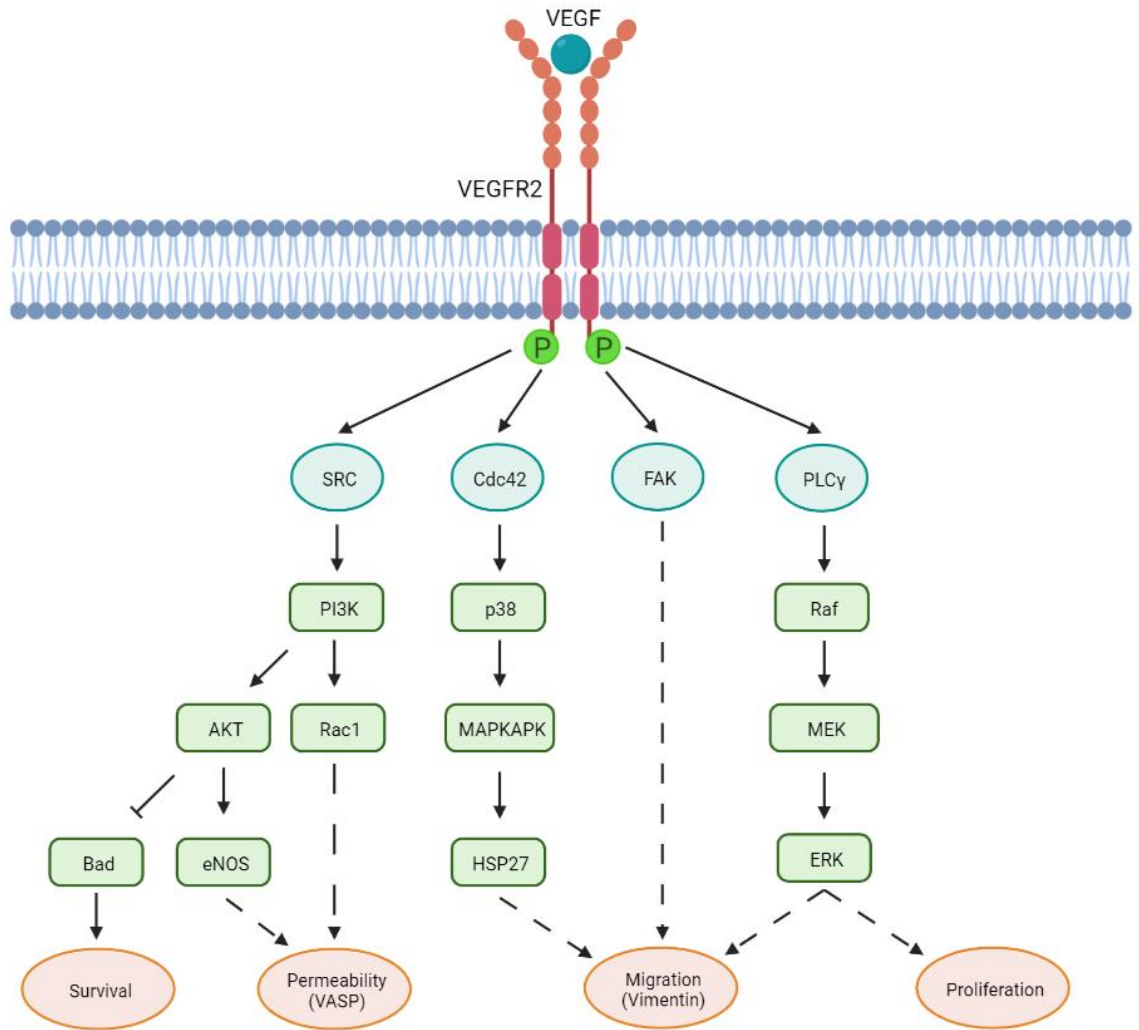
Figure 1.4 The VEGFR signalling pathway. Upon binding VEGF, VEGFR2 undergoes receptor dimerization and autophosphorylation. This subsequently leads to the upregulation of genes in multiple cellular pathway. Specifically, integrin upregulation via ERK and p38 for cell migration and proliferation and cell survivability and permeability via AKT [78].
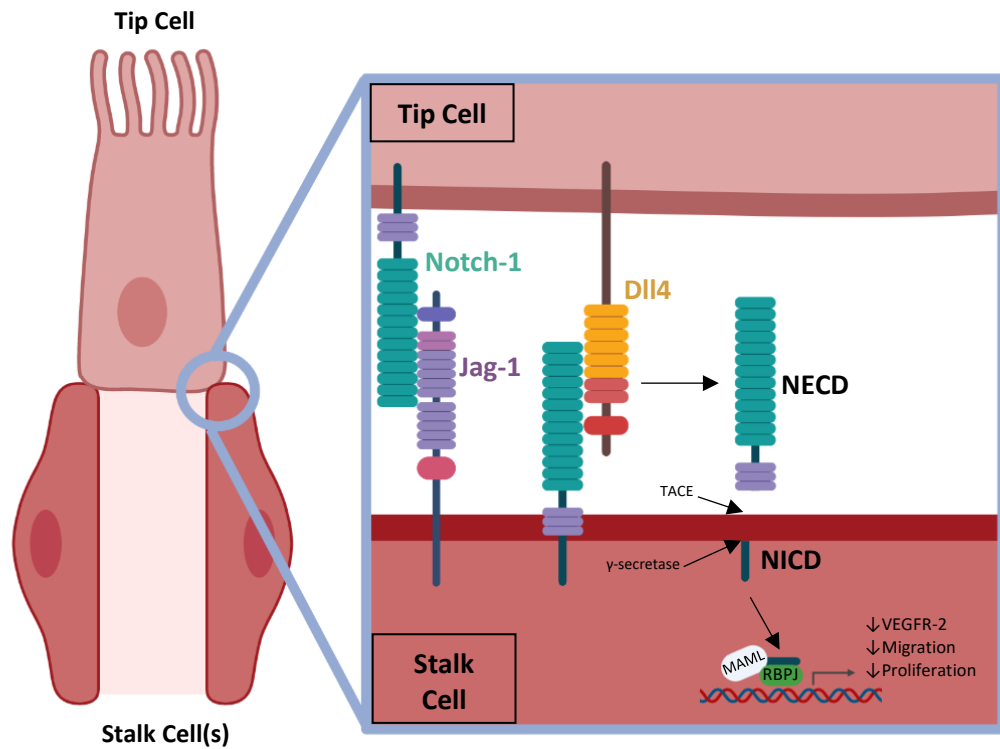
Figure 1.5 Notch-1/Dll4 Mediated tip cell selection. ECs exposed to VEGF express DLL4. DLL4 recognises and binds to notch on neighbouring ECs, triggering notch signalling. Activation of the notch signalling cascade inhibits the expression of VEGFR2, through the release of the Notch Intracellular Signalling Domain (NICD). NCID is then able to translocate to the nucleus where it forms a transcriptional complex (NCID-RBPJ-MAML). This complex upregulates HES/HEY1 genes which consequently downregulate VEGFR-2 expression, preventing the binding and signal transduction of VEGF (fating these cells as stalk cells), whilst also dampening migration and proliferation pathways [55].

1.2.2.4 Intussusceptive Angiogenesis

IA is a much rarer form of angiogenesis but occurs where dynamic remodelling of vasculature is required, such as the primitive vascular plexus or the mammary gland during late pregnancy [79]. IA is described as the process by which pre-existing vessels undergo internal division to increase the number of vessels within in given space; an increase in vascular density [80]. This type of blood vessel formation was first recorded in the 1980's by Caduff *et al*. who detected with scanning electron microscopy multiple tiny holes within vascular corrosion casts of rat pulmonary vessels [81]. It was later postulated, and confirmed, that these tiny holes were in fact the remnants of tissue posts, intra-luminal pillars which connected opposing sides of the vascular lumen which had been digested away during the vascular corrosion castings [82]. The process of IA has now been much further defined. The formation of the tissue posts, the fundamental aspect to the whole process, takes place via a regimented four step process: Phase I – Two opposing sides of a vessels lumen invaginate and make contact, Phase II – Inter-endothelial cell junctions are reorganised and perforation of the bilayer occurs, Phase III – An interstitial pillar core is formed and invaded by pericytes and myofibroblasts which then laydown collagen fibrils, Phase IV – The pillar increases in girth (**Figure 1.6**) [46].

The described process of pillar formation is a regimented process much like the steps involved in SA. However, the coordination, placement and sequential fusing of these pillars can result in varying morphological and functional outcomes. The process of IA can achieve two phenotypically distinct form of vessel expansion, namely, Intussusceptive Microvascular Growth (IMG) and Intussusceptive Arborisation (IAR) – IAR is followed by Intussusceptive Branching Remodelling (IBR) as a means of refinement (**Figure 1.7**) [83]. IAR is responsible for remodelling vasculature into the classical vascular tree pattern. This is achieved by several vertical pillars forming and then fusing in a linear fashion, creating new vessels, followed by horizontal pillar formation and fusion to segregate the new vessels from the capillary plexus (**Figure 1.7a-c**) [84]. On from IAR, IBR entails the refinement of vessels, adjusting for the hemodynamic requisites that exists throughout the vascular system. IBR is achieved by means of augmenting vessel geometry and, in some cases, vascular pruning to optimize perfusion and establish vessel hierarchy. This is accomplished through a series of transluminal pillars at points of branching (bifurcation points), culminating in vessel elongation or enlargement (**Figure 1.7d-f**) [85]. Lastly, IMG employs a sheer amplification in vessel density and is concomitant with capillary growth. Pillars arise sporadically throughout vascular the vascular plexus increasing its complexity, and thus surface area, permitting exchange of oxygen, carbon dioxide, nutrients and removal of metabolic waste (**Figure 1.7a and g-i**) [86].
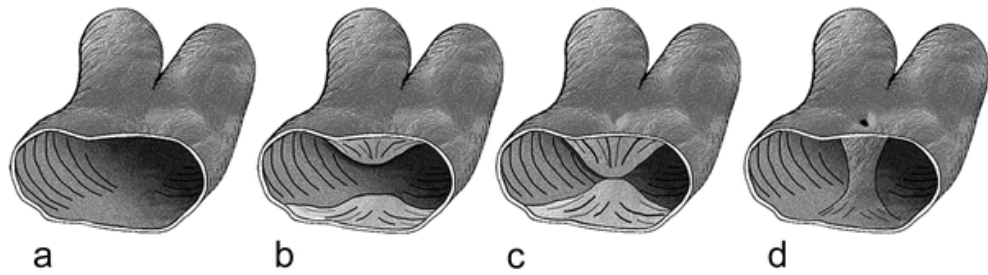
Figure 1.6 Schematic illustrating the four consecutive steps involved in intussusceptive pillar formation.(a-b) Opposing sides of the vascular lumen invaginate and encroach towards each other. **(c)** Contact is established, and perforation of the bilayer is preceded by inter-endothelial junctions having been reorganised. **(d)** The transluminal pillar is fully formed, pericytes and myofibroblasts are recruited to complete the structure by secreting collagen fibrils to amplify pillar girth (adapted from Djonov et al., 2003 [46]).
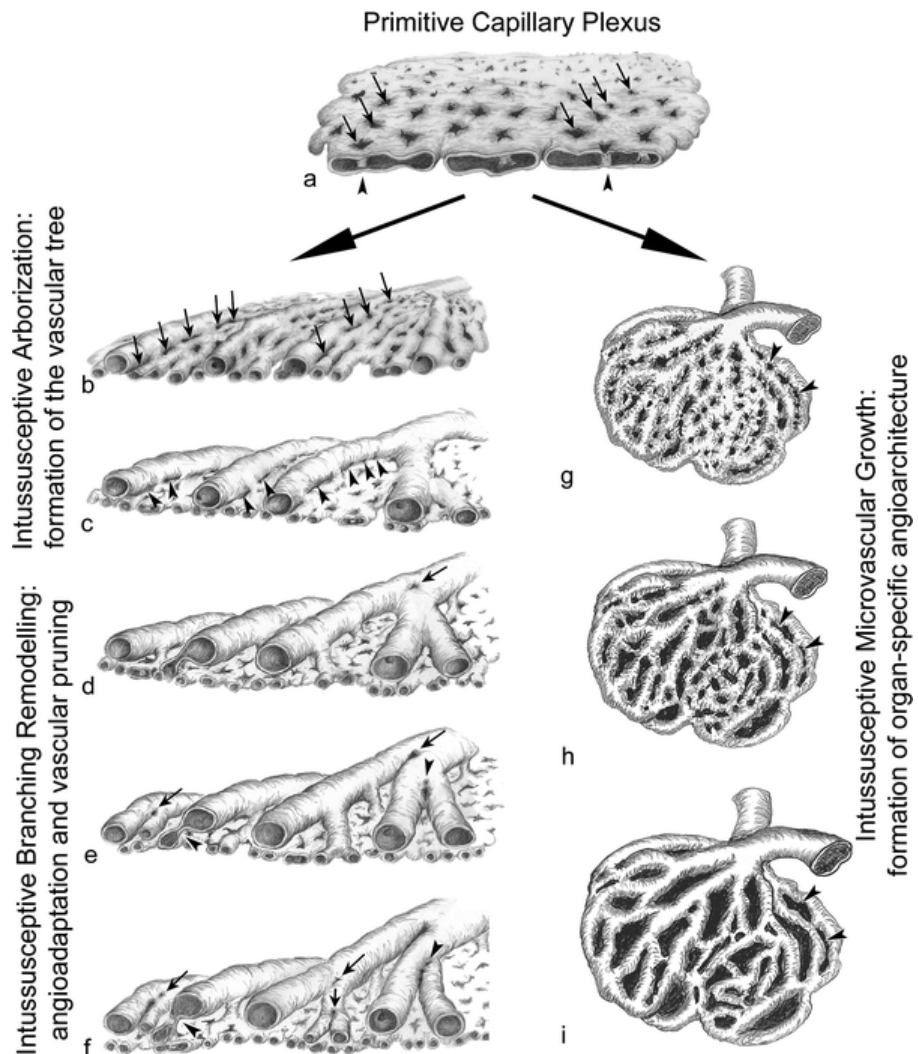
Figure 1.7 Phases of Intussusceptive Angiogenesis. The Primitive Capillary Plexus is a rudimentary vasculature through which vascular remodelling occurs. This simple tissue undergoes preliminary expansion via the insertion of pillars (black arrows) followed by either IMG or IAR; the latter proceeded by IBR (adapted from Makanya et al., 2009 [79])

1.2.2.5 Pathological Angiogenesis

As is common with many biological processes, it is no surprise that angiogenesis can be associated with the stigma of disease. Albeit a fundamental process, there exists a harmonic interplay between pro- and anti-angiogenic signals within the body. Given this, it is easy to imagine that disruption of this balance could result in the development and progression of disease – a tip in these balances being referred to as the angiogenic switch, on being pro-angiogenic and off being anti-angiogenic. Malfunction in the way of angiogenesis has been deemed the cause, or contributor, of a wide range of diseases. In the instance of an insufficient angiogenic response, diseases and ailments such as ischaemic heart disease, stroke, pre-eclampsia and delayed wound healing can occur [87–89]. Conversely, other diseases including cancer, psoriasis, retinopathies and diabetic nephropathy all derive from an excessive state of angiogenesis [90–93]. As the realms of disease besides cancer are beyond relevance for this thesis, this section shall focus on tumour growth and progression, and the role angiogenesis plays.

Tumorigenesis stems from the uncontrolled growth and proliferation of a cell, driven largely by mutation, and subsequent augmentation, of proto-oncogenes to oncogenes. Although essential in the human body for normal development, the proteins encoded for by proto-oncogenes, entailing processes such as cell proliferation, differentiation and apoptosis, highlights their potential volatility in terms of cancer formation and progression. However, in order to grow and metastasise around the body tumours require an adequate blood supply, which they obtain through hijacking angiogenesis. Fortunately, the human body favours an anti-angiogenic state, boding against tumour progression, and in most cases upregulates the expression of anti-angiogenic molecules to negate pro-angiogenic molecules being released by a tumour. Given this favoured state most tumours are gated to a size of 1mm or less in diameter, however, this innate mechanism is not fool-proof [94]. Upon achieving this dimension these avascular neoplasms undergo an angiogenic "switch" enabling them to recruit a blood supply to continue growth as well as opening the potential of metastatic spread; this switch is recognised as a hallmark of cancer [95]. It stems from this fundamentality that tumour angiogenesis is a highly relevant therapeutic target and hence a multitude of researchers have sought to develop drugs and therapies to mitigate the process from a variety of molecular angles.

In 1945, studies by Algire *et al*. alluded to the capacity of tumours to elicit the growth of new blood vessels to sustain and propagate tumour growth, overcoming the body's favoured anti-angiogenic state [96]. It was these early studies which set into motion the endeavour to target angiogenesis as a form of anti-tumorigenic therapy, justly pursued by Folkman *et al*. in 1971 [97]. Over the following years, a magnitude of work from this group yielded numerous purified and characterised pro- and anti-angiogenic factors, flooding the field with an array of targets, the modulation of which might serve as a means of anti-tumorigenic therapy [98]. As a consequence of these identified factors, and with prior research having demonstrated its fundamental role in angiogenesis, VEGF and its signalling pathway were swiftly set upon. In 2004 the first anti-angiogenic therapy was FDA approved, bevacizumab (commercial name Avastin); a monoclonal antibody against VEGF [99]. Initially used to treat colorectal cancer, administration of this antibody in combination with chemotherapy was shown to significantly improve patient survival [100]. Since the deployment of bevacizumab, many other anti-angiogenic drugs have been engineered including a range of Tyrosine Kinase Inhibitors (TKIs) and other monoclonal antibodies against a range of pro-angiogenic pathways, concomitant with the investigative utilisation of endogenous anti-angiogenics [101–103].

There exists a broad range of trials and tribulations in the field of anti-angiogenic drugs, with disappointing results ranging from failure at the start of clinical trials to cancer developing resistance to commissioned drugs [104–106]. Arguments are had that pre-clinical data affords some of these failures due to, in part, the tumours used during these studies being grown subcutaneously, as opposed to orthotopically, taking away physiological relevance [26]. Furthermore, some studies have added to this disarray in drug efficacy by administering inappropriate drug doses; those that are not safely achievable in humans as opposed to animal models [107]. A prime example of a drug boasting huge potential preclinically, bolstered by efficacy issues discussed, was sunitinib. Sunitinib is a TKI designed to target and inhibit primarily VEGF receptors, as well as Platelet-Derived Growth Factor Receptors (PDGFRs) and Fibroblast Growth Factor Receptors (FGFRs) [108]. Work by Abrams et al. produced compelling evidence for sunitinib as an effective clinical treatment for BC [109]. As a consequence of the promising pre-clinical data, four randomised phase III clinical trials took place. However, all four trials failed with all showing no benefit in progression free survival or overall survival [110]. Despite shortfalls, many FDA approved antiangiogenics are currently in use. These drugs range from antibody against VEGF (i.e. Ranibizumab), antibodies against VEGFR-2 (i.e. Ramucirumab), TKIs targeting downstream VEGF signalling (i.e. Sorafenib – multi-kinase targets, also inhibits downstream signalling from PDGFR and Raf [111]), soluble decoy receptors (i.e. Aflibercept), and antibodies against other growth factors known to stimulate angiogenesis (i.e.

Cetuximab against EGFR) with antibodies against FGF2 showing promise with no clinical trials to date – reviewed in [112,113].

Given the points discussed throughout this section, our lab harnesses the Cre/*Lox*P system (discussed in section 3) to study the anti-tumorigenic effects of deleting key players in the angiogenic cascade as a means of targeted therapy, specifically endothelial integrin-α5, integrin-β and neuropilin-1 [114]. Moreover, when utilising this system, we employ the use of a mouse breast carcinoma model derived from mouse mammary tumour virus-polyoma middle tumour-antigen (MMTV-PyMT) mice, acknowledging the use of the appropriate model with the appropriate disease; referencing the lack in physiological relevance some studies practiced.

A closing point to briefly touch upon is the inherent "oddity" of tumour vasculature. Hitherto I have discussed tumour angiogenesis as if it embodies that of normal angiogenesis; a sequential series of regimented, un-expendable, steps. This is not generally the case. Vascularisation of a tumour is achieved through the overexpression of pro-angiogenic factors in an uncontrolled manner, independent of the sequential cascade required to form functional, stable, vessels [115]. Consequently, vasculature within a tumour resembles a chaotic labyrinth of immature vessels, comprised of varying diameter and shape, which exhibit no vessel hierarchy (**Figure 1.8**) [116,117]. These facts in turn relate to functionality; vessels are hyperpermeable and falter in their ability to perform exchange of nutrients and metabolic waste, a knock-on effect being the delivery of anti-tumorigenic drugs [118,119]. As such, research groups are now commencing in studies that seek to "normalise" the tumour vasculature in a bid to enhance the delivery and retention of anti-tumorigenic drugs [120].

Normal angiogenesis:
- Functional
- Hierarchical
- Stable/mature

Tumour angiogenesis:
- Leaky/faulty
- Immature
- Unstable

Normalising vasculature
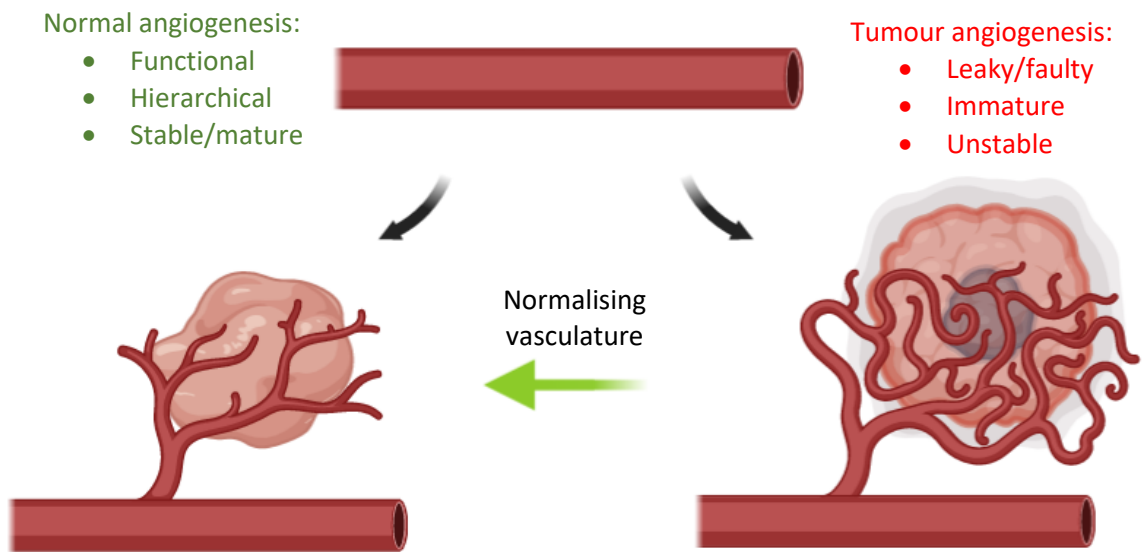
Figure 1.8 Basic schematic of angiogenesis resulting in either normal or abnormal (tumour) vasculature. Angiogenesis can follow two suits, normal or tumour. Normal angiogenesis generates functional, stable vessels which exhibit vessel hierarchy. Tumour angiogenesis is chaotic lacking all the former traits of normal angiogenesis. As such, normalising tumour vasculature as a means of improving drug delivery is being explored.

1.2.3 Integrins

Integrins play a key, non-exclusive, role in the modulation of angiogenesis in the body, through the interaction of ECs with their surroundings. These cell surface molecules are transmembrane, heterodimeric, glycoproteins comprised of non-covalently bonded α and β subunits [121]. To date, it is known 24 unique integrins exist comprised of 18 α and 8 β subunits [122]. The heterodimerisation of these subunits can be diverse, such that one α subunit can bind several different β subunits and vice versa (**Figure 1.9**) [123]. The functionality of these glycoproteins exists through their ability to bind ligands, either those on the surface of other cells or directly to proteins found within the ECM, such as fibronectin, collagen and laminin (**Figure 1.10**) [28]. The ligands to which specific integrins bind is an area governed by affinities. Hence, although integrins have predominant ligands to which they bind, they also possess low affinities for a wide range of other ligands ; hitherto perpetuating the ongoing debate as to whether integrins can "compensate" each other's function due to this overlap in viable ligands [124,125].

Integrins modulate cellular homeostasis through their ability to utilise bidirectional signalling; namely "outside-in" and "inside-out" signalling. Outside-in signalling is instigated when an integrin encounters, and binds, its extracellular ligand (**Figure 1.10**). Binding of an integrin to its ligand triggers homotypic clustering, forming organised aggregations of ligand bound integrins termed focal adhesion complexes [126]. These complexes in turn initiate a cascade of protein phosphorylation events resulting in the polymerisation of new actin filaments, anchoring the cell through the actin cytoskeleton, via the ligand bound integrin, to the ECM thus enabling cell adhesion and migration (**Figure 1.9**) [127]. Outside-in signalling assumes the integrin heterodimer is in a high affinity state, enabling sufficient binding to its ligand; the extracellular domain is in a straight, high-affinity, conformation as opposed to a bent, low-affinity, conformation (**Figure 1.10**) [128,129]. Inside-out signalling takes place from the former, bent, conformation and aims to achieve a straight conformation to permit outside-in signalling. Talin, a cytoskeletal linker protein, undergoes a conformational change in response to a G-protein coupled receptor (GPCR) signalling cascade, independent of integrins, enabling it to bind the β-cytoplasmic tail of an integrin heterodimer [130–133]. Binding of talin induces a conformational change in both integrin cytoplasmic tails, in turn inducing a conformational change in the extracellular domain to a high-affinity state, allowing outside-in signalling to ensue [134,135].

The heterodimers of interest to discuss are those formed by the integrin subunits α5 and β3. These subunits were temporally removed utilising the Cre/*Lox*P system as a tool throughout this thesis to study the effects of impeding angiogenesis on the life cycle of the murine mammary gland. Namely, the heterodimers comprised of these subunits are: α5β1, αVβ3 and αIIbβ3 (**Figure 1.9**), receptors for fibronectin, vitronectin and fibrinogen respectively [136–138]. In terms of spatial situation, α5β1 and αVβ3 integrins are expressed on ECs, whereas expression of αIIbβ3 integrin is restricted to cells of the megakaryocyte lineage, such as platelets, with functional roles in aggregation and adhesion [139]. Previous studies have demonstrated that integrins α5 and β3 play roles in angiogenesis. As early as 1994, Brooks *et al*. noted that during developmental angiogenesis in chicks, the chorioallantoic membrane had high expression of integrin αVβ3, and that application of a monoclonal antibody (mAb) against this integrin prevented angiogenesis; adducing fundamental evidence for β3 integrin in angiogenesis [140]. Ablation of αV- or α5-integrin in mice showed no lethality nor defects, with knockout mice being both viable and fertile. However, simultaneous ablation of both αV and α5 proved to be embryonic lethal, with an extremely low chance of survival (<4% survive). The majority of mice missing both subunit died at E14.5 (embryonic day), around the time branchial arch artery remodelling takes place [141]. This preliminary evidence demonstrated that α5 indeed plays a role in angiogenesis, but also alludes to the complex interplay between integrins – **Figure 1.9** highlights the broad range of heterodimers associated with αV. Given the fundamentality of these integrins in permitting angiogenesis, integrin-α5 and integrin-β3 can be seen as attractive anti-angiogenic targets, especially as their heterodimeric pairing is far more exclusive than other integrins; ablation of these two integrins will affect fewer tissue types.
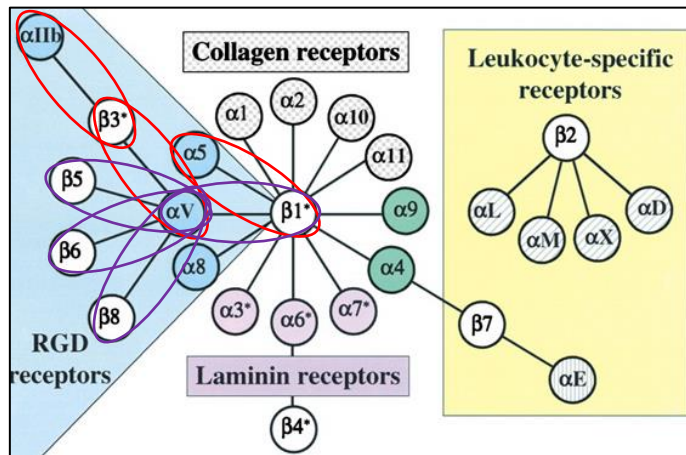
Figure 1.9 An illustration of the known pairing patterns of α and β subunits, and the potential integrin heterodimers that can form. The rings in red highlight the heterodimers affected by the genetic manipulation of either α5 or β3. The purple rings highlight the broad range of heterodimers affected upon manipulation of αV (adapted from Hynes, 2002a [142]).
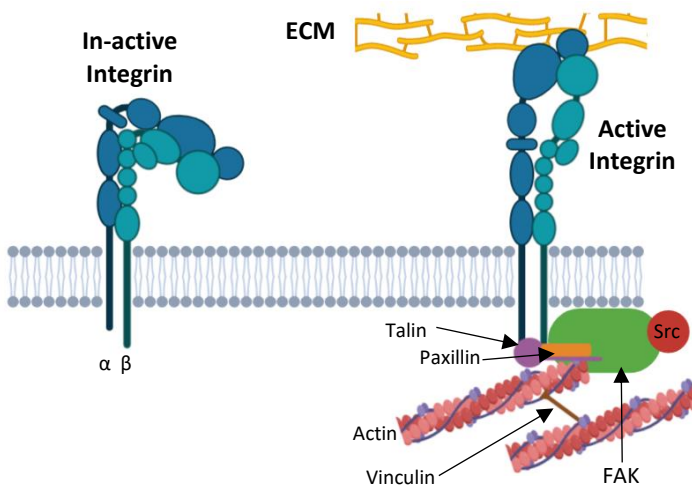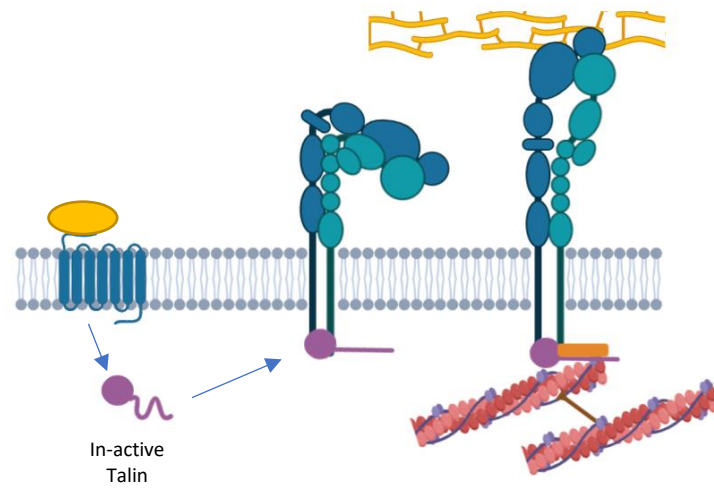
Figure 1.10 A schematic diagram of the structure and function of an integrin heterodimer. Binding of the integrin with the ECM results in the interaction of the N-terminal domain with a variety of intracellular molecules. Two, structural, cellular processes modulated by cell-ECM interactions, achieved through integrins, are the formation of focal adhesions, and intracellular signalling via FAK; signalling via FAK results in the expression of genes involved in cell migration. The ECM (yellow) represents a range of potential ligands (adapted from Millard *et al*., 2011 and Kechagia *et al*., 2019 [143,144]).

1.2.4   Neuropilin-1

Initially identified in the developing *Xenopus* as a semaphorin co-receptor for neuron development and guidance in the late 1990s, subsequent studies identified neuropilin-1 to have a high affinity for several VEGF isoform, specifically VEGF-A, thus mediating angiogenesis by acting as a co-receptor for VEGFR-2 [145–147]. Confirmation of neuropilin-1's involvement in angiogenesis was observed in both overexpression and knockout experiments where vascular formation was augmented or ablated, respectively, and resulted in major cardiovascular defects in both cases [148,149]. Furthermore, it has been documented that neuropilin-1 over-expression correlates with tumour angiogenesis and subsequently tumour progression, further demonstrating the role of neuropilin-1 in angiogenesis whilst highlighting its potential as therapeutic target [150].

Neuropilin-1 is transmembrane glycoprotein comprised of a large extracellular N-terminal domain, a transmembrane domain and a small cytoplasmic domain (**Figure 1.11**) [151]. The N-terminal domain is comprised of two semaphorin binding CUB (for complement C1r/C1s, Uegf, Bmp1 – a1 and a2) domains, two VEGF binding domains (FV/VIII – b1 and b2) and a single MAM (meprin, A5 antigen, receptor tyrosine phosphatase μ – c) domain [152]. The cytoplasmic domain of neuropilin-1 contains a PDZ-domain binding motif (SEA) which associates with neuropilin-interacting protein-1 (NIP1), synectin or RGS-GAIP-interacting protein GIPC, important for the internalisation of neuropilin-1 [153]. Despite this, mice expressing C-terminally truncated neuropilin-1 are normal with no angiogenic defects [154]. In terms of VEGF signalling, neuropilin-1 recognises and binds VEGF-A, moves towards VEGFR-2 and forms a complex. The formation of this complex augments VEGFR-2 activity and downstream signalling, described in section 1.2.2.3 [155].

Of note, a second member of the neuropilin family exists: neuropilin-2. Comprised of a same domain composition, two semaphorin binding CUB domains, two VEGF binding FV/VIII domains a MAM domain, and TM and a SEA cytoplasmic domain, neuropilin-1 and -2 share an overall amino acid homology of 44% [156]. Whilst studies have shown neuropilin-2 to play a pro-angiogenic role, knockout studies revealed neuropilin-2 null animals are viable showing only a significant reduction in small lymphatic vessels and capillaries during development [157,158]
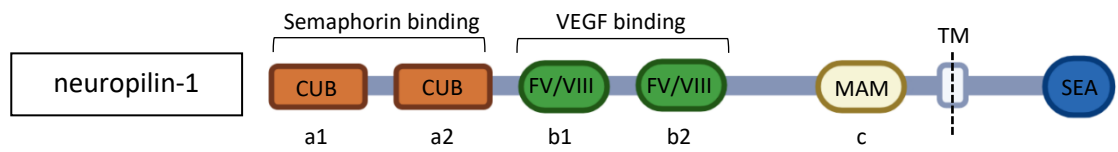
Figure 1.11 Structural diagram of neuropilin-1. Neuropilin-1 contains an extracellular domain comprised of two CUB semaphorin binding domains (a1 and a2), two VEGF binding domains (FV/VIII – b1 and b2) and a MAM domain, a single transmembrane domain (TM) and a cytoplasmic SEA domain. Adapted from Pellet-Many *et al*, 2008 [151].

1.3 The murine mammary gland

The mammary gland is a dynamic organ composed of a variety of tissues which collectively serve the sole purpose of supplying offspring with milk, a substance providing nutritional and immunological benefits [159]. In order to achieve this feat, the mammary gland must undergo morphological and physiological changes, driven both hormonally and non-hormonally, continually throughout the life of the animal; involving processes such as cellular proliferation, differentiation and apoptosis. [160]. This perpetual cycle of the mammary gland therefore requires a fluctuating demand on oxygen, nutrients and other biological molecules, all of which are supplied via the vasculature. As a consequence, angiogenesis in the mammary gland must mirror this dynamic behaviour, increasing and decreasing vascular density as required, and hence plays a vital role in permitting the functions of the mammary gland [161].

1.3.1 Embryonic development

As previously mentioned, the mammary gland is a complex and dynamic organ which serves a vital purpose when raising offspring through the production of milk, providing nutritional and immunological benefits. The development of the mammary gland is broken down into three main stages: embryonic, pubertal and reproductive. Utilising mice (*Mus musculus*) as a model organism to study these stages of development has enabled researchers to gain great insight into the human breast, with regards to both normal and pathological development.

The murine mammary gland begins development at around E10.5 with the formation of milk lines running bilaterally from anterior, forelimb bud, to posterior, hindlimb bud, on the ventral surface of the embryo (**Figure 1.12a**). These milk lines consist of multi-layered ectoderm that by E11.5 have resolved into compact spheroids of mammary epithelium referred to as placodes (**Figure 1.12b**). From here, the underlying mammary mesenchyme is what holds the key to further development of the mammary epithelium. Key inductive signals, to be discussed in more detail later, released from this mesenchyme propagate the differentiation of the mammary epithelium, driving its embryonic growth.

A variety of evidence exists which demonstrates mesenchyme tissue, not only mammary derived, can influence, drive and specify mammary epithelium differentiation. Work by Cunha *et al* (1995) provided grounding evidence for the ability of mammary mesenchyme to induce functional mammary differentiation in both mammary and non-mammary epithelium [162]. Skin epithelium harvested from either the mid-ventral or dorsal of E13 mice or rats was co-cultured with mouse mammary mesenchyme via renal capsule grafting. Histological analysis of the tissue revealed that hair bearing keratinised skin had formed, combined with underlying ducts reminiscent of that

ductal epithelium found within the mammary gland. Furthermore, addition of an adult pituitary gland to the mice hosting these combination engraftments triggered lactogenesis. In turn, this led to the expression of casein, a protein common in milk, detected by immunohistochemistry, as well as the detection of markers indicative of mammary epithelium. Interesting observations were also made when performing the same experiment in reverse. Mammary epithelium associated with salivary mesenchyme, though renal capsule grafting, resulted in the mammary epithelium morphologically resembling that of a salivary gland [163]. All in all, besides resounding evidence for the role of mesenchyme in defining the differentiation pattern of the epithelium, it also bodes true in the opposite direction. The mammary epithelium influences the mammary mesenchyme's differentiation, such that by E14 there becomes two clear distinct mesenchymal tissue types: the dense fibroblastic mesenchyme, closely associated with the mammary epithelium, and the fat pad mesenchyme [164].

To backtrack, the previously alluded inductive signal which enables the resolution of the milk line into placodes at E11.5 is of Wingless-related integration (Wnt) origin. To date, it is not known which Wnt is responsible for initiating this stage of mammogenesis but studies exist showing overexpression of Dickkopf (DKK1), a Wnt inhibitor, blocks entirely the formation of placodes signifying Wnt signals are fundamental to this process [165].

Moreover, from E11.5 to E12.5 the epithelium comprising the placode invaginates to form a compact sub-surface bulb (bud) within the underlying dense mesenchyme (**Figure 1.12c**) – this is when the mammary mesenchyme differentiates into the two distinct types mentioned previously [166]. In female embryos, the mammary epithelium remains predominantly quiescent until E16.5, besides allometric growth, at which point it begins to proliferate down through the mesenchyme until it reaches the dense fat pad (**Figure 1.12d-e**). Upon reaching the fat pad, the epithelium undergoes branching ductal morphogenesis in a dichotomous fashion (**Figure 1.12f**) [167]. Concomitant with this, epidermal cells situated above the bud begins to differentiate to form the nipple; hair follicles are suppressed, keratinocytes form a nipple sheath and the epidermis thickens [168]. Interestingly, the presence of androgens, and the subsequent lack in their receptors on male mammary mesenchyme, results in the termination of the mammary primordium in male embryos. Contrastingly, in female embryos the presence of androgen receptors on the mammary mesenchyme is what induces the differentiation of the tissue in the presence of androgens [169]. Signals which drive bud formation between E11.5 – 12.5 remain elusive and to date require further study. However, through E12.5 to E15 it has been shown that TOPGAL (TCF Optimal Promoter-beta-GALactosidase), a Wnt signalling reporter, is expressed along with many other Wnt genes, and that blocking Wnt signalling abolishes bud formation [165,170]. Furthermore, absence of Fibroblast

Growth Factor Receptor 2-IIIb (FGFR-2b) or its ligand, Fibroblast Growth Factor-10 (FGF-10) during embryonic development has been shown to prevent placode formation. Likewise, FGFR-1 and -2 have been shown to regulate post-natal branching, but this will be discussed in later sections [171].
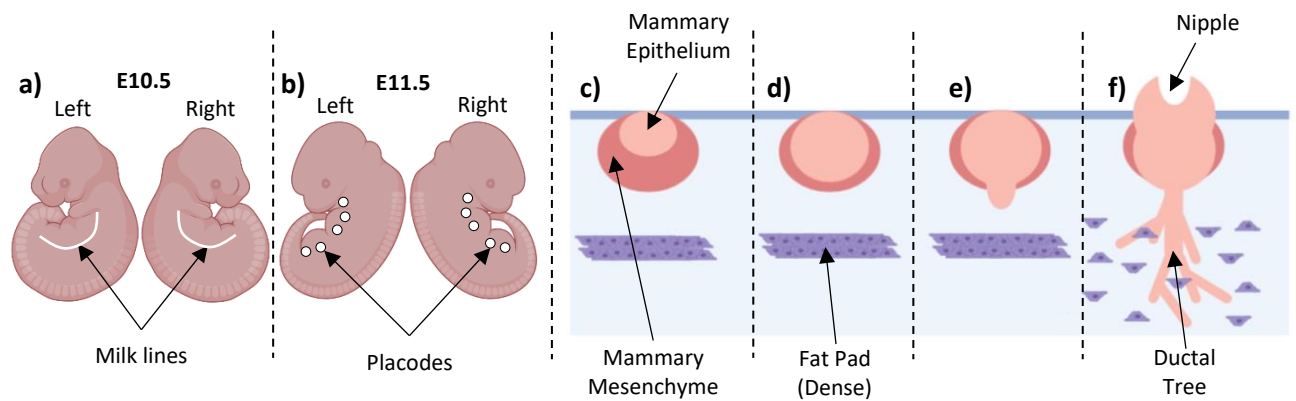
Figure 1.12 Embryonic milestones in the development of the mouse mammary gland. a) E10.5 – Formation of a pair of bilateral milk lines comprised of multi-layered ectoderm positioned on the ventral surface of the embryo running anterior to posterior situated from forelimb bud to hindlimb bud respectively. **b)** E11.5 – Milk line is resolved into 5 symmetrically located pairs of 'placodes'. **c)** E12.5 – Placodes invaginate into the underlying mesenchyme and the mesenchyme undergoes differentiation into fibroblastic mesenchyme and fat pad mesenchyme. **d)** E14.5 – Mammary epithelium undergoes a small amount of proliferation. **e)** E16.5 – Mammary epithelium undergoes rapid proliferation. Cells descend as a stalk down through the fibroblastic mesenchyme into the fat pad precursor mesenchyme. **f)** E18.5 – Epithelial stalk reaches the fat pad and undergoes branching ductal morphogenesis [172].

1.3.2 Pubertal development

Upon birth and up until puberty (4 weeks of age) the mammary gland remains quiescent besides allometric growth to maintain its size in proportion to the overall size of the animal. When puberty begins rapid and expansive proliferation of the mammary epithelium is required. This huge expansion is orchestrated by Terminal End Buds (TEBs), club shaped structures located at the ends of growing epithelium (**Figure 1.13a and f**). Cap cells, situated at the leading edge of TEBs, are highly proliferative and drive the elongation and penetration of the ducts into the fat pad. The cap cells that trail behind the proliferative leading edge differentiate into myoepithelial cells which go on to form the outer layer surrounding the luminal epithelial cells (**Figure 1.13h**) [173]. To achieve the tree like structure often observed within the mammary gland, lateral branching of off the primary ducts occurs to fill around 60% of the available fat pad; the 40% of space remaining is for expansion triggered under the influence of pregnancy hormones (**Figure 1.13c-f**) [174]. At 12 weeks of age the gland is mature and will exhibit transient changes in morphology during the estrus cycle; these changes are not permanent and mirror, on a small scale, what will occur under the influence of pregnancy hormones [175].

Despite transient epithelial changes during estrus, hormones play a vital role in epithelial development during puberty. Mice that have undergone ovariectomy or hypophysectomy exhibit a lack of TEB formation and consequently a lack of epithelial expansion. However, exogenous estrogen has been shown to rescue epithelial retardation in ovariectomised mice, but cannot rescue the same phenotype in hypophysectomised mice [176]. Interestingly, addition of Growth Hormone (GH) alongside estrogen to rats that have undergone both ovariectomy and hypophysectomy was sufficient to rescue this phenotype, demonstrating both are necessary to permit pubertal development [177]. Prolactin (Prl) has also been shown to contribute towards epithelial development during puberty. Work by Brisken *et al* revealed that Prl null mice exhibit a normal ductal tree by 6 weeks of age however present with a severe level of infertility come pregnancy [178]. Interestingly, studies utilising Prl receptor heterozygous mice (*Prl-R$^{+/-}$*) mice revealed a smaller, less dense, ductal tree with a more severe phenotype observed in Prl receptor knockout mice (*Prl-R$^{-/-}$*). Transplantation of *Prl$^{-/-}$* epithelium into wildtype fat pads rescued this phenotype, highlighting the importance of Prl-R in pubertal development, whilst the former study demonstrated the lack of Prl to severely impede pregnancy and not puberty [179,180]. Of note, mice lacking progesterone receptor, -A or -B (PgR-A and PgR-B), exhibit normal mammary epithelial development both embryonically and during puberty however they are unable to undergo side-branching and lobuloalveolar development during pregnancy (section 1.3.3) [181]. TGF-β is another key molecule in the branching of the epithelium during puberty. Absence of TGF-β demonstrated

excessive epithelial outgrowth whilst overexpression experiments showed the opposite – epithelial outgrowth during puberty was severely impeded, however alveologenesis was unaffected [182–184]. Downstream of estrogen signalling, the EGF pathway plays a pivotal paracrine signalling role. Produced by mammary epithelial cells in response to estrogen, Amphiregulin (AREG), a ligand for EGFR, mediates local hormone signals to neighbouring epithelial cells and the surrounding stroma to drive epithelial growth [185]. AREG knockout mice exhibit impaired ductal outgrowth during puberty, phenotypically mirroring that of ER knockout mice – exogenous AREG was shown to rescue the ER knockout phenotype, confirming AREG as a downstream mediator [186]. Of note, AREG is anchored to the expressing cells membrane post estrogen stimulation. As such, AREG requires cleavage by TACE to enable its activity [187]. FGFs -2, -3 and -10 have all been implicated as vital for pubertal branching morphogenesis. With only hypothetical evidence, FGF-10 null mice die shortly after birth showing severe defects in pulmonary branching morphogenesis, suggesting a morphogenic role in mammary branching morphogenesis [188]. Overexpression of FGF-3 revealed stunted ductal growth [189]. Lastly, FGFR-2 has been cleverly demonstrated, through use of genetic mosaic analysis, as essential for TEB proliferation and invasion; FGFR-2 heterozygous cells ultimately outcompeted FGFR-2 null cells throughout pubertal development [190].

1.3.3   Pregnancy and Lactation

The next hurdle for the mammary gland arises during pregnancy. On average, the female mouse gives birth to five pups, all of which require nourishment through milk. To achieve this feat, the adult mammary gland must undergo two tremendous transformations in the ways of maturation and alveologenesis [191]. These events are driven hormonally, specifically by progesterone and prolactin (PL) [192]. Differing to pubertal development, where estrogen is the predominant driver of ductal morphogenesis, during pregnancy the ovarian steroidal hormone progesterone drives epithelial morphogenesis by means of side branch development. Early on in pregnancy, a surge of progesterone stimulates the epithelial branches generated during puberty to undergo epithelial expansion perpendicular to the main branch – side branching. Binding of progesterone to its receptor, progesterone receptor (PgR), mobilises non-canonical Wnt signalling, specifically Wnt-4 paracrine signalling, instructing epithelial cells to proliferate. The absence of either Wnt-4 or PgR has been shown to severely impact gland development during pregnancy. Studies in mice lacking progesterone receptor ($PgR^{-/-}$) reveal only a simple epithelial tree forms, with the presence of progesterone availing to no ductal expansion, or alveologenesis, in gestation [193]. Furthermore, deletion of Wnt-4 has also been shown to have no effect on rudimentary branching morphogenesis during puberty, however exhibits the same phenotype as $PgR^{-/-}$ during pregnancy; failure to

undergo any form or expansion or differentiation [194,195]. Differing to pubertal expansion, these shorter side branches finalise their growth by undergoing alveologenesis; the formation of bud-like structures referred to as alveoli (lobuloalveolar) which encompass the side-branches. Alveologenesis requires a vital, synergistic, crosstalk between progesterone and PL shown to be heavily controlled through RANKL signalling [196,197]. Evidence for this crosstalk being paramount is seen upon the deletion of the prolactin receptor (PLR), where studies have shown its absence to impede progesterone driven epithelial expansion, as well as abolish alveologenesis [179]. Upon entering the secretory phase of gestation, alveoli undergo maturation, through differentiation, giving rise to secretory cells able to produce milk, and a contractile mesh of surrounding myo-epithelial cells capable of exerting mechanical force to move the milk from the secretory cells into the ductal lumen (**Figure 1.13e-f**) [192,198].

1.3.4   Involution

Post-lactation the mammary gland undergoes a process called involution. This process entails the remodelling of the ductal tree to that of a pre-pregnancy state; removal of alveolar buds, reduction in side-branches and regression of pregnancy derived vasculature. Involution has been shown by a multitude of studies, such as forced weaning and teat sealing, to be initiated via weaning; a lack of demand on the milk available [199,200]. Interestingly, and in support of the notion that weaning plays an anti-involution role, animals overexpressing T-antigen (promoting early apoptosis) exhibit early involution, however suckling throughout induction of T-antigen maintains the presence of the alveolar buds [201]. Moreover, involution is a two-stage process. The first stage is purely apoptotic, is primarily driven by the accumulation of milk in the alveolar buds and is reversible. An accumulation in milk results in the secretion of Leukaemia Inhibitory Factor (LIF), Transforming Growth Factor Beta3 (TGFβ3) and Death Receptor (DR) ligands within 12 hours of weaning. These three factors stimulate apoptosis of the epithelial cells for up to 36 hours after their secretion via both the DR pathway and the JAK/STAT pathway – stage one is reversible if suckling resumes between 0 – 48 hours post-wean [202,203]. Stage two of involution occurs 72 – 144 hours post-wean and is not reversible at any point. The predominant difference between both stages, besides stage one being reversible, is that no gross change in ductal architecture takes place during stage one. During stage two, however, the cells comprising the alveolar buds begin to collapse as their supporting basement membrane (BM) and ECM is degraded; phagocytosis removes the dead epithelial cells whilst adipocytes colonise the space left behind. The key propagators of this stage

are MMPs. MMPs become activated during stage one as a knock-on effect from the activation of serine proteases, which were activated by the induction of apoptosis, however, the MMPs remain inactive due to the expression of their suppressive counter parts TIMPs. It is after this the mammary gland has come full cycle and can now undergo the estrus and the pregnancy cycles again (**Figure 1.13g**). Although not explicitly discussed, it is noteworthy to mention that MMPs also contribute to branching morphogenesis during puberty as well as milk production during pregnancy [204,205].
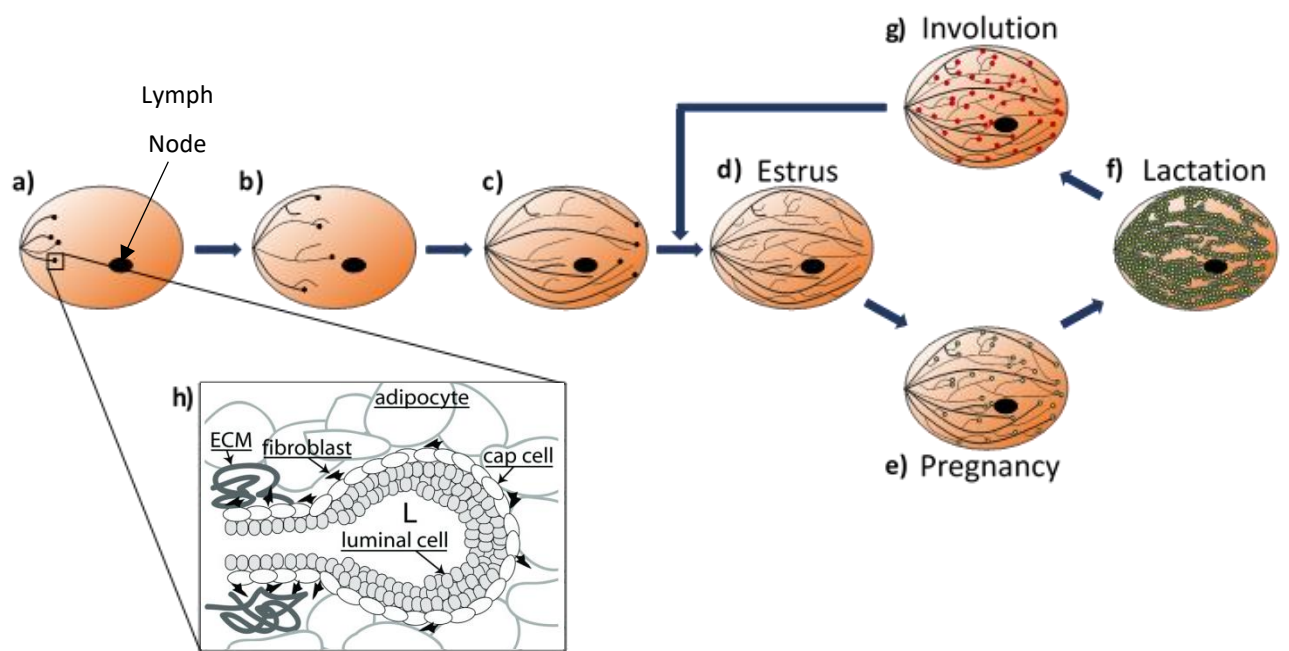
Figure 1.13 Diagram illustrating the post-embryonic development of the murine mammary gland. a) At birth, the epithelium is unbranched and contains mitotically inactive TEBs. **b-c)** At 4 weeks old the TEBs drive the expansion of the epithelium through the fat pad, accompanied by laterally branching, to fill 60% of the fat pad. At 12 weeks old the gland is fully mature and can undergo changes influenced by estrus and pregnancy. **d)** During estrus the epithelium experiences mild morphological changes such as those that occur during pregnancy. **e)** During pregnancy, a surge in hormones such as progesterone and prolactin stimulate further branching and alveologenesis. **f)** The alveolar buds formed during alveologenesis begin to secrete milk and swell, increasing the total volume of the mammary gland. **g)** The mammary gland undergoes involution post weaning and reverts to its pre-pregnancy state. **h)** Schematic of a TEB illustrating the cell types present and their locations [174].

1.3.5 Mammary gland vasculature

As alluded to, the mammary gland is a dynamic organ undergoing waves of epithelial expansion throughout puberty, estrus and pregnancy, the latter followed by involution; the vast undoing of gestational expansion. Concomitant with this transient behaviour, angiogenesis ensues to supply the expanding, ultimately lactating, epithelium with vital resources. Being that it is rare that organs exhibit angiogenesis outside of embryonic development, it is striking to note that during pregnancy the mammary gland utilises both forms of angiogenesis, SA and IA, to meet the increased requirement for oxygen and nutrients during the prolific expansion of the epithelium and during lactation. Vascular corrosion casts of the mouse mammary gland throughout the pregnancy cycle were the key to elucidating this dual angiogenic modality. During the first 14 days of gestation casts revealed the presence of capillary sprouts, with the final 7 days shifting from SA to IA through the emergence of capillary pillars (discussed in section 1.2.2.3.2) and a decline in sprouts [161]. The induction and signalling involved in triggering, and propagating, angiogenesis in the mammary gland is presumably identical to that previously described. Post-lactation the process of involution occurs, as previously described, concomitant with remodelling of the ductal tree. Hand in hand, with the regression of the ductal tree follows the revision of the vasculature which enabled the expansion of the epithelium initially. The process of how the vasculature undergoes regression is sparsely understood with only visual data, corrosion casts, illustrating the stages [25]. Regardless, it is apparent from these data that the vasculature responds to the decline in epithelium, and hence a decline in demand for oxygen and nutrients, following suit by reverting to its pre-pregnancy state.

1.3.6 Breast Cancer

In 2018 the World Health Organisation (WHO) deemed BC to be the second most common cancer worldwide (lung being the most), with BC being the most prevalent cancer in the UK (Cancer research UK – CRUK) [206,207]. Incidence of female BC in the UK has increased by 23% between 1993 to 2017, with a forecast increase of 2% between 2014 to 2034. These increases in BC cases coincide with the most common risk factor associated with BC, age. Since 2010, the UK population has risen from 63.4million to 67.5million in 2019, with a predicted increase to 70.4million by 2030. In conjunction, the median age rose from 39.5 to 40.1, with 2030 showing a median age of 42.4 [208]. Given these figures cumulatively take place over a period of only 20 years, it is more than apparent the UK population is not only growing, but ageing. In a non-mutually exclusive manner, an increasing prevalence of BC and aging population both infer costs, socially and economically. In addition, although age is the most common factor associated with BC development, through means discussed below, environmental and genetic factors are also of importance, and in some cases a root cause.

At first glance, ageing would seem to be the pre-dominant factor with regards to BC development due to an increased time in which cells could mutate through mitosis, be exposed to mutagenic factors or be influenced by other factors (i.e. lifestyle), resulting in BC formation. However, there is a substantial increase in BC cases during pre-menopausal years, with incidence rates doubling every 10 years until menopause, at which point a considerable decline in cases is seen [209]. Given the role of menopause, others factors have also been associated with BC development, such as diet, smoking, oral contraception, obesity and alcohol, all of which can be heavily associated with western culture; the globalisation of BC being accounted for by westernisation [210]. Aside from hormonal disarray and external factors, genetic abnormality is also heavily accountable for the aetiology of BC. In the UK up to 16% of BC cases are down to hereditary germline mutations in either of the Breast Cancer susceptibility genes, BRCA1 and BRCA2 [211]. These two genes are expressed in both breast and ovarian tissue and are fundamental in the repair of double stranded breaks through homologous recombination [212]. Mutation or absence of either of these two genes can result in chromosomal rearrangements through error prone means of DNA repair (i.e. non-homologous end joining) which, if stable and followed by successful rounds of division, could result in autonomous cell division – a hallmark of cancer [213]. Luminal epithelial cells, lining the ducts and milk producing lobules, are the predominant culprit for BC development, however, rarely, the basal cells from the outer layer of ducts can also be the root cause [214].

1.3.6.1 Diagnosis

Recent innovations in the way of BC diagnosis have paved the way for tailoring treatments to BC subtypes, improving the effectiveness of treatments and subsequently patient survival. Analysed histologically, BC biopsies are divided into one of three grading categories. Grade one describes tissue architecture where the vast majority of cells are differentiated showing normal morphology, whereas grade three describes highly undifferentiated cells lacking uniformity or structure, exhibiting severe nuclear pleomorphism [215]. More recently the hormone receptor status of tumours has come to light as an important indicator of effective treatment regimes. Utilising Immunohistochemistry (IHC), the expression of hormone receptors (HR), estrogen receptor (ER) and progesterone receptor (PgR), can be investigated and exploited therapeutically [216,217].

In conjunction with BC subtype, it is also vital oncologists deduce the current stage of a patients BC. Staging of BC is a summative way to discern the extent to which the cancer has progressed. Formally, BC staging is achieved through the Tumour Node Metastasis (TNM) staging system, classifying tumours based on these foremost morphological attributes. Summarised in **Table 1.1**, T refers to the presence and size of primary tumour, N to the presence and extent of lymph node involvement and M to the degree, if any, of metastasis [218].

Table 1.1 Summary of the TNM staging system, extrapolated from the American Joint Committee on Cancer (AJCC) 8th Edition [172].

Stage	Tumour Size (T)	Lymph Node Involvement (N)	Metastasis (M)
0	No evidence of primary tumour present	No evidence of lymph node involvement	No evidence of metastasis
I	≤ 20 mm	Metastases in 1 – 3 axillary lymph nodes	No evidence of metastasis
II	≤ 50 mm	Metastases in 4 – 9 axillary lymph nodes	No evidence of metastasis
III	≥ 50mm	Metastases in ≥ 10 axillary lymph nodes	No evidence of metastasis
IV	Any size in direct contact with chest wall and/or skin.	Any axillary lymph node involvement	Any distally located metastasis

1.3.6.2 Subtypes

Collectively, these histological techniques have culminated in the molecular classification of BC into three main subtypes: Luminal A and B, Basal-like (Triple-negative) and Human Epidermal Growth Factor Receptor-2 (HER2) enriched.

Luminal A is described as ER and/or PgR positive, HER2 negative and Ki67 negative, often grade low with a good prognosis. Like Luminal A, Luminal B are also described as ER and/or PgR positive, however can also be HER2 positive or negative, and are Ki67 positive. The presence of Ki67 is often a distinguishing factor between Luminal A and Luminal B, indicative of proliferative capacity and often correlates with poor prognosis; Luminal B often has a poorer prognosis [219].

Basal-like show no expression of ER, PgR or HER2 (often described as Triple-negative). Finally HER2-enriched may show expression of ER or PR, but heavily express HER2 [220,221]. Of note, there is also a Normal-like subtype which highly resembles Luminal A, bar some variation in gene expression, however yields a poorer prognosis [222,223]. In descending order, Luminal A/B accounts for the majority of BC cases (~70%), followed distantly by HER2 positive (~15-20%) and Basal-like (~15%) [224].

1.3.6.3 Treatment

Courtesy of detailed histological analysis, treatment regimens can be designed to best suit a patients BC subtype. In most cases, BC treatment begins with surgical removal of the tumour along with, if any, axillary lymph nodes to detain the tumours growth and potential to metastasise; stages 0 and I entail breast conserving surgery whereas stage II and III often involve mastectomy – stage IV is often treated palliatively [225]. Alongside surgical resection, chemotherapy and radiotherapy are administered, and depending on the patients BC subtype other targeted drugs may also be administered; chemotherapy can be both an adjuvant and neo-adjuvant therapy.

In instances where a patients BC presents as HR positive (ER+ and/or PgR+), endocrine therapy can be used to antagonise the appropriate HRs through administration of hormone therapy drugs, such as: Tamoxifen, Goserelin, Leuprorelin and Fulvestrant [226]. In a similar vein, use of aromatase inhibitors (i.e. Letrozole, Anastrozole, and Exemestane) act to inhibit estrogen produced by adipose tissue, as opposed to ovarian estrogen; limiting their use to predominantly post-menopausal women [227]. Patients who present with HER2 positive BC can also be given antibody therapy, specifically Trastuzumab (Herceptin), a monoclonal antibody against HER2. Likewise, other antibody therapies also exist, targeting other growth factor pathways: i.e. antibodies against FGF, VEGF and PDGF, the latter two crossing over into the anti-angiogenics, another treatment approach [228]. Targeting growth factor pathways is not limited to antibodies, other strategies also exist, for

example, TKIs, histone deacetylase inhibitors (HDACi) and PI3K inhibitors [229,230]. Other targeted therapies not mentioned above include Poly-ADP Ribose Polymerase inhibitors (PARPi) and Cyclin Dependent Kinase inhibitors (CDKi), both of which can be used alongside chemotherapy, radiotherapy or other targeted therapies. PARPi act by preventing damaged cancer cells from repairing, i.e. after chemotherapy, and examples include: Talazoparib, Rucaparib, Veliparib and Niraparib [231]. The purpose of CDKi is to prevent the cell cycle, aiming to slow down or prevent tumour growth. Over recent years, CDKi against CDK4/6 have been approved for use in HR positive BC [232]. Table 1.2 summarises BC subtype, treatments and prognosis [233].

Table 1.2 Summary of Breast Cancer Subtypes: IHC Status, Effective Treatments and Prognosis.

	Subtype		
	Luminal (A and B)	**Basal-like**	**HER2 Positive**
IHC Status	ER+ and/or PgR+ HER2 (A-, B-/+) Ki67 (A-, B+)	ER- and PgR- HER2-	ER-/+ and/or PgR-/+ HER2+
Effective Treatments	Chemotherapy Radiotherapy Endocrine Therapy PARPi CDKi	Chemotherapy Radiotherapy PARPi	Chemotherapy Radiotherapy Endocrine Therapy Trastuzumab CDKi
Prognosis	Good	Very poor	Poor

* Growth factor inhibitors require a biopsy and tests to ascertain effectiveness

1.4 The placenta

The placenta is a transient organ that arises during pregnancy orchestrating complex interactions between mother and embryo, whilst maintaining gestation through hormone production and perpetuating embryo growth through delivery of nutrients and gaseous exchange. In addition to nutritional input, the placenta also protects the embryo from the maternal immune system [234]. Achieving such remarkable feats is attributed to the placenta's structure, comprised of three distinct layers: the maternal decidua, the junctional zone, and the labyrinth (**Figure 1.14**). It is this triad of regions which enable complex interactions to occur between mother and embryo, collectively resulting in successful gestation.

1.4.1 Placental development

The blastocyst is comprised of two cell layers, the inner cell mass (ICM) and the trophectoderm. At E3.5 these two layers become distinguished resulting in the trophectoderm not in contact with the ICM to differentiate into trophoblast giant cells (TGCs). At E4.5, TGCs penetrate the uterine epithelium and implant into the endometrium, anchoring the placenta to the uterus [235]). Success of implantation permits decidualization of the uterine stroma surrounding the TGC contact, thus forming the maternal decidua. The decidua constitutes a vital layer within the placenta, mediating direct contact and interaction with the mother termed the maternal-fetal interface [236]. Although poorly understood, it is widely accepted that the maternal-fetal interface is vital in maintaining pregnancy through upholding maternal tolerance through modulation of the maternal immune cells at the site of the decidua [237]. Concomitantly, the polar trophectoderm gives rise to the extra-embryonic ectoderm and the ectoplacental cone [238]. At E7.5, the extra-embryonic ectoderm expands to form the chorionic ectoderm (chorion) whilst the allantois begins to form from the posterior mesoderm, contacting the chorion at E8.5 resulting in chorioallantoic fusion – this is deemed the primitive placenta, choriovitelline placenta [236]. Shortly after chorioallantoic fusion the chorion invaginates forming villi, laying foundation for the growth of feto-placental blood vessels from the allantois. As the allantois vascularisation proceeds, at E10 the ectoplacental cone gives structural support through development of a spongiotrophoblasts layer. Upon invasion of the feto-placental blood vessels into the chorion derived villi, the chorionic trophoblast cells differentiate into labyrinth cells [236,239,240]. The spongiotrophoblasts layer once supportive goes on to mature into the junctional zone, containing glycogen cells and executing endocrine functions (**Figure 1.14**) [241]. The mature placenta (chorioallantoic placenta) is seen at E14.5, exhibiting all three layers and perfused with maternal blood sinuses derived from maternal arteries, capable of maintaining and perpetuating embryonic growth [242].
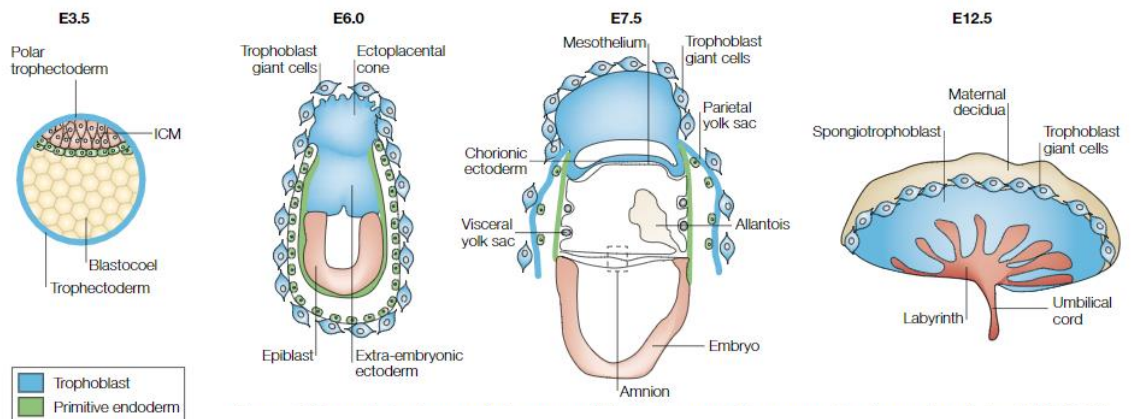
Figure 1.14 Schematic of murine placental development. At E3.5 the inner cell mass (ICM) and trophectoderm become distinguished, resulting in the trophectoderm differentiating into trophoblast giant cells (TGCs). TGCs penetrate the uterine epithelium, anchoring the placenta to the uterus and for the maternal decidua (DB). From E6 to E7.5 the extra-embryonic ectoderm expands and matures to form the chorionic ectoderm (chorion), with the formation and maturation of the allantois occurring from E7.5 to E8.5, fusing with the chorion – chorioallantoic fusion. Shortly after fusion, chorion invagination gives rise to villi, ultimately forming the labyrinth (LZ). E10 the ectoplacental cone gives rise to a supportive spongiotrophoblasts layer. Initially aiding in the formation of the labyrinth, this layer matures forming the junctional zone (JZ) (adapted from Rossant and Cross, 2001 [238]).

1.5 Research aims and hypotheses

In light of background literature discussed and findings of our lab, it is evident that integrin-β3, integrin-α5 and neuropilin-1 have a complex relationship with each other. The interactive balance between these molecules summating in successful angiogenesis. Nonetheless, complete deletion all of three molecules exhibits a potent anti-angiogenic effect in the systems we have investigated to date. This provides a valuable tool for impeding angiogenesis and studying the subsequent outcome on developmental systems, such as the murine mammary gland; the generation of this model will be discussed in section 3. Utilising this as a tool to study the role of fibronectin binding receptors (integrin-α5β1 and -αVβ3), and the VEGF co-receptor neuropilin-1, during the lifecycle of the mammary gland (pubertal development, pregnancy, lactation and involution). Furthermore, given the metabolically active state of the mammary gland during the majority of its lifecycle, including transiently during estrus, alongside literature demonstrating an expansion of vasculature during pregnancy, we propose the following hypothesis:

- The pubertal, gestational and lactational phases of epithelial growth will be impeded through a lack of angiogenesis, caused by the absence of key fibronectin binding receptors and neuropilin-1.

Additionally, tumour angiogenesis is a hallmark of cancer and as such offers a targetable means to try and prevent tumour growth. Having already discussed the premise of this concept in section 1.2.2.5, I sought to address whether the three molecules of interest could offer a robust approach to mitigating tumour growth. As such, I propose the following hypothesis:

- Tumour growth will be significantly reduced in the absence of all three molecules, with a decipherable interaction discernible from the differing combinatorial absence(s) of the three molecules in single and double deletion.

The results chapters within this thesis will be presented as follows. Chapter 1 shall divulge the process of generating the tools required to undertake the research questions being asked, followed by chapter 2 where I shall explore the role of angiogenesis during the pubertal phase of epithelial outgrowth. Chapters 3 and 4 shall investigate the role of angiogenesis in the mature mammary gland, specifically its effects on epithelium during pregnancy, lactation and involution (chapter 3), and breast cancer development (chapter 4). Lastly, in chapter 5, I shall begin to unpick tissue specific EC responses to angiogenic stimuli.

2 Materials and Methods

2.1 Reagents and Housekeeping

Unless otherwise noted, reagents used were purchased from Thermo Fisher Scientific (Loughborough, UK). This encompasses: Applied Biosystems, Corning, Fisher Scientific, Gibco, Invitrogen and Life Technologies. All other reagents were purchased from the following suppliers, listed below:

Abcam (Cambridge, UK)	Microzone Life Science (Stourbridge, UK)
Agilent – Dako (Cheshire, UK)	Nutacon B.V. (Leimuiden, Netherlands)
Amaxa Biosystems (Cologne, Germany)	Olympus (Massachusetts, USA)
Bio-Rad (Hertfordshire, UK)	Qiagen (Sussex, UK)
Brunel Microscopes (Chippenham, UK)	Rockland (Pennsylvania, USA)
CST (London, UK)	Santa Cruz (Dallas, Texas, USA)
eBioscience (Hatfield, UK)	Sigma-Aldrich (Poole, UK)
FlowJo (Oregon, USA)	UVP (Cambridge, UK)
Leica (Milton Keynes, UK)	Vector Laboratories (Peterborough, UK)
Medisave (Dorset, UK)	Zeiss (Cambridge, UK)
Microm (Bicester, UK)	

All methods and techniques employed to generate any work enclosed within this thesis are described throughout this chapter. Data generated in this thesis utilising methods which precede this work are referenced and briefly described. Unless otherwise stated, protocol steps were performed at room temperature and pressure (RTP).

VEGF-A[164] was utilised experimentally to induce pro-angiogenic behaviour of lung and mammary derived endothelial cells. This growth factor was made in-house following the protocol published by Krilleke *et al.,* [243].

2.1.1 Table(s) of Primary Antibodies

Table 2.1 List of primary antibodies used for western blotting.

Target/Anti-	Host	Reactivity	Conjugate	Application	Source	Cat. No.	Clone
ABL1/ABL2	Rabbit	Mouse	-	WB	Sigma-Aldrich	SAB4300641	871521530
AKT	Rabbit	Mouse	-	WB	CST	9272	-
CD31	Rabbit	Mouse	-	WB	CST	77699	-
claudin-V	Rabbit	Mouse	-	WB	Abcam	Ab131259	GR3261733
endomucin	Rat	Mouse	-	WB	Santa Cruz	Sc-65495	K1710
ERG 1/2/3	Rabbit	Mouse	-	WB	Abcam	Ab92513	GR305449
FAK	Rabbit	Mouse	-	WB	CST	3285	-
GAPDH	Mouse	Mouse	-	WB	Abcam	Ab9484	GR3257457
HSC-70	Mouse	Mouse	-	WB	Santa Cruz	Sc-7298	B2117
integrin-α5	Rabbit	Mouse	-	WB	CST	4705	-
integrin-β3	Rabbit	Mouse	-	WB	CST	4702	-
LYVE-1	Rabbit	Mouse	-	WB	Abcam	Ab14917	768540
neuropilin-1	Rabbit	Mouse	-	WB	CST	3725	-
p44-42 MAPK (ERK)	Rabbit	Mouse	-	WB	CST	9102	-
pABL1/ABL2 (Tyr393/429)	Rabbit	Mouse	-	WB	Sigma-Aldrich	SAB4300273	-
P-AKT (Ser473)	Rabbit	Mouse	-	WB	CST	4060	-
P-AKT (Thr308)	Rabbit	Mouse	-	WB	CST	9275	-
P-FAK (Y397)	Rabbit	Mouse	-	WB	CST	3283	-
P-p44-42 MAPK (ERK) (T202, Y204)	Rabbit	Mouse	-	WB	CST	9101	-
PROX-1	Rabbit	Mouse	-	WB	Abcam	Ab11941	811267
pVASP (Ser157)	Rabbit	Mouse	-	WB	CST	3111	-
P-VEGFR2 (Tyr1175)	Rabbit	Mouse	-	WB	CST	2478	-
pVIM (Ser56)	Rabbit	Mouse	-	WB	CST	3877	-
VASP	Rabbit	Mouse	-	WB	CST	3132	-
VE-cadherin (Cdh5)	Rabbit	Mouse	-	WB	Abcam	Ab205336	GR229866
VEGFR2	Rabbit	Mouse/Human	-	WB	CST	2479	-
VIM	Rabbit	Mouse	-	WB	Abcam	Ab92547	GR3186827

WB – Western blot.

Table 2.2 List of primary antibodies used for flow cytometry.

Target/Anti-	Host	Reactivity	Conjugate	Application	Source	Cat. No.	Clone
CD31	Rat	Mouse	eFlour-450	FC	Thermo Fisher	48-0311-80	390
endomucin	Rat	Mouse	AF-647	FC	Santa Cruz	Sc-65495	C1219
Integrin-α5	Hamster	Mouse	FITC	FC	eBioscience	11-0493-81	eBioHMa5-1
Integrin-β3	Hamster	Mouse	PE	FC	eBioscience	12-0611-81	2C9.G3
neuropilin-1	Rat	Mouse	Biotin	FC	Biolegend	145213	3E12
neuropilin-1	Rat	Mouse	PE/Cy7	FC	eBioscience	25-3041-82	3DS304M
neuropilin-1	Goat	Mouse	PE	FC	eBioscience	FAB566P	ABZF0212121
neuropilin-1 (Streptavidin)	-	Rat	BV711	FC	Biolegend	405241	B271307
VE-cadherin (Cdh5)	Rat	Mouse	BV421	FC	Biolegend	138013	BV13

FC – Flow cytometry.

Table 2.3 List of primary antibodies used for immunocytochemistry, immunofluorescence and endothelial cell sorting.

Target/Anti-	Host	Reactivity	Conjugate	Application	Source	Cat. No.	Clone
endomucin	Rat	Mouse	-	IF/ECS	Santa Cruz	Sc-65495	K1710
ERG	Rabbit	Mouse	-	IF	Abcam	Ab92513	GR3054491
Integrin-α5	Rabbit	Mouse	-	IF	Abcam	Ab150361	GR10593376
Integrin-β3	Rabbit	Mouse	-	IF	Abcam	Ab75872	-
neuropilin-1	Goat	Mouse	-	IF	R&D Systems	AF566	ETH0409111
Progesterone Receptor	Rabbit	Mouse/Human	-	ICC	Abcam	Ab63605	GR510226
TdTomato (RFP)	Rabbit	Mouse	-	IF	Rockland	600-401-379	42896

ICC – Immunocytochemistry, IF – Immunofluorescence, ECS – Endothelial Cell Sort.

2.1.2   Table(s) of Secondary Antibodies

Table 2.4 List of secondary antibodies used for western blotting.

Target/Anti-	Host	Conjugate	Application	Source	Catalogue
Mouse	Goat	HRP	WB	Dako	P0447
Rabbit	Goat	HRP	WB	Dako	P0448

HRP – Horseradish peroxidase, WB – Western blot.

Table 2.5 List of primary antibodies used for immunocytochemistry, immunofluorescence and endothelial cell sorting.

Target/Anti-	Host	Conjugate	Application	Source	Catalogue
Goat	Rabbit	Alexa®-488	ICC/IF	Thermo Fisher	A-21222
Rabbit	Donkey	Alexa®-488	IF	Thermo Fisher	A-21206
Rat	Donkey	Alexa®-488	IF	Thermo Fisher	A-21208
Donkey	Rabbit	Alexa®-555	IF	Thermo Fisher	A-31572
Rat	Donkey	Alexa®-594	IF	Thermo Fisher	A-21209
Rabbit	Donkey	Alexa®-647	IF	Thermo Fisher	A-31573
Rat	Sheep	Dynabeads	ECS	Thermo Fisher	11035

ICC – Immunocytochemistry, IF – Immunofluorescence, ECS – Endothelial Cell Sort.

2.2 Animals

Animals were bred on a mixed C57BL/6;129Sv background. All animal experiments were performed in accordance with UK Home Office regulations and the European Legal Framework for the Protection of Animals used for Scientific Purposes (European Directive 86/609/EEC). The study was also approved by the Animal Welfare and Ethical Review Board (AWERB) committee at the University of East Anglia, School of Biological Sciences.

2.2.1 Breeding

In order to study the effects of endothelial integrins in a temporal manner, the Cre/*Lox*P system was utilised. Mice containing an endothelial cell specific Cre-recombinase gene construct, Pdgfb/iCre^{ERT2} (located on the Rosa26 locus) in this instance, were crossed to mice containing our gene(s) of interest flanked by *lox*P sites (floxed) on both alleles. Briefly, Pdgfb/CRE^{ERT2} mice were crossed to integrin-β3$^{fl/fl}$ (β3$^{fl/fl}$), integrin-α5$^{fl/fl}$ (α5$^{fl/fl}$) and neuropilin-1$^{fl/fl}$ (Nrp1$^{fl/fl}$) mice, generating inducible knock-out animals for each of the respective genes [141,244–246]. Animals containing single target floxing were then crossed to generate all double floxed target, and the triple floxed target, combinations: β3.α5$^{fl/fl}$; β3.Nrp1$^{fl/fl}$; α5.Nrp1$^{fl/fl}$; β3.α5.Nrp1$^{fl/fl}$. In breeding trios, Pdgfb/iCre^{ERT2} was maintained only on the male mice allowing the generation of both Cre-positive and Cre-negative offspring; Cre-negative serving as littermate controls for all *in vivo* experiments.

2.2.2 Timed mating

To study the effects of angiogenesis on the murine mammary gland during pregnancy, female mice underwent timed mating. Female triple floxed mice were individually housed alongside a triple floxed male. In the evening, females were introduced into the male's cage, then the following morning all females were plug checked and returned to their home cages; presence or evidence of a vaginal plug was an indication of successful mating and was considered E0.5 [247]. If a plug was found, the female(s) were not paired again in the evening. Females who were plugged were weighed every other day to monitor weight gain (a positive indicator of pregnancy). Upon reaching the embryonic day of interest (E10.5 and E15.5 for work conducted in this thesis) the female and her embryo(s) were sacrificed, and tissue was harvested.

2.2.3 Genotyping

To ensure all animals contained our genes of interest, DNA genotyping was performed. All PCR reactions were run on a 1.8% agarose gel, to allow for sufficient separation of wildtype and floxed bands. Gels were imaged using BioDoc-It Transiluminator (UVP).

2.2.3.1 DNA Preparation

Ear punch biopsies from mice were collected and DNA was isolated for PCR analysis. Briefly, ear biopsies were digested overnight at 56°C in tissue lysis buffer (100µl): Tris-HCL (50mM, pH 8.5), EDTA (10mM, pH 8.0), NaCl (100mM), SDS (0.2%) plus proteinase-K (100µg/ml – Sigma-Aldrich). DNA was precipitated by the addition of isopropanol (100µl) then collected by centrifugation at 1200 X g for 30 minutes. The supernatant was removed, the pellet left to air dry at room temperature for 2 hours and once dry re-suspended in Tris-HCL/EDTA (TE) buffer (200µl): Tris-HCL (10mM, pH 7.5), EDTA (1mM).

2.2.3.2 PCR Reactions

Analysis of the floxed alleles (integrin-β3, integrin-α5 and neuropilin-1) and the Cre-recombinase PDGFb, and the TdTomato reporter gene were performed as follows. DNA (0.4µl), MegaMix-Blue (10µl) (Microzone: a 1.1X reaction buffer containing *Taq* polymerase, 2.75mM $MgCl_2$, 220µM dNTPs, blue agarose loading dye) and 0.08µl of the forward (F) and reverse (R) primers (from a 100 µM stock) were combined and loaded into a 96-well PCR plate.

The reaction conditions of oligonucleotide primers can be seen in **Table 2.6** (below).

Table 2.6 Primers and reaction conditions used for the PCR of all GEMMs.

Gene	Primers		Amplification Programme	
Integrin-β3	F:	5' – TTGTTGGAGGTGAGCGAGTC – 3'	**95°C**	2mins
	R:	5' – GCCCAGCGGATCTCCATCT – 3'	**95°C**	30secs
			56°C	90secs ⎱ 35x
			72°C	1min
			72°C	8mins
			4°C	Indefinitely
Integrin-α5	HT030:	5' –GCAGGATTTTACTCTGTGGGC– 3'	**95°C**	5mins
	HT0311:	5' –TCCTCTGGCGTCCGGCCAA– 3'	**94°C**	30secs
	HT032:	5' –GAGGTTCTTCCACTGCCTCCTA– 3'	**60°C**	90secs ⎱ 35x
			72°C	1min
			72°C	10mins
			16°C	Indefinitely
neuropilin-1	F:	5' –AGGTTAGGCTTCAGGCCAAT– 3'	**94°C**	3mins
	R:	5' –GGTACCCTGGGTTTTCGATT– 3'	**94°C**	30secs
			65°C	1min ⎱ 35x
			72°C	1min
			72°C	10mins
			16°C	Indefinitely
PDGFb	F:	5'–GCCGCCGGGATCACTCTC–3'	**94°C**	4mins
	R:	5' –CCAGCCGCCGTCGCAACT–3'	**94°C**	30sec
			57.5°C	45sec ⎱ 34x
			72°C	1min
			72°C	10mins
			4°C	Indefinitely
TdTomato	WT F:	5' – AAGGGAGCTGCAGTGGAGTA – 3'	**94°C**	3mins
	WT R:	5' – CCGAAAATCTGTGGGAAGTC – 3'	**94°C**	20sec
	Tom F:	5' – GGCATTAAAGCAGCGTATCC – 3'	**61°C**	30sec ⎱ 35x
	Tom R:	5' – CTGTTCCTGTACGGCATGG – 3'	**72°C**	30sec
			72°C	2mins
			4°C	Indefinitely

F – Forward, R – Reverse.

2.3 Tamoxifen Preparation

Tamoxifen was prepared by dissolving 0.3g of Tamoxifen (Sigma-Aldrich) into 1.5ml of corn oil (Mazola). To this, 13.5ml of 100% ethanol was added and the mixture was shaken at ~180rpm at 55°C for 6 hours. This produced a stock solution of 20mg/ml. Once dissolved, aliquots were prepared in UV-proof tubes (Eppendorf™) and stored at -20°C until use.

2.4 Orthotopic Mammary Gland Tumour Assays

Mouse breast carcinoma cells derived from MMTV-PyMT mice (B6BO1[1]) were prepared at 1×10^5 per 50µl in a 1:1 mixture of phosphate buffered saline (PBS) to Matrigel then injected, under anaesthesia, into the left number 4 abdominal mammary fat pad (MFP) of age matched (8 – 12 weeks) Cre-positive and Cre-negative littermate control female mice. Cre-recombinase activity was initiated and sustained as follows. One week prior to tumour cell implantation, Cre-positive and Cre-negative littermate control mice underwent thrice weekly (Monday, Wednesday and Friday) intraperitoneal (I.P.) injections of Tamoxifen (75mg/kg of bodyweight – Jackson Laboratory Protocol, Bar Harbor, Maine, USA); this thrice weekly regimen continued throughout the duration of the experiment(s). Post-implantation, tumour growth was permitted for 15 days, at which point all animals were sacrificed by cervical dislocation and tumours were harvested. Upon collection, tumours were weighed (g), measured (length x width) and imaged prior to being bisected then snap frozen for subsequent analysis. Tumour volume was calculated using the following formula:

(length x width^2) x 0.52 – length being the larger measurement recorded [248].

2.4.1 Immunofluorescent Staining and Analysis – Tumours

Frozen tumours were mounted and sectioned at 6µm using a Cryostat HM-560 (Microm) and mounted onto positively charged slides . Once sectioned, slides were air dried for 10 minutes before being fixed in 4% paraformaldehyde (PFA) for 10 minutes. Slides were then washed two times, for 15 minutes each, in PBS/0.3% Triton X-100. Next, slides were washed twice in PBLEC (1x PBS, 1% Tween 20, 0.1 mM $CaCl_2$, 0.1 mM $MgCl_2$, 0.1 mM $MnCl_2$), 15 minutes each, before being blocked for 30 minutes at 37°C with Dako Block (Agilent-Dako). Slides were then incubated with primary antibodies (Abs) (1:500 in PBLEC) o/n at 4°C (**Table 2.3**). The following day, slides were washed three times, for 5 minutes each, in PBS/0.3% Triton X-100 before being incubated in secondary Abs

---

[1] Kindly provided by Professor Katherine Weilbaecher (Washington University, St Louis, MO, USA).

(1:500 in PBS) for 2 hours (**Table 2.5**). Post-incubation, slides underwent three 5 minute washes in PBS, followed by one 5 minute wash in PBS/0.3% Triton X-100, before being blocked with 5% BSA/PBS for 15 minutes. Once blocked, slides were incubated with a second primary Ab (1:500 in 5% BSA/PBS) for 1 hour (**Table 2.3**). Next, slides underwent three 5 minute PBS washes before being incubated with a second secondary Ab (1:500 in PBS) for 1 hour (**Table 2.5**). Finally, slides were immersed in Sudan Black (0.1% in 70% EtOH) for 5 minutes (in order to quench auto-fluorescence), briefly rinsed in dH$_2$O before being mounted with Fluoromount-G™ with DAPI (4',6-diamidino-2-phenylindole – nuclear DNA stain). Note: not all slides underwent two rounds of primary/secondary Ab incubation. Only slides which required targets to be probed for using primary Abs of the same species received this preparation; all other slides went from secondary straight to the Sudan Black step.

2.5 Endothelial Cell Culture and Isolation

Incubation of cell cultures were performed under the following conditions: 37°C, 5% CO$_2$ and 95% humidity. Primary mammary endothelial cells (MECs) were seeded into flasks pre-coated with 0.1% gelatin (type A from porcine skin – Sigma-Aldrich), human plasma fibronectin (FN, 10µg/ml – Sigma-Aldrich) and PureCol (10µg/ml – Nutacon B.V.). Immortalised MECs were seeded into flasks pre-coated with 0.1% gelatin only. Cell detachment for sub-culturing was performed using a 0.25% Trypsin-EDTA solution (Sigma-Aldrich). Culturing of cells for experimental purposes is described within the relevant sections.

2.5.1 Triple-floxed Mammary Endothelial Cell Isolation

Primary MECs were isolated and prepared from the number 4 abdominal mammary glands of β3.α5.Nrp1$^{fl/fl}$ female mice, aged 8-12 weeks, as previously described [249]. Mice were sacrificed by cervical dislocation, the mammary glands were collected aseptically and placed into Mouse Lung Endothelial Cell media (MLEC – 1:1 Ham's F-12:DMEM (low glucose, 20% fetal bovine serum (FBS); penicillin/streptomycin (100units/ml), L-glutamine (2mM – Sigma-Aldrich), heparin (50µg/mL), endothelial mitogen (25mg – Bio-Rad)). Once extracted, the lymph node within the mammary gland was removed then the glands were rinsed in 70% EtOH before being placed into fresh MLEC. From here, glands were homogenised to a paste like consistency with scalpels (No. 10 – Medisave) then digested at 37°C for 1 hour in the following solution: PBS containing Ca^{2+}Mg^{2+} (1mM), 0.1% Collagenase I (Gibco), 0.01% DNase (Sigma-Aldrich), with agitation every 15 minutes. Post-digestion, the solutions were aspirated through a 19G needle (Medisave) five times followed by a

21G needle (Medisave) four times before being passed through a 100µm sterile cell strainer. Strained digests were then centrifuged at 300 X g for 3 minutes, resuspended in PBS and centrifugation repeated before finally being resuspended in MLEC and seeded into a pre-coated T75 flask. The next day, two PBS washes were performed to remove red blood cells and cellular debris generated from the digest, prior to fresh MLEC being added.

Upon reaching ~80% confluency, the MECs were positively sorted by their expression of endomucin using Magnetic-Activated Cell Sorting (MACS) [250]. Flask(s) were placed at 4°C for 20 minutes prior to incubation with rat-anti-mouse endomucin (Santa Cruz) (1:1000 in PBS) for a further 30 minutes at 4°C. Flask(s) then underwent one PBS wash before incubation with sheep-anti-rat IgG coated magnetic beads (Invitrogen) (1:1000 in MLEC) for 30 minutes at 4°C. Following this, three PBS washes were performed prior to the cells being detached with trypsin and placed into a magnetic rack for 3 minutes. Supernatant was re-seeded into a T75 (in case the positive sort failed), and MECs bound to the beads within the magnetic field were re-suspended in MLEC and placed back into the magnetic rack for a further 3 minutes. Supernatant from this sort was then discarded, MECs bound to the magnetic beads were then resuspended in MLEC and seeded into a pre-coated T25. Upon reaching confluency, a second positive sort was performed (as above) to ensure only MECs were isolated and expanded.

2.5.2 Mammary Endothelial Cell Immortalisation

Immortalized MECs were generated from primary MECs which underwent transfection with polyoma-middle-T-antigen (PyMT) retrovirus as previously described [251]. Briefly, primary MECs that had undergone 2 positive sorts and reached ~80 confluency were incubated with PyMT conditioned media supplemented with Polybrene for 6 hours at 37°C and 5% CO_2, then refreshed with MLEC media overnight (o/n). The following day the treatment was repeated however the MECs were fed with Immortalised Mouse Lung Endothelial Cell media (IMMLEC – 1:1 Ham's F-12:DMEM (low glucose), 10% FBS; penicillin/streptomycin (100units/mL), L-glutamine (2mM), heparin (50µg/mL)). Immortalised MECs were subsequently expanded, frozen down and used at between passages 4 – 24.

2.5.3 TAT.Cre-recombinase Nucleofection

The deletion of floxed target genes within immortalised MECs was achieved via the nucleofection of TAT.Cre-recombinase. Briefly, MECs were nucleofected, using programme T-005 on the Amaxa Nucleofector II (Amaxa Biosystems), with TAT.Cre-recombinase (70units – Sigma-Aldrich), seeded into pre-coated flasks and allowed to recover for two days, followed by a repeat of the nucleofection. Cells were than expanded, a portion of which were lysed and utilised to confirm target deletion via western blot.

2.6 Western Blotting

2.6.1 Western Blot Sample Preparation

Samples were manually lysed, with the aid of a rubber policeman, in electrophoresis sample buffer (ESB – Tris-HCl (65mM, pH 7.4), sucrose (60mM), SDS (3%)). Once lysed, lysates were transferred to a safe-lock microfuge tube containing acid-washed glass beads (Sigma-Aldrich) and homogenised in a tissue lyser (Qiagen) at 50Hz for 2 minutes, followed by centrifugation at 16,000 X g for 10 minutes. Protein concentration was then quantified using the BioRad DC protein assay (Bio-Rad). Prior to loading, the required volume of each sample for a given concentration was reduced by the addition of lithium dodecyl sulfate (LDS) sample buffer and sample reducing agent to a final concentration of 1X then boiled at 95°C for 5 minutes.

2.6.2 8% Polyacrylamide gel (SDS-PAGE) and Gradient gel (5 – 12%) Electrophoresis

Prepared lysates were loaded and run on either homemade (5% stacking, 8% resolving) or pre-cast gradient (NuPAGE™ 4 – 12%) polyacrylamide gels. Gels were run until sufficient resolution of proteins was achieved. Running buffer for homemade gels was used at 1X concentration in distilled water (dH$_2$O): 10X running buffer stock (glycine (1.92M), Tris (250mM), SDS (1%) in dH$_2$O). The running buffer used was the NuPAGE™ MOPS SDS 20X Running Buffer at 1X concentration in dH$_2$O with the running chamber supplemented with antioxidant (NuPAGE™ – 0.25%).

2.6.3   Protein Transfer and Immunoblot

Resolved proteins were transferred onto nitrocellulose at 30V for 3 hours. Transfer buffer used at 1X concentration in dH_2O with the addition of MeOH (20%): 10X transfer buffer stock (glycine (1.92M), Tris (250mM) in dH2O). The transfer buffer used for proteins resolved on gradient gels utilised the same buffer with the addition of antioxidant (NuPAGE™ − 0.25%). Post-transfer, membranes were incubated with Ponceau S stain (0.1% in 5% acetic acid) for 5 minutes to confirm the presence of proteins.

Following confirmation of complete transfer, membranes were blocked in 0.1% Tween-20/PBS (PBSTw) containing 5% milk powder for 1 hour. Once blocked, membranes underwent three 5 minute washes in PBSTw prior to incubation with the appropriate primary Ab, prepared in 5% milk/PBSTw, o/n at 4°C. All primary Abs, excluding loading controls, were used at a dilution of 1:1000 (**Table 2.1**). Primary Abs used for loading controls were all used at a dilution of 1:2000: anti-GAPDH and anti-HSC-70 (**Table 2.1**). Post-incubation with primary Ab, membranes were washed three times for 5 minutes in PBSTw then incubated with the appropriate horseradish peroxidase (HRP) conjugated secondary Ab(s) (**Table 2.4**) for 2 hours in the dark. Secondary Abs were prepared in 5% milk/PBSTw and used at a dilution of 1:2000 for proteins of interest and 1:5000 for loading controls. Membranes were again washed three times for 5 minutes in PBSTw, treated with Pierce® ECL Western Blotting Substrates and imaged via detection of chemiluminescence on a ChemiDoc XRS+ (Bio-Rad). Chemiluminescence was converted to densitometric readings and quantified using ImageJ [252].

2.7   Whole Mammary Gland Extraction

Female Cre-positive and Cre-negative mice were administered Tamoxifen (50µl – 2mg/ml) following either the pubertal or pregnancy regimen described in section 3.2 (**Figure 3.3**). Once induced mice reached the desired experimental endpoint, they were sacrificed by cervical dislocation, the lower thoracic and abdominal mammary glands were harvested into histological cassettes and placed into Tellyesniczky/Fekete (Telly's) fixative (100ml: 87% EtOH (70%), 8.5% formaldehyde (37% stock), 4.5% glacial acetic acid) o/n for haematoxylin whole gland staining, or into 4% PFA: 2 hours for whole gland clearing and immunofluorescence staining (section 2.7.2) or o/n at 4°C for haematoxylin and eosin (H&E) (section 2.7.3).

2.7.1 Haematoxylin Staining

Mammary glands fixed in Telly's were washed three times for 1 hour each in acetone before two subsequent washes in 100% EtOH and 95% EtOH respectively. The mammary glands then underwent whole gland staining for 3 hours in the following haematoxylin stain: 0.8% stock haematoxylin (10% in 95% EtOH), 93% EtOH (95%), 6.2% dH$_2$O, 0.06% FeCl$_3$, pH1.25, adjusted with concentrated HCl (~37%) once all components had been combined. Stained glands were then washed in the following regime: two times for 1 hour each in tap water, once for 1 hour in 50% EtOH containing 2.5% 1N HCl, once for 1 hour in 70% EtOH, one time for 1 hour in 95% EtOH, two times for 1 hour each in 100% EtOH and finally two times 1 hour each in Xylene washes. Glands were then transferred from the final xylene wash into methyl salicylate for long term storage before imaging.

2.7.1.1 Haematoxylin Analysis

Haematoxylin stained glands were imaged using a Brunel Stereoscope (Brunel Microscopes – BMDZ SD2) at 7.5x magnification unless otherwise stated. Epithelial expansion was analysed and quantified from the images obtained using ImageJ. Briefly, masks of the epithelium were manually sketched, binarized and subsequently quantified using the Simple Neurite Tracer plugin. Then epithelium was sketched and measured for each experimental timepoints accordingly. Pubertal glands utilised the lymph node within the abdominal gland as a consistent reference point to sketch and therefore measure epithelial expansion from (**supplementary Figure 9.3**). Pregnant glands at stage E10.5 were sketched and consequently measured at, and across, the lymph node region of the abdominal gland to provide a point of consistent measurement across all E10.5 glands (**supplementary Figure 9.4**).

2.7.2 Immunofluorescent Staining and Analysis – Mammary Glands

Mammary glands fixed in 4% PFA were blocked at 4°C o/n in a permeabilization-blocking buffer composed of: 10% BSA/PBS containing 1% Triton X-100. The following day the glands were incubated in primary antibody prepared in the permeabilization-blocking buffer at 4°C for 4 days. Primary Abs were used at a dilution of 1:200 (**Table 2.1**). After incubation with primary Abs, glands were washed three times each for 1 hour in PBS/1% Triton X-100 before being incubated with secondary Abs (1:500) at 4°C for 2 days (**Table 2.5**). Glands were then washed three times each for 1 hour in PBS/1% Triton X-100, two times each for 30 minutes with PBS and incubated with DAPI for 2 hours at a dilution of 1:1000. Once staining was complete, glands were serially incubated with fructose solutions (w/v in dH$_2$O containing 0.5% 1-thioglycerol (Sigma-Aldrich)) for a minimum of

16 hours each; solutions respectively were 20%, 40%, 60%, 80%, 100% and 115%. Glands were imaged using Zeiss LSM880 Airyscan confocal (Zeiss) at 10X magnification.

2.7.3 H&E Staining

Post-fixation (section 2.7), cassettes containing mammary glands were placed into the Leica Tissue Processor ASP-300S (Leica) for tissue processing prior to H&E staining. Briefly, cassettes are moved through a series EtOH, increasing in concentration: 70% (1 hour); 80% (90 minutes); 90% (2 hours); 100% (1 hour); 100% (90 minutes); 100% (2 hours), before undergoing three xylene washes: 30 minutes, 1 hour and 90 minutes respectively. Lastly, cassettes were passed through three Paraffin wax incubations: 2 hours, 2 hours and 1 hour respectively. Once processed, mammary glands were embedded in paraffin using a Leica EG-1150H Paraffin Embedding Station (Leica) before being sectioned using a HM-355S Microtome (Microm). Sectioning was performed at 10μm and sections were mounted onto positively charged slides; sections were dried o/n at 37°C. Deparaffinisation and H&E staining was performed using a Leica Tissue Multistainer ST5020 (Leica). Briefly, slides were washed twice in Xylene for 5 minutes, washed in a series of ethanol's, of decreasing concentrations, 2 minutes each: 100%, 80% and 70%. Next, slides were submerged H_2O 5 minutes before being placed into haematoxylin for 5 minutes. Next, slides were moved through a series of H_2O, five 1 minute washes, before 15 seconds in 1% HCl/70% EtOH, a dip in H_2O before by 1 minute in 0.1% Sodium Bicarbonate (). Follow this, slides were moved through a series of H_2O, five 1 minute washes before 30 seconds in eosin. Slides were then washed in a series of ethanol's, of increasing concentrations, 2 minutes each: 70%, 80% and 100%, before two 5 minutes washes in xylene and finally being mounted with Neo-Clear® hard set mounting medium (Sigma-Aldrich). Slides were imaged using an Olympus BX60 (Olympus).

2.8 Placental Extraction and Processing

Alongside extraction of the mammary glands, placentas were harvested from the embryos of the pregnant female mice, both Cre-positive and Cre-negative, at E15.5. Placentas were carefully removed from the embryonic sack, weighed, and bisected; with half fixed in 4% PFA for 2 hours then stored in 70% EtOH while the other was snap-frozen in liquid nitrogen and stored at -80°C.

2.8.1   Placental Immunohistochemistry and Stereology

Post-extraction, subsequent embedding, sectioning, staining and analysis were performed by Jorge López-Tello as described [253]. Briefly, the PFA fixed placental halves were paraffin embedded and sectioned at 7μm. Of the sections collected, three non-adjacent sagittal sections (spaced by at least 200μm) underwent immunohistochemical analysis to enable visualisation of the three distinct layers of the placenta, the Decidua (DB), Junctional Zone (JZ) and Labyrinth Zone (LZ). Stereology was performed on these sections to determine the proportion of each of the three regions within each placenta, then compared to the relative controls (e.g. Cre-positive to Cre-negative).

2.9   Flow Cytometry

Flow cytometry was performed on immortalised ECs (see Section 2.5) and tumour homogenates to confirm EC status plus check the absence or presence of the proteins of interest (the floxed targets).

2.9.1   Cell Isolation

2.9.1.1   Tumour Lysate

Tumour bearing mice (Section 2.4) were sacrificed by cervical dislocation and tumours removed. Tumours were manually homogenised to a paste like consistency using scalpels (No. 10 – Medisave) and then digested at 37°C for 1 hour in the following solution with agitation every 15 minutes: 0.2% Collagenase IV (Invitrogen); 0.01% Hyaluronidase (Sigma-Aldrich); 2.5U/ml DNAse I (Sigma-Aldrich) in hanks' balanced salt solution (HBSS). The homogenate was passed through a 70μm cell strainer before being centrifuged at 300 X g for 5 minutes at 4°C. Post-centrifugation, the pellet was washed twice in PBS under the same centrifugal conditions and subsequently stained (Section 2.9.2)

2.9.1.2   Immortalised Endothelial Cells

Immortalised ECs were detached non-enzymatically with citric saline buffer (135mM potassium chloride, 15mM sodium citrate in dH_2O. Once detached, cells were stained according to Section 2.9.2 omitting the incubation step with the red blood cell lysis buffer.

2.9.2 Staining Protocol

Cells from homogenised tumour tissue were resuspended and incubated in 1X red blood cell lysis buffer (Invitrogen) for 5 minutes. Cells, from homogenised tumour tissue or immortalised ECs, were then washed in PBS, 300 X g for 5 minutes, before being resuspended in flow cytometry staining (FACS) buffer (1% FBS in PBS) and counted using a haemocytometer (Sigma-Aldrich). Into a 96-well plate (Corning), cells were aliquoted at $1x10^6$ per well, centrifuged at 300 X g for 5 minutes at 4°C and resuspended in Fc Block (1:200 – Miltenyi, Bergisch Gladbach, Germany) for 10 minutes at 4°C. Once blocked, cells were resuspended in 100µl of the appropriate primary Ab solution and incubated for 30 minutes at 4°C in the dark (**Table 2.2**). Cells were then washed twice in FACS buffer prior to fixation in 4% PFA for 30 minutes at 4°C, washed once in PBS, and finally resuspended in FACS buffer and stored at 4°C before analysis.

2.9.3 Data Collection and Analysis

Data was collected using a Becton Dickinson (BD, Franklin Lakes, NJ, USA) LSR II Fortessa with standard filter sets and five lasers. Data were analysed using FlowJo software (BD).

2.10 Immunocytochemistry

Acid washed coverslips, one per well of a 24-well plate (Corning), were coated with FN prepared in PBS (10µg/ml – Sigma-Aldrich) o/n at 4°C. The coverslips were then washed in PBS before being blocked with a 1% BSA/PBS solution for 1 hour. Cells were then detached from their flask using a 0.25% trypsin-EDTA solution (Sigma-Aldrich), counted and seeded at $2.5x10^4$ per well o/n at 37°C. Coverslips were then washed once in PBS before being incubated with 4% PFA for 10 minutes. Once fixed, coverslips were blocked in 10% goat serum/0.3% Triton X-100 in PBS for 1 hour before being incubated with primary Abs o/n at 4°C. All primary Abs were prepared in PBS and used at 1:200 (**Table 2.3**). Coverslips were then washed three times (3 second submerge) in PBS before being incubated with secondary Abs for 2 hours (**Table 2.5**). The coverslips were then washed three times (3 second submerge) in PBS before being mounted onto glass slides using Prolong Gold with DAPI (Thermo Fisher) and stored at 4°C in the dark until imaging. Imaging was performed on the Axioplan Epifluorescent microscope (Zeiss) and the AxioCam MRm camera (Zeiss) at 63X oil immersion.

2.11 *In Vitro* Assays

2.11.1 VEGF Stimulation and Signalling Assay

Immortalised endothelial cells were seeded at densities of 2×10^5 and 5×10^6 per well on 6-well plates and 15cm dishes respectively (Corning), pre-coated o/n at 4°C with FN in PBS (10µg/ml – Sigma-Aldrich), and left to adhere o/n. The following morning, all cells were starved for 3 hours in reduced serum media (Opti-MEM™) prior to being stimulated with VEGF (30ng/ml in Opti-MEM™) for 5, 10, 15 and 30 minutes – one well remained in Opti-MEM™ only to serve as an unstimulated control. Post-stimulation, wells were lysed in ESB and prepared for western blot analysis as detailed in Section 2.6.1. Cells seeded and treated in 15cm dishes were prepared for Microarray analysis (Section 2.11.3).

2.11.2 Non-Pregnant Serum and Pregnant Serum Stimulation and Signalling Assays

Non-pregnant serum (S) was collected from virgin female mice aged between 8-12 weeks. Pregnant serum (PS) was collected from Cre-negative and Cre-positive female mice at E15.5 of pregnancy – alongside the harvest of mammary glands, embryos and placentas detailed in Section 2.8. Briefly, blood was extracted via cardiac puncture from freshly euthanised mice, left to coagulate at room temperature for 20 minutes, and then spun for 15 minutes at 2600 x g at 10°C. Serum was the carefully aliquoted off the pelleted blood, pooled and stored at -80°C until use.

Immortalised endothelial cells were seeded at densities of 2×10^5 and 5×10^6 per well of 6-well plates and 15cm dishes respectively (Corning), pre-coated o/n at 4°C with FN in PBS (10µg/ml – Sigma-Aldrich), and left to adhere o/n. The following morning, all cells were starved for 3 hours in reduced serum media (Opti-MEM™), prior to being stimulated with either S or P serum (5% in Opti-MEM™) for 15 minutes – one well remained in Opti-MEM™ only to serve as an unstimulated control. Post-stimulation, wells were lysed in ESB and prepared for western blot analysis as detailed in Section 2.6.1 or were prepared for microarray analysis (see Section 2.11.3).

2.11.3 Microarray Sample Preparation

Microarray analysis was performed by Kinex™ KAM-1325 Antibody Microarray Services (Kinexus, Vancouver, Canada). Samples were prepared according to sample preparation guidelines and sent to Kinexus for quantification and analysis (KAM-Kit Instruction manual, Kinexus). Briefly, cells ready for lysis were washed twice in ice-cold PBS before being added to Kinexus Lysis Buffer containing 1X HALT™ protease and phosphatase inhibitor cocktail at 4°C. Lysed samples were then collected

into safe-lock Eppendorf tubes containing acid-washed glass beads and homogenised in a tissue lyser (Qiagen) at 50Hz for 2 minutes. Next, lysates were cleared by centrifugation at 21,000 X g on a benchtop centrifuge for 30 minutes at 4°C. The supernatant was then transferred to a new safe-lock Eppendorf and protein quantification was performed using BioRad DC protein assay (Bio-Rad). Samples were used at 50μg of protein for protein labelling and purification with the appropriate volume being aliquoted into an Eppendorf for proceeding steps. Each sample underwent chemical cleavage for 30 minutes at 37°C before being incubated with biotin for 1 hour. Next, samples were aliquoted into and spun in Microspin columns for 2 minutes at 750 X g. Meanwhile, microarray slides were blocked for 1 hour, prior to incubation with samples, using reagents supplied in the Kinex™ KAM-1325 Antibody Microarray kit. The recovered samples were then loaded onto the now blocked microarray slides and incubated in a humidity chamber for 2 hours. The microarray(s) then underwent eight 5 minute washes in the supplied wash buffers before being incubated in the dark with a supplied biotin antibody for 15 minutes. The microarray slides were then washed twice more, 5 minutes, in supplied wash buffers before being stored in the dark at 4°C prior to shipping to Kinexus for analysis and quantification. Excess sample was stored at -70°C for use in follow up analysis and validation studies.

2.12 Statistical Analysis

Statistical analysis was performed on Cre-positive cells/mice (induced *in vivo* by Tamoxifen administration or *in vitro* by TAT-Cre recombinase as detailed in Sections 2.4 and 2.5 respectively) against their appropriate Cre-negative controls. Values for *in vitro* experiments were calculated and presented as a percentage normalised to Cre-negative controls – controls response being arbitrarily set to 100% for comparison. In order to determine significance between Cre-positive and Cre-negative mammary glands at the various time points investigated, unpaired T-tests were performed. To establish significance between the several mouse models used to study tumorigenesis, unpaired T-tests were performed on data normalised to the respective Cre-negative controls (e.g. each genetic line compared to its own Cre-negative). Welch's correction was performed where variances were significantly different – an F test was used to compare variances. All statistical analysis was performed using GraphPad Prism 6. Error bars shown on graphs represent the Standard Error of the Mean (SEM). Asterisks represent P values that have fallen into the following ranges: (* = P<0.05), (** = P<0.01), (*** = P<0.001) and (**** = P<0.0001). NS = not significant.

Graphical figures were designed on either Microsoft PowerPoint or BioRender (Biorender.com).

2.12.1 Power Calculations

As an initial estimate for tumour studies we analysed similar experiments in animals carrying B6BO1 orthotopic allografts. The variation in statistical power as a function of sample size is presented below. The calculations were based on performing two separate two-sided Welch T-tests where the group means (standard deviation) were assumed to be 5.50 (0.33), 6.27 (0.54) and 4.93 (0.33) for Control, Antibiotic treatment "X" and Antibiotic treatment "Y", respectively (based on preliminary data). The desired significance level was set to $\alpha = 0.025$ to control the family-wise error rate. Each tumour experiment will aim to have a minimum of 12 animals (**Table 2.7**). Due to a lack of preliminary data we were unable to perform power calculations for mammary gland studies.

Table 2.7 Power calculation for B6BO1 tumour experiments.

Group Size	Power Calculation vs "X"	Control vs "Y"
8	0.793	0.802
9	0.854	0.859
10	0.898	0.902
11	0.930	0.932
12	0.953	0.954

3 Generating the *in vivo* and *in vitro* tools and models required to study the role of angiogenesis in the functional lifecycle of the murine mammary gland

As alluded to in the introductory sections of angiogenesis (Section 1.2.2) and integrins (section 1.2.3), integrins play a fundamental role in the successful modulation of angiogenesis. Our lab utilizes genetic tools to investigate the roles, interactions, and mechanistic functions of integrin-β3, integrin-α5 and neuropilin-1, in the process of angiogenesis [114,254,255]. We have generated genetically engineered mouse models (GEMMs) that allow us to inducibly delete the endothelial expression of these three molecules, either alone or in various double/triple combinations. Given their fundamental role in angiogenesis, depletion of all three of these pro-angiogenic targets grants us access to a powerful anti-angiogenic tool that can be used to study the rudimentary and progressive role of angiogenesis in developing systems; in the case of this thesis that system is the murine mammary gland (unpublished – Robert Johnson, Thesis, 2019). Given the (at times cyclical) proliferative capacity of the murine mammary gland, we hypothesized that angiogenesis must be dynamic within the mammary gland throughout its lifecycle to enable such mitogenic feats to occur in a temporally strict window. Supported by studies demonstrating an expansion in vasculature during pregnancy followed by regression, alongside an upregulation of VEGF throughout this process, angiogenesis should play a key role in mammary gland development and function [161]. With this hypothesis in mind, this section shall describe and detail the trials, tribulations, and successes in generating the tools required to explore the effects of angiogenesis in lifecycle of the murine mammary gland.

3.1 The Cre/*Lox*P system – breeding and generating genetically engineered mouse models as an *in vivo* tool

The modern era of biological science has yielded many powerful research tools, specifically ones that enable genome editing; one such tool is the Cre/*Lox*P system. Cre-recombinase (Cre) was originally isolated from bacteriophage P1 and was identified as a unique site-specific recombinase functioning through the recognition of 34-bp sequences referred to as *Lox*P sites (**Figure 3.1b**); an exploitable system for application in gene editing [256,257]. Harnessing this technology through means of molecular biology has yielded an invaluable gene editing tool, not only deleting genes of interests, but doing so in either a constitutive and/or temporal manner. First considerations when designing a Cre gene construct is the promoter region. The promoter region is vital in design consideration as this governs the tissue in which Cre is expressed and, in turn, the tissue in which

Cre can become active. Once Cre is expressed, excision of its target, *Lox*P sites, can be utilised to enable specific gene deletion through Cre-mediated recombination (**Figure 3.1a**). Target gene constructs are engineered to contain the gene(s) of interest with *Lox*P sites situated in flanking positions of a coding region – a floxed gene (**Figure 3.1b**). In circumstances where the Cre construct is devoid of an exogenously inducible element, Cre will be expressed under the deemed promoter region, translocate to the nucleus post-translation, and proceed to recognise and mediate Cre recombination of the floxed gene(s). Further advances in this system have enabled a temporal adaptation; through incorporating an estrogen receptor with a mutated ligand binding domain, ER^{t2}, within the Cre gene construct restricts the transcribed Cre to the cells cytoplasm upon transcription – the nuclear localisation signal (NLS) responsible for the translocation of Cre to the nucleus is blocked [258]. This $CreER^{t2}$ is exogenously inducible through administration of Tamoxifen, which subsequently metabolised to 4-hydroxytamoxifen (4-OHT) *in vivo* via hepatocytes, binds to ER^{t2} receptor on $CreER^{t2}$ (**Figure 3.1d**). Successful binding of 4-OHT enables the translocation of $CreER^{t2}$ into the nucleus through NLS reveal, where Cre-mediated recombination can occur [259]. The consequence of Cre-mediated recombination between the *Lox*P sites results in the deletion of the floxed gene(s) from the genomic DNA, and creation of a circular closed loop of DNA consisting of the excised gene (**Figure 3.1e**) [260,261].

The breeding regimen followed to generate the triple floxed GEMM used throughout this thesis can be seen in Table. 3.1. Briefly, $\beta3^{fl/fl}$, $\alpha5^{fl/fl}$, and $Nrp1^{fl/fl}$ (FL0) mice were crossed to $Pdgfb.iCreER^{T2}$ heterozygous mice to generate each of the single floxed GEMMs with and without the Cre construct, producing i.e.: $\beta3^{fl/fl}.Pdgfb.iCreER^{T2}$ and $\beta3^{fl/fl}$, respectively (FL1); Pdgfb is an endothelial cell specific promoter [244]. Crossing of the single floxed GEMMs to one another proceeded to generate double floxed variations, i.e.: $\beta3.\alpha5^{fl/fl}.Pdgfb.iCreER^{T2}$ and $\beta3.\alpha5^{fl/fl}$ (FL2). Finally, crossing of the double floxed variations to one another resulted in the generation of the triple floxed GEMM – $\beta3.\alpha5.Nrp1^{fl/fl}.Pdgfb.iCreER^{T2}$ and $\beta3.\alpha5.Nrp1^{fl/fl}$ (FL3); for simplicity throughout rest of this thesis, Cre-positive refers to the triple floxed GEMM containing Cre ($\beta3.\alpha5.Nrp1^{fl/fl}Pdgfb.iCreER^{T2}$) whereas Cre-negative refers to the triple floxed GEMM lacking Cre ($\beta3.\alpha5.Nrp1^{fl/fl}$) which serves as a wild-type littermate control. In a similar vein, we crossed GEMMs containing a TdTomato Cre-reporter gene to our $Pdgfb.iCreER^{T2}$ GEMMs to generate $TdTomato.Pdgfb.iCreER^{T2(Cre-neg/Cre-pos)}$ GEMMs that upon administration of Tamoxifen should express red fluorescent protein (RFP); enabling us to test the efficacy of our Cre system [262].
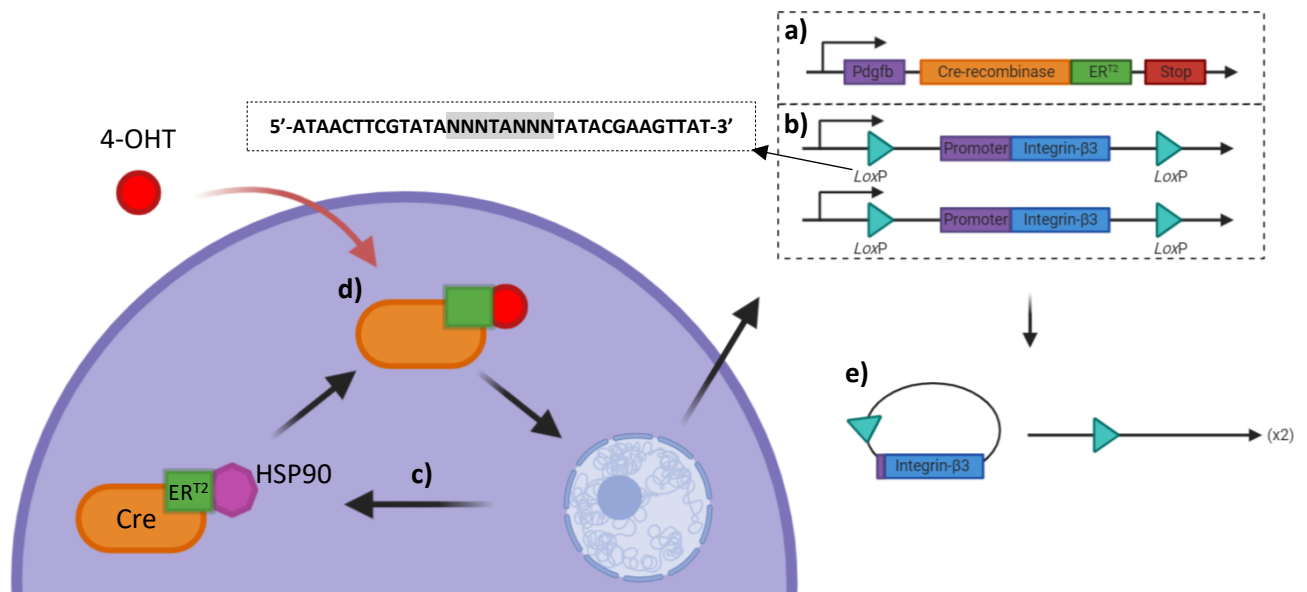
Figure 3.1 Illustration of the Cre/LoxP system. a) A single copy of the Cre-recombinase construct is present within the animal's genome, located on the Rosa26 locus, containing CreER^{T2} driven by a Pdgfb promoter. **b)** For a complete homozygous deletion of the target gene(s), the gene(s) of interest are a flanked by *Lox*P sites as depicted. In the case of the triple, integrin-β3, integrin-α5 and neuropilin-1 are all floxed on both alleles (integrin-β3 is shown alone for simplicity). **c)** Under normal biological circumstances Cre is expressed and remains in the cytoplasm, HSP90 binds to ER^{T2}. **d)** Post-administration, Tamoxifen is converted by hepatocytes to 4-OHT, and binds ER^{T2} enabling the translocation of Cre to the nucleus. **e)** Once inside the nucleus, Cre-mediated recombination ensues at *Lox*P sites, resulting in the excision of the floxed gene to a non-expressible closed loop; all floxed targets are deleted and are no longer expressed inside the promoter specific cell types.

Table 3.1 Simple breeding schematic for the phases of breeding to achieve the triple floxed GEMM (FL3).

Start (FL0)	FL1	FL2	FL3
β3$^{fl/fl}$	β3$^{fl/fl}$.Pdgfb.iCreER$^{T2(pos/neg)}$	β3.α5$^{fl/fl}$.Pdgfb.iCreER$^{T2(pos/neg)}$	β3.α5.Nrp1$^{fl/fl}$.Pdgfb.iCreER$^{T2(pos/neg))}$
α5$^{fl/fl}$	α5$^{fl/fl}$.Pdgfb.iCreER$^{T2(pos/neg)}$	α5.Nrp1$^{fl/fl}$.Pdgfb.iCreER$^{T2(pos/neg)}$	
Nrp1$^{fl/fl}$	Nrp1$^{fl/fl}$.Pdgfb.iCreER$^{T2(pos/neg)}$	β3.Nrp1$^{fl/fl}$.Pdgfb.iCreER$^{T2(pos/neg)}$	
Pdgfb.iCreER^{T2}			

3.2 Deduction of an effective tamoxifen regimen to induce target depletion without impeding epithelial growth

The successful generation of the triple GEMM provided us an *in vivo* model in which we could study the effects of angiogenic disruption throughout the mammary gland's life cycle. However, given this model is inducible, a regimen of Tamoxifen administration needed to be determined to ensure effective target deletion was consistently achieved. Given that Tamoxifen can inhibit mammary epithelial proliferation (see below for more detail) we felt it important to establish an administration regimen that allowed Cre activity without having deleterious effects on the mammary epithelium [263]. Previous work by my supervisor investigated the role of Transforming Growth Factor Beta (TGFβ) in mammary gland development, specifically epithelial outgrowth [264]. The experimental design for these studies was centred on the local delivery of TGFβ to the mammary gland whilst preventing systemic circulation of such a biologically promiscuous growth factor. To achieve this, TGFβ was delivered locally via slow release implantable pellets made from Elvax-40P® copolymer resin. Elvax-40P is a biologically inert material capable of the sustained release of biological molecules. Using these implants, dose administration curves can be performed to determine at which point local effects, but not systemic effects, occur, using the contralateral gland as a control to measure systemic responses [264,265]. Once an appropriate dose is determined, an empty implant can be implanted into the contralateral mammary gland, as a control for measuring potential effects of surgical manipulation, such that each animal serves as its own control.

I decided I might be able adapt Elvax-40P® implants to administer Tamoxifen locally to the mammary gland. Unfortunately, this endeavour ended swiftly. It was with great difficulty that the pellets were produced given the equipment available to me at the time. Furthermore, pellets were tricky to prepare, very small pellets needed to be prepared from the larger stock pellet, followed by even greater difficulty in implantation and recovery at experimental endpoint; pellets were very small to handle and upon performing histological analysis, and post-tissue harvest it was difficult to identify whether the pellet had remained in the gland, and if so its location. Additionally, despite the physical preparation and recovery of the pellet proving difficult, immunofluorescent analysis of Cre-activity, assessed by TdTomato expression discussed in the following section, revealed systemic delivery of Tamoxifen (**supplementary Figure 9.1**). The failure of this approach was disappointing, as it could have granted me a definitive negative control, in that the opposing mammary gland (implanted with an empty implant) would have served as a contralateral control as opposed to a Cre-negative littermate providing the control glands; subject to tittering down the pellet's Tamoxifen dose to prevent the observed systemic effects. Furthermore, continual administration

of Tamoxifen by Elvax-40P® implants would have required pellet resection to avoid the caveat discussed in the following passage.

I therefore turned my attention to Tamoxifen regimens already used in the lab to induce endothelial target depletion in other biological systems. For example, the Robinson Lab routinely administers Tamoxifen via I.P. injection to deplete endothelial receptors in subcutaneously growing tumours (unpublished – Robert Johnson, Thesis, 2019). Following doses recommended by Jackson Laboratory (**supplementary Figure 9.2**), the regimen entails thrice weekly I.P. injections of Tamoxifen over the experimental period (Section 2.3). This regimen produces phenotypic effects on tumour growth through modulation of angiogenesis, implying it activates the Cre/*Lox*P system within our GEMMs (unpublished – see section 6). I decided to test a similar regimen in the mammary gland. Confirmation of Cre activity within the mammary gland using this regimen was achieved by testing it in a Cre-reporter mouse line that expresses TdTomato (a red fluorescent protein) in response to Cre activity. In this reporter line, the promoter region of the TdTomato gene is followed by a floxed stop codon, preventing reporter expression; the stop codon is removed upon Cre activation, thus allowing the expression of the TdTomato reporter. Crossing this reporter line to Pdgfb.iCreER^{T2} animals generated TdTomato.Pdgfb.iCreER$^{T2(pos/neg)}$ animals that, upon addition of Tamoxifen, would reveal where Cre is active in the mammary gland under the regimen being tested (section 2.2.1). I administered Tamoxifen to TdTomato.Pdgfb.iCreERT$^{2(pos/neg)}$ animals thrice weekly over two weeks (**Figure 3.2a**). Mammary glands were then harvested on day 14 and examined for TdTomato expression by immunofluorescence. As can be seen in Figure 3.2, the expression of TdTomato (red) overlaps with endomucin (a marker of endothelial cells) staining (green) indicating Cre-activity within ECs (**Figure 3.2b-c**). This not only indicates the EC specificity of the Pdgfb.iCreER^{T2} within the mammary gland (which has not previously been tested), but it also demonstrates the effectiveness of this particular administration regimen in activating Pdgfb.iCreER^{T2} in the gland. Whilst these parameters were important to establish, systemic administration of Tamoxifen, at the dose being used, has been shown to inhibit epithelial growth in the developing mammary gland from between 3-8 weeks post treatment, with complete recovery observed after 8 weeks [263].

Taking this into consideration, I wanted to design an experimental setup that would allow me to examine the effects of disrupted angiogenesis, without having Tamoxifen toxicity on the mammary epithelium as a confounder. I decided to start Tamoxifen administration when animals weighed 15g. This experimental start point was decided upon for two reasons: (1) a multitude of literature exists demonstrating that early deletion of our EC targets results in embryonic lethality [266–270], and we have shown that even early postnatal deletion of the proposed EC targets leads to lethality (unpublished data); (2) 15 g is a documented indicator of the onset of puberty in C57/BL6 mice

[271,272]. Therefore, a start weight of 15 g allowed me to have a consistent point at which to activate Cre and to then harvest glands in windows outside of the reported Tamoxifen toxicity. Thus, for <u>all</u> non-cancer studies, Tamoxifen treatment began when animals weighed ~15g. Developing glands were then harvested when animals weighed ~20g (mid puberty), which was generally two-weeks after the last Tamoxifen injection (before the beginning of Tamoxifen toxicity) [271]. I further modified the Tamoxifen regimen such that mice only received three I.P. Tamoxifen injections, administered every other day. I decided to only administer these three doses in order to further mitigate against potential Tamoxifen toxicity (**Figure 3.3a**). For all other non-pubescent studies (e.g. pregnancy, lactation, and involution) required the mice to be sexually mature. As such, the same Tamoxifen treatment regimen was followed, with mating not instigated until 8 weeks post final injection, thus well outside the window of potential Tamoxifen toxicity (**Figure 3.3b**). Late in my studies, I was able to confirm this adapted regimen provided effective Cre activity, in the mammary glands of mice that underwent the pregnancy regimen, by testing it in the TdTomato Cre-reporter mouse line (**Figure 3.3b**). Post-induction, 8 weeks later, TdTomato expression was detectable in vasculature, demonstrating that not only was our adapted regimen inducing Cre activity, but the vasculature of a mature gland was fully expressing TdTomato, implying the activity of the Cre extended into adulthood (**Figure 3.4**).
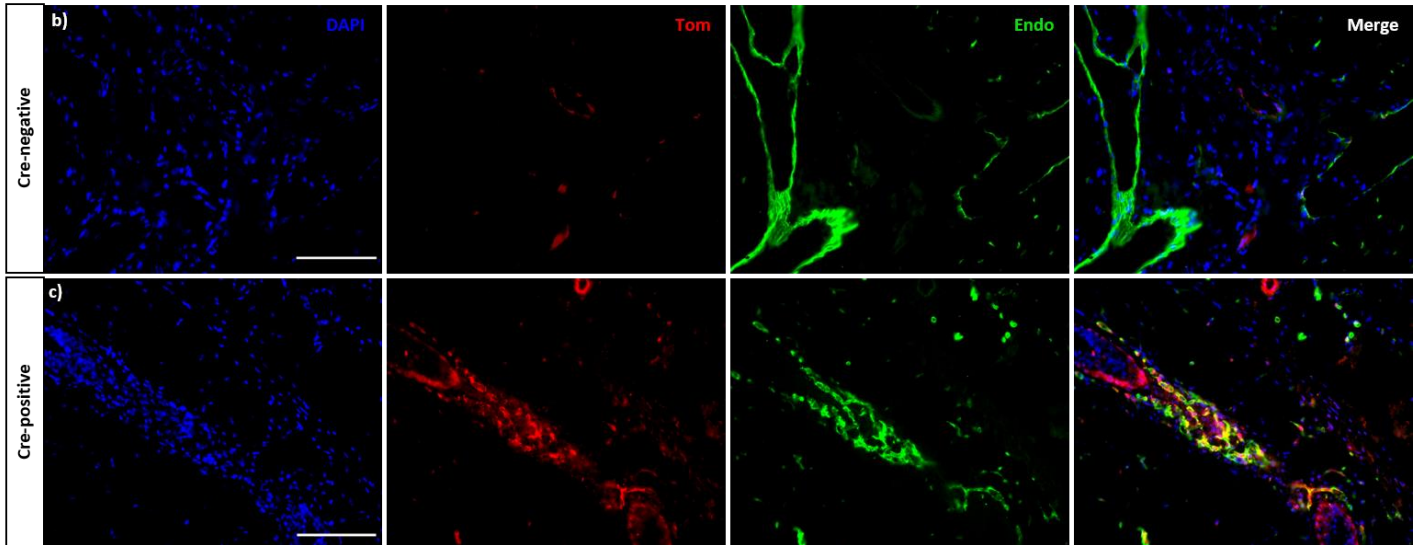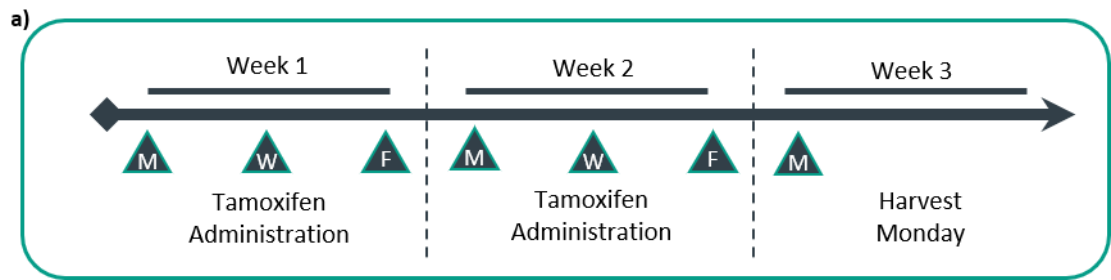
Figure 3.2 Immunofluorescent staining shows co-expression of TdTomato and endomucin in the pubertal gland. TdTomato.Pdgfb.iCreER$^{T2(neg/pos)}$ mice underwent the initial, experimental, Tamoxifen regimen in (**a**). **b)** Representative image of Cre-negative staining for DAPI (blue), TdTomato (red) and endomucin (green). **c)** Representative image of Cre-positive staining for DAPI (blue), TdTomato (red) and endomucin (green). Scale bar = 100μm.
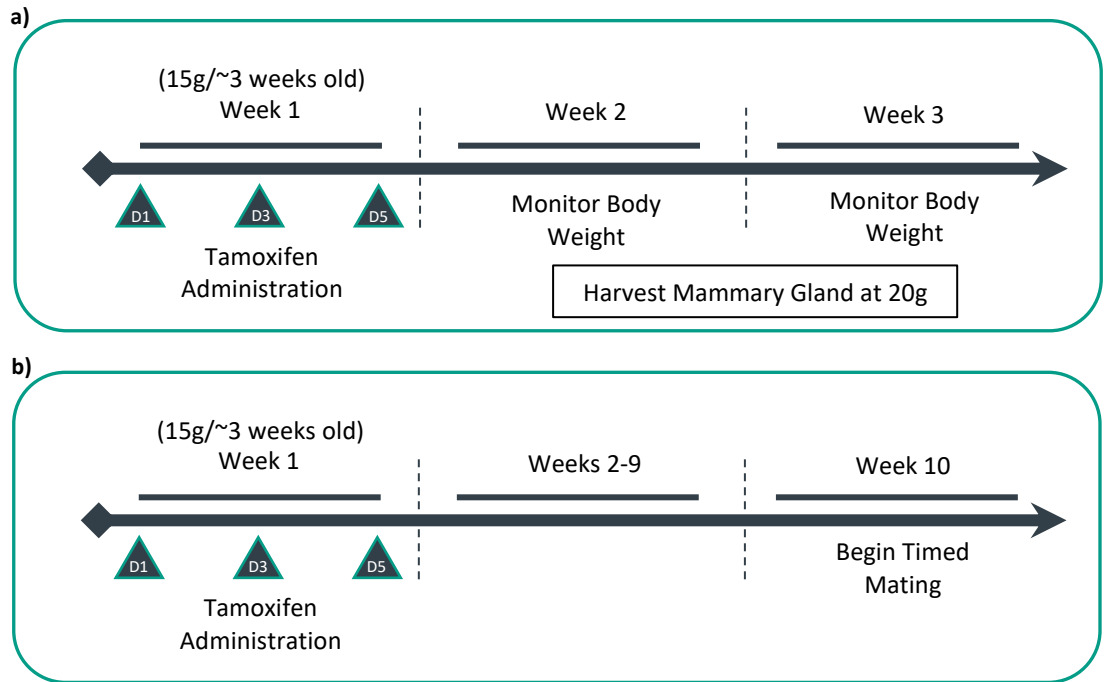
Figure 3.3 Experimental Tamoxifen regimens used for studying mammary morphogenesis at various stages. Pubertal and pregnancy experiments were performed under these regimens to ensure consistent timepoints for experimental start and harvest, and to avoid adverse effects of Tamoxifen. **a)** The Tamoxifen regimen used for all pubertal experiments. Mice weighing 15g underwent one round of three injections of Tamoxifen on alternating days and were monitored until their body weight reached 20g. Upon reaching 20g, approximately 2 weeks post final injection, mice were mid-puberty and the glands were harvested. **b)** The Tamoxifen regimen used for all experiments regarding pregnancy, lactation, and involution of the mammary gland is the same as the developmental regimen (**a**), following which mice were aged for 8-weeks to avoid potential effects of Cre toxicity, prior to timed mating.
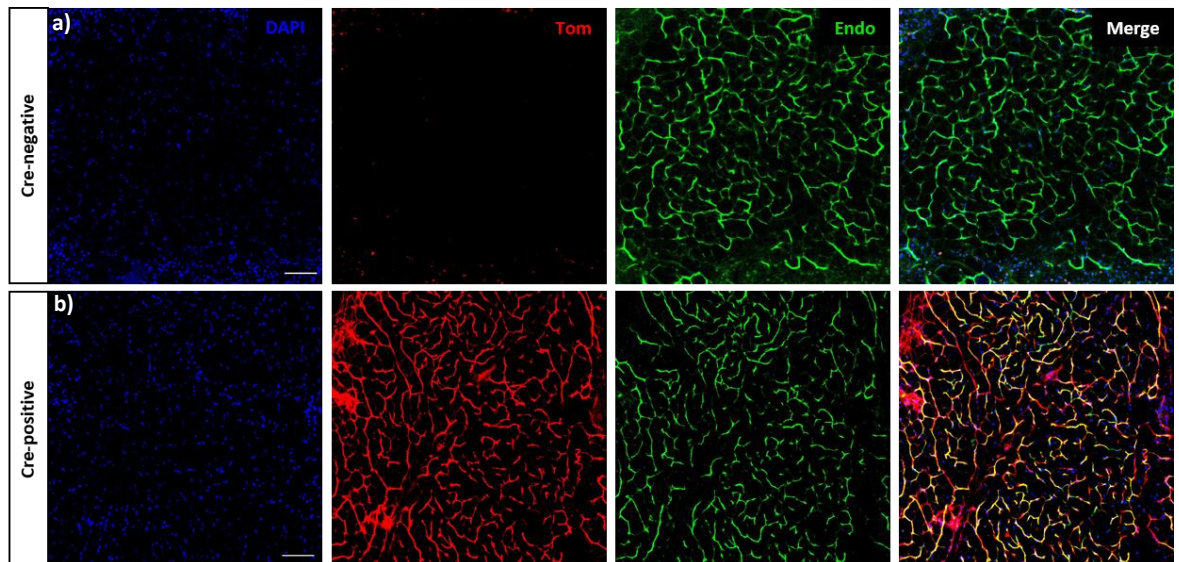
Figure 3.4 Immunofluorescent whole gland staining shows co-expression of TdTomato and endomucin in the mature virgin gland, 8 weeks post Tamoxifen administration. TdTomato.Pdgfb.iCreER[T2(neg/pos)] mice underwent Tamoxifen administration following the pregnancy regimen. **a)** Representative image of Cre-negative staining for DAPI (blue), TdTomato (red) and endomucin (green). **b)** Representative image of Cre-positive staining for DAPI (blue), TdTomato (red) and endomucin (green). Scale bar = 100μm.

3.3 Isolation, transfection, and immortalisation of mammary derived endothelial cells provides a tool to study mammary endothelial cell behaviour *in vitro*

The Robinson Lab has a history of studying EC biology and biochemistry using ECs derived from the lung microvasculature [254]. However, given the mammary focus of this project, and other literature identifying unique EC populations from different organs / systems, we sought to investigate how mammary derived ECs would differ to those from the lung, and attempt to have an EC line that might provide mechanistic insight into any mammary specific *in vivo* phenotypes (e.g. enabling me to unpick signalling pathways and interactions between the three molecules of interest in mammary-derived ECs) [10,273,274]. A previous researcher in the lab (Dr Robert Johnson) generated working immortalised lung microvascular EC (LECs) lines which are missing the expression of integrin-β3, integrin-α5 and neuropilin-1 (**Table. 3.1** – F1, F2 and F3). Endothelial cells were isolated from lung microvasculature and were immortalised through transfection with polyoma-middle-T-antigen (PyMT) retrovirus (section 2.5.1 and 2.5.2). Target depletion was achieved by tat-Cre transfection after isolation of floxed/floxed cells, which allows us to have a 'parental' control (mock transfected) line for **each** individual line we isolate (Section 2.5.3). Deleted lung EC lines will henceforth be referred to as LEC-KO, whilst floxed/floxed (e.g. essentially wild-type cells) will be referred to as LEC-WT.

I was able to successfully modify this approach to isolate and generate triple floxed endothelial cells from the mammary gland (mammary endothelial cells – MECs) as described for the LECs. The predominant modification added to the process was the removal of the lymph node from the number four mammary gland prior to tissue homogenisation, in an attempt to enrich our capillary population and reduce the proportion of lymphatic cells cultured post-homogenisation. Immortalisation and target deletion were achieved as described before, generating both MEC-KO and MEC-WT populations. Target depletion was confirmed through Western blot analysis (**Figure 3.5**). A fibroblast cell line (3T3) lysate was probed alongside MEC lysates to provide a negative control for EC markers and target deletion, acknowledging 3T3 cells are known to express low levels of integrin-α5 (Unpublished – Jordan Lambert, Thesis, 2019). To note, the second, higher, band observed when probing for integrin-β3 is a commonly observed non-specific band (which appears in lysates from β3-null animals).
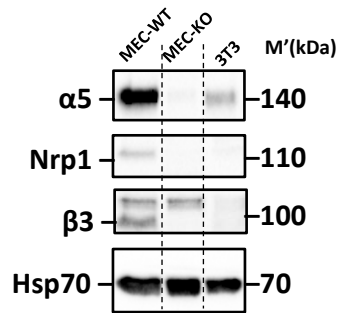
Figure 3.5 Representative Western blot showing in vitro depletion of floxed target genes in MECs through tat-Cre-recombinase transfection. Mammary endothelial cells (MECs) were isolated from β3.α5.Nrp1$^{fl/fl}$.Pdgfb.iCreER^{T2} triple floxed mice, immortalised through PyMT mediated retroviral infection and transfected with tat-Cre-recombinase (MEC-KO), and then immunoblotted for the targets of interest. Mock-transfected MECs (MEC-WT) serve as a wild-type parental line. Lysates from 3T3 fibroblasts were run alongside as controls because they are known to possess low (integrin-α5) or no (integrin-β3, neuropilin-1) target expression [275] – (representative of 3 lysates).

3.4   Confirmation of mammary endothelial cell identity prior to *in vitro* studies

Having successfully isolated, immortalised, and partitioned triple floxed MECs into KO and WT populations, I proceeded to confirm their identity as ECs. During the MEC preparation, endomucin was used as a marker to positively sort for ECs from the mammary gland homogenate; this step was performed twice (see Section 2.5.1). Though well established as an EC marker, endomucin is only one potential marker of EC identity, and it can be expressed by other cell types, specifically those from the hematopoietic cell lineage, such as myeloid and lymphoid cells [276,277]. Best practise entails the confirmation of newly generated cell line identities to ensure all work performed can be confidently attributed to the acclaimed cell type [278–280]. In addition, when isolating ECs from microvasculature, there is potential of co-isolating lymphatic ECs [281,282]. In addition, though we and others have shown that immortalised ECs maintain their identity post-immortalisation, we routinely confirm EC identity throughout the passaging of the cells during their culture [114,251,283,284].

Endothelial identity was assessed throughout the experimental study period, and up to passage 24, the maximum passage at which MECs were used. As expected, MECs continue to express endomucin, the marker against which they were originally isolated (**Figure 3.6**). In addition, we confirmed the expression of VEGFR2, a key receptor expressed by endothelium for the transduction of VEGF signals (**Figure 3.6**) [30]. Furthermore, the expression of CD31 (PECAM-1) and VE-Cadherin (Cdh5) were also detected, both highly expressed at, and essential in maintaining, EC cell-cell junctions (**Figure 3.6**) [285,286]. We also examined the expression of two more recently recognised markers of EC identity: claudin-V and ETS-Related Gene (ERG). The respective function of claudin-V and ERG on endothelium is to modulate tight junctions between ECs and control of vascular permeability respectively [287,288]. Both proteins were expressed by MECs, reinforcing the conclusion that I had successfully isolated ECs from the mammary gland, and their identity was maintained throughout culture (**Figure 3.6**). I also examined the expression of known lymphatic markers, namely LYVE-1 and PROX-1 [289,290]. PROX-1 expression was very low, and LYVE-1 expression was not detected (**Figure 3.6**). Lysates from 3T3 fibroblasts were included as a negative control for all markers (note, low PROX-1 expression was observed in MECs and 3T3 fibroblasts, suggesting the antibody used detects a non-specific band).
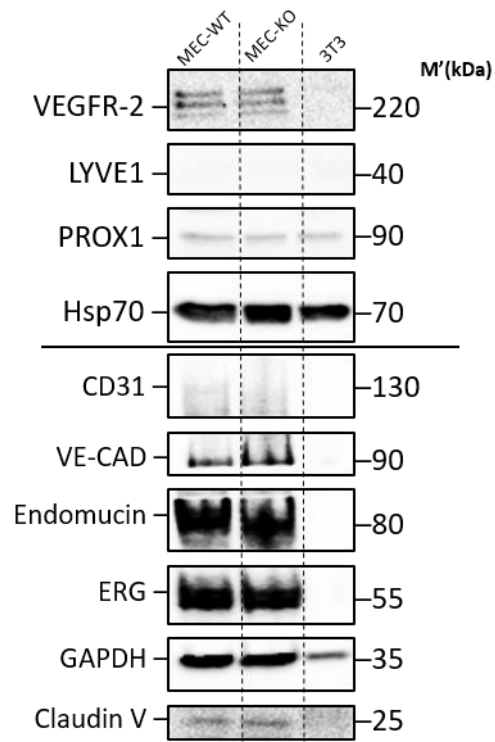
Figure 3.6 Western blot confirmation of endothelial cell status. An immune blot of MECs for endothelial and lymphatic markers. 3T3 is a fibroblast cell line used as a negative control for the expression of endothelial and lymphatic markers (representative of 2 independent lysates).

3.5 Discussion

The GEMMs used in my studies had already largely been established at the start of this project, thus there was little delay in undertaking *in vivo* studies. The ultimate task in hand which had been achieved prior to the project was the generation of the triple floxed animal ($\beta3.\alpha5.Nrp1^{fl/fl}.Pdgfb.iCreER^{T2}$) upon which the entire project, *in vivo* and *in vitro*, was pinned. Aside the GEMM utilised for the developmental studies throughout this project, all other GEMMs generated (listed in Table. 3.1) were used for cancer studies in a bid to ascertain the value of each molecule individually in modulating pathological angiogenesis with respect to the cancer model used (see section 6).

Although the tools required to pursue this project had successfully been generated, there are several drawbacks. First and foremost is the efficacy of our Cre, specifically its off-target activity. Pdgfb.iCreER^{T2} has been shown to lack sole EC specificity [291,292]. Expression of Pdgfb has been documented in neurons, smooth muscle, macrophages and megakaryocytes [293–296]. Despite this, Pdgfb.iCreER^{T2} has demonstrated, and continues to demonstrate, efficient target depletion in our GEMMs [114,254]. Having stated Pdgfb is not exclusive to ECs, without experimental evidence we cannot say for certain any findings observed can be solely a result of a lack of angiogenesis. Specifically, macrophages are known to play a vital role in remodelling the ECM during mammary gland morphogenesis. As such, phenotypes associated with epithelial development could be a consequence of macrophage related deletions of our targets as opposed to endothelial [297]. Advances in the Cre/*Lox*P system have resulted in the development of new inducible EC specific Cre-promoters, one worthy of mention is Cdh5.iCreER^{T2}. Cdh5 driven Cre demonstrates EC specificity whilst boasting no off target expression [291,298]. Our lab is now in the possession of Cdh5 Cre, however we had already established our GEMMs on the Pdgfb Cre prior to its obtainment.

Coinciding with the effort to generate and maintain these GEMM lines, we developed a routine of "best breeding practice", involving: genotype confirmation by PCR of all GEMMs to be used for breeding trios to ensure the correct animals are bred, PCR analysis of all floxed alleles for every first litter across all breeding trios in all of our GEMM lines to confirm the former checkpoint, and confirmation of the allelic status, post-harvest, for all experimental animals to ensure correct genotypic parameters; Pdgfb.iCreER^{T2} status was also checked and confirmed at these checkpoints, as well as on every litter weaned.

Having access to the triple floxed animals at the start of this project not only facilitated the *in vivo* studies but it also enabled the isolation of MECs. LECs are often widely used as an *in vitro* model to

study angiogenesis [284,299,300]. Albeit valid, this wholistic approach overlooks literary evidence for differences between "identical" cells isolated from unique locations, i.e. ECs from lung vs mammary gland [10,273,274]. The success of isolating MECs, in conjunction with already having access to triple LECs, grants us the opportunity to begin exploring the tissue specificity of ECs, and whether they differ enough to warrant tissue specific isolation.

4 Angiogenic signalling mediated through integrin-β3, integrin-α5 and neuropilin-1 is not required for successful epithelial morphogenesis in the murine mammary gland during pubertal development

Having determined a Tamoxifen regimen suitable to induce target depletion that should not impact normal epithelial growth, the exploration into the role of angiogenesis in the murine mammary gland could begin. I initially explored the role of angiogenesis during the rapid epithelial expansion the mammary gland undergoes during puberty. As with any tissue, allometric growth alone requires angiogenic activity to ensure growing tissues stay within sufficient range of blood vessels to allow diffusion of oxygen and nutrients [301,302]. During puberty, the mammary gland undergoes expansion at exceptional speed, faster than that of allometric growth; I hypothesised this rapid growth would require angiogenesis to meet the needs of the developing organ.

4.1 Epithelial outgrowth of the murine mammary gland during pubertal development is not affected by angiogenic impediment

The ventral surface of the mouse is comprised of five pairs of mammary glands running in parallel, cranial to caudal (**Figure 4.1**). Of the five pairs, the easiest to harvest are the mammary glands located at positions three and four, with the number three also lying the flattest, and therefore offering the greatest clarity in terms of visualisation post-staining (**Figure 4.1a**). In fact, the number three gland is that which is most often used for examining the effects of experimental manipulations on mammary gland morphogenesis. However, for my studies the quantitation of the number three glands proved difficult due to a lack of a reference point from which epithelial outgrowth could be measured consistently. To facilitate easy visualisation, this gland requires manual stretching to original size over a tissue cassette before fixation and staining. Because this stretching exercise varies from gland to gland, and from user to user, we felt this manipulation might lead to variability in the quantification of total epithelial growth, if, for example, we were to measure distance from nipple to epithelial front (**Figure 4.2**). Moreover, the margins of glands in positions two and three overlap, and the number three glands sits in close proximity to muscle situated on the forelimbs and spine. Practically speaking, this means that part of the number two gland and some muscle is inevitably harvested along with the number three gland, and these must be manually separated after whole gland staining, which generally leads to structural damage in the number three gland. Thus, we decided to harvest and perform analyses in the number four, abdominal, mammary gland. Although this gland is thicker than the number three gland, and consequently lacks the same level of clarity in epithelial structure post whole gland stain (WGS), it

requires very little stretching back to original size and it contains a central lymph node: a structure which can be used as a landmark for quantifying epithelial outgrowth that occurs during puberty.
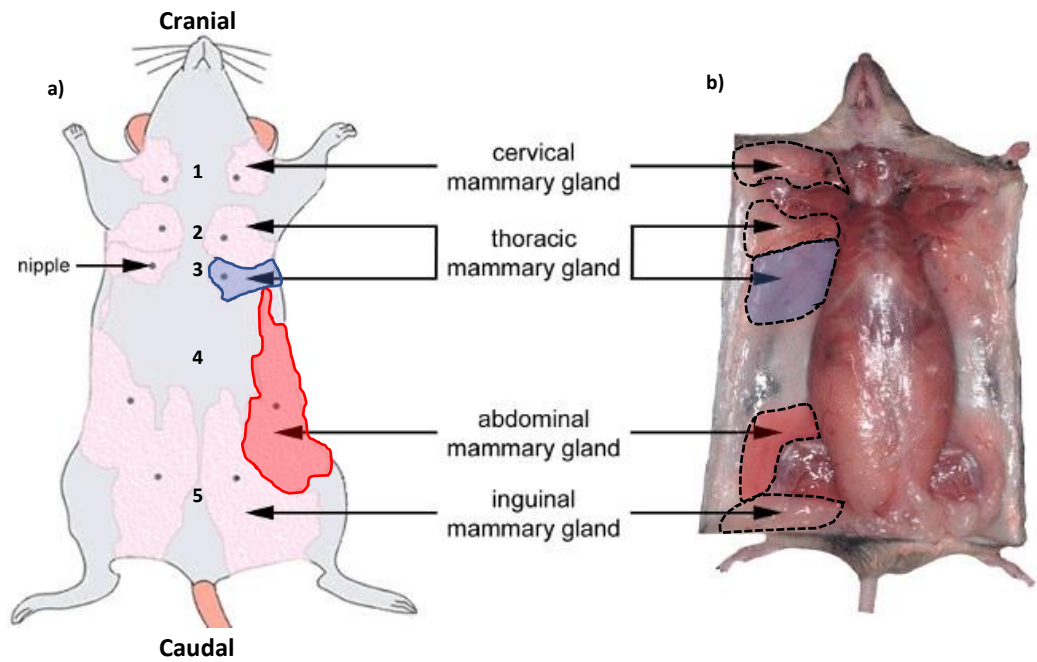
Figure 4.1 Ventral diagrams of the mouse depicting the position and location of all five pairs of mammary glands. Mouse possess five pairs of mammary glands on the ventral surface. **a)** A sketched ventral diagram of the mouse displaying the five pairs of mammary glands located on the ventral surface. The numbers running down the centre denote the position of the mammary glands. Highlighted are one of the two number three glands (blue) and one of the number four glands (red). **b)** An anatomical photo displaying the five pairs of mammary glands. Note, the situation of glands two and three with respect to each other and muscle from the forelimb and spine. Adapted from Honvo-Houéto and Truchet [303].
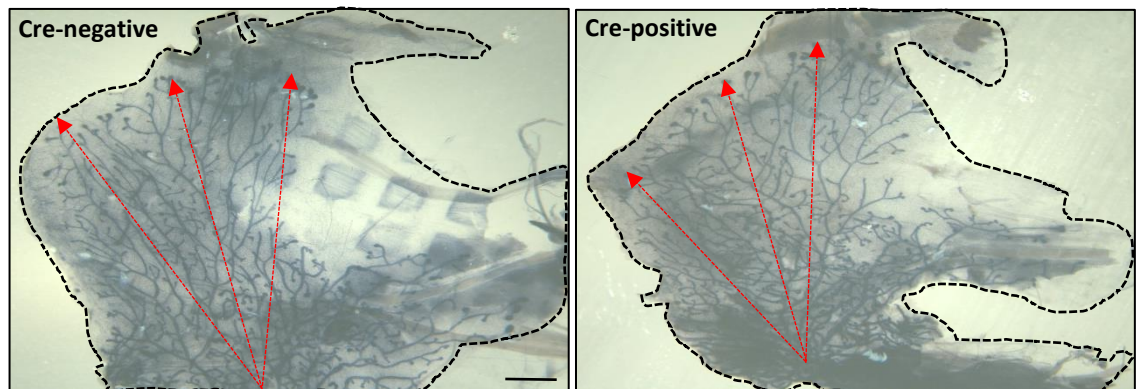
Figure 4.2 Quantification of epithelial outgrowth of the number three gland proved difficult due to imaging limitations. Representative images of the number three glands following WGS with haematoxylin, highlighting the difficulties in quantifying the number three mammary gland. The peripherally located tissue (black dashed lines) highlights the boundary of the mammary gland, demonstrating the artificial area produced by the manual spreading of the gland into the tissue cassette. Depicted by the red arrows, measuring epithelial outgrowth from nipple to epithelial front can be difficult due to the high density of tissue situated at the nipple's location. Scale bar = 2mm.

Having established the number four gland to be optimal for my studies, I proceeded to treat 15g female mice with the Tamoxifen regimen discussed previously (section 3.2) (**Figure 3.3a**) and harvested their glands when they reached 20g. Glands were then processed for WGS so that the epithelium was discernible and visual interpretation of epithelial outgrowth ensued. To my surprise, upon visual inspection, it appeared that impeding angiogenesis through the co-depletion of integrin-β3, integrin-α5, and neuropilin-1 in Cre-positive animals showed no gross deviation in epithelial expansion compared to their Cre-negative counterparts (**Figure 4.3a-b**). I then proceeded to quantify a number of epithelial parameters. First, the epithelium adjacent to, and extending past, the lymph node was traced as a separate image layer (GNU Image Manipulation Program – GIMP) and measured using the Simple Neurite Tracer plugin (ImageJ) (**Supplementary Figure 9.3**). This quantification supported the observation from the WGS; epithelial outgrowth measured in this way showed no significant difference between Cre-positive and Cre-negative animals (**Figure 4.3c**). Because visually there seemed to be differences in the epithelial distribution about the lymph node, I next quantified the maximum directional epithelial outgrowth (from the lymph node) to assess whether direction of growth was affected in Cre-positive animals. The top edge (above) and either side of the lymph node were measured (**Figure 4.3a**). Although total epithelial outgrowth was not altered between Cre-positive and Cre-negative animals, the extent to which the epithelium at the top edge of the lymph node grew was significantly greater in Cre-positive mice (**Figure 4.3d-e**).
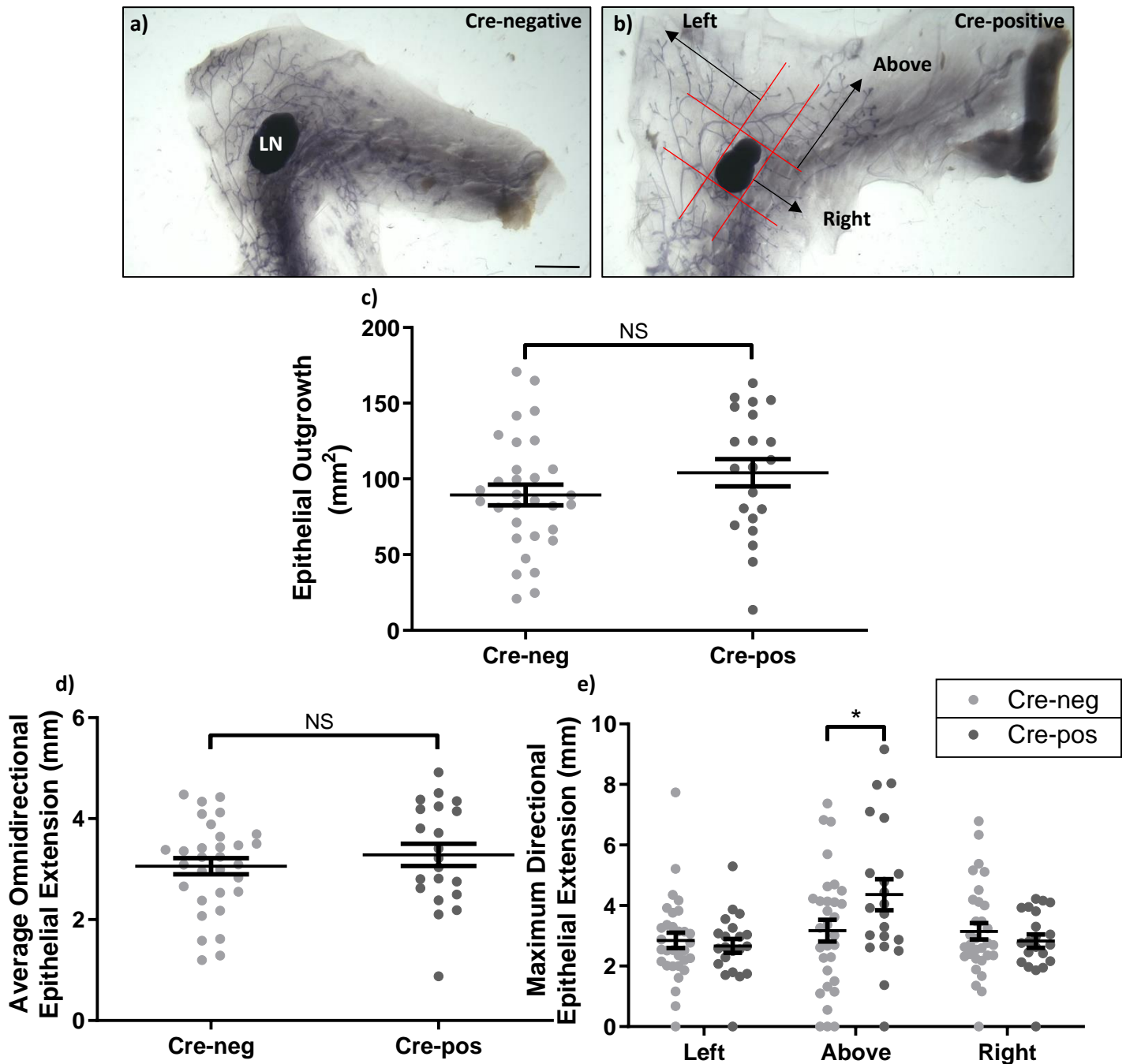
Figure 4.3 Epithelial outgrowth of the mammary gland during pubertal development is not impeded by co-depletion of endothelial integrin-β3, integrin-α5 and neuropilin-1. Cre-positive and Cre-negative animals underwent Tamoxifen-induced Cre-recombinase activation following the pubertal Tamoxifen regimen described in section 3.2. **a-b)** Representative images of whole gland stained number four mammary glands. **c)** Quantification of the area of total epithelial outgrowth measured from the base of the lymph node outward. **d)** Average omnidirectional epithelial extension (right – overlaid with an example of quantification method). **e)** Maximum directional extension of mammary epithelium from the lymph node, left, above and right respectively. LN = Lymph Node. N=11, Cre-negative n=31, Cre-positive n=21. Scale bar = 2mm. Error bars = ±SEM. (* = P<0.05).

Finally, I also measured epithelial density and number of branch points within each of the three measured areas near the lymph node (e.g. top edge (above), left and right). Like overall outgrowth, I observed no statistical difference in these two measurements when comparing Cre-positive to Cre-negative glands (**Figure 4.4**). Taken collectively, these findings suggest that impeding angiogenesis during pubertal development does not influence epithelial outgrowth.
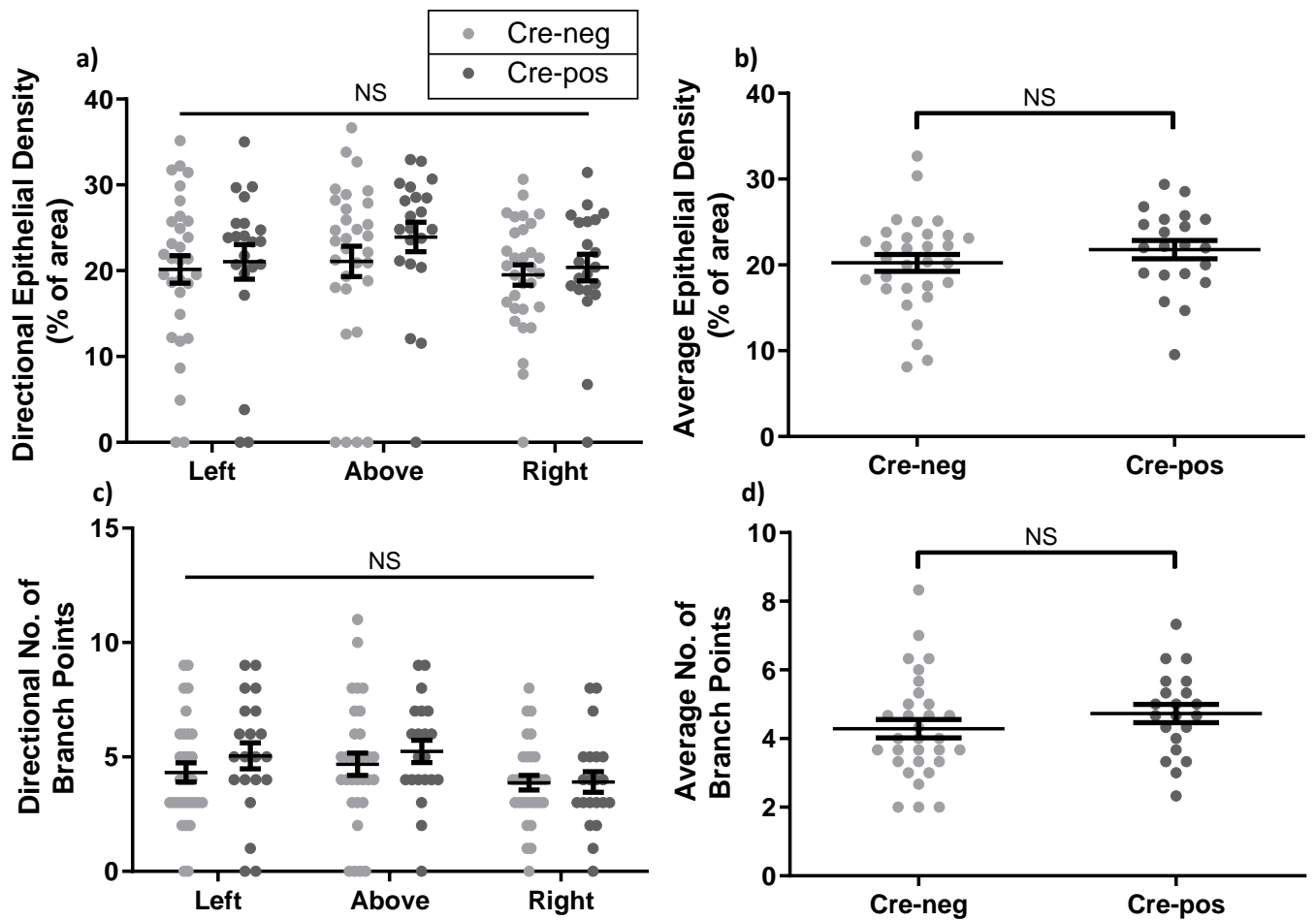
Figure 4.4 Epithelial density and the number of branch points are unaffected when endothelial integrin-α5, integrin-β3 and neuropilin-1 are depleted. Cre-positive and Cre-negative animals underwent Tamoxifen-induced Cre-recombinase activation following the pubertal Tamoxifen regimen described in section 3.2. Three $1 \times 10^6 \, \mu m^2$ regions around the lymph node were quantified (left, above, right) for epithelial density and number of branch points. **a)** Area specific quantification of epithelial density as a percentage of the $1 \times 10^6 \mu m^2$ region. **b)** Average epithelial density as a percentage of the $1 \times 10^6 \mu m^2$ region. **c)** Area specific quantification of the number of branch points. **d)** Average number of branch points. N=11, Cre-negative n=31, Cre-positive n=21. Error bars = ±SEM.

4.2 Terminal end bud trifurcation events are significantly increased in the absence of pro-angiogenic targets

Upon closer visual inspection of stained whole glands, I noted occasional trifurcation at branching points (**Figure 4.6a**)**,** suggesting that whilst overall epithelial outgrowth may not be affected by angiogenic perturbation, other aspects of developmental morphogenesis might be. Thus, I decided to quantify additional morphometric parameters.

Terminal end buds (TEBs) are small robust structures found within the post-natal mammary gland, fundamental in permitting epithelial expansion through their motility and proliferative capacity [304]. Found at the migratory front of the mammary epithelium during pubertal development, hormonal stimulation of TEBs during puberty is responsible for instigating mitotic events which summate in the growth, and subsequent penetration, of the epithelium through the mammary fat pad [305]. As they grow through the fat pad, TEBs branch, filling the available space as they grow, but maintaining sufficient space for alveoli to form during later stages of the mammary gland cycle [306]. Bifurcations are the most common form of branching, but trifurcations do form on occasion. The mechanisms leading to rare trifurcation events are poorly defined, but increased trifurcations are more frequently associated with an over expression of the Rho GTPase CDC42, a key protein in regulating mammary morphogenesis whose aberrant expression has been linked with BC formation, suggesting the process is tightly controlled [307]. Thus, I decided to examine TEBs and branch points in greater detail, with the aim of addressing whether the modality in which the epithelium is expanding via TEBs differs between Cre-negative and Cre-positive animals. Given the lack of an overall phenotype with respect to epithelial "coverage" in Cre-positive animals, I hypothesised that the type of branching is altered such that overall epithelial density, which may be essential for later stages of mammary gland differentiation and function, is maintained even when angiogenesis is impaired.

As mentioned, TEBs are the drivers of epithelial growth during pubertal development and can be considered to directly relate to epithelial growth; the greater the number of TEBs the greater the growth rate [308]. Thus, I first quantified the overall number of TEBs per gland, using the multi-point tool on ImageJ (section 2.7.1.1, **Figure 4.5**). There was no significant difference observed in the number of TEBs in the Cre-positive mammary glands compared to Cre-negative glands.
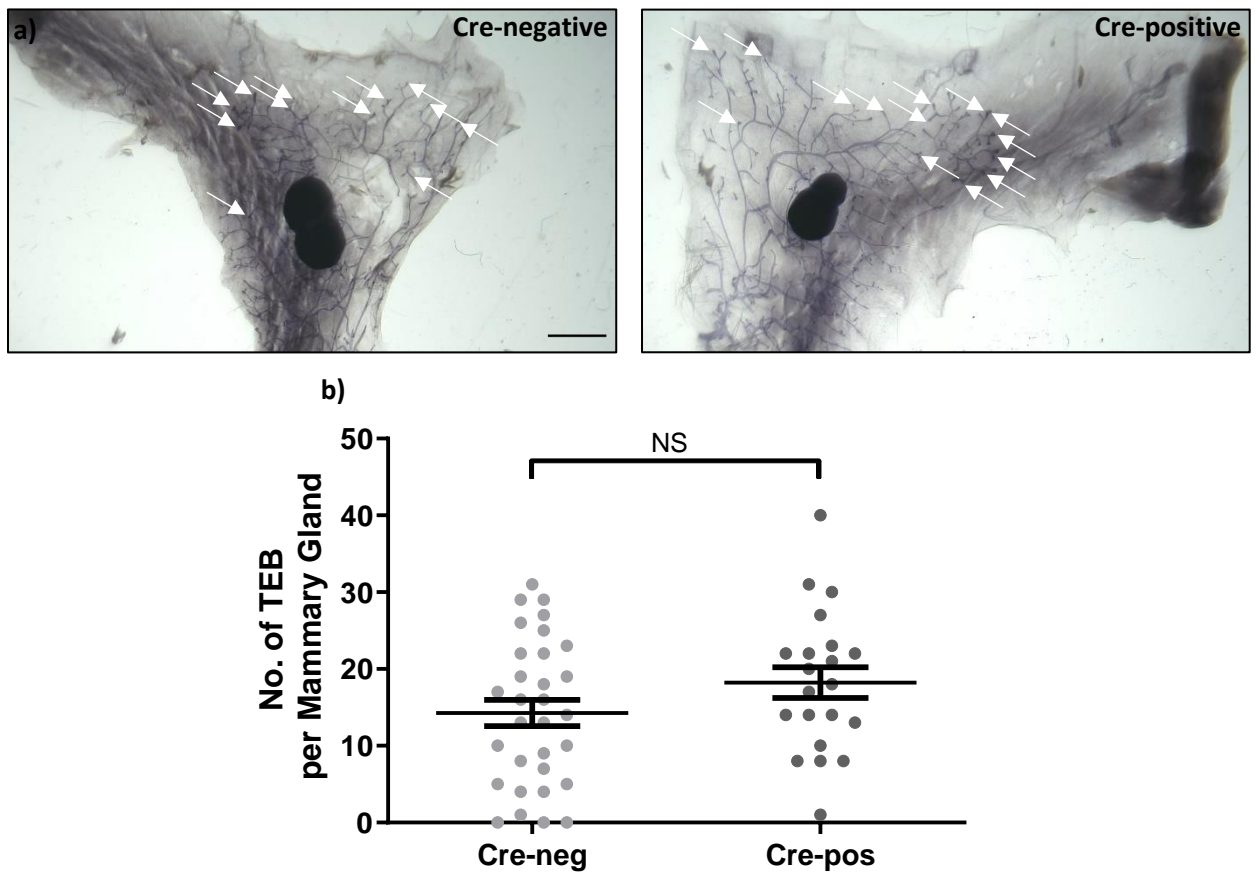
Figure 4.5 Depletion of endothelial integrin-α5, integrin-β3 and neuropilin-1 does not affect terminal end bud (TEB) number. Cre-positive and Cre-negative animals underwent Tamoxifen-induced Cre-recombinase activation following the pubertal Tamoxifen regimen described in section 3.2. Total TEB counts were enumerated from WGS images using ImageJ. **a)** Representative images of WGS mammary glands with TEBs marked (white arrows). **b)** TEB quantification from WGS images. N=11, Cre-negative n=31, Cre-positive n=21. Scale bar = 2mm. Error bars = ±SEM.

I next counted the number of epithelial trifurcations in Cre-negative and Cre-positive glands. This quantification revealed a significantly greater number of these events in the Cre-positive mammary glands compared to the Cre-negative (**Figure 4.6**). This finding suggests that epithelial outgrowth in Cre-positive animals is maintained by increasing the number of trifurcated branch points. Finally, during my enumeration of TEBs, I noted they were not always easy to identify in Cre-positive glands as they occasionally lacked typical TEB size, they appeared smaller, but were exhibiting bifurcation or were located at the migratory front (**Figure 4.5a**). Thus, I decided to investigate the histoarchitecture of TEBs and bifurcations is H&E sections.

An explanation for this given the data discussed so far, is that an increase in TEB trifurcations is a response to impaired angiogenesis to supplement epithelial growth. In turn, increased mitotic activity at TEBs, to accommodate impaired angiogenesis, could consequently be coming at a structural cost, resulting in TEBs losing their traditional shape. Altogether, this suggests the robust bulb like structure normally exhibited by TEBs may not have fully recovered prior to the next bifurcation, or trifurcations, event, perpetuating this lack of typical structure.
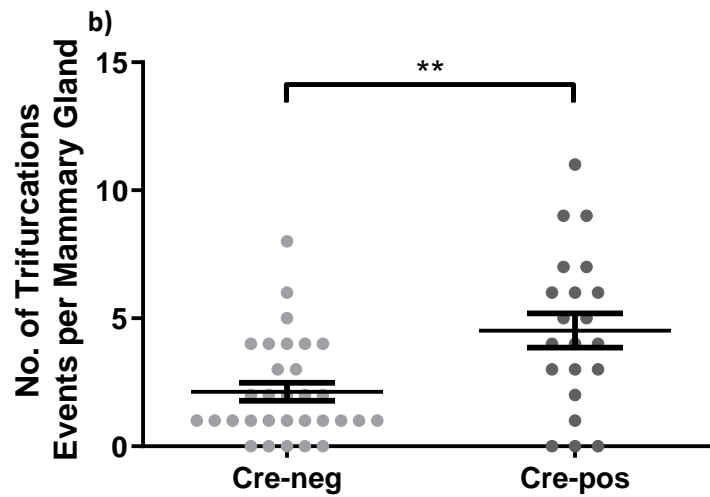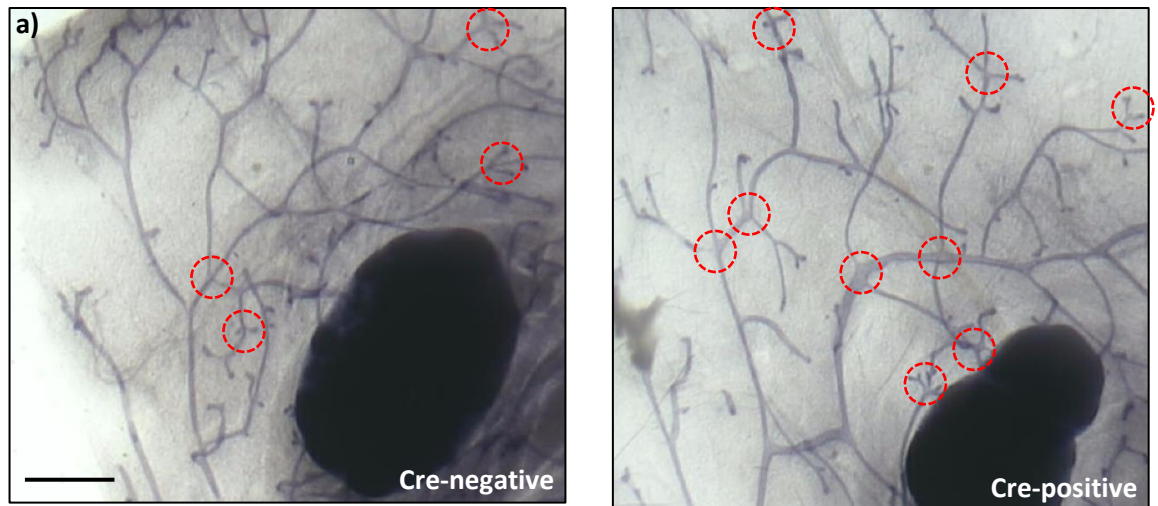
Figure 4.6 Trifurcation events take place more frequently in the mammary gland when when endothelial integrin-α5, integrin-β3 and neuropilin-1 are depleted. Cre-positive and Cre-negative animals underwent Tamoxifen-induced Cre-recombinase activation following the pubertal Tamoxifen regimen described in section 3.2.Total trifurcation events were quantified from WGS images. **a)** Representative WGS images of mammary glands with points of trifurcation highlighted (red rings). **b)** Quantification of trifurcation events in Cre-negative and Cre-positive mammary glands. N=11, Cre-negative n=31, Cre-positive n=21. Scale bar = 1mm. Error bars = ±SEM. (** = P<0.01).

Investigating regions of bifurcation and trifurcation at a structural level was achieved through H&E staining (section 2.7.3). Serial sections of Cre-negative and Cre-positive glands were collected in their entirety and stained, enabling clear visualisation of epithelium undergoing bifurcation and trifurcation (**Figure 4.7**). Despite the typical TEB structure being infrequent, reminiscent of the observation made in the WGS images, points of bifurcation were discernible based upon their known location, the end of epithelium, alluding to the location of TEBs. Close examination of these areas confirmed their identity as TEBs, exhibiting bifurcation or trifurcation whilst showing no abnormalities in terms of structure (**Figure 4.7a-b**). Clearly visible were the cap cells followed by a larger layer of cells, the body cells, trailed further by the luminal and myoepithelial cells (**Figure 4.7a**). Additionally, we were successful in identifying trifurcation events in both Cre-negative and Cre-positive glands, both of which exhibited normal structure as observed in normal bifurcation events (**Figure 4.7c-d**).
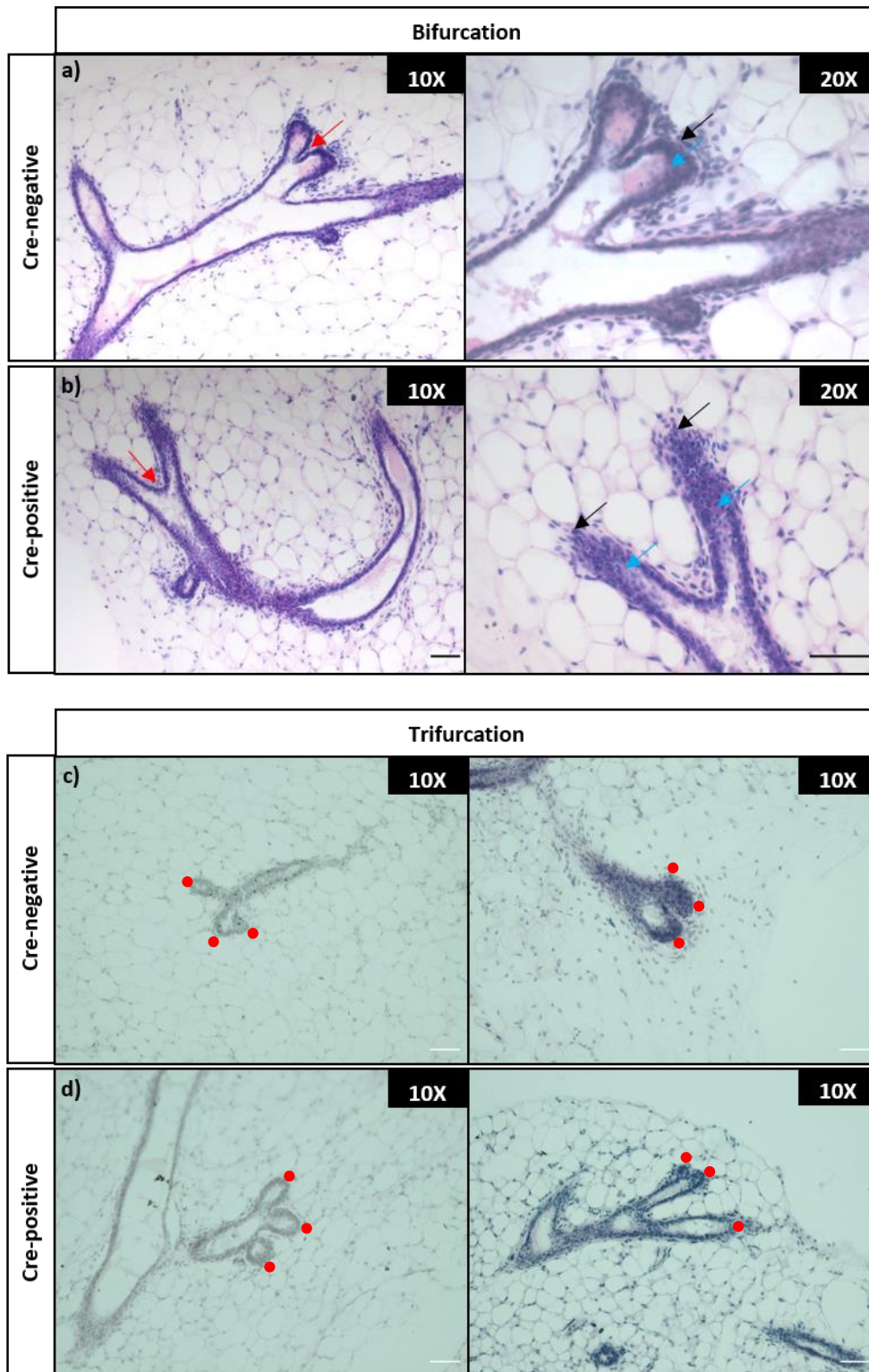
Figure 4.7 H&E staining shows terminal end bud (TEB) structure is unaffected when endothelial integrin-α5, integrin-β3 and neuropilin-1 are depleted. Cre-negative and Cre-positive mice underwent Tamoxifen-induced Cre-recombinase activation following the pubertal Tamoxifen regime, whole mammary glands were paraffin embedded and serial sectioned at 10μm before H&E staining. **a)** Top panel – representative images of Cre-negative epithelium undergoing bifurcation (red arrows), cap cells (black arrows) and body cells (blue arrows). **b)** Bottom panel – representative images of Cre-positive epithelium undergoing bifurcation (red arrows), cap cells (black arrows) and body cells (blue arrows). **c)** Top panel – representative images of Cre-negative epithelium undergoing trifurcation. **d)** Bottom panel – representative images of Cre-positive epithelium undergoing trifurcation. Red dots indicate the heads of trifurcation. N=2, Cre-negative n=3, Cre-positive n=3. Scale bar(s) = 100μm.

4.3   Discussion

Angiogenesis is a fundamental process throughout embryogenesis and postnatal development [309]. Besides allometric growth, angiogenesis also occurs to supplement developing tissues, e.g. the retina, and to accommodate new biological functions, e.g. pregnancy, when a demand for oxygen and nutrients is not being met [310,311]. This chapter sought to determine the role, if any, angiogenesis plays during the process of epithelial growth in the murine mammary gland during pubertal development. Through targeted co-depletion of endothelial integrin-β3, integrin-α5 and neuropilin-1, we sought to impair angiogenesis *in vivo*, during puberty (section 3.2). Previous work in our lab, utilising the retinal angiogenesis assay, has demonstrated their collective depletion elicits a potent anti-angiogenic effect (unpublished – Robert Johnson, Thesis, 2019). In addition, tumour studies performed by our lab utilising this same combination of target depletion leads to a significant reduction in tumour volume and weight. Together, this indicates co-depletion of these targets effectively impairs both physiological and pathological angiogenesis (unpublished – Robert Johnson, Thesis, 2019, and see section 6). All in all, given epithelial growth during pubertal development is a rapid process, that undoubtedly requires a steady supply of oxygen and nutrients, I was keen to explore the effects that impairing the process of angiogenesis, using this combination of target depletion, would have on the developing mammary gland.

To address whether the collective removal of these molecules affected epithelial development I quantified the growth of the epithelium from a range of perspectives. Specifically, I measured: epithelial outgrowth, epithelial extension, epithelial density, number of branch points, number of TEBs, number of trifurcation events and TEB structure. To my surprise, and in stark contrast to my initial hypothesis that impeding angiogenesis would impair epithelial morphogenesis, there was little change in morphogenesis when endothelial integrin-β3, integrin-α5 and neuropilin-1 were co-depleted. Only two of the parameters measured showed any significant change when comparing Cre-positive (angiogenesis impaired) to Cre-negative (normal angiogenesis) animals: maximum epithelial growth at the top edge of the lymph node and the number of trifurcation events. Even here, I felt the differences were relatively subtle. The mean trifurcation events were 2.1 and 4.5 and mean distance from the top edge (above) of the lymph node were 3.2 and 4.4 mm, when comparing Cre-negative and Cre-positive glands, respectively. There are three easy explanations for the lack of a phenotype at this developmental stage of the gland, which I see as being related to the EC proteins we chose to disrupt: (1) I have not impaired angiogenesis as expected (i.e. the Tamoxifen regimen did not work in the mammary gland); (2) epithelial outgrowth at this stage does not require what is considered classical angiogenesis; and (3) angiogenesis in the mammary gland is not driven by the VEGF pathway, meaning I chose the wrong EC targets to impede angiogenesis

and/or cross-talk between the vasculature and the epithelium in the mammary gland. I will discuss each of these possibilities in turn.

Despite our target deletion having previously demonstrated potent anti-angiogenic effects we were unable to demonstrate target deletion in the pubertal, and subsequently pregnancy, studies. However, we were successful in demonstrating target deletion in tumour studies, discussed in section 6. Furthermore, as we were unsuccessful in obtaining a WGS of our TdTomato Cre-reporter at the experimental start and end point of the pubertal studies, we cannot comment on the extent to which Cre was active in the pubertal gland, nor whether the vasculature of the pubertal gland was formed at experimental start point. However, we were successful in obtaining this information for proceeding pregnancy experiments (section 5) – Cre activity following our Tamoxifen regimen is near fully active amongst mammary endothelium.

Through the use of corrosion casts, Djonov *et al* showed between 5 and 12 weeks of age that Swiss MORO mouse mammary gland exhibits a slight increase in capillary size and complexity, whilst also noting morphological characteristics of sprouting angiogenesis [161]. However, if we assume that depleting our EC targets during puberty would impair angiogenesis (if it is occurring), we can only conclude that the vasculature required for mammary epithelial morphogenesis is pre-existing throughout the fat pad and not formed during puberty.

Aside from *de novo* vascular formation playing a role in epithelial morphogenesis, there is precedence in the literature to suggest that signal from the endothelium are essential for tissue/organ formation (coined angiocrine signalling) [312]. For example, Barry *et al*. recently deciphered a complex interplay between kidney vascularisation and gross kidney development. Utilising bulk and single RNA-seq they managed to identify six unique vessel types within the kidney. In addition, they also noted several unique gene signatures within kidney vasculature all of which became robustly expressed upon birth, with loss of function experiments demonstrating their tissue specific importance. The group hypothesise that this post-birth shift in gene expression could be related to physiological load not previously experienced by the kidney whilst *in utero*, a concept that is supported by noting that transport proteins essential for kidney function are not expressed until after birth [313]. Relating this field of study to the results of this section, it seems feasible to suggest that angiocrine signalling between the native vasculature of the mammary gland and the mammary epithelium is a driving force in propagating epithelial expansion during puberty, but the EC molecules we have chosen to deplete are not involved in the angiocrine signalling that is taking place. Literature, and our own findings discussed later in this thesis, point to hormonal cues, specifically progesterone, as a potential mechanism by which the vasculature of the mammary

gland is modulated; in part supporting the angiocrine theory given the tissue specific response of the mammary vasculature. Although debated, literature exists for progesterone being both pro- and anti-angiogenic, however this will be discussed in greater detail in chapter 7 [273,314–319].

5 Maturation and alveologenesis of the mammary epithelium during pregnancy is moderately reduced when angiogenesis is impaired, but lactation and involution appear unaffected

The mammary gland is a unique organ in the way it demonstrates post-embryonic feats of rapid proliferation, functional differentiation, milk production and organised cell regression (involution), with the ability to repeat the cycle over multiple times. Pregnancy is the ultimate phase of the mammary lifecycle, exhibiting all the aforementioned processes, and in the case of the mouse, in a relatively small timeframe. Given the massive changes in epithelial growth and restructuring that occur, it seems rational to propose that angiogenesis and/or vascular remodelling would occur alongside; especially since epithelial activity during pregnancy is even greater than during puberty. Supporting this proposal, corrosion cast data collected by Matsumoto *et al.* detected an increase in capillary number, density and ramification during pregnancy [320]. Therefore, although epithelial outgrowth during pubertal development was unaffected by impeding angiogenesis, we hypothesised that the increased metabolic state of epithelium during pregnancy would be dependent on sufficient angiogenesis, specifically VEGF driven; expression of VEGFs and VEGFRs have been detected in the virgin gland with a marked increase in expression during pregnancy [321]. To test this hypothesis, I assessed the maturation of the mammary epithelium at two timepoints during pregnancy, E10.5 and E15.5, one timepoint during lactation (P2) and one timepoint at which involution was induced (P10+48hours).

Between E0.5 and E10.5 the mammary gland undergoes rapid epithelial expansion through means of secondary and tertiary branching. From E10.5 up until birth the mammary gland transitions from epithelial maturation to alveologenesis; the formation of bud-like structures referred to as alveoli (lobuloalveolar) which encompass the side-branches [306,322,323]. E10.5 and E15.5 coincide with the two major phases of epithelial growth, thus I decided to examine phenotypic consequences of impeding angiogenesis at these two time points.

5.1 Epithelial maturation during mid-gestation (E10.5) is unaffected by angiogenic impairment however embryo weight is significantly reduced

The triple GEMMs used for E10.5 pregnancy studies received the same Tamoxifen regimen that was used for the induction of Cre in the developmental studies; at a body weight of 15g, animals received three injections of Tamoxifen, once every other day (**Figure 3.4b**). Post Cre-induction, animals were left to age for a further 8 weeks to accommodate for any stunting in epithelial growth caused by the Tamoxifen administration (Tamoxifen toxicity) (previously discussed – section 3.2). At 8 weeks post injection, female triple GEMM mice were paired with triple GEMM males in the evening followed by unpairing and plug checking in the morning; evidence of a plug was considered E0.5 and the female(s) were weighed to track weight gain as a positive indicator of pregnancy [324]. Upon reaching mid-gestation, E10.5, the female(s) were sacrificed, and the number four glands were harvested, fixed and WGS was performed (see section 2.7). Of note, the embryos at this timepoint were collected (placenta included), counted and weighed. Interestingly, despite no significant difference observed in the number of embryos in the Cre-positive females when compared to Cre-negative females, the weight of the embryos was significantly different (**Figure 5.1a-b**). The glands that underwent WGS allowed clear visual discernment of the epithelium (**Figure 5.1c-d**). Casual visual examination of images suggested that some areas within the fat pad of Cre-positive glands exhibited lower epithelial density compared to Cre-negative glands (**Figure 5.1c-d**). Quantification was then performed on the epithelium directly adjacent to the lymph node. This region was chosen to allow a consistent point in which the epithelium could be measured across all E10.5 glands (**supplementary Figure 9.4**). Whilst the overall measured mean difference between Cre-negative and Cre-positive glands supported the visual observations, it did not reach statistical significance (**Figure 5.1e**).

Whilst not wanting to fall into a trap of believing a "trend" that is not supported by statistical analysis is meaningful, in this particular instance I felt that the quantification of the epithelial density near the lymph node did not reflect the overall picture of what I was observing across the entire gland. I felt that perhaps by measuring the epithelial density across the entire WGS, I might achieve a better reflection of what I was observing. However, having attempted to utilise ImageJ numerous times to automate epithelial quantification to no avail (at all stages of development), and with the density of the epithelium too great at E10.5 to reliably execute manual quantification, entire gland quantification was unachievable – see **supplementary Figure 9.5** for all E10.5 gland images. Thus, I conclude that impeding angiogenesis impairs epithelial outgrowth in the mammary gland during the early stages of pregnancy, but I cannot yet support that statement mathematically.
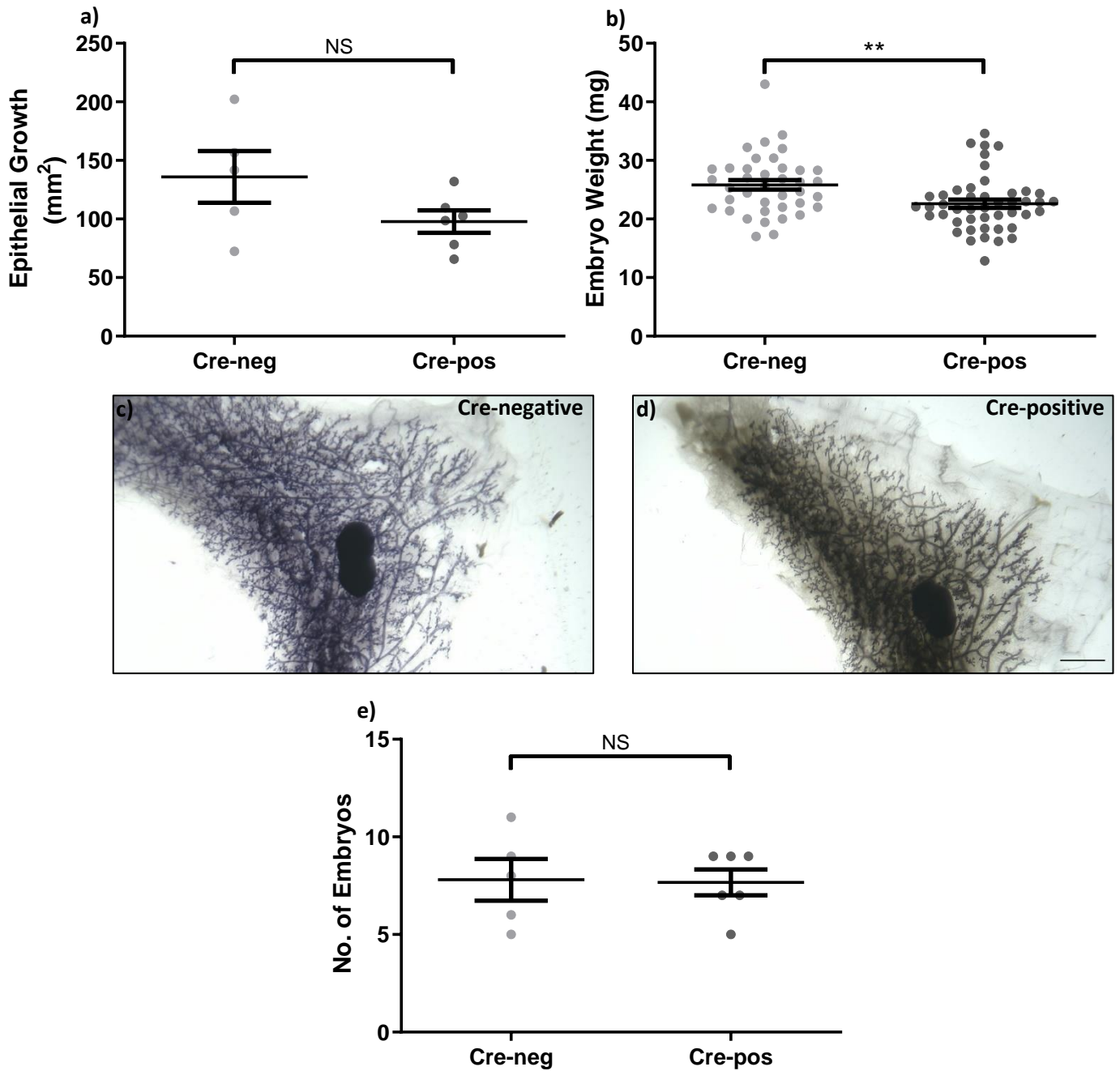
Figure 5.1 E10.5 embryonic weight is significantly reduced, and embryonic number and epithelial maturation are (statistically) unaffected when endothelial integrin-α5, integrin-β3 and neuropilin-1 are depleted. Cre-negative and Cre-positive females underwent Tamoxifen-induced Cre-recombinase activation following the pregnancy Tamoxifen regimen described in section 3.2. **a)** Number of embryos present at E10.5. **b)** Embryo weights at E10.5 (P=0.0033). **c-d)** Representative images of E10.5 whole gland stained number four mammary glands. **e)** Quantification of epithelial growth on both sides of the lymph node. Cre-negative, N=5. Cre-positive, N=6. Embryos: Cre-negative, n=39 and Cre-positive n=46. Scale bar = 2mm. Error bars = ±SEM. (** = P<0.01).

5.2 Epithelial maturation during late gestation (E15.5) is unaffected by angiogenic impediment through the co-depletion of endothelial integrin-β3, integrin-α5, and neuropilin-1

Encouraged by my observations in the E10.5 mammary gland, I proceeded to explore the same parameters at a later stage of pregnancy, E15.5. As mentioned above, I chose this stage of pregnancy because it serves as a transition point between the final stages of epithelial maturation and alveologenesis within the gland. Alveologenesis primes the mammary gland for lactation. During this stage of pregnancy, epithelial growth and side-branching quiesces and proliferative cells within newly formed side-branches generate alveolar buds which mature, through cleavage and differentiation, into alveoli [306]. Furthermore, the period of time between E10.5 and E15.5 is approximately a quarter of the entire gestation period; five days. I considered this time difference sufficient to explore whether the phenotype observed at E10.5 persisted, and/or was augmented, without the gland becoming entirely saturated with alveoli, which I thought might make quantification even more difficult than it already was.

Finally, E15.5 was also chosen because of difficulties I had early on in my pregnancy studies with achieving successful timed mating in Cre-positive animals. When I began studying the mammary gland at E10.5, I was finding it very difficult to obtain Cre-positive females that were carrying any pups when they were harvested at E10.5. I began to question whether this lack of success stemmed from a lack of a proper angiogenic response in the placenta, resulting in the inability to support embryo growth. In later months, I was able to implement a modified timed mating scheme (proposed by technicians in our animal facility) which alleviated this problem, but by this time I had already (fortuitously) begun to explore the placentas of E15.5 animals (see section 5.3).

As in E10.5 pregnancy studies, Cre-negative and Cre-positive animals were treated with Tamoxifen as described in section 3.2, and at E15.5 the number four glands were harvested, fixed and processed for WGS (section 2.7). As well as the mammary glands, embryos and placentas from these animals were collected, weighed, the uterine position of embryos recorded, and any reabsorption events were documented along with their respective uterine locations (**Figure 5.2**); at this timepoint the placenta can easily be separated from the embryo and subsequently fixed in 4% PFA overnight and stored in 70% ethanol until further processed (see section 5.3 below). All of these parameters measured yielded no significant difference in Cre-positive animals when compared to Cre-negative (**Figure 5.2**); between E10.5 and E15.5 a loss in significance in embryo weight was observed.
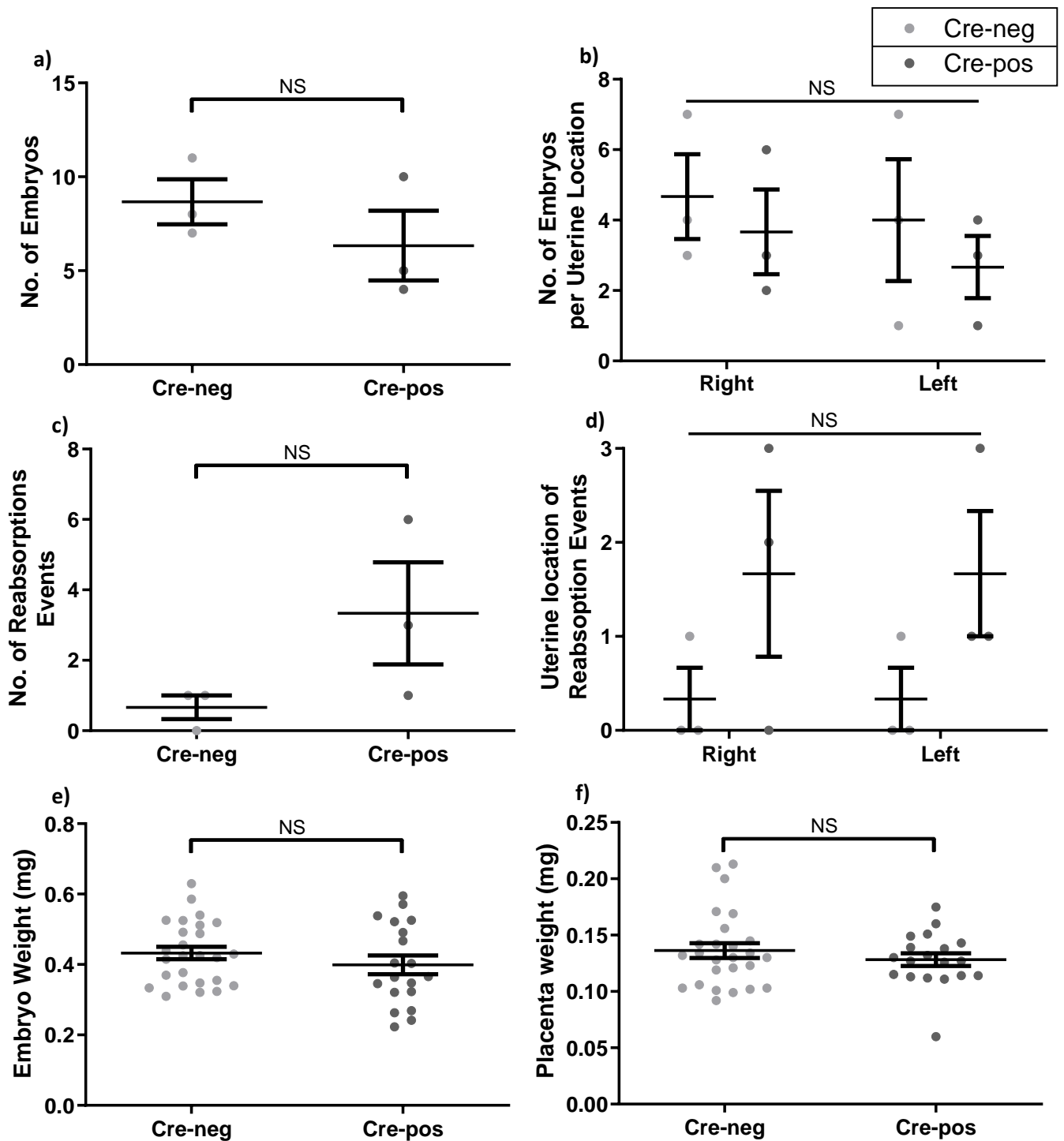
Figure 5.2 Number of embryos, embryonic weight, placental weight, uterine line position, number of reabsorption events and location of reabsorption events at E15.5 are when endothelial integrin-α5, integrin-β3 and neuropilin-1 are depleted. Cre-negative and Cre-positive female mice underwent Tamoxifen-induced Cre-recombinase activation following the pregnancy Tamoxifen regimen as described in section 3.2. **a)** Total number of embryos present at E15.5. **b)** Number of embryos per uterine line. **c)** Total number of reabsorption events observed. **d)** Number of reabsorption events per uterine line. **e)** Embryo weight at E15.5. **f)** Placental weight at E15.5. Cre-negative, N=3. Cre-positive, N=3.Embryos: Cre-negative, n=26 and Cre-positive, n=19. Error bars = ±SEM.

At E15.5 the mammary gland is saturated with epithelium beyond that of the E10.5 gland and begins to saturate the fat pad further by the addition of alveoli through alveologenesis, taking place on secondary and tertiary epithelia, in preparation for postpartum milk production. Having quantified the epithelium of the E10.5 WGSs, we sought to stain and quantify glands collected from E15.5. However, the level of epithelial density at E15.5 rendered manual quantification impossible, and automated quantification was not considered given the inability of the method to yield representative epithelial masks of developmental glands which provided fewer, yet more distinct, epithelia. Aside from this drawback to quantifying the WGSs, wholistic examination of E15.5 WGS yielded no grossly obvious differences in the epithelia of the Cre-positive glands when compared to Cre-negative (**Figure 5.3**).
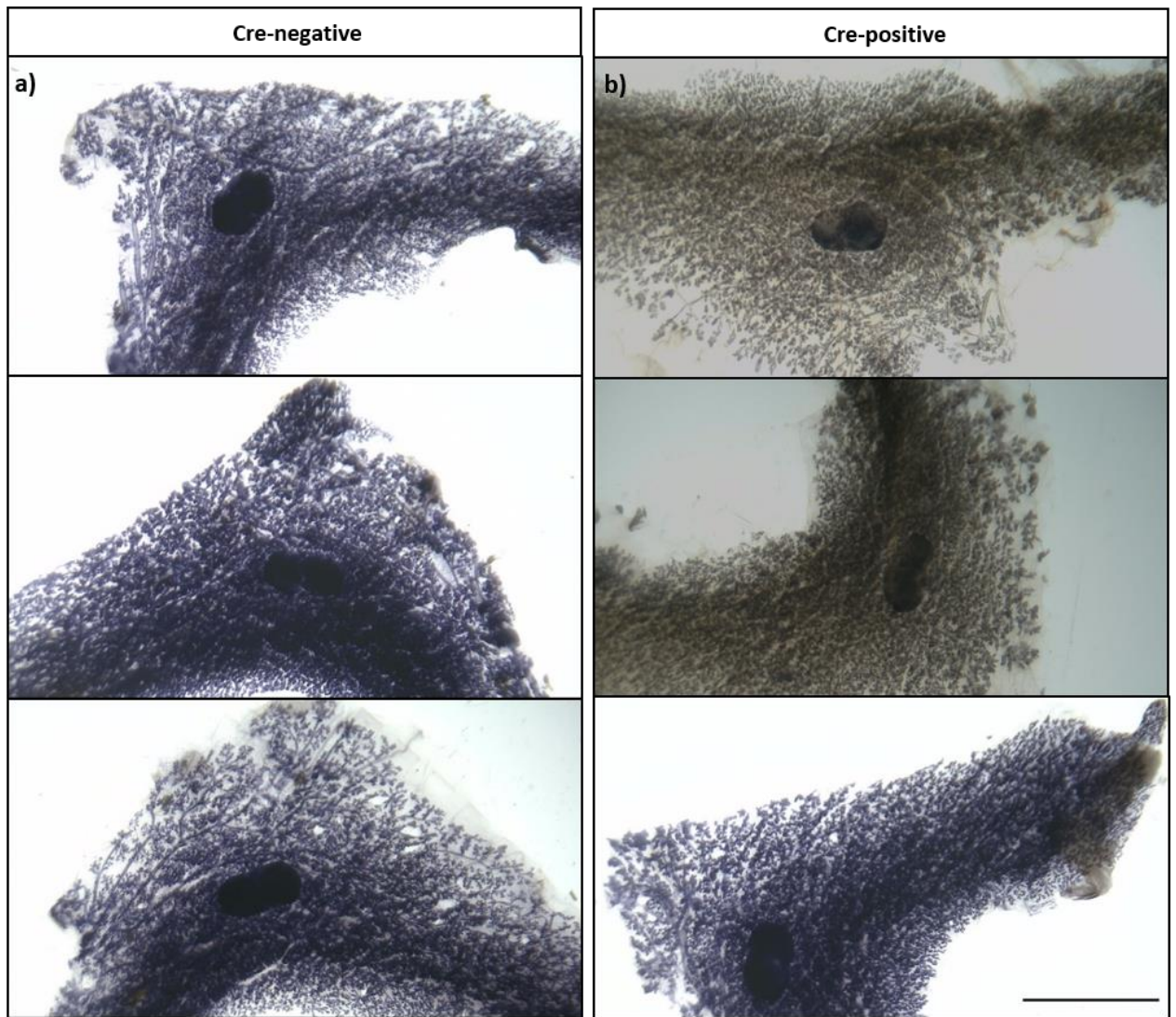
Figure 5.3 Epithelial development at E15.5 is unaffected when endothelial integrin-α5, integrin-β3 and neuropilin-1 are depleted. Cre-negative and Cre-positive female mice underwent Tamoxifen-induced Cre-recombinase activation following the pregnancy Tamoxifen regimen as described in chapter 3.2. Cre-negative, N=3. Cre-positive, N=3. Scale bar = 5mm.

5.3 The junctional zone of the placenta is larger when endothelial integrin-β3, integrin-α5, and neuropilin-1 are co-depleted

The placenta is an organ which brings together embryo and mother, allowing their interaction and function, permitting nutrient supply and subsequently embryo growth, whilst preventing tissue rejection; development of the placenta is paramount to successful gestation [325]. Intrauterine Growth Restriction (IUGR) is a common problem that can occur during pregnancy, often stemming from defects/failure of the placenta. This disorder manifests in foetuses being stillborn, premature birth and lifelong risk of adverse health (i.e. poor neurological development and immune deficiencies) [239]. As mentioned, my initial attempt at timed mating for the E10.5 experiments proved difficult, vaginal plugs were infrequently found and when they were, they rarely resulted in a successful pregnancy; I was unable to track abortion therefore I cannot comment on whether litters were lost pre-term. As such, alongside the mammary gland, I proceeded to explore placental development at E15.5. I reached out to Amanda Sferruzzi-Perri (Cambridge University), and started a collaboration with Jorge Lopez-Tello, a postdoctoral researcher in her lab.

Placentas from the embryos of E15.5 mice underwent stereology. Two placentas per litter, based on mean placental weights, were chosen. Analysis was performed on three sagittal sections, non-adjacent and evenly spaced by 200µm. Subsequent analysis was performed using the Image J Grid tool to quantify the regions of the placentas (section 2.8). Despite the weight of Cre-positive placentas showing no significant difference when compared to Cre-negative placentas (**Figure 5.2f**), the quantification of placental regions, the decidua (DB), junctional zone (JZ) and labyrinth (LZ), revealed something interesting. The DB and LZ are comparable between Cre-positive and Cre-negative (**Figure 5.3a and c**). However, the JZ was significantly larger in Cre-positive placentas when compared to Cre-negative (**Figure 5.3b**). This finding was unexpected given the roles of these regions, specifically the JZ and the LZ. The LZ is the vascular region of the placenta, vital for physically connecting the embryo to the uterine wall whilst also permitting the exchange of nutrients and gas between mother and embryo [326]. As such, I hypothesised if a region of the placenta were to show alteration in response to a lack of maternal angiogenesis this would be the region; it might increase in size to compensate the uterine wall failing to sufficiently vascularise to permit nutrient and gas exchange. To my surprise, instead I observed changes in the JZ, the endocrinal powerhouse of the placenta.

The JZ produces hormones, growth factors and cytokines which collectively perpetuate normal pregnancy by modulating the physiology of both mother and foetus [239]. Given the normality of the pups, one would assume fetoplacental growth and placental efficiency were unaltered through the deletion of my EC targets, and as such the mouse work to explore this phenotype halted. However, I pursued an understanding of this phenotype *in vitro,* utilising mammary and lung ECs, in a bid to explore whether hormonal response of the endothelium in the mammary gland was aiding in normalising angiogenesis following target deletion, and whether any response was specific to mammary endothelium. This work is discussed in section 6.1.
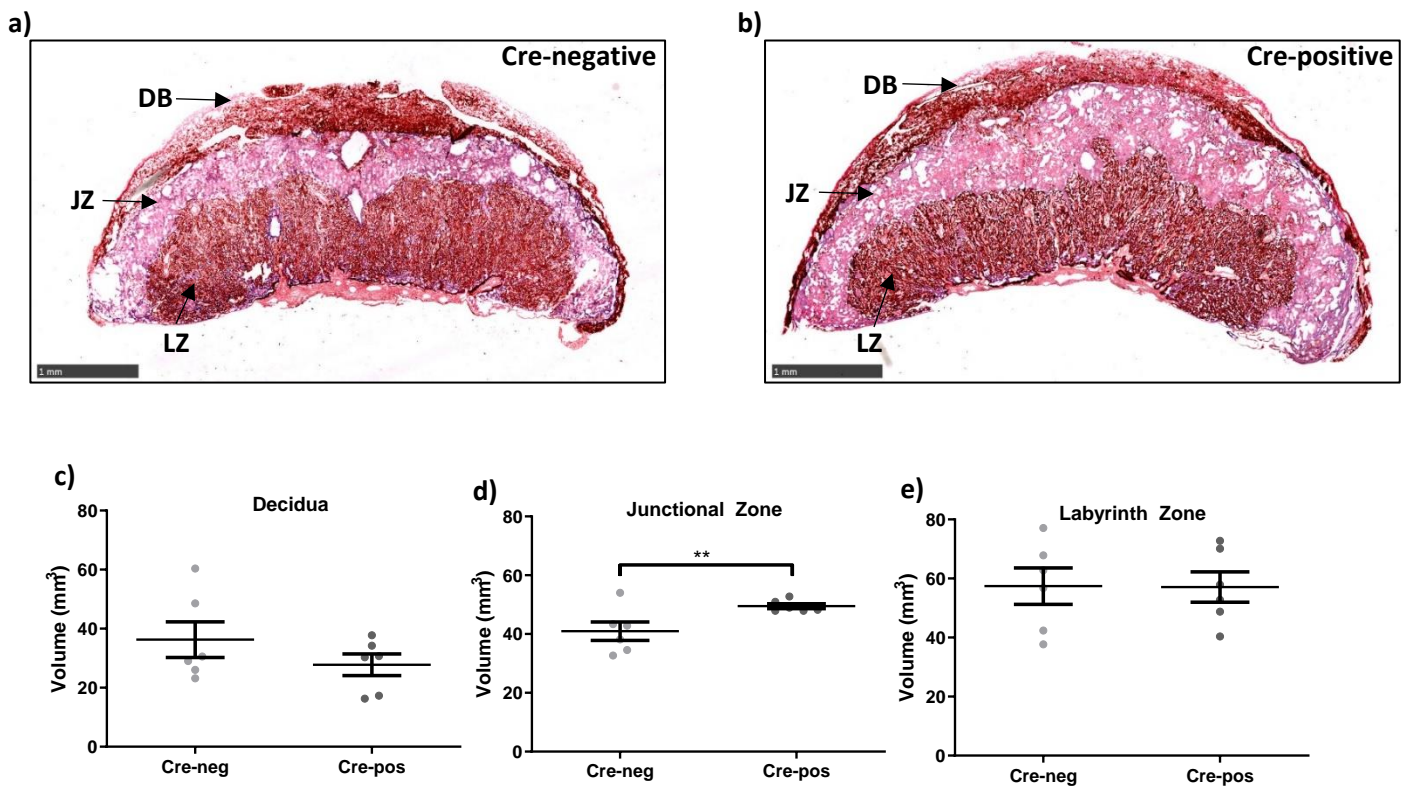
Figure 5.4 The volume of the junctional zone (JZ) is significantly increased, at E15.5, when endothelial integrin-α5, integrin-β3 and neuropilin-1 are depleted. Cre-negative and Cre-positive female mice underwent Tamoxifen-induced Cre-recombinase activation following the pregnancy Tamoxifen regimen as described in chapter 3. Following timed-mating, placentas were collected at E15.5. **a)** Representative image of Cre-negative placenta. **b)** Representative image of Cre-positive placenta. Volume of the decidua (DB) **(c)**, junctional zone (JZ) **(d)** and labyrinth (LZ) **(e)** compared to Cre-negative counterparts. Cre-negative, N=3. Cre-positive, N=3. Scale bar = 1mm. Error bars = ±SEM. (* = P<0.05).

5.4 Lactation (P2) and involution (P12) were not affected by the depletion of integrin-β3, integrin-α5, and neuropilin-1

To come full circle in my endeavour to explore the role of angiogenesis in the lifecycle of the mammary gland, I proceeded to investigate lactation, at P2, and involution, at P12. I chose P2 as a timepoint for lactation for two reasons. Firstly, P2 is soon after the gland has transitioned from alveologenesis to lactation, making it an ideal timepoint to explore whether the gland is functional; pups will have gained a small amount of weight and will have milk present in their stomachs. Secondly, exploring an early timepoint reduces the possibility for a phenotype to be missed, be it by the epithelium recovering as lactation persists, or being visually undiscernible come later days of lactation as alveoli become engorged with milk, and thus opaque.

5.4.1 The epithelium of the mammary gland during lactation (P2) and involution (P12) by the depletion of integrin-β3, integrin-α5, and neuropilin-1 resembles that of the Cre-negative

Cre-negative and Cre-positive females underwent the experimental regimen discussed in section 5.1 and were sacrificed at P2. Following sacrifice, the number four glands were harvested, fixed and processed for WGS. Visual examination of the glands at P2 revealed no gross morphological changes in the epithelium when comparing the two genotypes (**Figure 5.5**). Equally, WGS images of the gland at P12 revealed no gross morphological changes in the epithelium (**Figure 5.6**) – for entire gland images of both experimental timepoints see **supplementary Figure 9.6 and 9.7**.

Unfortunately, glands at these two timepoints were difficult to collect. More often than not, animals which were gaining weight or visually pregnant seemingly aborted/lost their pups as litters were not found. Similarly, litters were sometimes found dead upon birth or were consumed prior to one of the two timepoints being reached. Without surmountable evidence it is very difficult to comment on the cause, although we did not observe this as a trend in Cre-positive animals therefore it is unlikely to be a phenotype arising from target depletion. Other factors may have contributed to this outcome. It is not uncommon for first litters to be lost, whether loss is through poor practice on the mothers part, behavioural changes postpartum, or due to infanticide which is not largely understood [327,328]. Furthermore, some of the females being bred were older than would be advisable by best breeding practice (a result of Covid-19 lockdown); a diminished economic breeding life could impede successful mating. Lastly, as an overarching consequence of the factors discussed, extrapolating data from the pups that were successfully weaned may vary. The ability of the mother to produce milk is thought to correlate with the number of pups, which is

subsequently thought to diminish to reduce in utero competition to avoid recombination events resulting in abnormalities [329–331]. Taken collectively many of these factors may explain the difficulty I had in obtaining sufficient data to fully discuss the effects of angiogenesis on the murine mammary gland during lactation and involution.

Cre-negative	Cre-positive
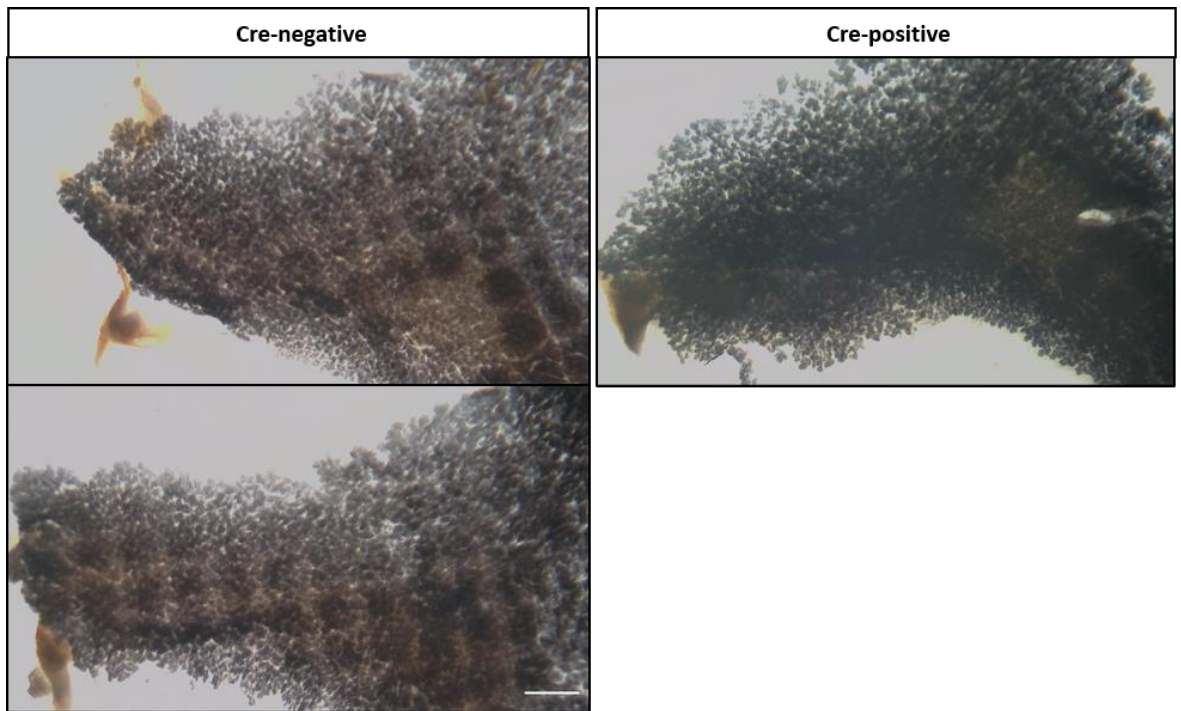
Figure 5.5 Epithelial density is unaffected during lactation (P2) when endothelial integrin-α5, integrin-β3 and neuropilin-1 are depleted. Cre-negative and Cre-positive female mice underwent Tamoxifen-induced Cre-recombinase activation following the pregnancy Tamoxifen regimen as described in chapter 3.2. **a)** Cre-negative mammary glands. **b)** Cre-positive mammary gland. Cre-negative, N=2. Cre-positive, N=1. Scale bar = 2mm.

Cre-negative	Cre-positive
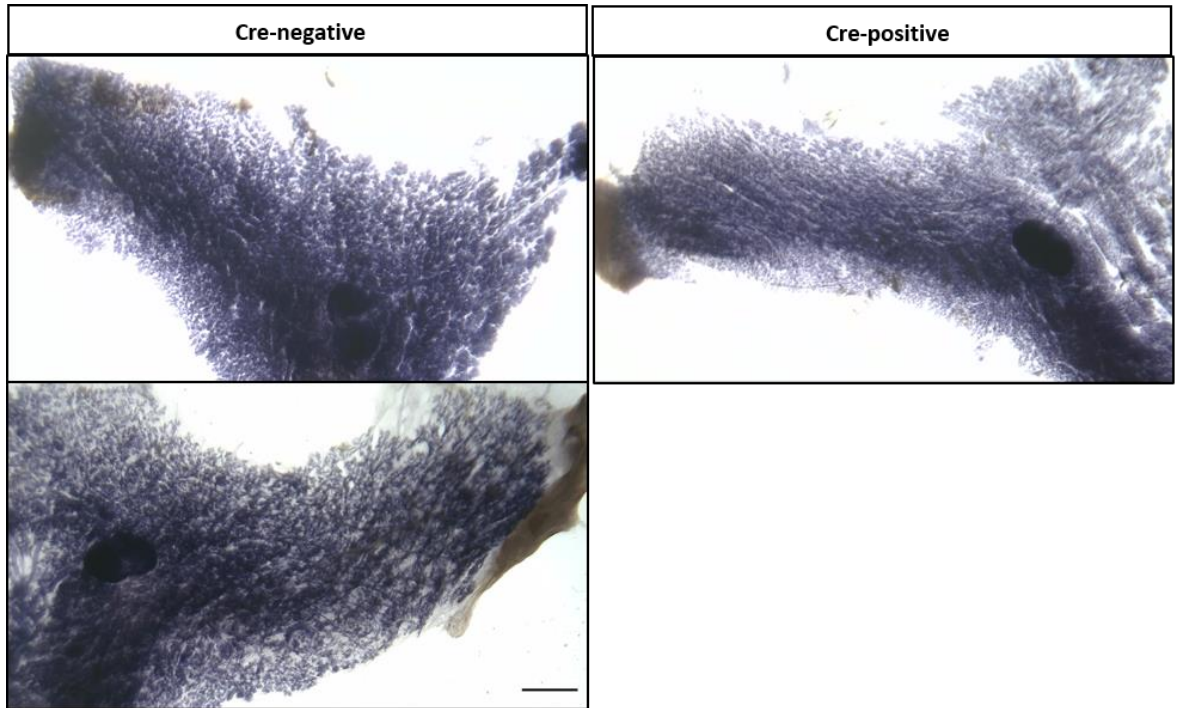
Figure 5.6 Epithelial density is unaffected during involution (P12) when endothelial integrin-α5, integrin-β3 and neuropilin-1 are depleted. Cre-negative and Cre-positive female mice underwent Tamoxifen-induced Cre-recombinase activation following the pregnancy Tamoxifen regimen as described in chapter 3.2. **a)** Cre-negative mammary glands. **b)** Cre-positive mammary gland. Cre-negative N=2, Cre-positive N=1. Scale bar = 2mm.

5.5 Discussion

The lifecycle of the murine mammary gland begins during embryogenesis and completes once the virgin gland has successfully nurtured offspring and returned to its pre-pregnancy state. Having assessed the role of angiogenesis in the developing gland in the previous chapter, this chapter sought to address the role of angiogenesis in the mammary gland during pregnancy, E10.5 and E15.5 through to lactation, P2, and ultimately involution, P12. Angiogenesis is vital in permitting tissues and organs sufficient gas exchange and nutrient access, specifically where rapid growth or development is occurring. As with pubertal development, the demand for oxygen and nutrients increases throughout pregnancy to accommodate epithelial maturation and alveologenesis, and in pre-emption to support the generation of milk during lactation. Furthermore, it has been documented that during pregnancy, concomitant with epithelial expansion and morphogenesis, the vasculature of the mammary gland also undergoes rapid expansion, ramification and anastomosis to increase vascular density, in turn increasing oxygen and nutrient supply [161]. Given this, combined with evidence demonstrating an increased expression of VEGFs during pregnancy, modulating angiogenesis throughout pregnancy using our model has the potential to elicit potent angiogenic effects on the maturation of the mammary gland [321].

To assess the role of our pro-angiogenic targets in the maturation of the mammary gland, we examined the epithelium of E10.5 and E15.5 mammary glands. Accompanying this we also measured and recorded the number, and weight, of embryos present per pregnant female, with the position in the uterine line also recorded for E15.5 embryos – discussed later. Gross observation of WGS images from E10.5 glands suggested epithelial maturation (e.g. epithelial density) of Cre-positive glands was decreased compared to Cre-negative glands. However, manual quantification of the epithelium flanking the lymph node of E10.5 glands indicated there was no significant differences in the density of epithelium when comparing the two genotypes, though the caveats associated with this analysis have been discussed above. For the sake of further discussion, and until a better method of quantification can be devised (one where the entire epithelial tree can be measured), I will assume there is a small change in epithelial density in the E10.5 mammary gland when angiogenesis is disrupted by EC depletion of integrin-β3, integrin-α5, and neuropilin-1. As mentioned previously, Djonov *et al*. (2001) demonstrated angiogenesis to be active during pregnancy by noting an increase in vascular density throughout [161]. Therefore, although my findings are not as robust as might be expected given the extent to which Djonov *et al*. noted a change in vasculature, my findings do suggest that angiogenesis is required for mammary epithelial morphogenesis during pregnancy. The lack of a more robust phenotype lends weight to the idea (as proposed in section 4.2) that perhaps angiogenesis in the mammary gland is not primarily driven

by the EC targets we have chosen to deplete, targets we know to mediate VEGF-driven migration responses [114,254,255]. Whatever changes in epithelial growth I observed at E10.5, they were gone by E15.5. Also gone was the significant reduction in embryo weight that was observed at E10.5. Both observations suggest some sort of compensatory mechanism in Cre-positive animals kicks in between E10.5 and E15.5 that allows mammary and embryo development to overcome an early delay. A likely mechanism is signals coming from the placenta.

The exploration of the placenta was originally conceived through the difficulty in successfully time-mating our Cre-positive females. I hypothesised this difficulty was a consequence of embryos failing to develop due to a lack of maternal angiogenesis, specifically affecting the development of the placenta. Whilst the uterus undergoes rapid neovascularisation early on during embryo implantation, a subset of uterine stromal cells proliferate and differentiate, forming the decidua. Maternally derived, the decidua becomes the first vascular interface between mother and embryo – vital for embryo survival and pregnancy success. Interestingly, although somewhat debated, the process of decidual angiogenesis is driven by VEGF-A, regulated by the steroid hormones progesterone and estrogen [315,316,332]. Indeed, I noted decreased embryo weights at E10.5 (**Figure 5.1b**), suggesting that defects in decidual angiogenesis, if present, might retard early embryonic development. To date, I have not had time to revisit placental analyses at E10.5. However, examination of the placentas from E15.5 females shows no significant difference in the decidua region of the placenta in Cre-positive mothers, compared to Cre-negative mothers. At E9.5 in mice the formation of the labyrinth begins [239]. The labyrinth proceeds the role of the decidua as the fetal-maternal interface that will orchestrate oxygen and nutrient supply. Being foetal-derived, the labyrinths in both Cre-positive and Cre-negative mothers is derived from wild-type embryos – although the embryos may express Cre-recombinase, an absence of Tamoxifen renders the Cre inactive and thus embryos express all floxed targets. Given our phenotype of embryo weight is lost by E15.5, a timepoint at which the labyrinth is mature and has taken over the decidua's vascular interface role, it could be speculated that this shift from a potentially under vascularised decidua to an embryo-derived labyrinth resolves the lagging embryo development. In fact, the labyrinth at E15.5 does not differ between Cre-positive and Cre-negative, an observation which might support the above conclusions – early defects in maternally derived decidual angiogenesis are overcome by normal embryo-derived labyrinth angiogenesis. Although there is no change in volume, this region could still compensate the decidua by E15.5.

Strikingly, however, the junctional zone (JZ) in the Cre-positive mothers was significantly larger than that of Cre-negative mothers. The JZ is an endocrinal region vital in permitting successful pregnancy through the production of hormones, growth factors and cytokines that regulate pregnancy through modulating mother and embryo physiology [241,333,334]. Like the labyrinth, the JZ is embryo derived. Why would there be a larger JZ in Cre-positive mothers? Does this zone become enlarged in Cre-positive animals to compensate for early defects in placental angiogenesis? Is there increased production of hormones/growth factors in Cre-positive animals that lead to increased angiogenesis, and the loss of the mammary epithelial phenotype observed at E10.5? The timing would certainly coincide with changes in circulating factors produced by the placenta (e.g. increased progesterone production occurs between E10.5 and E15.5 [335]). Further studies are certainly warranted and must occur before I can begin to answer these questions. Nonetheless, chapter 6 explores (at least in part) the idea that MECs derived from Cre-negative and Cre-positive animals are differentially responsive to angiogenic signals, including progesterone.

To backtrack, although there was no significant difference observed in embryo number in Cre-positive compared with Cre-negative at E15.5, there was a near significant increase in the number of reabsorptions in Cre-positive females (P=0.0573). Unfortunately, the practice of recording the position of embryos as well as occurrence of reabsorption events was not implemented until E15.5 experiments when suggested by Jorge as a best practice when exploring fetoplacental growth – E10.5 experiments are lacking this parameter. Despite this, these trends at E15.5 support further the hypothesis that our target deletion is modulating embryo development, such that embryo viability is compromised. Of note, the uterus undergoes profound levels of angiogenesis during pregnancy to supplement the embryo with oxygen and nutrients, prior to the placenta becoming structurally and functionally competent, driven by VEGF-A [336]. Given our model utilises this pathway as a means to impair angiogenesis, this may allude as to why reabsorptions were greater in the Cre-positive mothers.

Glands from lactation and involution experiments were impossible to quantify due to the density of the epithelium at both experimental timepoints. However, as no phenotypic trends were observed in E15.5 glands it is not surprising there is no observable difference in the epithelium at P2 (lactation); discussed previously E15.5 marks the process of alveologenesis where angiogenesis may proceed via intussusception, increasing vascular density around alveoli through basket like modification of existing vessels – independent of VEGF [320,337].

6 Exploring the effects of combinatorial depletion of endothelial integrin-β3, integrin-α5 and neuropilin-1 in the development of breast cancer

Breast cancer (BC) is the most common form of cancer in the United Kingdom, impacting people and societies on financial, emotional and personal levels [338]. Often with disease a strong understanding of its aetiology, development and progression naturally leads to the conception of an effective treatment or treatment strategy. The same is true with BC. Tumour angiogenesis is one of the classic hallmarks of cancer, enabling tumours to grow and ultimately metastasise about the body [95]. Conceptualised and demonstrated over four decades ago, cancer cells infused into vascular regions were able to grow to and exceed a volume of $2mm^3$ by hijacking angiogenesis [339,340]. Conversely, tumour cells situated in avascular regions were restricted to a growth of $2mm^3$, even exhibiting necrosis and becoming apoptotic [341,342]. To no surprise, these early findings triggered a cascade of research into developing anti-angiogenics to mitigate the ability of tumours to grow and spread, with the extended benefit of potentially initiating apoptotic regression – discussed in detail in sections 1.2.2.5 and 1.2.3. Despite the variety of studies demonstrating, and in some cases opposing, the role of certain molecules in the angiogenic response, integrin-β3, integrin-α5 and neuropilin-1 have all been shown to elicit an anti-angiogenic response when inhibited or removed [343,344]. As touched upon in section 1.2.2.5, some studies extrapolate too greatly the implications of their findings, arguably using cancer models lacking in physiological relevance or drug doses beyond human efficacy; subsequent, humanised, studies do not reflect the preliminary findings [26,107].

In a bid to address the final point made above, in conjunction with coming full circle in my studies of the murine mammary gland, I proceeded to explore the effects of our EC targets in an orthotopic model of BC. In line with previous findings from our lab using different (non-breast) cancer models, I hypothesised that depletion of EC integrin-β3, integrin-α5 or neuropilin-1 alone would have minimal effects on tumour growth, but co-depletions would inhibit growth, with the greatest effects seen when all three targets are depleted simultaneously.

6.1 Triad depletion of endothelial integrin-β3, integrin-α5 and neuropilin-1 significantly impairs tumour growth and vascularisation

To begin exploring the angiogenic contribution of endothelial integrin-β3, integrin-α5 and neuropilin-1 in the progression of BC, I chose to investigate the effects of each molecule in singular depletion, dual depletion and triad depletion. This approach allowed me to explore the role of each molecule, individually and in combinations, in modulating tumour angiogenesis. Tumours were allowed to grow for 14 days post-implantation, with collection on day 15; sufficient time for tumours to grow past 1mm in diameter and hijack angiogenesis as a means to enhance growth [95]. Furthermore, to enhance the clinical relevance of this work, in contrast to tumour studies previously performed by the Robinson Lab, we altered the Tamoxifen administration from slow release Tamoxifen pellets (5mg, 21 day release) to thrice weekly I.P. injections of Tamoxifen (75mg/kg Tamoxifen per bodyweight) (Monday, Wednesday and Friday), starting one week prior to tumour cell implantation (**Figure 6.1a**); the Robinson Lab has already demonstrated thrice weekly injections elicits target depletion in another cancer model (unpublished – Robert Johnson, Thesis, 2019). To model BC, we utilised a murine breast carcinoma cell line, B6BO1, isolated from MMTV-PyMT mice (gifted from Dr Katherine Weilbaecher, Washington University, St Louis, MO, USA), known to readily metastasise to lung and bone. Under anaesthesia, 1×10^5 B6BO1 cells were injected into the abdominal, number four, mammary gland of female mice – section 2.4. After 14 days of growth, tumours were harvested at day 15, weighed, measured and volume calculated using the follow formula: (length x width^2) x 0.52 [248]. Given these experiments were conducted across all seven of our GEMM lines, tumour weight and volume from Cre-positive mice were expressed as a percentage of their relative Cre-negative littermates (controls). This data processing step was taken to account for potential genetic background differences of the mice used for each EC depleted strain; that is to say, the GEMMs are on a mixed C57BL/6;129Sv background, and the contribution of each individual strain (C57BL/6 and 129Sv respectively) may vary from GEMM line to GEMM line.

Single depletion of either integrin-β3 or neuropilin-1 did not result in a significant reduction in tumour weight nor volume, corroborating previous findings by our group and others (**Figure 6.1c-d**) [114,345]. Controversially, despite Murphy *et al*. agreeing with our β3 findings, our α5 data does not support their findings, and also contradicts recent findings in our lab utilising the same GEMM with a different cancer model (unpublished) [345]. Instead, results shown here suggest single depletion of integrin-α5 does significantly reduces tumour volume; though this result is caveated by the fact that , due to time constraints, I was unable to complete three experimental repeats for the α5 genotype (**Figure 6.1c-d**). Interestingly, dual depletion (EC-KO**β3/α5**, EC-KO**β3/Nrp1** and EC-KO**α5/Nrp1**) resulted in no significant reduction in tumour weight or volume when compared to their

respective Cre-negative littermates (controls). This is surprising given recent findings by our lab showing that dual depletion, in any combination, markedly deceases tumour weight and volume in other cancer models (**Supplementary Figure 9.12)**. However, triple-depletion of our EC targets (EC-KO$^{\alpha 5/Nrp1/\beta 3}$), showed significant inhibition of BC tumour growth (**Figure 6.1**). This is consistent with findings in other cancer models in the Robinson Lab (**Supplementary Figure 9.12**).

I attempted to confirm target depletion in tumour blood vessels by flow cytometry. Whole tumour homogenates were prepared and stained for two out of three endothelial markers (endomucin, CD31 (PECAM-1) and Cdh5) along with staining for the three molecules, integrin-$\beta 3$, integrin-$\alpha 5$ and neuropilin-1 (section 2.9). Despite my best efforts, I was not able to sufficiently optimise the flowcytometry enough to convince myself that I was uniquely detecting ECs (**Supplementary Figure 9.8, 9.9 and 9.10**). However, I was able to stain for the targets and confirm target deletion in tumour blood vessels (**supplementary Figure 9.11**). In line with modulating angiogenesis, I would expect to see trends reminiscent of the tumour volumes (**Figure 6.1d**) in terms of vascular density – BAN Cre-positive tumours should exhibit significantly fewer blood vessels compared to BAN Cre-negative tumours. Unfortunately, due to time constraints I was unable to quantify the vasculature of the tumours from all the genotypes, however these data shall be available for the defence of this thesis.

a)

Monitor Body Weight Throughout

(8-12 weeks of age)

Week 1 | Week 2 | Week 3 | Week 4

M W F | M W F M W F M T

Tamoxifen Administration
(continued thrice weekly)

B6BO1 Implantation
(Day 8)

Harvest Tumour
(Day 15)

b)

Cre-neg

Cre-pos

EC-KO: β3 α5 Nrp1 β3/α5 β3/Nrp1 α5/Nrp1 β3/α5/Nrp1

c)

% Tumour Weight (relative to Cre-neg controls)

**

Cre-Neg A B N BA AN BN BAN

Target(s) Expressed	β3 α5 Nrp1	β3 Nrp1	α5 Nrp1	β3 α5	Nrp1	α5	β3	-
Effect on Growth	-	-	-	-	-	-	-	↓

d)

% Tumour Volume (relative to Cre-neg controls)

*   **

Cre-Neg A B N BA AN BN BAN

	β3 α5 Nrp1	β3 Nrp1	α5 Nrp1	β3 α5	Nrp1	α5	β3	-
	-	↓	-	-	-	-	-	↓

Figure 6.1 Triad-depletion of integrin-β3, integrin-α5 and neuropilin-1 impairs tumour growth. Female GEMMs of the indicated genotypes were implanted with 1×10^5 B6BO1 breast carcinoma cells, orthotopically into the inguinal mammary gland. **a)** Experimental regimen: Thrice weekly I.P. injections (Monday, Wednesday and Friday) of Tamoxifen (75mg/kg bodyweight) for three weeks, B6BO1 implantation on day 8 (red) post-initial I.P., and tumour harvest on day 15 (red) post-implantation. **b)** Representative images of Cre-negative and Cre-positive B6B01 tumours at day 15. **c)** Tumour weight at day 15 as a percentage of relative Cre-negative littermate controls. **d)** Tumour volume ((length x width^2) x 0.52) at day 15 as a percentage of relative Cre-negative littermate controls. A: N=1, n=13, Others: N=3, Cre status, n≥7. Scale bar = 5mm. Error bars = ±SEM. (* = P<0.05), (** = P<0.01).

6.2   Discussion

Having discussed extensively the targeted approach researchers have taken to prevent angiogenesis as a means of treatment for cancer (section 1.2.2.5) whilst also illustrating the global impact of BC (section 1.3.6), we sought to take a step back and re-assess the potential of pro-angiogenic molecules as a target for preventing/impeding tumour growth. Mentioned previously (section 1.2.2.5), the experimental design, models used, and findings extrapolated do not always lend themselves to success in terms of follow up studies or pre-clinical trials. In line with this, we executed our BC studies using orthotopically implanted, MMTV-PyMT derived, mouse BC cells (section 2.4) to enable physiologically relevant data to be collected and commented on.

Of the single and combinatorial deletion of our targets we only observe a significant reduction in tumour volume in integrin-α5 single (A) depleted, and triple depleted (BAN) tumours (**Figure 6.1d**). We see a similar trend with the weights for these two genotypes, however due to the heterogeneity of tumour tissue and large tumours exhibiting necrotic cores, weight may not always correlate with tumour size (**Figure 6.1c**). To reiterate, the integrin-α5 single depleted experiment is an N of 1, therefore biological repeats in this genotype may see this statistical difference evaporate. However, for the sake of the data presented I shall discuss this result as it is. Previous work by a former PhD student in the lab (Dr Robert Johnson, unpublished) performed in the same GEMMs has elicited different findings. In contrast to the findings I present here, Dr Johnson analysed CMT19T tumours growing subcutaneously and showed that the depletion of two targets in any combination significantly decreased tumour volume (**supplementary Figure 9.12**); both models show the greatest inhibition of tumour growth with simultaneous depletion of all three targets. Why the difference? The cancer model used throughout this work was an orthotopic model of BC implanted into the mammary gland. The other data referred to is a lung carcinoma subcutaneously implanted into the flank. Furthermore, although both studies follow thrice weekly injections, the latter study ran longer (tumours harvested on day 18) and started with a higher baseline of cells per animal ($1x10^6$ as opposed to $1x10^5$). Having noted these two points, it is important to consider that both studies findings are accurate – maybe lung tumours respond robustly to anti-angiogenic treatment compared to breast tumours? This example of disparity between two tumour experiments highlights the short-term differences that can arise when modelling different cancer models in genetically similar mice, not to mention the potential differences which could occur over longer experimental periods or in instances of metastasis.

Integrin-β3, integrin-α5 and neuropilin-1 have all been implemented as targets for anti-angiogenic drug development, having all been shown to exhibit anti-tumorigenic effects when their expression or function is impeded. Our group has previously demonstrated that inhibition of integrin-β3

provides short-term anti-tumorigenic effects with tumours recapitulating wild-type levels of growth, whilst others have shown inhibition to result in enhanced pathological angiogenesis [114,254,346]. Likewise, integrin-α5 was identified as a prime anti-tumorigenic target in mice however these results did not fully translate to clinical trials [347,348]. Studies have also demonstrated the upregulation of neuropilin-1 to be present in primary tumours of both mouse and human, whilst also demonstrating inhibition of neuropilin-1 to markedly decrease tumour angiogenesis and tumour size [150,349]. Despite a multitude of evidence for these three molecules as candidates for anti-tumorigenic therapies, the tumour data presented here does not coincide with these published findings, pre-clinically, but does fit with the lack of benefit observed in clinical trials. Granted, we see a large reduction in tumour volume when all three molecules are depleted, suggesting the presence of one of the three molecule is sufficient to execute tumour angiogenesis. The complementary nature of these findings with regards to the clinical trial failures also attributes the point touched upon in section 1.2.2.5. Physiologically, findings from mouse models can lack relevance in terms of drug dose, tumour model or even study type (e.g. intervention and prevention) owing failure come clinical application.

Furthermore, anti-angiogenic treatment, targeting the VEGF pathway, has proven largely ineffective in the long term survival of BC patients whilst being effective in the treatments of other cancer, such as renal cell carcinoma, colorectal cancer and non-small cell lung cancer [99,350–352]. Given other types of cancer utilise VEGF as a major driver of tumour angiogenesis, and as such respond to VEGF targeted anti-angiogenics, BC was assumed to respond in a similar manner [353]. However, it has been shown that VEGF expression in primary breast tumours compared with contralateral, normal/healthy, breast tissue shows no significant change in VEGF expression [354]. Therefore, whilst BC does exhibit tumour angiogenesis, the pathway through which it achieves vascularisation is seemingly independent of VEGF. Furthermore, studies have demonstrated the use of anti-angiogenics against the VEGF pathway can consequently lead to the upregulation of alternative pro-angiogenic factors, such a basic fibroblast growth factor (bFGF), interleukin-8 and stromal derived factor-1 (SDF-1) [355–357]. This upregulation is thought to be subject to the inhibition of the VEGF pathway, in turn inducing tumour hypoxia, increasing HIF-1 expression and consequently the expression several compensatory pro-angiogenic factors – potentially exacerbating tumour growth as opposed to no change at all or a reduction [353]. As such, it is reasonable to perceive that BC utilises an alternative, VEGF independent, form of angiogenesis. Of note, literature also presents a disputed role for hormones in the process of angiogenesis, however this will be explored, in a non-malignant setting, in section 7.

7 Mammary gland derived endothelial cell isolation, characterisation and comparison to lung derived endothelial cells

To enable researchers to follow up on specific findings they often require a model *in vitro* system upon which to administer the same treatment or condition to extrapolate detailed cellular responses. Often stemming from the result of an *in vivo* study, or from large scale multiplex analysis to follow up a specific hit, the isolation and use of an individual cell type *in vitro* enables targeted follow up of cellular behaviour and/or mechanism [358]. Typically, when exploring the behaviour or signalling response of specific cells, an organ rich in the desired cell type is harvested, followed by the extraction and isolation of that cell type for subsequent study. As such, we hope to assess the credibility of utilising system/tissue specific ECs for studying a respective system/tissues angiogenic behaviour. LECs are widely used to study angiogenesis, even within the Robinson Lab. For my project, I wanted to explore and characterise the differences, if any, between MECs and LECs, whilst also seeking to understand if there is a role for progesterone in angiogenesis during pregnancy [284,299,300].

In light of the placental findings discussed in section 5.3, where we observed a significant increase in the size of the JZ, we became interested in whether hormonal input was playing a significant role in angiogenesis throughout pregnancy. More so, we wondered whether hormones present during pregnancy were helping to orchestrate angiogenesis, either with or without VEGF. Although an array of hormones, growth factors and cytokines are produced by the JZ, we set our sights on progesterone for two reasons. Firstly, a multitude of literature exists arguing both for and against the pro- or anti-angiogenic role of progesterone – the takeaway message being it plays a disputed role during angiogenesis [273,314–319]. Secondly, our placental phenotype was seen at E15.5, the point at which serum levels of progesterone are at their highest during pregnancy (81.9ng/ml) [335]. Having successfully isolated MECs from both Cre-negative and Cre-positive animals, alongside having access to LECs isolated from the same genotype (triple GEMM – β3.α5.Nrp1$^{fl/fl}$ mice), I hypothesised that these two different types of ECs would differ in their responses to VEGF and pregnant serum (a rich source of progesterone, and other factors secreted by the placenta).

7.1 Target depleted mammary derived endothelial cells show only modest changes in VEGF signalling

To begin characterising target depleted mammary endothelial cells (MEC-KO), we performed a VEGF-induced time course to assess their response to VEGF in terms of phosphorylated ERK 1/2 (pERK) expression, and at the same time, compare it to that observed in LECs. Given VEGF is a predominant stimulant of ECs *in vivo*, inducing an angiogenic response, it is commonly used to stimulate cells in culture as a means to study angiogenic signalling. ECs were seeded onto fibronectin coated plates and treated with VEGF for 0, 5, 15 or 30 minutes, lysed, and western blot analysis performed (sections 2.6 and 2.11.1). Much like their LEC-KO counterparts (**supplementary Figure 9.13**), MEC-KOs show a dampened response to VEGF compared to MEC-WT cells when examining pERK expression (**Figure 7.1**). Given ECs generally respond to VEGF, is it not surprising a pERK signal is detected in the MECs. However, since only mild phenotypes in both developing and pregnant mammary glands are observed when angiogenesis is impaired, it was surprising to see a reduced response in MEC-KO ECs; wild-type responses to VGEF in these cells would have been expected given the lack of robust phenotype(s).

Having observed similar VEGF-induced responses in MECs compared to LECs, alongside an reduced PgR expression upon target deletion (see below), I proceeded to explore the potential for other differences in signalling between these two cell types in a bid to understand how they might differ in their responses to other angiogenic stimuli, such as hormones/growth factors of pregnancy (e.g. progesterone).
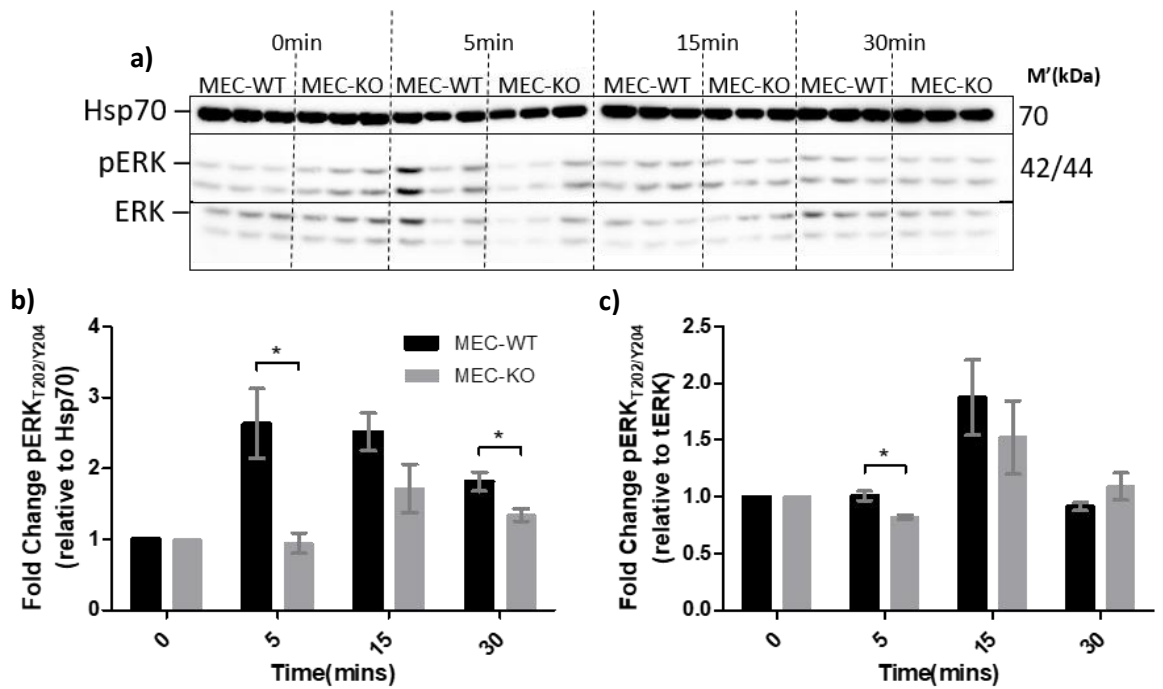
Figure 7.1 VEGF stimulation of triple MECs shows a dampened response to VEGF as determined through pERK expression. PyMT immortalised ECs (MEC-WT and MEC-KO[β3/α5/Nrp1]) were seeded onto fibronectin and were subsequently treated with VEGF for 0, 5 15 and 30 minutes. Post-treatment, cells were lysed and western blot analysis was performed to compare protein expression between MEC-WT and MEC-KO[β3/α5/Nrp1]. **a)** Western blot of lysates from MEC VEGF time-course. **b-c)** Densitometric analysis of western blot (a) normalised to Hsp70 or total ERK. N=3. Error bars = ±SEM. (* = P<0.05).

7.2 Progesterone receptor is profoundly decreased in target deleted lung endothelial cells compared to mammary endothelial cells

Having already alluded to the potential of progesterone playing a key role in modulating angiogenesis in the mammary gland, expression of the progesterone receptor (PgR) seemed a logical place to begin examining responses to other angiogenic stimuli. I first sought to compare the expression of PgR in LECs and MECs, with and without target depletion. PgR has been shown to exhibit differing levels of expression in ECs derived from different tissues, specifically showing human lung ECs lack PgR expression [273].

Assessment of PgR was performed through immunocytochemistry (ICC) of both WT and KO LECs and MECs. MECs and LECs were seeded onto fibronectin coated coverslips and left to adhere overnight prior to fixation and staining (section 2.10). ICC and subsequent Corrected Total Cell Fluorescence (CTCF – QBI, The University of Queensland, Australia) revealed an interesting expression profile of PgR. Both LEC- and MEC-WTs express PgR and do so at a similar level (**Figure 7.2**). However, target depletion alters this expression. LEC-KOs show a significant reduction in PgR expression whereas MEC-KOs show a very minor, non-significant, reduction in PgR expression (**Figure 7.2**). I found this interesting given the speculated importance of progesterone in modulating angiogenesis during pregnancy [336]. Our working hypothesis entailed the involvement of progesterone as a pro-angiogenic molecule aiding in overcoming the anti-angiogenic phase we were inducing through our target depletion. In light of our hypothesis and current literature, the MEC finding fits this supposition; target depletion does not affect PgR expression, therefore progesterone could still positively modulate angiogenesis in MEC-KO cells. The LEC finding not only demonstrates mouse LECs express PgR, it also shows LEC-WTs have an equivalent level of PgR as MEC-WTs with a marked decrease in PgR expression post-target deletion. This is an interesting finding which demonstrates the differences in ECs isolated from different tissues [273,359]. Of note, I attempted to assess PgR expression further by Western blot analysis, but my attempts were unsuccessful.
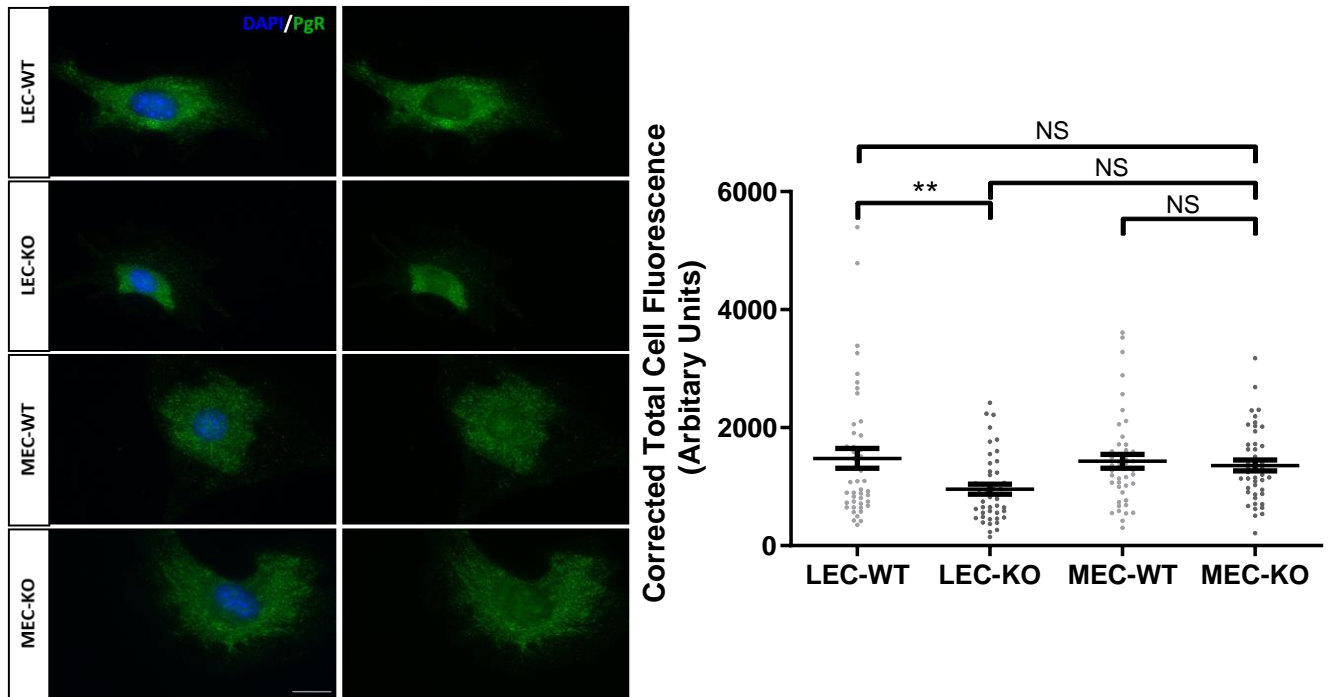
Figure 7.2 Target deletion in lung derived endothelial cells significantly reduces progesterone receptor (PgR) expression. LECs and MECs were seeded overnight on fibronectin coated coverslips before being stained and fixed the following day. **a)** Representative images of immunocytochemistry stained LEC-WT, LEC-KO, MEC-WT and MEC-KO cells: PgR (green) and Dapi (blue). **b)** Corrected Total Cell Fluorescence (CTCF) of immunocytochemistry in (a). N=3, Cre-negative, n=45. Cre-positive, n=45. Scale bar = 20µm. Error bars = ±SEM. (** = P<0.01).

7.3 Treatment of mammary derived endothelial cells with pregnant serum results in altered signalling responses when EC targets are depleted

Having established differences in PgR expression between LEC-KOs and MEC-KOs, we proceeded to explore the role of progesterone in angiogenic signalling pathways in ECs. In a bid to assess progesterone's involvement in MEC signalling, we extracted blood, and subsequently serum, from non-pregnant and pregnant mice (E15.5) to stimulate MECs with. MEC-WT and MEC-KO cells were seeded overnight on pre-coated fibronectin plates and were treated with non-pregnant serum (S) or pregnant serum (PS) the following day (section 2.11.2). To ascertain whether progesterone was indeed stimulating signalling pathways, and whether these pathways differed between MEC-WTs and MEC-KOs, we probed for several proteins known to be involved in angiogenic signalling. PS was used as opposed to neat progesterone to maintain physiological relevance when assessing signalling responses. Target proteins for western blot analysis post-treatment included VEGFR2, AKT, FAK, ERK and p38 (**Figure 7.3**).

I initially wanted to examine changes in VEGFR2 phosphorylation (pVEGFR2). VEGFR2 is a key component of the angiogenic signalling cascade vital in transducing VEGF signals in ECs. Our target depletion affects VEGF signalling directly as the molecules depleted are involved both down- and upstream of VEGF stimulation. Given we are treating cells with S and PS, and our target depletion is directly relatable to VEGFR2, it seemed a relevant protein to investigate [360–362]. We were unable to detect pVEGFR2 within our samples however we detected a significant reduction in **total** VEGFR2 in cells treated with PS, and a marked decrease in cells treated with S (**Figure 7.4a**). An absence of a pVEGFR2 signal suggests there is no VEGF present in the serums used for these studies. The fact that total VEGFR2 decreases in response to serum stimulation suggests that VEGFR2 is quickly degraded in response to these treatments (VEGFR2 is known to be degraded post-activation by endocytosis, ubiquitination and proteolysis), but there appears to be no difference between MEC-KO and MEC-WT cells [363,364]. Probing for pERK revealed both S and PS stimulated ERK phosphorylation, but there were no differences between MEC-KOs and MEC-WTs (**Figure 7.3**). This reinforces the idea that S and PS contain little to no VEGF, as the previous section demonstrated a depressed pERK response to VEGF in MEC-KOs (**Figure 7.4b**). Another VEGF thematic signalling pathway is AKT, commonly activated in response to VEGF to promote EC survival with literature supporting progesterone upregulating the AKT signalling pathway to support EC viability [365]. However, whilst target depletion in MEC-KOs led to reduced total AKT expression, no significant differences were noted when comparing pAKT relative to tAKT levels (**Figure 7.4c**). The two final signalling proteins we explored were FAK and p38. Both FAK and p38 are downstream signalling proteins of VEGF stimulation, orchestrated via neuropilin-1, with downstream effects on EC

proliferation and migration [366–368]. We were unable to detect pFAK however we did detect total FAK, which showed a slight, but non-significant, decrease in expression when MECs were treated with either S or PS (**Figure 7.4d**). Examining p38 expression was problematic as expression seemed low and background was relatively high, making accurate quantification impossible. It appears, however, that p38 phosphorylation was decreased in MEC-KO cells, in both S and PS conditions, but I cannot currently comment on whether this is statistically significant.
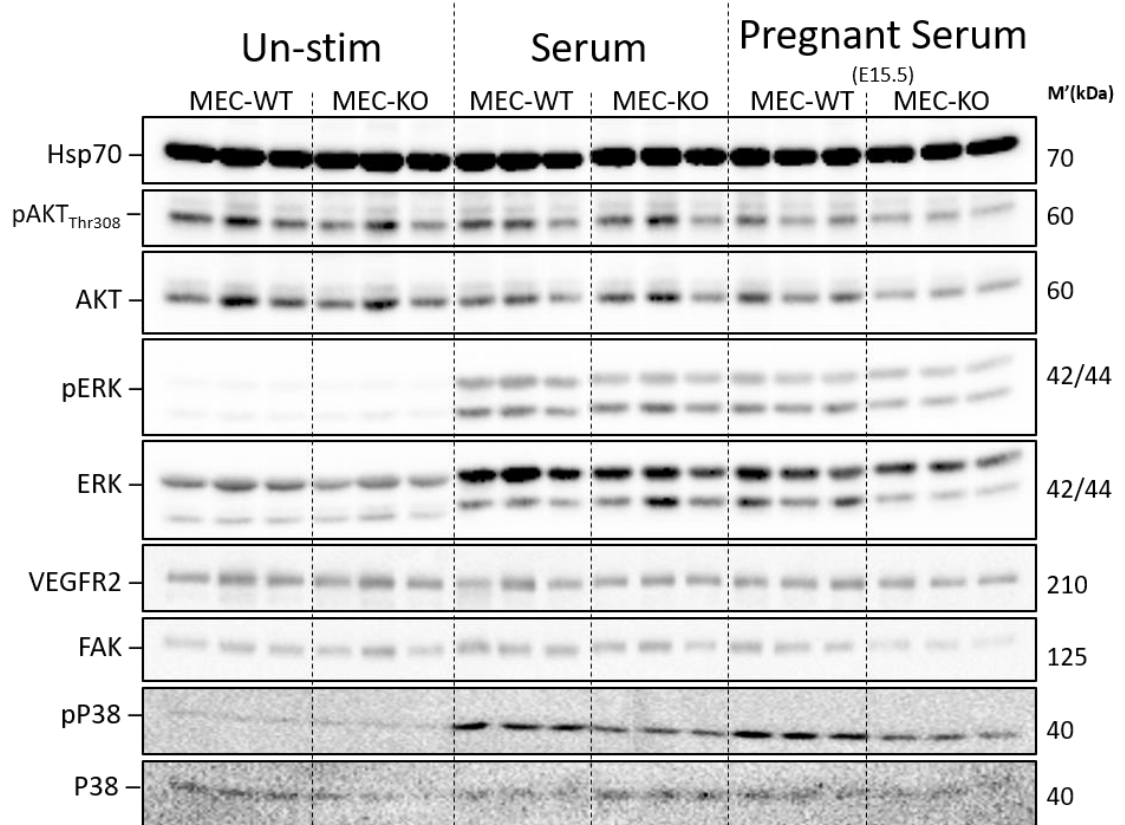
Figure 7.3 Western blot analysis of MECs treated with serum and pregnant serum. MECs were seeded overnight on fibronectin coated plates, serum starved and treated with serum or pregnant serum. Lysates were collected and probed for the indicated proteins labelled above. N=3 lysates per condition.
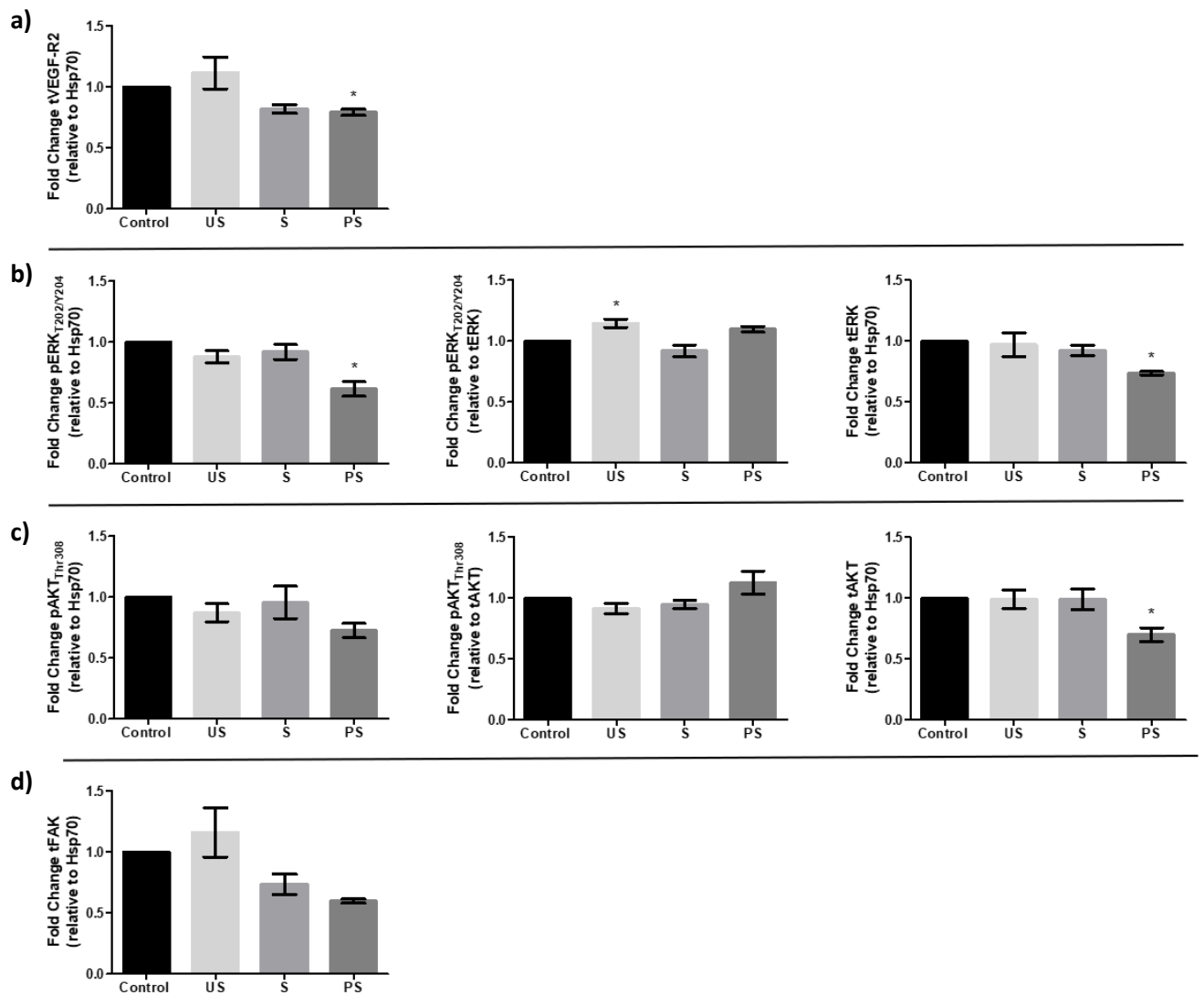
Figure 7.4 Densitometric analysis of western blotting performed on MECs treated with serum and pregnant serum. Densitometric analysis of western blot targets normalised to Hsp70 or respective total protein. **a)** Total- VEGFR2 (tVEGFR2) relative to Hsp70. **b)** Phospho-ERK relative to Hsp70 and total-ERK (tERK), and tERK relative to Hsp70 respectively. **c)** Phospho-AKT (pAKT) relative to Hsp70 and total-AKT (tAKT), and tAKT relative to Hsp70 respectively. **d)** Total-FAK (tFAK) relative to Hsp70. N=3. Expression levels are presented relative to those observed in control (MEC-WT – black bar) for each treatment. US = unstimulated, S = Serum and PS = Pregnant Serum (E15.5). N=3 per condition. Error bars = ±SEM. (* = P<0.05).

7.4 Microarray, and subsequent STRING analysis, reveals signalling differences between mammary and lung derived endothelial cells in response to VEGF, serum and pregnant serum

The Western blots described above pointed toward a couple of signalling leads, but were, overall, rather disappointing. Thus, I sought to investigate the signalling response of MECs and LECs on a larger scale. To provide a broad insight into potential signalling pathways at work, I proposed performing microarray analyses on the following cells and treatments: LEC-WT, LEC-KO, MEC-WT and MEC-KO treated with VEGF; MEC-WT and MEC-KO treated with serum; MEC-WT and MEC-KO treated with serum from pregnant mice (E15.5). This combination of treatments would enable comparative discernment between LEC and MEC in terms of signalling responses to VEGF, whilst the latter would enable me to explore the effects of our target depletion with regards to how MECs respond to bio-actives found in serum and pregnant serum.

The microarray analysis I chose to perform was the Kinex™ KAM-1325 Antibody Microarray. This microarray provides exclusive readings for 627 signalling proteins alongside duplicate measurements to enhance accuracy and internal cross-validation using antibodies to the same signalling protein specified to a different epitope. Samples were prepared as per section 2.11.1-3. Briefly, LEC/MEC-WT and LEC/MEC-KO cells were seeded onto fibronectin coated plates, stimulated with the designated treatment and lysed before being loaded onto the microarray; microarrays were subsequently shipped and analysed by Kinexus™ (**supplementary Figure 9.14**). Unfortunately, the LEC-KO +VEGF sample leaked out of the chamber during incubation, so this treatment was lost from subsequent analyses, and consequently, so too was the LEC-WT +VEGF sample. Initial analyses performed by Kinexus highlighted changes that the company considered to be significant (based on fold differences in expression between comparisons). Comparing the MEC-WT to the MEC-KO for each treatment, nothing "jumped out" as being an obvious lead to follow. However, I thought I might increase the power of the comparisons by pooling all the data into a single analysis, even if the treatments were different (that is all the MEC-WT samples and all the MEC-KO samples were considered as biological repeats) I surmised that I might be able to uncover common signalling hubs through which my EC targets were functioning, even if the treatment was different. To do this, I used Qlucore™ bioinformatics software to bring together all "priority" leads from the microarray reports for the three MEC-WT and MEC-KO conditions; VEGF, serum, pregnancy serum. Using this software to generate a hierarchical protein clustering heatmap, I narrowed down the proteins of interest – cut offs for considering a pathway to be of interest were set to P<0.05 (**Figure 7.5**). This clustering algorithm compares the mean reading for each protein and compares them between MEC-WT and MEC-KO samples. Out of the 627 unique signalling proteins assayed, we identified 33

leads from the microarray analysis and subsequent hierarchical clustering (**Figure 7.5**). These leads were fed into STRING in order to generate a protein interaction network, proposing a visual map of how signalling proteins detected between samples may be interacting. Of note, we performed Qlucore™ analysis on samples denoted by Kinexus™ as "priority" leads. Besides these leads, there were also numerous potential leads, however we did not pursue these. To enable us to perform analysis with Qlucore™ we pooled the "priority" leads for the three MEC-WT samples and for the three MEC-KO samples, VEGF, Serum and Pregnant Serum respectively, to grant us a refined panel of signalling proteins which we could follow up with string analysis and ultimately western blot analysis (**Figure 7.6**).
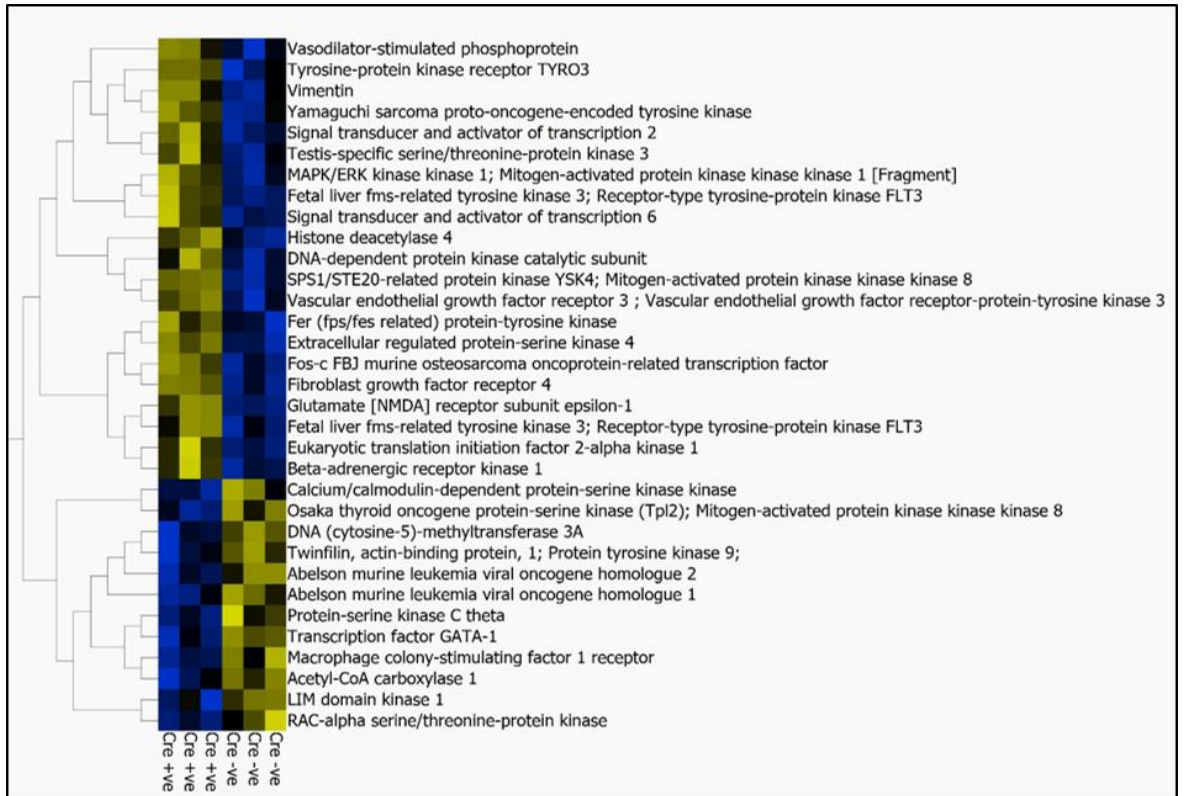
Figure 7.5 Hierarchical protein cluster analysis, performed on Qlucore™, from the three MEC-WT and MEC-KO samples. MEC-WT and MEC-KO samples were treated with either VEGF, serum or pregnant serum and microarray analysis performed – samples are not replicates but are VEGF, serum or pregnant serum treated, respectively. Yellow = high expression, blue = low expression.
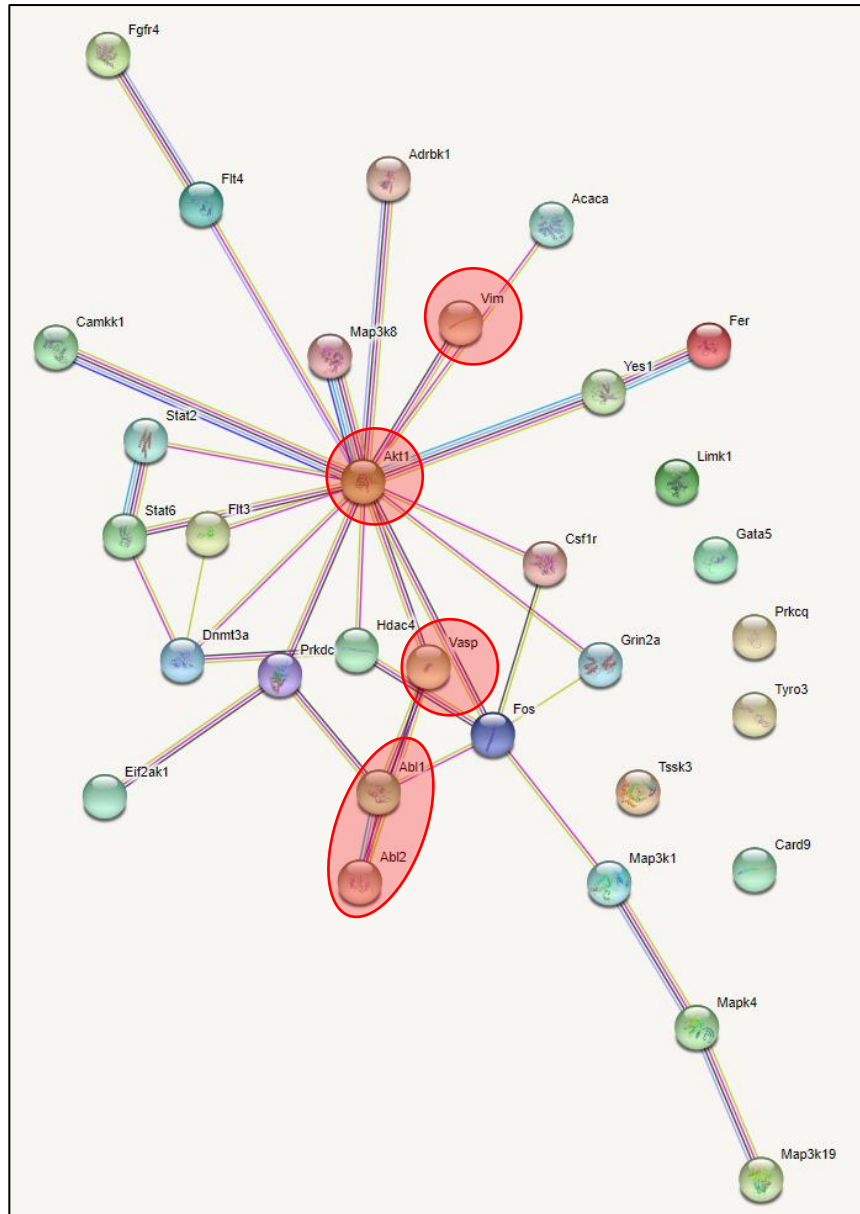
Figure 7.6 STRING analysis generated from hierarchical protein clustering. The output from hierarchical protein clustering, from data generated from the microarray analysis, were inputted into STRING (String Consortium 2020©). Signalling proteins of interest, highlighted in **red**, were chosen for follow up analysis via western blot.

7.5 Subsequent western blot analysis for signalling proteins identified by STRING analysis reveals differential signalling responses to hormonal input

Directed by the results of the Qlucore™ analysis, and subsequent STRING analysis, follow up western blotting was performed on the lysates that were generated for the microarray. Of the proteins inputted into, and interactions mapped by, STRING, I decided to follow up on four proteins, namely: Protein Kinase B or RAC-alpha serine/threonine-protein kinase (AKT), Vimentin (VIM), Vasodilator-stimulated phosphoprotein (VASP), and Abelson tyrosine-protein kinase (ABL). Situated at the centre of the STRING analysis. AKT is accountable for many of the downstream responses, induced by growth factors, in ECs and has been shown to mediate the recycling and trafficking of integrins-αVβ3 and α5β1 – two targets which we have depleted [369,370]. Thus, even though earlier findings were disappointing, I decided to reanalyse signalling through this molecule. Both VIM and VASP are key molecules in generating and mediating focal adhesion formation, maturation and subsequent signalling, as previously demonstrated by our lab when integrin-β3 is depleted, and by others demonstrating VIM to be essential in the localisation and phosphorylation of VASP, subsequently controlling EC migration and proliferation [255,371]. ABL is directly related to neuropilin-1 activity; dependent on the presence of neuropilin-1 to enable subsequent VEGFR2 activation, ABL phosphorylation and SFK activation, and ultimately vascular permeability [372]. Of note, as I only possessed one lysate per microarray condition, I did not perform densitometry, and I cannot comment statistically on any observed differences. I also decided to include lysates from the LECs since I had them and was interested in potential differences between LECs and MECs.

At the heart of the STRING analysis, AKT was our first protein of interest for follow up. I performed the western blot analysis on the microarray samples for both AKT_{Thr308} and AKT_{Ser473}; covering all of the phosphorylation sites of AKT [373]. Western blot analysis of AKT_{Thr308} revealed increased phosphorylation, and expression, of AKT_{Thr308} in MEC-KOs treated with VEGF or S, but decreased expression in MEC-KO treated with PS and LEC-KO treated with VEGF (relative to their WT counterparts) (**Figure 7.7a**). In contrast, AKT_{Ser473} phosphorylation only changed in MEC-KO +S. (**Figure 7.7b**). The reason for the discrepancy with earlier findings (see above) is unknown, but the array findings, on whole, suggest this is an important signalling hub to pursue in future work.

I next probed for VIM and VASP; separately on freshly prepared lysates. Phosphorylated VIM (pVIM) was really only detected in the MEC+VEGF samples. However, total VIM (tVIM) levels look as if they are decreased in MEC-KO +VEGF cells, and tVIM levels drop dramatically in MEC cells in response to PS treatment (though there does not appear to be a difference between KO and WT ECs (**Figure 7.7c**). Examining VASP expression turned out to be quite interesting. In general, both LEC and MEC

KO cells show a reduction in total VASP. However, taking this into consideration relative changes in phosphorylated VASP, in relation to total VASP, look unchanged. (**Figure 7.7d)**. Finally, I probed for ABL, but was unable to detect any phosphorylated ABL in any of the samples. In general, total levels of ABL were unaltered when comparing WT ECs to KO ECs, with an absence of total ABL when MECs were treated with PS (**Figure 7.7e**).

A summary of signalling responses for all treatments and EC types can be seen in **Figure 7.7f**.

Figure 7.7 Western blot analysis of mammary and lung derived endothelial cells treated with VEGF, and MECs treated with serum (S) or pregnant serum (PS).MECs and LECs were seeded overnight on fibronectin coated plates, serum starved and treated with VEGF, serum or pregnant serum f0r 30 minutes. Lysates were collected and probed for phosphorylated (p) and total (t) levels of **(a, b)** AKT$_{Thr308}$ and AKT$_{Ser473}$; **(c)** VIM; **(d)** VASP; and **(e)** ABL. **f)** Graphical depiction of the results from the western blot analyses. N=1, n=1.

7.6 Discussion

In this section I sought to not only characterise the difference in signalling response between MEC-WT and MEC-KO cells, when treated with either VEGF, S or PS, but I also began to explore whether there are fundamental signalling differences between MECs and LECs. I began this journey predominantly for two reasons. Firstly, the phenotype observed during pubertal development, (e.g. a lack of any robust phenotype in animals missing EC expression of integrin-a5, integrin-b3 and neuropilin-1) contrasts significantly with the depletion of these three molecules in other systems in the lab, such as retinal angiogenesis. This suggest these molecules may not play a role in mammary gland angiogenesis. Secondly, this intimates that LECs may differ from MECs in their response to common angiogenic stimuli, such as VEGF.

The ECs isolated from the mammary gland and the lungs of our triple floxed mice have been grown, isolated, immortalised, and a subset nucleofected with TAT-Cre, to generate WT (MEC-WT and LEC-WT) and target depleted populations (MEC-KO and LEC-KO) respectively from each organ. We have demonstrated the identity of our MECs (section 3.4) and LECs (data not shown) through their expression of known endothelial markers, whilst also showing our WT cells express our targets and our KO cells do not. As such, we proceeded to explore the response of MECs to VEGF, the major driver of sprouting angiogenesis. Interestingly, despite deleting three of the major receptors involved in VEGF signal transduction the MECs showed only modest changes in ERK signalling, especially in comparison to their lung counterparts; LECs exhibit a harsh reduction in ERK expression and phosphorylation. This result prompted us to question whether angiogenic signalling in these cells is tissue specific, potentially offering an explanation as to why genotypically identical ECs differ in their response to VEGF.

Although repeats and follow up signalling assays need to be performed, findings can be extrapolated from what we have found. Generally, stimulation of MEC-KOs with VEGF summated in no change, or a decrease, in the expression of proteins measured, with the exception of AKT_{Ser473}, compared to LEC-KOs where only a small decrease in AKT_{Ser473} and tVASP was observed (**Figure 7.7f**). Interestingly, the decrease in the signalling proteins measured in MEC-KOs treated with PS would suggest ablation of our targets is impacting the ability of either a growth factor or hormone present in PS to transduce a signal, especially when compared with S treated MEC-KOs where we do not see the same changes in expression. On from this point, S treated MEC-KOs show an increase in the phosphorylation of AKT. This suggests our target ablation dampens a signalling pathway via a molecule present within PS, whilst concomitantly increasing a signalling pathway via a molecule present within S. To tie back to the ICC for PgR, LEC-KOs exhibit significantly less PgR than LEC-WTs, MEC-WTs and MEC-KOs, all of which display equivalent levels to one another. This reduction in PgR

may suggest a homeostatic balance whereby a decrease in a pro-angiogenic pathway (induced by our target depletion) also reduces an anti-angiogenic pathway, potentially progesterone. Although there is insufficient evidence to support the previous claim, it is certain that we have a phenotype in the expression of PgR between LECs and MECs, and that our target depletion in MECs is altering their signalling in response to both PS and S.

8 Final discussion and future work

Angiogenesis has long been deemed a fundamental process by which tissues and organs undergo vascular expansion. Occurring allometrically, in response to tissue and organ growth, and pathologically, angiogenesis is a valuable process to have an understanding of. In the instance of this thesis, the focus was the murine mammary gland. With considerable evidence for the pro-angiogenic involvement of integrin-β3, integrin-α5, and neuropilin-1, both collectively and individually, our lab possesses a powerful tool to ascertain the level of importance of angiogenesis during the normal and malignant lifecycle of the mammary gland [114,140,141]. Our overarching hypothesis was that the depletion of key fibronectin binding receptors and neuropilin-1 would impede the pubertal and gestational expansion of the mammary epithelium. As such, we required a suitable model. Fortunately, the conception of this project required no creation of an *in vivo* angiogenic model as the triple floxed GEMM had already been generated (**Table. 3.1**). Additionally, this facilitated the establishment of the MECs from the mammary glands of the triple GEMM following an adapted LEC isolation protocol; isolated, immortalised and transfected with tat-Cre-recombinase we were able to generate target depleted and Cre-negative (wild-type) lines (**Figure 3.3**). Whilst having both an *in vivo* and *in vitro* model of angiogenesis, caveats exist. The activity of our Pdgfb Cre, albeit active in ECs, needs to be investigated for off target expression as studies have demonstrated PDGFb expression in a variety of cell types. Funa and Sasahara demonstrated neuronal cell expression of PDGFb and noted its importance in neurogenesis [374]. Furthermore, a comparative study exploring the cell specificity between Cdh5 driven Cre compared to PDGFb discovered a small number of hematopoietic cells to be expressing PDGFb [294]. Of specific importance, macrophages fall under the hematopoietic lineage and have well defined roles in the expansion of the mammary epithelium; to fully account for our partial phenotype(s) observed in section 4 to angiogenic impediment we need to verify cell specificity [297]. Furthermore, to fully describe the anti-angiogenic model we are generating through target depletion we should quantify the expression of other integrins, namely the heterodimeric partners of our targets, integrin-αV and integrin-β1; the expression profile of integrin-αV and integrin-β1 may differ between MEC and LEC.

Utilising our triple GEMM as a model for angiogenic impediment, we set out to assess the involvement of angiogenesis in the pubertal, gestational, and pathological lifecycle of the murine mammary gland. Beginning with pubertal growth, we delved into assessing the direct effects of ablating our three molecules of interest (as a means to impede angiogenesis) on the epithelial growth in the pubertal mammary gland. Establishing the number four gland as the gland of study, for reasons previously discussed (section 4), we proceeded to collect pubertal glands that had

undergone the pubertal Tamoxifen regimen (section 3.2), followed by WGS to assess the epithelium. To our surprise we saw no change in epithelial outgrowth, however we noted a significant increase in epithelial outgrowth directionally in Cre-positive mammary glands; at the top edge (above) the lymph node (**Figure 4.3c and e**). However, despite this finding, when we attempted to quantify other parameters as a means to explore and understand why we were seeing this change we found little of note. Namely, epithelial density and number of branch points did not significantly differ between Cre-positive and Cre-negative animals, either overall or in a specific direction about the lymph node (**Figure 4.4**). However, upon visual inspection it appeared the Cre-positive glands may be exhibiting more trifurcations than Cre-negative glands. Quantitation of these events led us to discover that whilst TEB number did not vary between Cre-negative and Cre-positive, Cre-positive glands were displaying significantly more trifurcations events. Subsequent H&E analysis revealed no structural alteration in TEB structure (**Figure 4.7**). Taken collectively, perturbation of angiogenesis by our target depletion results in no significant changes in the mammary epithelium during puberty, with the exception of a significant increase in trifurcation events and a directional increase in epithelial growth – of note, position of trifurcations were not predominant at top edge (above) the lymph node and hence do not account for the significant increase in epithelial growth observed in that direction. The obvious explanation for these findings is that the significant increase in trifurcation events is a result of impeded angiogenesis in a bid to maintain epithelial growth. Consequently, towards the end of puberty the migratory front naturally exists at the top edge (above) the lymph node. As such, TEBs will predominantly be present at the top edge (above) of the lymph node and could therefore amplify epithelial growth, beyond that of a Cre-negative when measured and compared. Taken further, previously mentioned was the observation by Matsumoto *et al*. noting the close association of endothelium with epithelium [320]. Given the endothelium of the pubertal gland is likely largely formed prior to pubertal onset, the instance of trifurcation may be consequence of the interaction of the epithelium with the endothelium – via angiocrine signalling. Although we have not shown the endothelial composition of the mammary gland during, or before, puberty, corrosion casts previously discussed would suggest a vasculature of some degree pre-exists within the pre/pubertal gland [161]. In line with these findings, it is plausible that angiocrine signalling is affected as a result of our target depletion, resulting in a mild phenotype. Rafii *et al*. comment on the organ specific role of ECs in inducing, specifying and guiding organ regeneration via angiocrine signalling [375]. Although focussed on tissue regeneration, it is conceivable that these signals equally propagate epithelial growth via TEBs; faulty angiocrine signalling could result in trifurcations instead of bifurcations. Although no unique chemoattractant has been defined for aiding epithelial expansion, Fibroblast Growth Factors

(FGFs), Epidermal Growth Factors (EGFs) and Wnts have all been implicated in branching morphogenesis [376]. Additionally, Transforming Growth Factor-β (TGF-β) has been shown to restrict branching morphogenesis, negatively modulating the process [264]. Many of these growth factors can be produced by the endothelium. As such an array of EC-derived growth factors may play a cumulative role in regulating branching morphogenesis throughout the lifecycle of the mammary gland, and target depletion may disrupt the balance of these molecules resulting in trifurcation events.

I next proceeded to assess the effect of angiogenic disruption on the cycle of pregnancy, specifically mid-gestation (E10.5), late gestation (E15.5), lactation (P2) and Involution (P12). Starting with E10.5, we observed only mild differences in epithelial outgrowth between Cre-negative and Cre-positive mammary glands, saw no changes in embryo numbers, but did observe a significant reduction in embryo weight. Following up our E10.5 studies, E15.5 mammary glands proved too difficult to quantify in terms of epithelium, but visual examination revealed no grossly obvious differences between Cre-negative and Cre-positive glands (**Figure 5.3**). Furthermore, the number of embryos and their uterine location revealed no striking differences between genotypes, however the E10.5 phenotype of embryo weight differences was lost (**Figure 5.2a-b and e**). Also, despite a greater number of reabsorption events detected in Cre-positive E15.5 mice, specifically in the left position of the uterus, no significant changes were observed (**Figure 5.2c-d**). Lastly, I collected placentas from E15.5 mothers in a bid to address the difficulty I had when performing timed mating – was placental angiogenesis resulting in miscarriage or failure to fall pregnant? Despite new "best practice" for timed mating being implemented by our animal facility, and as such alleviating our difficulty to a degree, we had already begun our placental investigation. Although there was no difference in placental weight (**Figure 5.2f**), I did observe a significant change in the proportion of the placental zones, namely a significant increase in the JZ in Cre-positive mothers (**Figure 5.3**). Unfortunately, due to undefined circumstances of litter loss, I possess very little data bar WGS observations as to the effect of our target depletion on the lactating and involuting mammary gland, though no obvious changes are observed between genotypes. The takeaway message from this results section is that the phenotype observed in embryo weight differences was transient, observed at E10.5 but lost by E15.5, with the mechanism for normalising/redeeming embryo weight thought to be placenta derived.

The maternal decidua is the first vascular interface, preluding the labyrinth, between mother and embryo, with angiogenesis within the decidua being driven by VEGF-A signals, which are hormonally regulated by progesterone and estrogen [315,316,332]. An emerging idea from my pregnant studies is that early defects in angiogenesis (both within the mammary gland and the

uterus) that occur as a result of target depletion, are overcome by increases in progesterone-driven angiogenesis later on. In line with this concept, I detect a significant increase in the size of the JZ, the endocrinal compartment of the placenta responsible for cytokine, growth factor and hormone production; bolstering progesterone as a vital player [239]. Thus, come E15.5, augmentation of the JZ occurs in Cre-positive mothers leads to increased progesterone production, which in turn increases angiogenesis, thus abrogating the effects of target depletion. Granted, as previously stated, the JZ is also responsible for the production of a range of other growth factors and cytokines; cumulative upregulation of an array of pro-angiogenic molecules could equally circumvent the lack of angiogenesis incurred through our target depletion. This is, of course, entirely speculative. In order to confidently correlate the augmentation of the JZ to hormone production I would need to culture the JZ of both Cre-negative and Cre-positive mothers and subsequently perform mass spectrometry on the conditioned media – at which point I would also be able to gauge differences in growth factor and cytokine excretion.

Coming full circle in the lifecycle of the mammary gland, we proceeded to explore the pathological side of angiogenesis, specifically during BC. The BC experiments performed in this thesis aimed to assess the involvement of all three of our target molecules in tumour angiogenesis and subsequently BC progression. Utilising a MMTV-PyMT derived breast carcinoma cell line (B6BO1) for our model of BC, we proceeded with tumour experiments (described in section 2.4) in all of our GEMM lines (**Table. 3.1**). Given previous findings by our lab, the findings from the cancer studies in this thesis were lacklustre, at least with respect to double EC knockouts; single and double target depleted experiments yielded no significant reduction in tumour volume. However, the triple EC knockout did show a significant reduction in tumour growth, providing evidence that the triumvirate might serve as an anti-angiogenic "target" in BC, though this concept needs to be considered alongside the clinical feasibility of inhibiting all three molecules simultaneously. To contrast my findings with those achieved in other cancer models, we have shown in lung cancer models that dual target depletion is sufficient to block tumour growth (see **supplementary Figure 9.12**). Clearly, there exists a difference between the cancer models used (section 6.3), highlighting the importance of studying organ-specific responses when considering the design of anti-cancer therapeutics. Interestingly, the B6BO1 cell line is PgR positive (unpublished).

In an effort to address the potential role of progesterone in orchestrating a pro-angiogenic response, and to ascertain whether the mammary gland yields a tissue specific EC population, I generated ECs from the mammary gland(s) of our triple GEMM for stand-alone studies, and comparative analysis to LECs. MEC-WT and MEC-KO cells were treated with VEGF, S or PS, whilst LECs were treated with VEGF, to answer: (1) do mammary and lung ECs differ in their response(s)

to VEGF; (2) do MEC-WT and MEC-KO cells respond differently to VEGF, S and PS. The findings from these studies (particularly with respect to VEGF-induced responses) are somewhat ambiguous, and there is clearly plenty more comparisons that need to be performed when comparing LECs to MECs. Moreover, there is huge scope to explore differences that might occur in the ECs isolated from the different organs in response to target depletion. The most interesting finding to emanate from my *in vitro* analyses relate to responses to pregnant serum (presumably driven by progesterone). There is a clear reduction in total VIM and total VASP levels in MEC-KO cells in response to PS. These observations certainly merit further investigation.

In summary, this thesis aimed to address how impaired angiogenesis, mediated by the collective depletion of EC integrin-β3, integrin-α5 and neuropilin-1, impacts on epithelial morphogenesis throughout the lifecycle of the murine mammary gland. Summarised in **Figure 8.1**, the mammary gland was largely unaffected by the absence of these molecules, with the exception of early-on during pregnancy. The ultimate reasons for this are largely unknown but are likely **not** related to inefficient target depletion in the gland (see **Figure 3.4**, section 3.2). I postulate that in the pubertal gland, the most likely explanation is that what we think of as "classical" angiogenesis is not needed; it may well be that the empty mammary fat pad into which the developing gland is growing is sufficiently vascularised such that additional vessel growth is not required. Further careful analyses of the interplay between growing epithelium and existing vasculature should help answer this question, and this is now possible given the recently acquired ability to perform meaningful whole gland immunostaining. That said, I cannot rule out that the signals governing angiogenesis in the pubertal gland, if it does occur, might not be transmitted through the targets we have chosen to delete. This this seems unlikely given the targets would generally be considered essential for EC migration, which itself is essential for angiogenesis, but, again, this requires further testing, and the tools are in hand to do so. Findings in the pregnant gland intimate that angiogenesis as mediated by our EC targets is required early on, but then some other process takes over such that the targets are no longer involved. This could be through some as yet unidentified compensatory pathway, or it may be the result of a shift in what factors are driving EC responses (for example, a transition from VEGF-driven angiogenesis to progesterone-driven angiogenesis). Where I see a clear connection between angiogenesis and mammary epithelial growth is in the pathological setting. Depletion of our chosen targets, at least simultaneously, impairs BC growth. Whilst it might be impractical to target all three molecules in a patient, if we can understand on what signalling pathways the three molecules impinge upon during the tumour development, it might throw up anti-angiogenic targets that have yet to be explored.

Puberty
- Overall epithelial outgrowth is unaffected
- Directional epithelial growth above lymph node is increased
- Epithelial denisty and number of branch points are unaffected
- TEB number is unchanged
- Trifurcation events are observed significantly more

The role of angiogenesis, mediated by endothelial adhesion receptors integrin-β3, integrin-α5 and neuropilin-1 in the lifecycle of the mammary gland

Breast Cancer
- Single and dual target depletion show no significant change in tumour weight or volume
- Triad target depletion reduces both tumour weight and volume

Pregnancy
Mid gestation (E10.5)
- Epithelial maturation is unaffected
- Embryo numbers the same, but embryos are smaller
Late gestation (E15.5)
- Epithelial maturation appears unaffected
- Embryo number, position, and weight are unaffected
- Reabsorption events occur more frequently
- Placental weight is unaffected, but the JZ region is larger

Post Pregnancy
Lactation (P2) and Involution (P12)
- Visually the epithelium at both time points is unaffected

Figure 8.1 Schematic summary of the findings from the work presented in this thesis.

9   Appendix – Supplementary figures
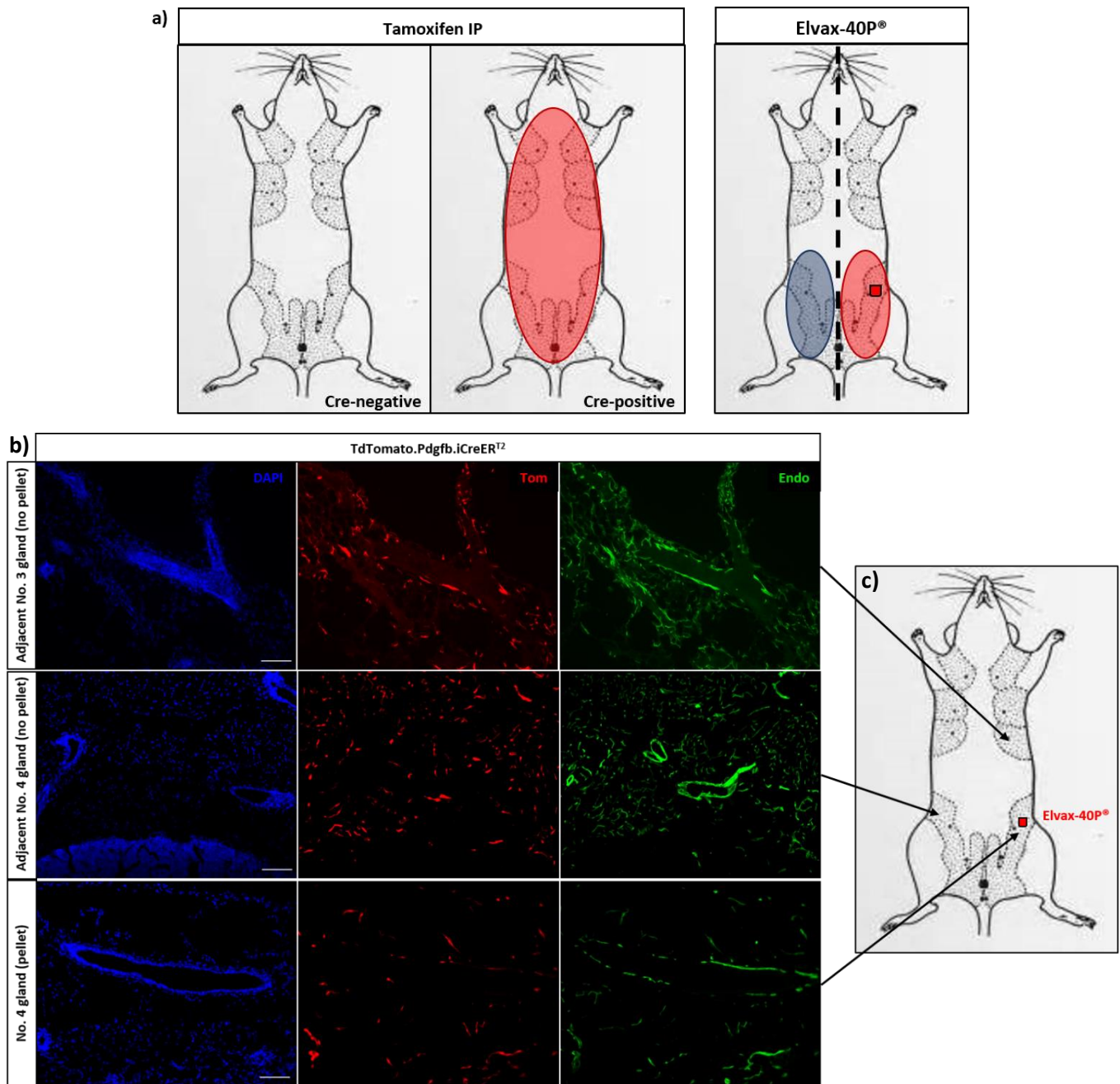
Figure 9.1 Tamoxifen delivery through Elvax-40P® yielded systemic administration of Tamoxifen, not local to the implanted mammary gland. TdTomato.Pdgfb.iCreER$^{T2(pos)}$ mice underwent Elvax-40P® (containing Tamoxifen) implantation in the left abdominal mammary gland. **a)** Schematic depicting the difference between I.P. and Elvax-40P® pellet method of Tamoxifen administration. I.P. administration is systemic and requires Cre-negative littermate controls (left). Elvax-40P® can provide local Tamoxifen administration, leaving the remaining mammary glands as contralateral controls (right). **b)** Representative images of mammary glands adjacent to the gland that underwent Elvax-40P® implantation exhibiting TdTomato expression (top and middle row), alongside the implanted gland also exhibiting TdTomato expression (bottom row): DAPI (blue), TdTomato (red) and endomucin (green). **c)** Diagrammatic representation of pellet implantation and the location of the glands shown in (b) respectively. Scale bar = 100µm.

Weight of Mouse (g)	Tamoxifen (mg)	Volume to Inject (µl)
18	1.35	67.5
19	1.425	71.25
20	1.5	75
21	1.575	78.8
22	1.65	82.5
23	1.725	86.25
24	1.8	90
25	1.875	93.75
26	1.95	97.75
27	2.025	101.25
28	2.1	105
29	2.175	108.75
30	2.25	112.25
31	2.325	116.25
32	2.4	120
33	2.475	123.75
34	2.55	127.75
35	2.625	131.25

Figure 9.2 Tamoxifen administration doses as recommended by Jax Lab. Tamoxifen, 0.3mg – Sigma-Aldrich, was resuspended in 1.5ml ethanol, diluted with 13.5ml of corn oil giving a final concentration of 20mg/ml and administered by intraperitoneal injection (section 2.3) [262,377].
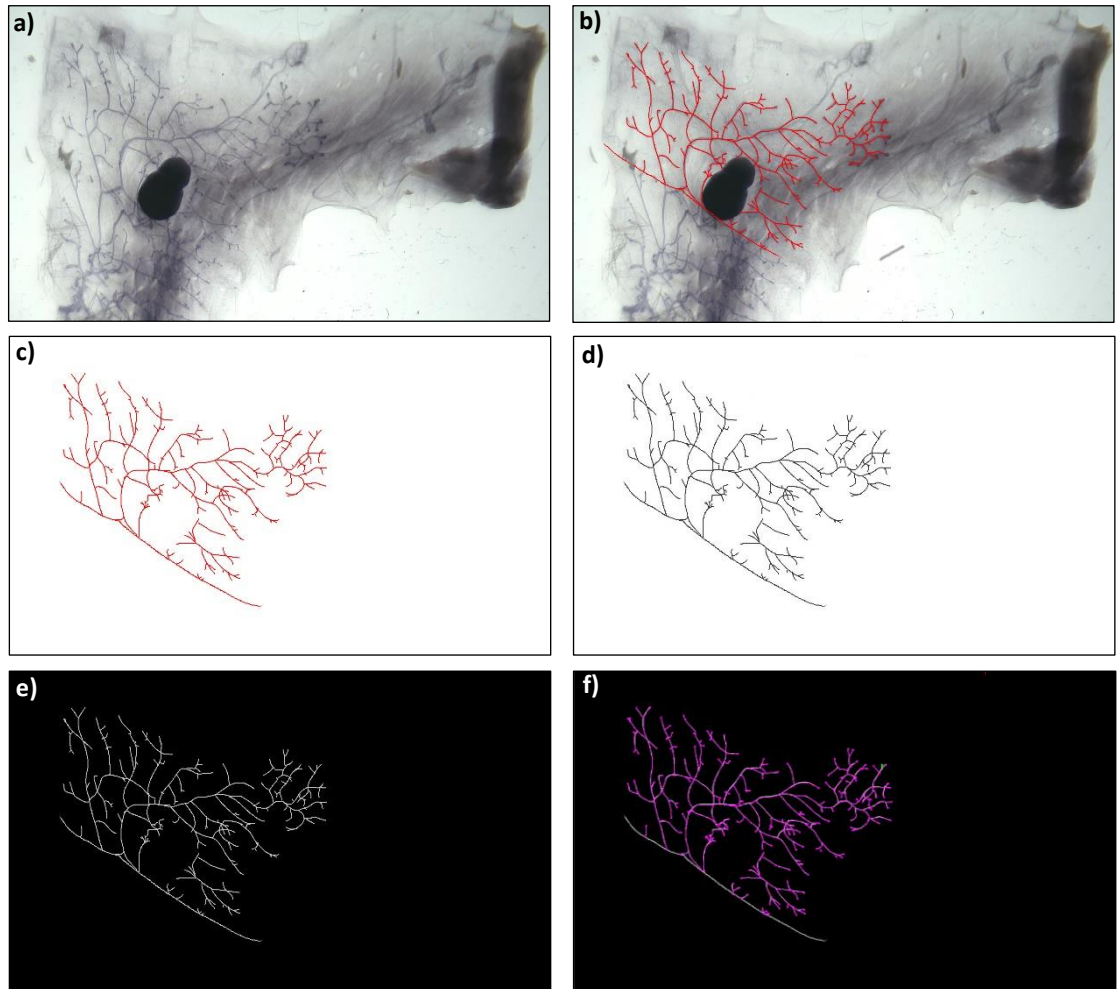
Figure 9.3 Quantification of mammary gland epithelial outgrowth in a pubertal gland after whole gland staining (WGS). Cre-negative and Cre-positive animals underwent the pubertal Tamoxifen regimen described in section 3. Following WGS epithelial outgrowth was quantified. **a)** Representative image of harvested number four mammary gland post WGS. **b)** The mammary epithelium is manually sketched to create a mask of the epithelium extending beyond the base of the lymph node. **c-e)** The mask of the epithelium is opened with ImageJ (c), Simple Neurite Tracer is loaded creating a copy of the mask in 8-bit (d) and is manually inverted to aid with quantification (e). **f)** Simple Neurite Tracer is used to mirror the mask (pink) and quantify the measured area.
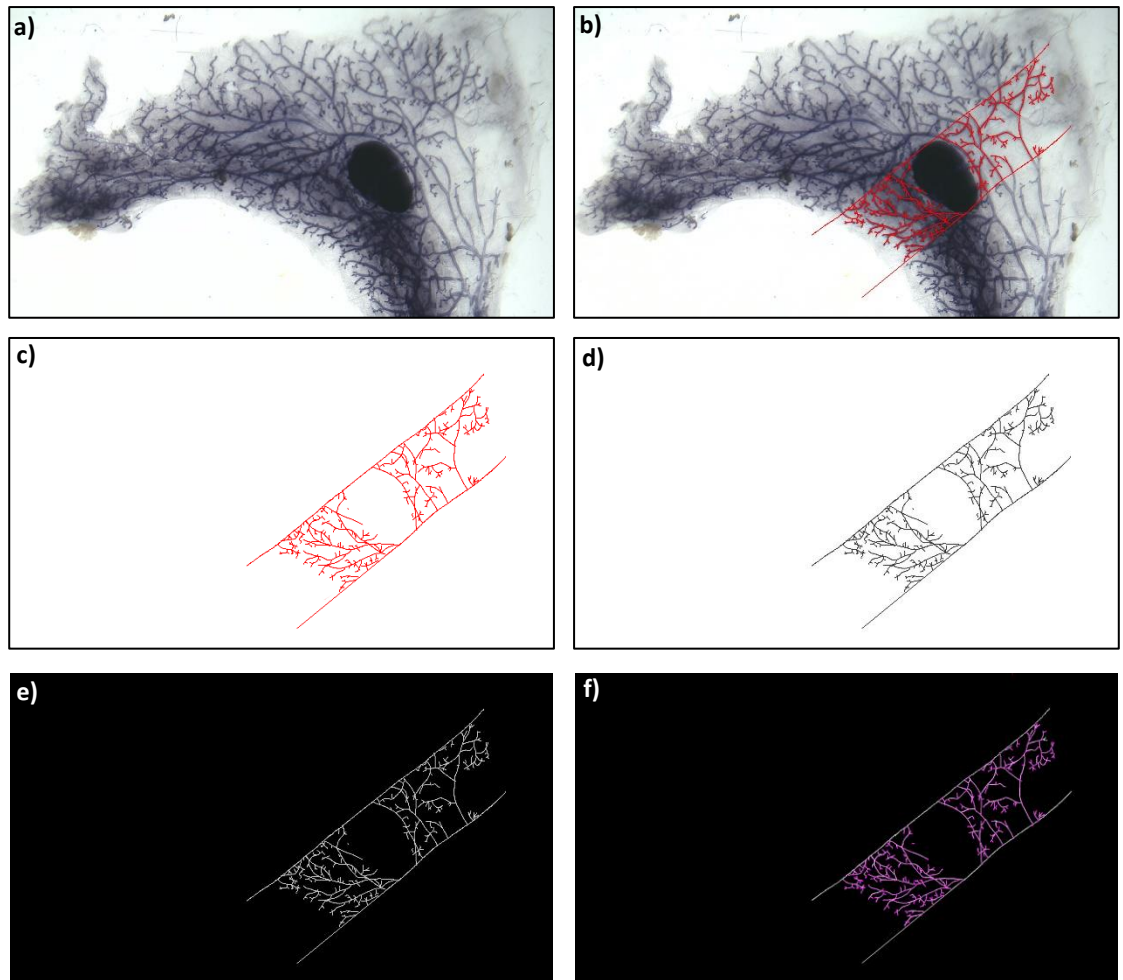
Figure 9.4 Quantification of mammary gland epithelial outgrowth in a E10.5 pregnant mammary gland after whole gland staining (WGS). Cre-negative and Cre-positive animals underwent the pregnancy Tamoxifen regimen described in chapter 3.2. Following WGS epithelial outgrowth was quantified. **a)** Representative image of harvested number four mammary gland post WGS. **b)** The mammary epithelium is manually sketched to create a mask of the epithelium adjacent to the lymph node; left and right. **c-e)** The mask of the epithelium is opened with ImageJ (c), Simple Neurite Tracer is loaded creating a copy of the mask in 8-bit (d) and is manually inverted to aid with quantitation (e). **f)** Simple Neurite Tracer is used to mirror the mask (pink) and quantify the measured area.
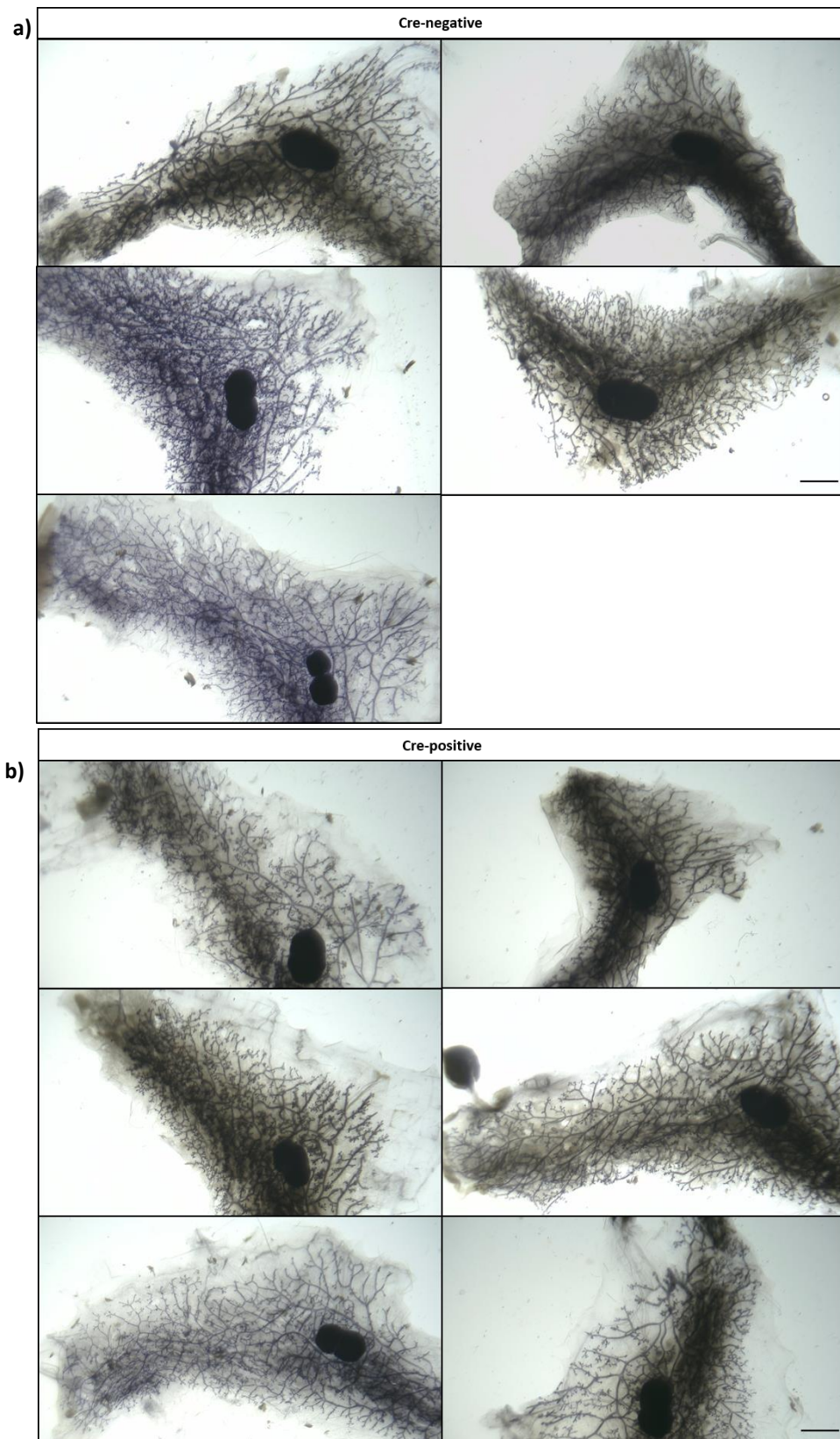
Figure 9.5 All E10.5 whole gland stain images. Cre-negative and Cre-positive animals underwent the pregnancy Tamoxifen regimen described in chapter 3.2, underwent WGS and subsequently epithelial outgrowth was quantified. a) All Cre-negative E10.5 glands. **b)** All Cre-positive E10.5 glands. Cre-negative, N=5, Cre-positive, N=6. Scale bar = 2mm.
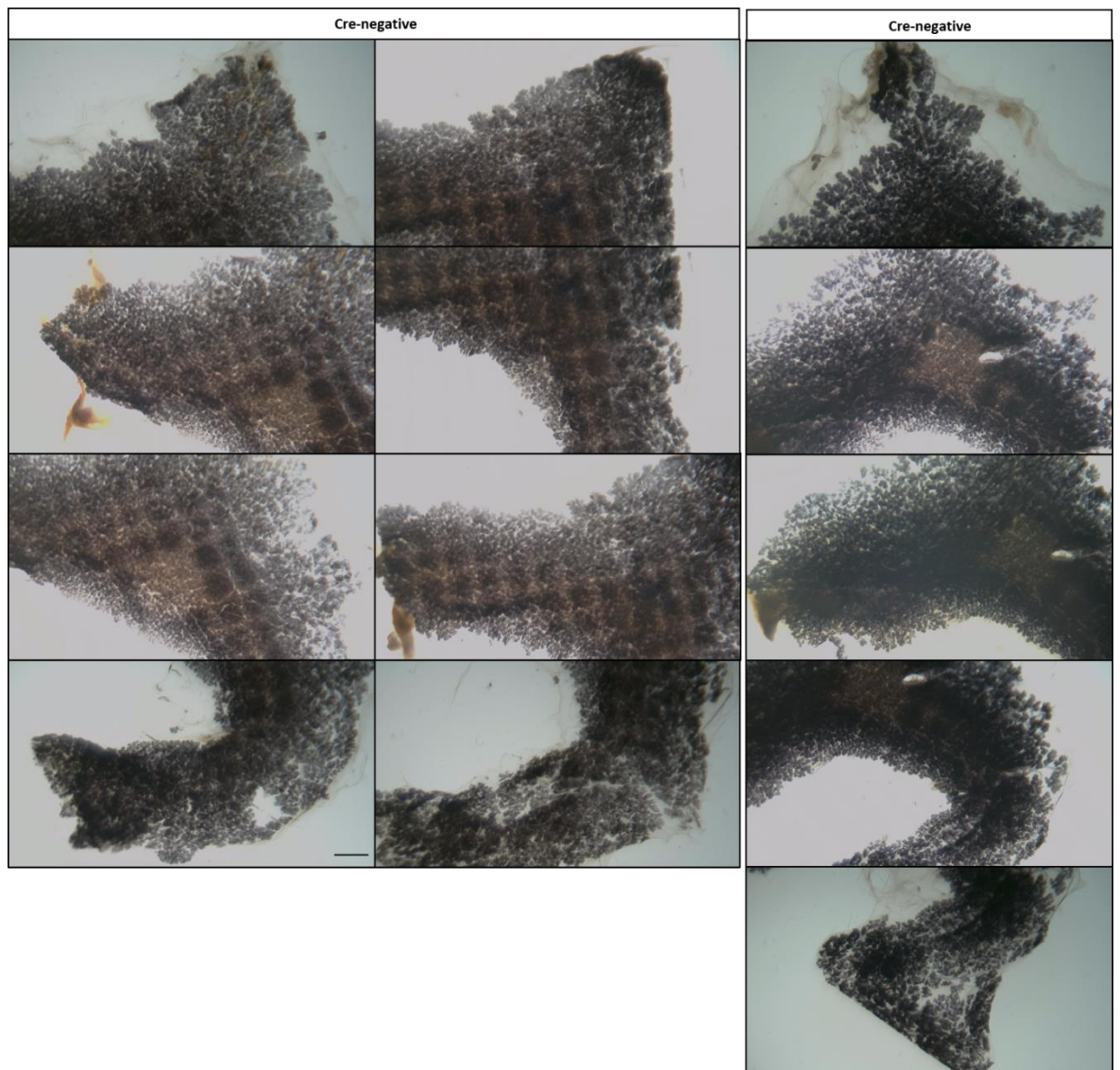
Figure 9.6 All lactating (P2) whole gland stain images. Cre-negative and Cre-positive animals underwent the pregnancy Tamoxifen regimen described in section 3.2. a) All Cre-negative P2 glands. **b)** All Cre-positive P2 glands. Cre-negative, N=2. Cre-positive, N=1. Scale bar = 2mm.
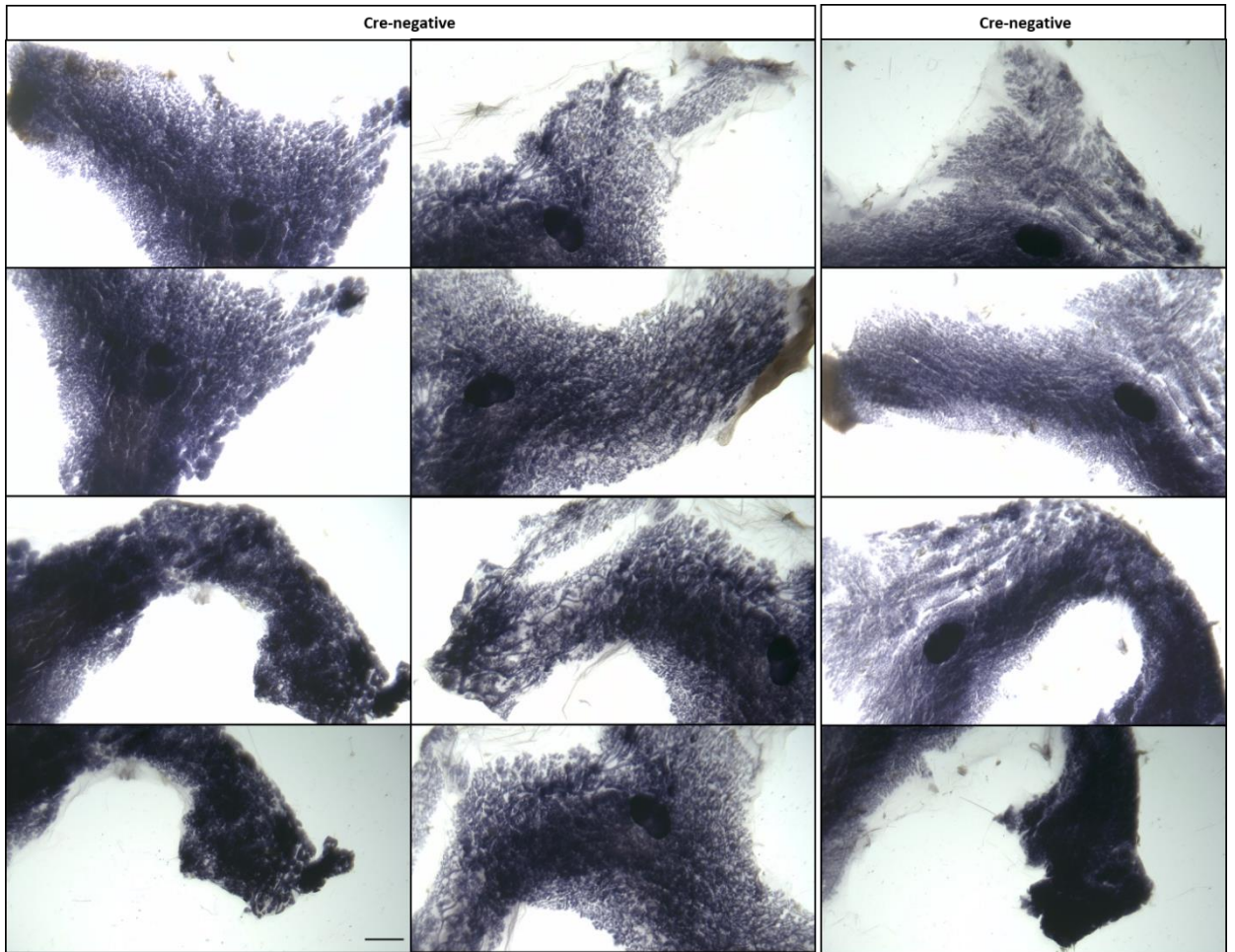
Figure 9.7 All involuting (P12) whole gland stain images. Cre-negative and Cre-positive animals underwent the pregnancy Tamoxifen regimen described in section 3.2. a) All Cre-negative P12 glands. **b)** All Cre-positive P12 glands. Cre-negative, N=2. Cre-positive, N=1. Scale bar = 2mm.
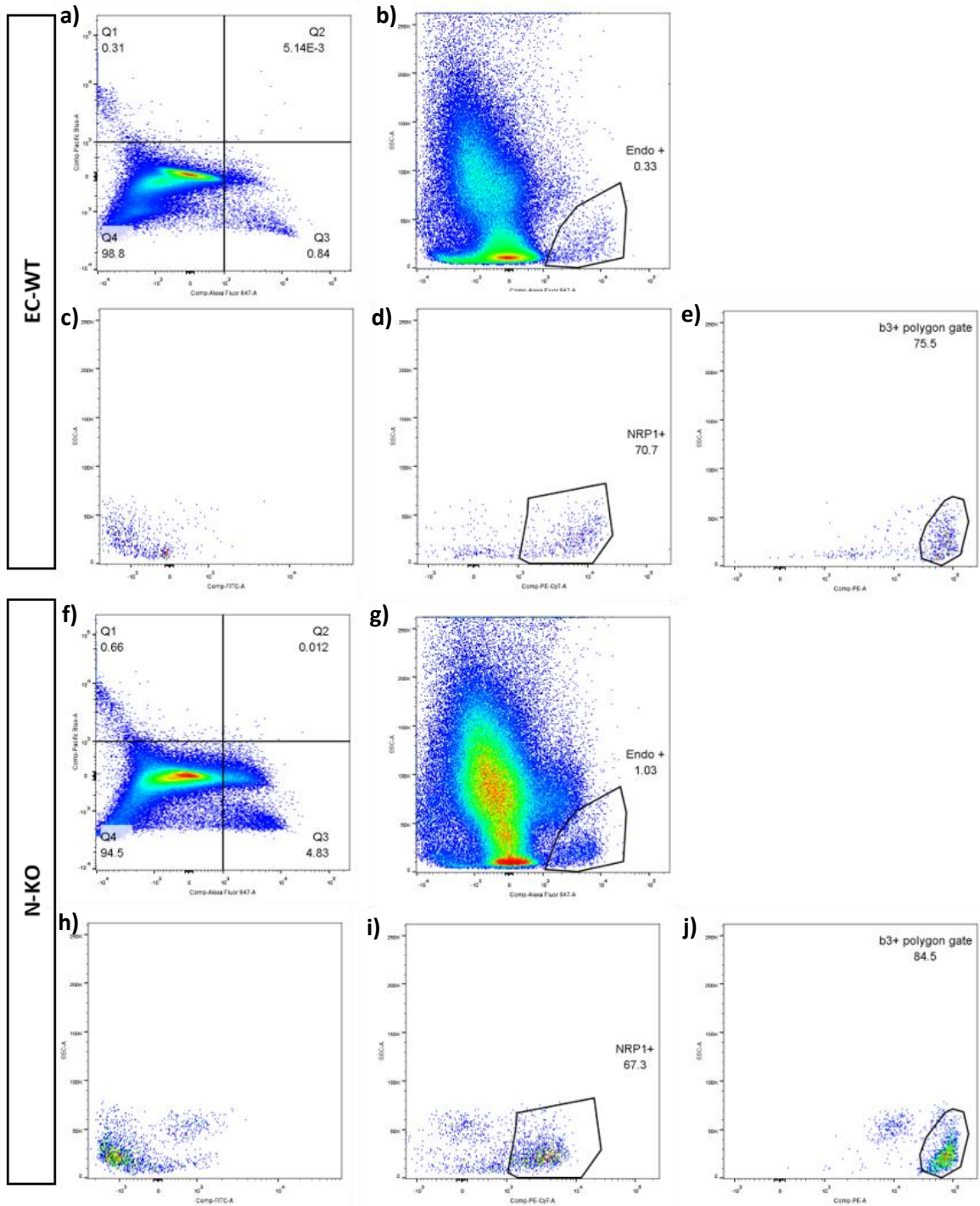
Figure 9.8 Flow cytometric analysis on Nrp1^{fl/fl}.Pdgfb.iCreERT2^(pos/neg) tumours proves ineffective at identifying ECs, preventing confirmation of target deletion. Nrp1$^{fl/fl}$.Pdgfb.iCreER$^{T2(pos/neg)}$ mice were implanted with 1x10^5 B6BO1 breast carcinoma cells, orthotopically into the abdominal mammary gland (section 2.4) following the experimental regimen shown in Figure. 6.1. Both EC-WT, top panel, and N-KO, bottom panel, tumours were stained and gated on endothelial markers CD31 (eFlour450) and endomucin (AF647). **a-b, f-g)** The lack of positive staining for CD31 resulted in subsequent gating for target deletion being performed on endomucin alone. **c-e)** EC-WT staining for integrin-α5 (FITC), integrin-β3 (PE) and neuropilin-1 (PE/Cy7), gated on the endomucin population. **h-j)** EC-WT staining for integrin-α5 (FITC), integrin-β3 (PE) and neuropilin-1 (PE/Cy7), gated on the endomucin population.
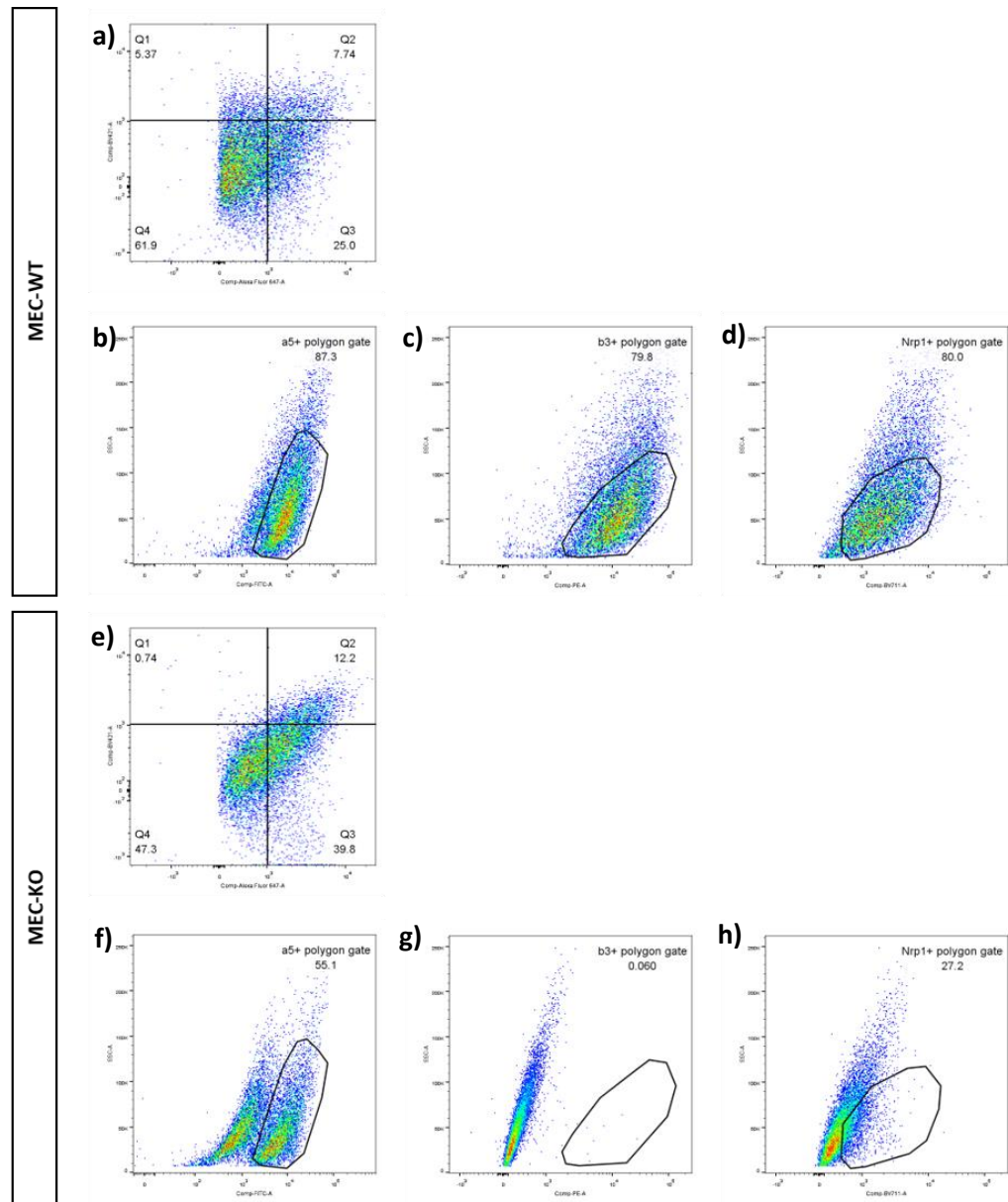
Figure 9.9 Using confirmed MEC-WT and MEC-KO cells to optimise tumour EC flow cytometry did not provide a straightforward answer. MECs were seeded into pre-coated flasks containing 0.1% gelatin and grown to confluency before being prepared for flow cytometry as described in section 2.9.1.2. Both MEC-WT, top panel, and MEC-KO, bottom panel, cells were stained and gated on endothelial markers Cdh5 (BV421) and endomucin (AF647). **a, e)** Despite western blot analysis proving these markers to be expressed in MECs, only a small proportion expressed both markers. Cells positive for both markers were gated on for target deletion. **b-d)** Subsequent MEC-WT staining for integrin-α5 (FITC), integrin-β3 (PE) and neuropilin-1 (BV711) shows all MEC-WT cells express all three targets. **f-h)** Subsequent MEC-KO staining for integrin-α5 (FITC), integrin-β3 (PE) and neuropilin-1 (BV711) shows a mixed population of MEC-KO cells expressing integrin- α5 with no expression of integrin-β3 and neuropilin-1.
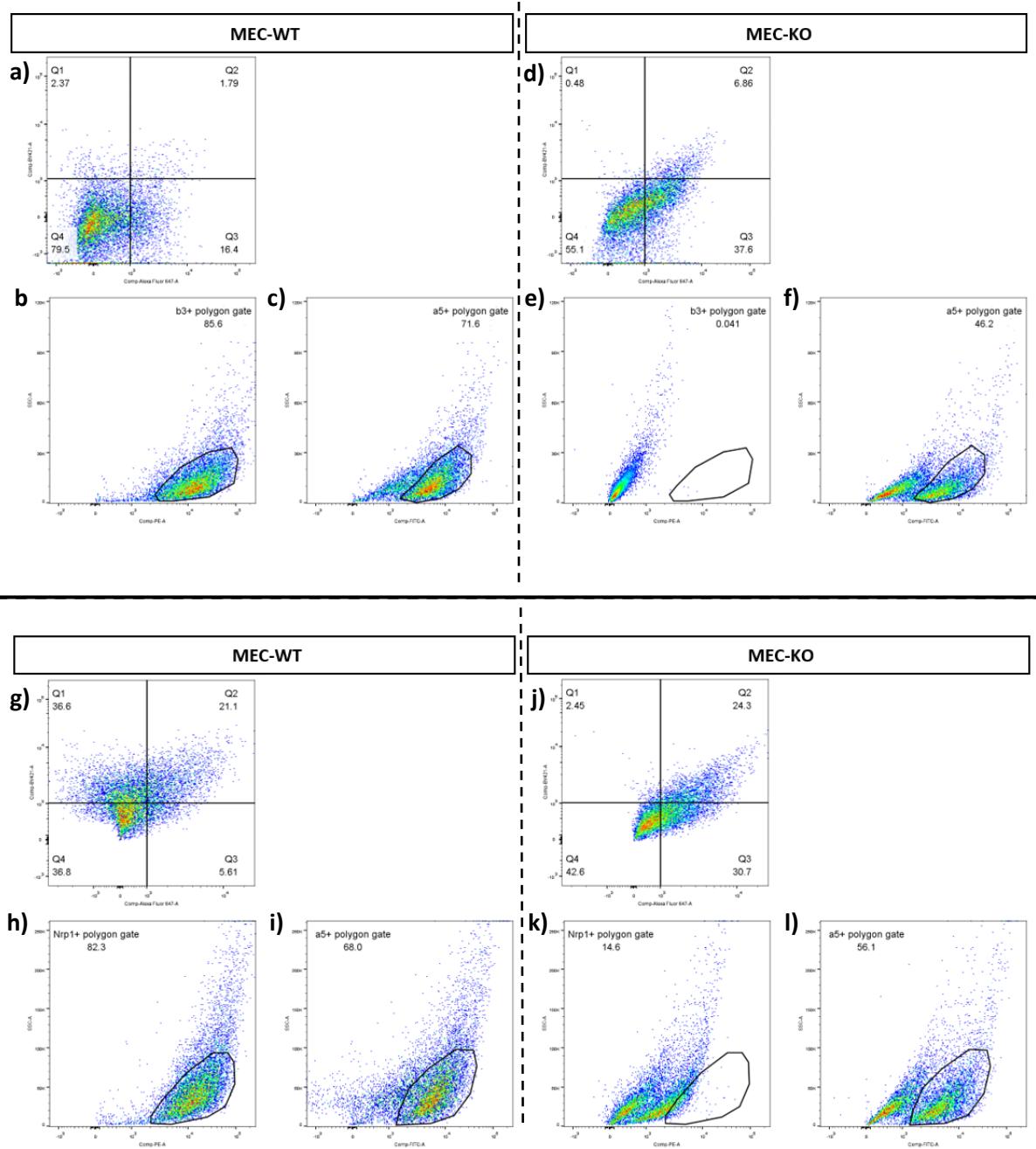
Figure 9.10 Further tumour EC flow optimisation using confirmed MEC-WT and MEC-KO cells, using a simplified antibody panel, yielded no improvement in optimisation. MECs were seeded into pre-coated flasks containing 0.1% gelatin and grown to confluency before being prepared for flow cytometry as described in section 2.9.1.2 – this panel of optimisation used the same fluorophore, separately, for two separate targets, specifically PE for integrin-β3 (top panel) and neuropilin-1 (bottom panel). **Top panel – a, d)** MECs cells were stained and gated on endothelial markers Cdh5 (BV421) and endomucin (AF647). **b-c)** Subsequent MEC-WT staining for integrin-α5 (FITC), integrin-β3 (PE) shows all MEC-WT cells express both targets. **e-f)** Subsequent MEC-KO staining for integrin-α5 (FITC), integrin-β3 (PE) shows a mixed population of MEC-KO cells expressing integrin- α5 with no expression of integrin-β3. The bottom panel shows the same as the top, with neuropilin-1 in PE as opposed to integrin-β3.
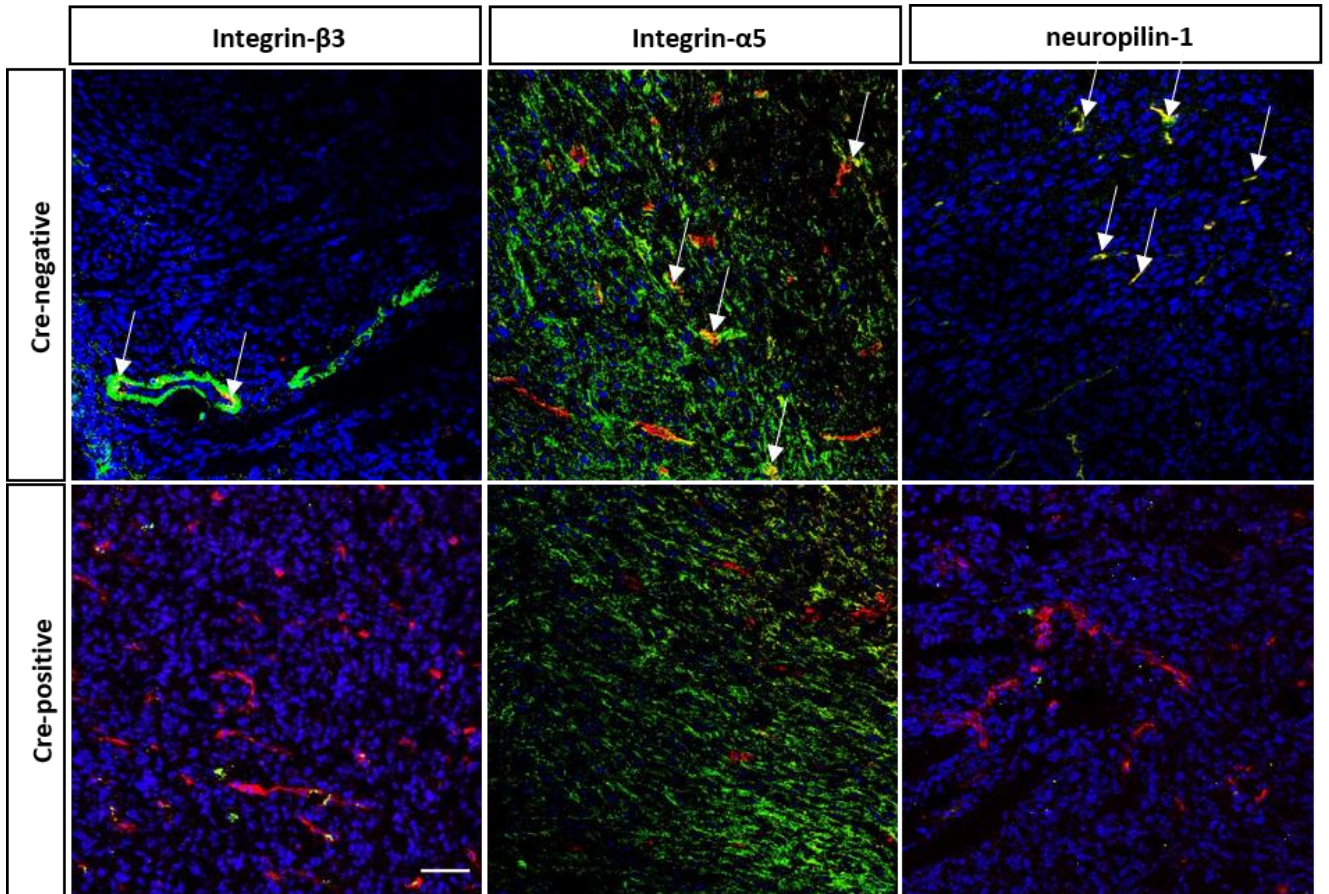
Figure 9.11 Immunofluorescent staining of tumours derived from triple floxed GEMMs for our targets confirms target deletion. Triple floxed female GEMMs implanted with 1×10^5 B6BO1 breast carcinoma cells, orthotopically into the inguinal mammary gland following the experimental regimen shown in **Figure 6.1a**. **a)** Representative images of Cre-negative staining for DAPI (blue), endomucin (red) and respective target (labelled above – green). **b)** Representative images of Cre-positive staining for DAPI (blue), endomucin (red) and respective target (labelled above – green). White arrows indicate areas of overlap (yellow) between endomucin (red) and target (green).
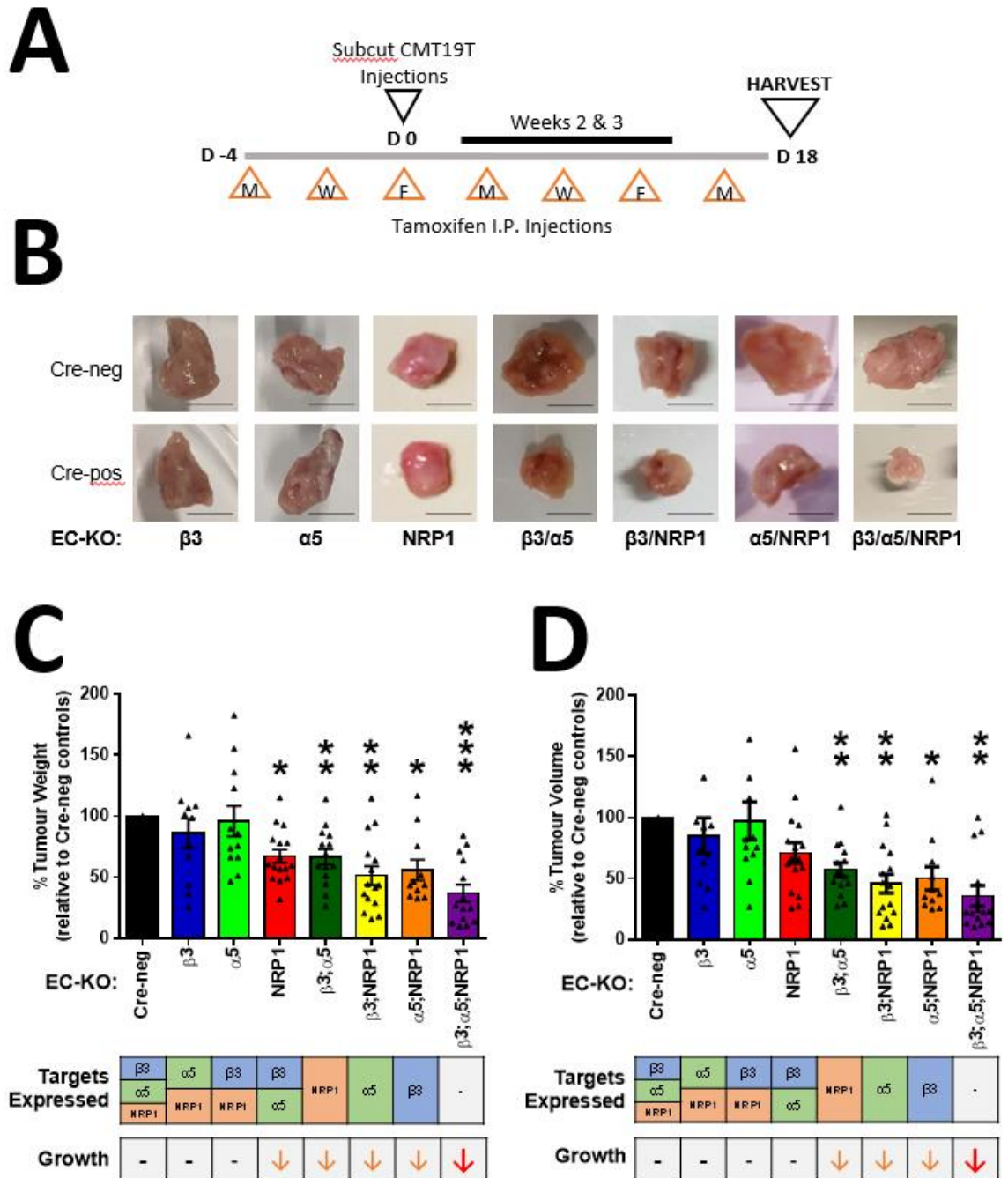
Figure 9.12 Co-depletion of endothelial fibronectin receptors impairs tumour angiogenesis. CMT19T lung carcinoma cells (1×10^6) were implanted subcutaneously into the flank of GEMMs and allowed to grow for 18 days. **(A)** Experimental schematic – thrice weekly (Monday, Wednesday & Friday) I.P. injections of Tamoxifen (75 mg/kg bodyweight) were administered for the duration of the experiment, inducing Cre-recombinase activity. **(B)** Representative images of CMT19T tumours harvested following 18 days of growth (Scale bar = 1 cm) (N =3, n ≥ 11 mice). **(C & D)** Ex vivo tumour measurements were expressed as a percentage of the average growth of their Cre-negative littermate controls. **(C)**. Tumour weight at Day 18. **(D)** Tumour volume at Day 18 calculated by the formula: length x width2 x 0.52. S.E.M. displayed as error bars. (* = P<0.05), (** = P<0.01), (*** P<0.001). Work by Dr Robert Johnson.
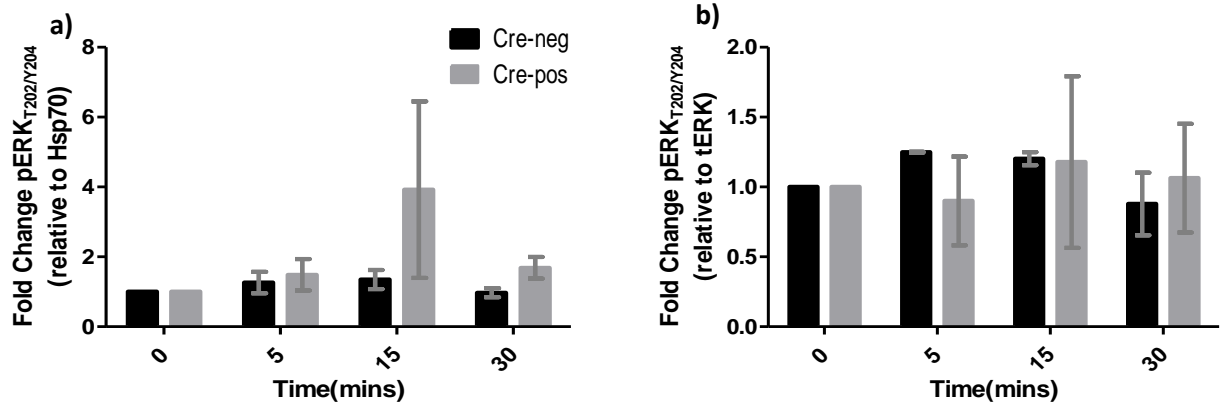
Figure 9.13 VEGF stimulation of triple-depleted lung ECs (LECs) shows a dampened response to VEGF as determined through phosphorylated ERK (pERK) expression. PyMT immortalised LECs (LEC-WT and LEC-KO$^{\beta3/\alpha5/Nrp1}$) were seeded onto fibronectin and were subsequently treated with VEGF for 0, 5 15 and 30 minutes. Post-treatment, cells were lysed and western blot analysis was performed to compare protein expression between LEC-WT and LEC-KO$^{\beta3/\alpha5/Nrp1}$. **a-b)** Densitometric analysis of western blot (a) normalised to Hsp70 or total ERK (b). N=2. Work by Dr Robert Johnson.

Figure 9.14 Microarray plate layout and sample comparisons made. MECs and LECs were seeded overnight onto pre-coated fibronectin plates and treated the following day with either VEGF, S or PS. **a)** Position of respective samples, their treatments and comparisons made (red and blue arrows). **b)** Sample IDs and the respective comparison made.

10 Abbreviations

Ab – Antibody

ABL – Abelson tyrosine-protein kinase

ADAM – A disintegrin and metalloproteinases

AKT – Protein Kinase B or RAC-alpha serine/threonine-protein kinase

ANG – Angiopoietin

BC – Breast cancer

BM – Basement membrane

BRCA – Breast cancer gene

BSA – Bovine serum albumin

CDC42 – Cell division control protein 42

CDH5 – Vascular endothelial cadherin

CTCF – Corrected total cell fluorescence

DAG – Diacylglycerol

DAPI – 4'6-diamidino-2-phenylindole

DB – Decidua

dH$_2$O – Distilled water

DKK1 – Dickkopf-related protein-1

DLL4 – Delta-like ligand 4

DMEM – Dulbecco's modified eagle medium

DR – Death receptor

E(x) – Embryonic day (x)

EC – Endothelial cell

EC-KO – Endothelial cell knock-out

ECL – Enhanced chemiluminescence

ECM – Extracellular matrix

EC-WT – Endothelial cell wildtype

EDTA – Ethylenediaminetetraacetic acid

eNOS – NO synthase

ER – Estrogen receptor

ERG – ETS related gene

ERK – Extracellular regulated kinase

ESB – Electrophoresis sample buffer

EtOH – Ethanol

F-12 – Ham's F12 nutrient mixture

FACS – Fluorescent-activated cell sorting

FAK – Focal adhesion kinase

FBS – Fetal bovine serum

FGF – Fibroblast growth factor

Fl – Floxed

Floxed – flanked by loxP sites

FN – Fibronectin

GAPDH – Glyceraldehyde 3-phosphate dehydrogenase

GEMM – Genetically engineered mouse model

GIMP – GNU Image Manipulation Program

GPCR – G-protein coupled receptor

H&E – Haematoxylin and eosin

HBSS – Hank's balanced salt solution

HCl – Hydrochloric acid

HER – Human epidermal growth factor receptor

HIF-1 – Hypoxia inducible factors

HR – Hormone receptor

HRP – Horse radish peroxidase

HSCs – Hematopoietic stem cells

Hsp70 – Heat shock protein-70

I.P. – Intraperitoneal

IA – Intussusceptive angiogenesis

IAR – Intussusceptive Arborisation

IBR – Intussusceptive Branching Remodelling

ICC – Immunocytochemistry

ICM – Inner cell mass

IF – Immunofluorescence

IHC – Immunohistochemistry

IMG – Intussusceptive Microvascular Growth

IMMLEC – Immortalised mouse lung endothelial cell

IP3 – Inositol trisphosphate

JAK – Janus Kinase

JZ – Junctional zone

KO – Knock-out

LEC – Lung microvascular endothelial cell

LEC-KO – Lung microvascular endothelial cell Knock-out

LEC-WT – Lung microvascular endothelial cell wildtype

LIF – Leukaemia Inhibitory Facto

LYVE-1 – Lymphatic vessel endothelial hyaluronan receptor-1

LZ – Labyrinth zone

M' – Molecular weight

mAb – Monoclonal antibody

MACS – Magnetic activated cell sorting

MAPK – Mitogen activated protein kinase

MEC – Mammary endothelial cell

MEC-KO – Mammary endothelial cell Knock-out

MEC-WT – Mammary endothelial cell wildtype

MeOH – Methanol

MFP – Mammary fat pad

MLEC – Mouse lung endothelial cell

MMP – Matrix metalloproteases

MMTV-PyMT – Mammary tumour virus-polyoma middle tumour-antigen

MOPS – (3-(N-morpholino)propanesulfonic acid)

NO – Nitric oxide

Nrp1 – Neuropilin-1

o/n – Overnight

p38 – p38 mitogen-activated protein kinase

PAGE – Polyacrylamide gel electrophoresis

PBS – Phosphate buffered saline

PBSTw – PBS supplemented with 0.1% Tween-20

PCR – Polymerase chain reaction

PDGF – Platelet derived growth factor

PECAM1 – Platelet and endothelial cell adhesion molecule-1

PFA – Paraformaldehyde

PgR – Progesterone receptor

PI3K – Phosphoinositide 3-kinase

PL – Prolactin

PLC- γ – Phospholipase C gamma

PLGF – Placenta Growth Factor

PLR – Prolactin receptor

PROX-1 – Prospero homeobox protein-1

PS – Pregnant serum

RFP – Red fluorescent protein

ROI – Region of interest

S – Serum

SA – Sprouting angiogenesis

SDF-1 – Stromal cell-derived factor-1

SDS – Sodium dodecyl sulfate

SEM – Standard error of the mean

Src – proto-oncogene tyrosine protein kinase

STAT – Signal Transducer and Activator of Transcription

TE – Tris-HCl-EDTA

TEB – Terminal end bud

TGC – Trophoblast giant cell

TGF-β – Transforming growth factor-β

TIMP – Tissue inhibitors of metalloproteinases

TNF-α – Tumour Necrosis Factor-α

TNM – Tumour Node Metastasis

TOPGAL – TCF Optimal Promoter-beta-GALactosidase

VASP – Vasodilator-stimulated phosphoprotein

VEGF – Vascular endothelial growth factor

VEGFR – Vascular endothelial growth factor receptor

VIM – Vimentin

WGS – Whole gland stain

Wnts – Wingless-related integration sites

WT – Wildtype

11 References

[1]   Noden, D.M. (1989) Embryonic Origins and Assembly of Blood Vessels. *American Review of Respiratory Disease*. 140 (4), 1097–1103.

[2]   Demir, R., Kaufmann, P., Castellucci, M., Erbengi, T., and Kotowski, A. (1989) Fetal Vasculogenesis and Angiogenesis in Human Placental Villi. *Cells Tissues Organs*. 136 (3), 190–203.

[3]   Conway, E.M., Collen, D., and Carmeliet, P. (2001) Molecular mechanisms of blood vessel growth. *Cardiovascular Research*. 49 (3), 507–521.

[4]   Patan, S. (2000) Vasculogenesis and angiogenesis as mechanisms of vascular network formation, growth and remodeling. *Journal of Neuro-Oncology*. 50 (1–2), 1–15.

[5]   Chung, A.S. and Ferrara, N. (2011) Developmental and Pathological Angiogenesis. *Annual Review of Cell and Developmental Biology*. 27 (1), 563–584.

[6]   His Wilhelm (1868) Untersuchungen über die erste Anlage des Wirbelthierleibes: die erste … - Wilhelm His - Google Books. *FCW Vogel*. Vol. 1.

[7]   Risau, W., Sariola, H., Zerwes, H.-G., Sasse, J., Ekblom, P., Kemler, R., et al. (1988) Vasculogenesis and angiogenesis in embryonic-stem-cell-derived embryoid bodies. .

[8]   Haase, K. and Kamm, R.D. (2017) Advances in on-chip vascularization. *Regenerative Medicine*. 12 (3), 285–302.

[9]   Patel-Hett, S. and D'Amore, P.A. (2011) Signal transduction in vasculogenesis and developmental angiogenesis. *International Journal of Developmental Biology*. 55 (4–5), 353–369.

[10]   Bautch, V.L. (2011) Stem cells and the vasculature. *Nature Medicine*. 17 (11), 1437–1443.

[11]   Park, C., Kim, T.M., and Malik, A.B. (2013) Transcriptional Regulation of Endothelial Cell and Vascular Development. *Circulation Research*. 112 (10),.

[12]   Risau, W. and Flamme, I. (1995) Vasculogenesis. *Annual Review of Cell and Developmental Biology*. 11 (1), 73–91.

[13]   Risau, W. (1991) Embryonic angiogenesis factors. *Pharmacology and Therapeutics*. 51 (3), 371–376.

[14]   Schatteman, G.C. and Awad, O. (2004) Hemangioblasts, Angioblasts, and Adult Endothelial

Cell Progenitors. *Anatomical Record - Part A Discoveries in Molecular, Cellular, and Evolutionary Biology*. 276 (1), 13–21.

[15]   Tsuji-Tamura, K. and Ogawa, M. (2018) Morphology regulation in vascular endothelial cells. *Inflammation and Regeneration*. 38 (1), 25.

[16]   Herbert, S.P. and Stainier, D.Y.R. (2011) Molecular control of endothelial cell behaviour during blood vessel morphogenesis. *Nature Reviews Molecular Cell Biology*. 12 (9), 551–564.

[17]   Vokes, S.A. and Krieg, P.A. (2002) Endoderm does not specify angioblasts. .

[18]   Huber, T.L., Kouskoff, V., Joerg Fehling, H., Palis, J., and Keller, G. (2004) Haemangioblast commitment is initiated in the primitive streak of the mouse embryo. *Nature*. 432 (7017), 625–630.

[19]   Ramírez-Bergeron, D.L., Runge, A., Dahl, K.D.C., Fehling, H.J., Keller, G., and Simon, M.C. (2004) Hypoxia affects mesoderm and enhances hemangioblast specification during early development. *Development*. 131 (18),.

[20]   Wang, Z., Cohen, K., Shao, Y., Mole, P., Dombkowski, D., and Scadden, D.T. (2003) Ephrin receptor, EphB4, regulates ES cell differentiation of primitive mammalian hemangioblasts, blood, cardiomyocytes, and blood vessels. *Blood*. 103 (1),.

[21]   Risau, W. and Flamme, L. (1995) V ASCULOGENESIS. *Cell Dev. Bioi*. 1 73–91.

[22]   Carstens, M. (2017) Pathologic anatomy of the soft palate, part 1: Embryology, the hard tissue platform, and evolution. *Journal of Cleft Lip Palate and Craniofacial Anomalies*. 4 (1), 37.

[23]   Nissen, N.N., Polverini, P.J., Koch, A.E., Volin, M. V, Gamelli, R.L., and DiPietro, L.A. (1998) Vascular endothelial growth factor mediates angiogenic activity during the proliferative phase of wound healing. *The American Journal of Pathology*. 152 (6), 1445–52.

[24]   Maas, J.W., Groothuis, P.G., Dunselman, G.A., de Goeij, A.F., Struyker Boudier, H.A., and Evers, J.L. (2001) Endometrial angiogenesis throughout the human menstrual cycle. *Human Reproduction (Oxford, England)*. 16 (8), 1557–1561.

[25]   Andres, A.C. and Djonov, V. (2010) The mammary gland vasculature revisited. *Journal of Mammary Gland Biology and Neoplasia*. 15 (3), 319–328.

[26]   Carmeliet, P. and Jain, R.K. (2000) Angiogenesis in cancer and other diseases. *Nature*. 407 (6801), 249–257.

[27]   Ucuzian, A.A., Gassman, A.A., East, A.T., and Greisler, H.P. (2010) Molecular mediators of angiogenesis. *Journal of Burn Care & Research : Official Publication of the American Burn Association*. 31 (1), 158–75.

[28]   Avraamides, C.J., Garmy-Susini, B., and Varner, J.A. (2008) Integrins in angiogenesis and lymphangiogenesis. *Nature Reviews Cancer*. 8 (8), 604–617.

[29]   Ogawa, S., Oku, A., Sawano, A., Yamaguchi, S., Yazaki, Y., and Shibuya, M. (1998) A Novel Type of Vascular Endothelial Growth Factor, VEGF-E (NZ-7 VEGF), Preferentially Utilizes KDR/Flk-1 Receptor and Carries a Potent Mitotic Activity without Heparin-binding Domain. *Journal of Biological Chemistry*. 273 (47), 31273–31282.

[30]   Holmes, K., Roberts, O.L., Thomas, A.M., and Cross, M.J. (2007) Vascular endothelial growth factor receptor-2: structure, function, intracellular signalling and therapeutic inhibition. *Cellular Signalling*. 19 (2007), 2003–2012.

[31]   Dvorak, H.F. (2000) VPF/VEGF and the angiogenic response. *Seminars in Perinatology*. 24 (1), 75–8.

[32]   Ferrara, N., Carver-Moore, K., Chen, H., Dowd, M., Lu, L., O'Shea, K.S., et al. (1996) Heterozygous embryonic lethality induced by targeted inactivation of the VEGF gene. *Nature*. 380 (6573), 439–442.

[33]   Carmeliet, P., Ferreira, V., Breier, G., & Pollefeyt, S. (1996) Abnormal blood vessel development and lethality in embryos lacking a single VEGF allele. *Nature*. 380 (6573), 435.

[34]   Ferrara, N., Gerber, H.-P., and LeCouter, J. (2003) The biology of VEGF and its receptors. *Nature Medicine*. 9 (6), 669–676.

[35]   Shibuya, M., Yamaguchi, S., Yamane, A., Ikeda, T., Tojo, A., Matsushime, H., et al. (1990) Nucleotide sequence and expression of a novel human receptor-type tyrosine kinase gene (flt) closely related to the fms family. *Oncogene*. 5 (4), 519–24.

[36]   Terman, B.I., Carrion, M.E., Kovacs, E., Rasmussen, B.A., Eddy, R.L., and Shows, T.B. (1991) Identification of a new endothelial cell growth factor receptor tyrosine kinase. *Oncogene*. 6 (9), 1677–83.

[37]   Yamaguchi, T.P., Dumont, D.J., Conlon, R.A., Breitman, M.L., Rossant, J., Uzan, G., et al. (1993) flk-1, an flt-related receptor tyrosine kinase is an early marker for endothelial cell precursors. *Development (Cambridge, England)*. 118 (2), 489–98.

[38]   Kendall, R.L. and Thomas, K.A. (1993) Inhibition of vascular endothelial cell growth factor activity by an endogenously encoded soluble receptor (endothelial ceils/mitogenic inhibitor/alternative transcription/angiogenesis). *Biochemistry*. 90 10705–10709.

[39]   Hiratsuka, S., Minowa, O., Kuno, J., Noda, T., and Shibuya, M. (1998) Flt-1 lacking the tyrosine kinase domain is sufficient for normal development and angiogenesis in mice. *Developmental Biology*. 95 9349–9354.

[40]   Shalaby, F., Rossant, J., Yamaguchi, T.P., Gertsenstein, M., Wu, X.F., Breitman, M.L., et al. (1995) Failure of blood-island formation and vasculogenesis in Flk-1-deficient mice. *Nature*. 376 (6535), 62–6.

[41]   Cross, M.J., Dixelius, J., Matsumoto, T., and Claesson-Welsh, L. (2003) VEGF-receptor signal transduction. *Trends in Biochemical Sciences*. 28 (9), 488–494.

[42]   Carmeliet, P. and Jain, R.K. (2011) Molecular mechanisms and clinical applications of angiogenesis. *Nature*. 473 (7347), 298–307.

[43]   Grainger, S.J. and Putnam, A.J. (2013) ECM Remodeling in Angiogenesis. in: pp. 185–209.

[44]   Mongiat, M., Andreuzzi, E., Tarticchio, G., and Paulitti, A. (2016) Extracellular matrix, a hard player in angiogenesis. *International Journal of Molecular Sciences*. 17 (11),.

[45]   Burri, P.H. and Djonov, V. (2002) Intussusceptive angiogenesis—the alternative to capillary sprouting. *Molecular Aspects of Medicine*. 23 (6), 1–27.

[46]   Djonov, V., Baum, O., and Burri, P.H. (2003) Vascular remodeling by intussusceptive angiogenesis. *Cell and Tissue Research*. 314 (1), 107–117.

[47]   Pugh, C.W. and Ratcliffe, P.J. (2003) Regulation of angiogenesis by hypoxia: role of the HIF system. *Nature Medicine*. 9 (6), 677–684.

[48]   Ward, J.P.T. (2008) Oxygen sensors in context. *Biochimica et Biophysica Acta - Bioenergetics*. 1777 (1), 1–14.

[49]   Fong, G.H. (2009) Regulation of angiogenesis by oxygen sensing mechanisms. *Journal of Molecular Medicine*. 87 (6), 549–560.

[50]   Krock, B.L., Skuli, N., and Simon, M.C. (2011) Hypoxia-Induced Angiogenesis: Good and Evil. *Genes and Cancer*. 2 (12), 1117–1133.

[51]   MARXSEN, J.H., STENGEL, P., DOEGE, K., HEIKKINEN, P., JOKILEHTO, T., WAGNER, T., et al.

(2004) Hypoxia-inducible factor-1 (HIF-1) promotes its degradation by induction of HIF-α-prolyl-4-hydroxylases. *Biochemical Journal*. 381 (3),.

[52]   Forsythe, J.A., Jiang, B.H., Iyer, N. V, Agani, F., Leung, S.W., Koos, R.D., et al. (1996) Activation of vascular endothelial growth factor gene transcription by hypoxia-inducible factor 1. *Molecular and Cellular Biology*. 16 (9), 4604–13.

[53]   Takahashi, H. and Shibuya, M. (2005) The vascular endothelial growth factor (VEGF)/VEGF receptor system and its role under physiological and pathological conditions. *Clinical Science*. 109 (3),.

[54]   Lakshmikanthan, S., Sobczak, M., Chun, C., Henschel, A., Dargatz, J., Ramchandran, R., et al. (2011) Rap1 promotes VEGFR2 activation and angiogenesis by a mechanism involving integrin αvβ3. *Blood*. 118 (7),.

[55]   Kopan, R. (2012) Notch signaling. *Cold Spring Harbor Perspectives in Biology*. 4 (10),.

[56]   Fryer, C.J., Lamar, E., Turbachova, I., Kintner, C., and Jones, K.A. (2002) Mastermind mediates chromatin-specific transcription and turnover of the notch enhancer complex. *Genes and Development*. 16 (11), 1397–1411.

[57]   Taylor, K.L., Henderson, A.M., and Hughes, C.C.W. (2002) Notch activation during endothelial cell network formation in vitro targets the basic HLH transcription factor HESR-1 and downregulates VEGFR-2/KDR expression. *Microvascular Research*. 64 (3), 372–383.

[58]   Holderfield, M.T. and Hughes, C.C.W. (2008) Crosstalk between vascular endothelial growth factor, notch, and transforming growth factor-β in vascular morphogenesis. *Circulation Research*. 102 (6), 637–652.

[59]   Phng, L.K. and Gerhardt, H. (2009) Angiogenesis: A Team Effort Coordinated by Notch. *Developmental Cell*. 16 (2), 196–208.

[60]   Gerhardt, H., Golding, M., Fruttiger, M., Ruhrberg, C., Lundkvist, A., Abramsson, A., et al. (2003) VEGF guides angiogenic sprouting utilizing endothelial tip cell filopodia. *Journal of Cell Biology*. 161 (6), 1163–1177.

[61]   Serini, G., Valdembri, D., and Bussolino, F. (2006) Integrins and angiogenesis: A sticky business. *Experimental Cell Research*. 312 (5), 651–658.

[62]   Neufeld, G., Cohen, T., Gengrinovitch, S., and Poltorak, Z. (1999) Vascular endothelial growth factor (VEGF) and its receptors. *FASEB Journal : Official Publication of the Federation*

of American Societies for Experimental Biology. 13 (1), 9–22.

[63]   Zhao, X. and Guan, J.-L. (2011) Focal adhesion kinase and its signaling pathways in cell migration and angiogenesis. *Advanced Drug Delivery Reviews*. 63 (8), 610–615.

[64]   Herbst, R.S. and Fidler, I.J. (2000) Angiogenesis and Lung Cancer: Potential for Therapy. *Clinical Cancer Research*. 6 (12),.

[65]   Betz, C., Lenard, A., Belting, H.G., and Affolter, M. (2016) Cell behaviors and dynamics during angiogenesis. *Development (Cambridge)*. 143 (13), 2249–2260.

[66]   Fantin, A., Vieira, J.M., Gestri, G., Denti, L., Schwarz, Q., Prykhozhij, S., et al. (2010) Tissue macrophages act as cellular chaperones for vascular anastomosis downstream of VEGF-mediated endothelial tip cell induction. *Blood*. 116 (5), 829–840.

[67]   Potente, M., Gerhardt, H., and Carmeliet, P. (2011) Basic and therapeutic aspects of angiogenesis. *Cell*. 146 (6), 873–887.

[68]   Jain, R.K. (2003) Molecular regulation of vessel maturation. *Nature Medicine*. 9 (6), 685–693.

[69]   Thurston, G., Suri, C., Smith, K., McClain, J., Sato, T.N., Yancopoulos, G.D., et al. (1999) Leakage-resistant blood vessels in mice transgenically overexpressing angiopoietin-1. *Science*. 286 (5449), 2511–2514.

[70]   Loughna, S. and Sato, T.N. (2001) Angiopoietin and Tie signaling pathways in vascular development. *Matrix Biology*. 20 (5–6), 319–325.

[71]   Logsdon, E.A., Finley, S.D., Popel, A.S., and MacGabhann, F. (2014) A systems biology view of blood vessel growth and remodelling. *Journal of Cellular and Molecular Medicine*. 18 (8), 1491–1508.

[72]   Kuijper, S., Turner, C.J., and Adams, R.H. (2007) Regulation of Angiogenesis by Eph-Ephrin Interactions. *Trends in Cardiovascular Medicine*. 17 (5), 145–151.

[73]   Gerety, S.S., Wang, H.U., Chen, Z.F., and Anderson, D.J. (1999) Symmetrical mutant phenotypes of the receptor EphB4 and its specific transmembrane ligand ephrin-B2 in cardiovascular development. *Molecular Cell*. 4 (3), 403–414.

[74]   Wang, H.U., Chen, Z.F., and Anderson, D.J. (1998) Molecular distinction and angiogenic interaction between embryonic arteries and veins revealed by ephrin-B2 and its receptor Eph-B4. *Cell*. 93 (5), 741–753.

[75]   Adams, R.H., Wilkinson, G.A., Weiss, C., Diella, F., Gale, N.W., Deutsch, U., et al. (1999) Roles of ephrinB ligands and EphB receptors in cardiovascular development: demarcation of arterial/venous domains, vascular morphogenesis, and sprouting angiogenesis. .

[76]   Héroult, M., Schaffner, F., and Augustin, H.G. (2006) Eph receptor and ephrin ligand-mediated interactions during angiogenesis and tumor progression. *Experimental Cell Research*. 312 (5), 642–650.

[77]   Krebs, L.T., Shutter, J.R., Tanigaki, K., Honjo, T., Stark, K.L., and Gridley, T. (2004) Haploinsufficient lethality and formation of arteriovenous malformations in Notch pathway mutants. *Genes and Development*. 18 (20), 2469–2473.

[78]   Matsumoto, T. and Claesson-Welsh, L. (2001) VEGF receptor signal transduction. *Science's STKE : Signal Transduction Knowledge Environment*. 2001 (112),.

[79]   Makanya, A.N., Hlushchuk, R., and Djonov, V.G. (2009) Intussusceptive angiogenesis and its role in vascular morphogenesis, patterning, and remodeling. *Angiogenesis*. 12 (2), 113–123.

[80]   Djonov, V., Schmid, M., Tschanz, S.A., and Burri, P.H. (2000) Intussusceptive Angiogenesis. *Circulation Research*. 86 (3),.

[81]   Caduff, J.H., Fischer, L.C., and Burri, P.H. (1986) Scanning electron microscope study of the developing microvasculature in the postnatal rat lung. *The Anatomical Record*. 216 (2), 154–164.

[82]   Burri, P.H. and Tarek, M.R. (1990) A novel mechanism of capillary growth in the rat pulmonary microcirculation. *The Anatomical Record*. 228 (1), 35–45.

[83]   Djonov, V.G., Kurz, H., and Burri, P.H. (2002) Optimality in the developing vascular system: Branching remodeling by means of intussusception as an efficient adaptation mechanism. *Developmental Dynamics*. 224 (4), 391–402.

[84]   Kurz, H., Burri, P.H., and Djonov, V.G. (2003) Angiogenesis and Vascular Remodeling by Intussusception: From Form to Function. *Physiology*. 18 (2),.

[85]   Styp-Rekowska, B., Hlushchuk, R., Pries, A.R., and Djonov, V. (2011) Intussusceptive angiogenesis: pillars against the blood flow. *Acta Physiologica*. 202 (3), 213–223.

[86]   Döme, B., Hendrix, M.J.C., Paku, S., Tóvári, J., and Tímár, J. (2007) Alternative Vascularization Mechanisms in Cancer: Pathology and Therapeutic Implications. *The American Journal of Pathology*. 170 (1), 1–15.

[87]   Levine, R.J., Maynard, S.E., Qian, C., Lim, K.-H., England, L.J., Yu, K.F., et al. (2004) Circulating Angiogenic Factors and the Risk of Preeclampsia. .

[88]   Krupinski, J., Kaluza, J., Kumar, P., Kumar, S., and Wang, J.M. (1994) Role of Angiogenesis in Patients With Cerebral Ischemic Stroke. .

[89]   Jenkinson, L., Bardhan, K.D., Atherton, J., and Kalia, N. (2002) Helicobacter pylori prevents proliferative stage of angiogenesis in vitro: Role of cytokines. *Digestive Diseases and Sciences*. 47 (8), 1857–1862.

[90]   Carmeliet, P. (2003) Angiogenesis in health and disease. *Nature Medicine*. 9 (6), 653–660.

[91]   Leong, T.T., Fearon, U., and Veale, D.J. (2005) Angiogenesis in psoriasis and psoriatic arthritis: clues to disease pathogenesis. *Current Rheumatology Reports*. 7 (4), 325–329.

[92]   Schrijvers, B.F., Flyvbjerg, A., Tilton, R.G., Lameire, N.H., and De Vriese, A.S. (2006) A neutralizing VEGF antibody prevents glomerular hypertrophy in a model of obese type 2 diabetes, the Zucker diabetic fatty rat. *Nephrol Dial Transplant*. 21 324–329.

[93]   Campochiaro, P.A. (2004) Ocular neovascularisation and excessive vascular permeability. *Expert Opinion on Biological Therapy*. 4 (9), 1395–1402.

[94]   FOLKMAN, J. (2002) Role of angiogenesis in tumor growth and metastasis. *Seminars in Oncology*. 29 (6), 15–18.

[95]   Hanahan, D. and Weinberg, R.A. (2000) The Hallmarks of Cancer. *Cell*. 100 (1), 57–70.

[96]   Algire, G.H., Chalkley, H.W., Legallais, F.Y., and Park, H.D. (1945) Vasculae reactions of normal and malignant tissues in vivo. i. vascular reactions of mice to wounds and to normal and neoplastic transplants. *Journal of the National Cancer Institute*. 6 (1), 73–85.

[97]   Folkman, J., Merler, E., Abernathy, C., and Williams, G. (1971) Isolation of a tumor factor responsible for angiogenesis. *Journal of Experimental Medicine*. 133 (2), 275–288.

[98]   Folkman, J. and Klagsbrun, M. (1987) Angiogenic factors. *Science*. 235 (4787), 442–447.

[99]   Hurwitz, H., Fehrenbacher, L., Novotny, W., Cartwright, T., Hainsworth, J., Heim, W., et al. (2004) Bevacizumab plus Irinotecan, Fluorouracil, and Leucovorin for Metastatic Colorectal Cancer. *New England Journal of Medicine*. 350 (23), 2335–2342.

[100]   Ilic, I., Jankovic, S., and Ilic, M. (2016) Bevacizumab combined with chemotherapy improves survival for patients with metastatic colorectal cancer: Evidence from meta analysis. *PLoS*

ONE. 11 (8),.

[101]   Ribatti, D., Annese, T., Ruggieri, S., Tamma, R., and Crivellato, E. (2019) Limitations of Anti-Angiogenic Treatment of Tumors. *Translational Oncology*. 12 (7), 981–986.

[102]   Nyberg, P., Xie, L., and Kalluri, R. (2005) Endogenous inhibitors of angiogenesis. *Cancer Research*. 65 (10), 3967–3979.

[103]   Rao, N., Lee, Y.F., and Ge, R. (2015) Novel endogenous angiogenesis inhibitors and their therapeutic potential. *Acta Pharmacologica Sinica*. 36 (10), 1177–1190.

[104]   Faivre, S., Demetri, G., Sargent, W., and Raymond, E. (2007) Molecular basis for sunitinib efficacy and future clinical development. *Nature Reviews Drug Discovery*. 6 (9), 734–745.

[105]   Jain, R.K., Duda, D.G., Clark, J.W., and Loeffler, J.S. (2006) Lessons from phase III clinical trials on anti-VEGF therapy for cancer. *Nature Clinical Practice Oncology*. 3 (1), 24–40.

[106]   Bergers, G. and Hanahan, D. (2008) Modes of resistance to anti-angiogenic therapy. *Nature Reviews Cancer*. 8 (8), 592–603.

[107]   Kung, A.L. (2006) Practices and Pitfalls of Mouse Cancer Models in Drug Discovery. *Advances in Cancer Research*. 96 191–212.

[108]   Le Tourneau, C., Raymond, E., and Faivre, S. (2007) Sunitinib: a novel tyrosine kinase inhibitor. A brief review of its therapeutic potential in the treatment of renal carcinoma and gastrointestinal stromal tumors (GIST). *Therapeutics and Clinical Risk Management*. 3 (2), 341–8.

[109]   Abrams, T.J., Murray, L.J., Pesenti, E., Walker Holway, V., Colombo, T., Lee, L.B., et al. (2003) Preclinical evaluation of the tyrosine kinase inhibitor SU11248 as a single agent and in combination with "standard of care" therapeutic agents for the treatment of breast cancer. *Molecular Cancer Therapeutics*. 2 (10),.

[110]   Kerbel, R.S., Guerin, E., Francia, G., Xu, P., Lee, C.R., Ebos, J.M.L., et al. (2013) Preclinical recapitulation of antiangiogenic drug clinical efficacies using models of early or late stage breast cancer metastatis. *The Breast*. 22 S57–S65.

[111]   Wilhelm, S., Carter, C., Lynch, M., Lowinger, T., Dumas, J., Smith, R.A., et al. (2006) Discovery and development of sorafenib: A multikinase inhibitor for treating cancer. *Nature Reviews Drug Discovery*. 5 (10), 835–844.

[112]   Madu, C.O., Wang, S., Madu, C.O., and Lu, Y. (2020) Angiogenesis in breast cancer

progression, diagnosis, and treatment. *Journal of Cancer*. 11 (15), 4474–4494.

[113]   Chen, M., Bao, L., Zhao, M., Cao, J., and Zheng, H. (2020) Progress in Research on the Role of FGF in the Formation and Treatment of Corneal Neovascularization. *Frontiers in Pharmacology*. 11 111.

[114]   Steri, V., Ellison, T.S., Gontarczyk, A.M., Weilbaecher, K., Schneider, J.G., Edwards, D., et al. (2014) Acute Depletion of Endothelial β3-Integrin Transiently Inhibits Tumor Growth and Angiogenesis in Mice. *Circulation Research*. 114 (1), 79–91.

[115]   Siemann, D.W. (2011) The unique characteristics of tumor vasculature and preclinical evidence for its selective disruption by Tumor-Vascular Disrupting Agents. *Cancer Treatment Reviews*. 37 (1), 63–74.

[116]   Nagy, J.A., Chang, S.H., Shih, S.C., Dvorak, A.M., and Dvorak, H.F. (2010) Heterogeneity of the tumor vasculature. *Seminars in Thrombosis and Hemostasis*. 36 (3), 321–331.

[117]   Ruoslahti, E. (2002) Specialization of tumour vasculature. *Nature Reviews Cancer*. 2 (2), 83–90.

[118]   Gee, M.S., Procopio, W.N., Makonnen, S., Feldman, M.D., Yeilding, N.M., and Lee, W.M.F. (2003) Tumor vessel development and maturation impose limits on the effectiveness of anti-vascular therapy. *American Journal of Pathology*. 162 (1), 183–193.

[119]   Hashizume, H., Baluk, P., Morikawa, S., McLean, J.W., Thurston, G., Roberge, S., et al. (2000) Openings between defective endothelial cells explain tumor vessel leakiness. *American Journal of Pathology*. 156 (4), 1363–1380.

[120]   Tong, R.T., Boucher, Y., Kozin, S. V., Winkler, F., Hicklin, D.J., and Jain, R.K. (2004) Vascular normalization by vascular endothelial growth factor receptor 2 blockade induces a pressure gradient across the vasculature and improves drug penetration in tumors. *Cancer Research*. 64 (11), 3731–3736.

[121]   Humphries, J.D., Byron, A., and Humphries, M.J. (2006) Integrin ligands at a glance. *Journal of Cell Science*. 119 (19),.

[122]   Brower, D.L., Brower, S.M., Hayward, D.C., Ball, E.E., Schmidt, A., Reichardt, L., et al. (1997) Molecular evolution of integrins: Genes encoding integrin   subunits from a coral and a sponge. *Proceedings of the National Academy of Sciences*. 94 (17), 9182–9187.

[123]   Hynes, R.O. (1992) Integrins: Versatility, modulation, and signaling in cell adhesion. *Cell*. 69

(1), 11–25.

[124]   Hynes, R.O. (2002) A reevaluation of integrins as regulators of angiogenesis. *Nature Medicine*. 8 (9), 918–921.

[125]   De Arcangelis, A. and Georges-Labouesse, E. (2000) Integrin and ECM functions: roles in vertebrate development. *Trends in Genetics*. 16 (9), 389–395.

[126]   Qin, J., Vinogradova, O., and Plow, E.F. (2004) Integrin Bidirectional Signaling: A Molecular View. *PLoS Biology*. 2 (6), e169.

[127]   Rüegg, C. and Mariotti, A. (2003) Vascular integrins: Pleiotropic adhesion and signaling molecules in vascular homeostasis and angiogenesis. *Cellular and Molecular Life Sciences*. 60 (6), 1135–1157.

[128]   Takagi, J., Petre, B.M., Walz, T., and Springer, T.A. (2002) Global conformational earrangements in integrin extracellular domains in outside-in and inside-out signaling. *Cell*. 110 (5), 599–611.

[129]   Schürpf, T. and Springer, T.A. (2011) Regulation of integrin affinity on cell surfaces. *EMBO Journal*. 30 (23), 4712–4727.

[130]   Margadant, C., Monsuur, H.N., Norman, J.C., and Sonnenberg, A. (2011) Mechanisms of integrin activation and trafficking. *Current Opinion in Cell Biology*. 23 (5), 607–614.

[131]   Wang, J.H. (2012) Pull and push: Talin activation for integrin signaling. *Cell Research*. 22 (11), 1512–1514.

[132]   Critchley, D.R. and Gingras, A.R. (2008) Talin at a glance. *Journal of Cell Science*. 121 (9), 1345–1347.

[133]   Das, M., Subbayya Ithychanda, S., Qin, J., and Plow, E.F. (2014) Mechanisms of talin-dependent integrin signaling and crosstalk. *Biochimica et Biophysica Acta - Biomembranes*. 1838 (2), 579–588.

[134]   Tadokoro, S., Shattil, S.J., Eto, K., Tai, V., Liddington, R.C., De Pereda, J.M., et al. (2003) Talin binding to integrin β tails: A final common step in integrin activation. *Science*. 302 (5642), 103–106.

[135]   Calderwood, D.A., Zent, R., Grant, R., Rees, D.J.G., Hynes, R.O., and Ginsberg, M.H. (1999) The talin head domain binds to integrin β subunit cytoplasmic tails and regulates integrin activation. *Journal of Biological Chemistry*. 274 (40), 28071–28074.

[136]   Zhang, Z., Vuori, K., Reed, J.C., and Ruoslahti, E. (1995) The alpha 5 beta 1 integrin supports survival of cells on fibronectin and up-regulates Bcl-2 expression. *Proceedings of the National Academy of Sciences of the United States of America*. 92 (13), 6161–5.

[137]   Charo, I.F., Nannizzi, L., Smith, J.W., and Cheresh, D.A. (1990) The vitronectin receptor alpha v beta 3 binds fibronectin and acts in concert with alpha 5 beta 1 in promoting cellular attachment and spreading on fibronectin. *The Journal of Cell Biology*. 111 (6),.

[138]   Savage, B., Shattil, S.J., and Ruggeri, Z.M. (1992) Modulation of platelet function through adhesion receptors. A dual role for glycoprotein IIb-IIIa (integrin alpha IIb beta 3) mediated by fibrinogen and glycoprotein Ib-von Willebrand factor. *The Journal of Biological Chemistry*. 267 (16), 11300–6.

[139]   Bennett, J.S. (2005) Structure and function of the platelet integrin alphaIIbbeta3. *The Journal of Clinical Investigation*. 115 (12), 3363–9.

[140]   Brooks, P.C., Clark, R.A., and Cheresh, D.A. (1994) Requirement of vascular integrin alpha v beta 3 for angiogenesis. *Science (New York, N.Y.)*. 264 (5158), 569–71.

[141]   van der Flier, A., Badu-Nkansah, K., Whittaker, C.A., Crowley, D., Bronson, R.T., Lacy-Hulbert, A., et al. (2010) Endothelial alpha5 and alphav integrins cooperate in remodeling of the vasculature during development. *Development (Cambridge, England)*. 137 (14), 2439–49.

[142]   Hynes, R.O. (2002) Integrins: bidirectional, allosteric signaling machines. *Cell*. 110 (6), 673–87.

[143]   Millard, M., Odde, S., and Neamati, N. (2011) Integrin Targeted Therapeutics. *Theranostics*. 1 154.

[144]   Kechagia, J.Z., Ivaska, J., and Roca-Cusachs, P. (2019) Integrins as biomechanical sensors of the microenvironment. *Nature Reviews Molecular Cell Biology*. 20 (8), 457–473.

[145]   He, Z. and Tessier-Lavigne, M. (1997) Neuropilin is a receptor for the axonal chemorepellent semaphorin III. *Cell*. 90 (4), 739–751.

[146]   Soker, S., Takashima, S., Miao, H.Q., Neufeld, G., and Klagsbrun, M. (1998) Neuropilin-1 is expressed by endothelial and tumor cells as an isoform- specific receptor for vascular endothelial growth factor. *Cell*. 92 (6), 735–745.

[147]   Takagi, S., Tsuji, T., Amagai, T., Takamatsu, T., and Fujisawa, H. (1987) Specific cell surface

labels in the visual centers of Xenopus laevis tadpole identified using monoclonal antibodies. *Developmental Biology*. 122 (1), 90–100.

[148]   Kitsukawa, T., Bekku, Y., Matsuda, Y., and Sanbo, M. (1999) A requirement for neuropilin-1 in embryonic vessel formation Genetic diversity of chickens and quail View project Cardiac Progenitor Cells View project. .

[149]   Kitsukawa, T., Shimono, A., Kawakami, A., Kondoh, H., and Fujisawa, H. (1995) Overexpression of a membrane protein, neuropilin, in chimeric mice causes anomalies in the cardiovascular system, nervous system and limbs. *Development*. 121 (12),.

[150]   Starzec, A., Vassy, R., Martin, A., Lecouvey, M., Di Benedetto, M., Crépin, M., et al. (2006) Antiangiogenic and antitumor activities of peptide inhibiting the vascular endothelial growth factor binding to neuropilin-1. *Life Sciences*. 79 (25), 2370–2381.

[151]   Pellet-Many, C., Frankel, P., Jia, H., and Zachary, I. (2008) Neuropilins: Structure, function and role in disease. *Biochemical Journal*. 411 (2), 211–226.

[152]   Nakamura, F. and Goshima, Y. (2002) Structural and functional relation of neuropilins. *Advances in Experimental Medicine and Biology*. 515 55–69.

[153]   Koch, S., Van Meeteren, L.A., Morin, E., Testini, C., Weströ, S., Bjö, H., et al. (2014) NRP1 Presented in trans to the Endothelium Arrests VEGFR2 Endocytosis, Preventing Angiogenic Signaling and Tumor Initiation. *Developmental Cell*. 28 633–646.

[154]   Fantin, A., Schwarz, Q., Davidson, K., Normando, E.M., Denti, L., and Ruhrberg, C. (2011) The cytoplasmic domain of neuropilin 1 is dispensable for angiogenesis, but promotes the spatial separation of retinal arteries and veins. *Development*. 138 (19), 4185–4191.

[155]   Gelfand, M. V., Hagan, N., Tata, A., Oh, W.J., Lacoste, B., Kang, K.T., et al. (2014) Neuropilin-1 functions as a VEGFR2 co-receptor to guide developmental angiogenesis independent of ligand binding. *ELife*. 3 e03720.

[156]   Chen, H., Chédotal, A., He, Z., Goodman, C.S., and Tessier-Lavigne, M. (1997) Neuropilin-2, a novel member of the neuropilin family, is a high affinity receptor for the semaphorins Sema E and Sema IV but not Sema III. *Neuron*. 19 (3), 547–559.

[157]   Favier, B., Alam, A., Barron, P., Bonnin, J., Laboudie, P., Fons, P., et al. (2006) Neuropilin-2 interacts with VEGFR-2 and VEGFR-3 and promotes human endothelial cell survival and migration. *Blood*. 108 (4), 1243–1250.

[158]   Sulpice, E., Plouët, J., Bergé, M., Allanic, D., Tobelem, G., and Merkulova-Rainon, T. (2008) Neuropilin-1 and neuropilin-2 act as coreceptors, potentiating proangiogenic activity. *Blood*. 111 (4), 2036–2045.

[159]   Vorbach, C., Capecchi, M.R., and Penninger, J.M. (2006) Evolution of the mammary gland from the innate immune system? *BioEssays*. 28 (6), 606–616.

[160]   Asselin-Labat, M.-L., Sutherland, K.D., Barker, H., Thomas, R., Shackleton, M., Forrest, N.C., et al. (2007) Gata-3 is an essential regulator of mammary-gland morphogenesis and luminal-cell differentiation. *Nature Cell Biology*. 9 (2), 201–9.

[161]   Djonov, V., Andres, A.C., and Ziemiecki, A. (2001) Vascular remodelling during the normal and malignant life cycle of the mammary gland. *Microscopy Research and Technique*. 52 (2), 182–189.

[162]   Cunha, G.R., Young, P., Christov, K., Guzman, R., Nandi, S., Talamantes, F., et al. (1995) Mammary phenotypic expression induced in epidermal cells by embryonic mammary mesenchyme. *Acta Anatomica*. 152 (3), 195–204.

[163]   Kratochwil, K. (1969) Organ specificity in mesenchymal induction demonstrated in the embryonic development of the mammary gland of the mouse. *Developmental Biology*. 20 (1), 46–71.

[164]   Kass, L., Erler, J.T., Dembo, M., and Weaver, V.M. (2007) Mammary epithelial cell: Influence of extracellular matrix composition and organization during development and tumorigenesis. *The International Journal of Biochemistry & Cell Biology*. 39 (11), 1987–1994.

[165]   Chu, E.Y., Hens, J., Andl, T., Kairo, A., Yamaguchi, T.P., Brisken, C., et al. (2004) Canonical WNT signaling promotes mammary placode development and is essential for initiation of mammary gland morphogenesis. *Development*. 131 (19),.

[166]   Sakakura, T. (1987) Embryogenesis. in: R. and F. Neville M.C. and Daniel C.W. Development (Ed.), Plenum Press, New Yorkpp. 37–65.

[167]   Cowin, P. and Wysolmerski, J. (2010) Molecular mechanisms guiding embryonic mammary gland development. *Cold Spring Harbor Perspectives in Biology*. 2 (6), a003251.

[168]   Foley, J., Dann, P., Hong, J., Cosgrove, J., Dreyer, B., Rimm, D., et al. (2001) Parathyroid hormone-related protein maintains mammary epithelial fate and triggers nipple skin differentiation during embryonic breast development. *Development (Cambridge, England)*. 128 (4), 513–25.

[169]   Drews, U. and Drews, U. (1977) Regression of mouse mammary gland anlagen in recombinants of Tfm and wild-type tissues: testosterone acts via the mesenchyme. *Cell*. 10 (3), 401–404.

[170]   Eblaghie, M.C., Song, S.-J., Kim, J.-Y., Akita, K., Tickle, C., and Jung, H.-S. (2004) Interactions between FGF and Wnt signals and Tbx3 gene expression in mammary gland initiation in mouse embryos. *Journal of Anatomy*. 205 (1), 1–13.

[171]   Howard, B.A. and Lu, P. (2014) Stromal regulation of embryonic and postnatal mammary epithelial development and differentiation. *Seminars in Cell and Developmental Biology*. 25–26 43–51.

[172]   Hens, J.R. and Wysolmerski, J.J. (2005) Key stages of mammary gland development: molecular mechanisms involved in the formation of the embryonic mammary gland. *Breast Cancer Research : BCR*. 7 (5), 220–4.

[173]   Howlin, J., McBryan, J., and Martin, F. (2006) Pubertal Mammary Gland Development: Insights from Mouse Models. *Journal of Mammary Gland Biology and Neoplasia*. 11 (3–4), 283–297.

[174]   Jackson-Fisher, A.J., Bellinger, G., Ramabhadran, R., Morris, J.K., Lee, K.-F., Stern, D.F., et al. (2004) ErbB2 is required for ductal morphogenesis of the mammary gland. *Proceedings of the National Academy of Sciences*. 101 (49), 17138–17143.

[175]   Richert, M.M., Schwertfeger, K.L., Ryder, J.W., and Anderson, S.M. (2000) An Atlas of Mouse Mammary Gland Development. *Journal of Mammary Gland Biology and Neoplasia*. 5 (2), 227–241.

[176]   Daniel, C.W., Silberstein, G.B., and Strickland, P. (1987) Direct Action of 17β-Estradiol on Mouse Mammary Ducts Analyzed by Sustained Release Implants and Steroid Autoradiography. *Cancer Research*. 47 (22),.

[177]   Kleinberg, D.L., Feldman, M., and Ruan, W. (2000) IGF-I: An Essential Factor in Terminal End Bud Formation and Ductal Morphogenesis. .

[178]   Brisken, C., Kaur, S., Chavarria, T.E., Binart, N., Sutherland, R.L., Weinberg, R.A., et al. (1999) Prolactin Controls Mammary Gland Development via Direct and Indirect Mechanisms. *Developmental Biology*. 210 (1), 96–106.

[179]   Ormandy, C.J., Camus, A., Barra, J., Damotte, D., Lucas, B., Buteau, H., et al. (1997) Null mutation of the prolactin receptor gene produces multiple reproductive defects in the

mouse. *Genes and Development*. 11 (2), 167–178.

[180] Gallego, M.I., Binart, N., Robinson, G.W., Okagaki, R., Coschigano, K.T., Perry, J., et al. (2001) Prolactin, growth hormone, and epidermal growth factor activate Stat5 in different compartments of mammary tissue and exert different and overlapping developmental effects. *Developmental Biology*. 229 (1), 163–175.

[181] Soyal, S., Ismail, P.M., Li, J., Mulac-Jericevic, B., Conneely, O.M., and Lydon, J.P. (2002) Progesterone's role in mammary gland development and tumorigenesis as disclosed by experimental mouse genetics. *Breast Cancer Research*. 4 (5), 191–196.

[182] Pierce, D.F., Johnson, M.D., Matsui, Y., Robinson, S.D., Gold, L.I., Purchio, A.F., et al. (1993) Inhibition of mammary duct development but not alveolar outgrowth during pregnancy in transgenic mice expressing active TGF-β1. *Genes and Development*. 7 (12 A), 2308–2317.

[183] Ewan, K.B., Shyamala, G., Ravani, S.A., Tang, Y., Akhurst, R., Wakefield, L., et al. (2002) Latent transforming growth factor-β activation in mammary gland: Regulation by ovarian hormones affects ductal and alveolar proliferation. *American Journal of Pathology*. 160 (6), 2081–2093.

[184] Silberstein, G.B. and Daniel, C.W. (1987) Reversible inhibition of mammary gland growth by transforming growth factor-β. *Science*. 237 (4812), 291–293.

[185] McBryan, J., Howlin, J., Napoletano, S., and Martin, F. (2008) Amphiregulin: Role in mammary gland development and breast cancer. *Journal of Mammary Gland Biology and Neoplasia*. 13 (2), 159–169.

[186] Ciarloni, L., Mallepell, S., and Brisken, C. (2007) Amphiregulin is an essential mediator of estrogen receptor α function in mammary gland development. *Proceedings of the National Academy of Sciences of the United States of America*. 104 (13), 5455–5460.

[187] Sternlicht, M.D., Sunnarborg, S.W., Kouros-Mehr, H., Yu, Y., Lee, D.C., and Werb, Z. (2005) Mammary ductal morphogenesis requires paracrine activation of stromal EGFR via ADAM17-dependent shedding of epithelial amphiregulin. *Development*. 132 (17), 3923–3933.

[188] Sekine, K., Ohuchi, H., Fujiwara, M., Yamasaki, M., Yoshizawa, T., Sato, T., et al. (1999) Fgf10 is essential for limb and lung formation. *Nature Genetics*. 21 (1), 138–141.

[189] Ngan, E.S.W., Ma, Z.Q., Chua, S.S., DeMayo, F.J., and Tsai, S.Y. (2002) Inducible expression of FGF-3 in mouse mammary gland. *Proceedings of the National Academy of Sciences of the*

United States of America. 99 (17), 11187–11192.

[190]   Lu, P., Ewald, A.J., Martin, G.R., and Werb, Z. (2008) Genetic mosaic analysis reveals FGF receptor 2 function in terminal end buds during mammary gland branching morphogenesis. *Developmental Biology*. 321 (1), 77–87.

[191]   Watson, C.J. and Khaled, W.T. (2008) Mammary development in the embryo and adult: A journey of morphogenesis and commitment. *Development*. 135 (6), 995–1003.

[192]   Oakes, S.R., Hilton, H.N., and Ormandy, C.J. (2006) Key stages in mammary gland development: The alveolar switch: Coordinating the proliferative cues and cell fate decisions that drive the formation of lobuloalveoli from ductal epithelium. *Breast Cancer Research*. 8 (2), 207.

[193]   Lydon, J.P., DeMayo, F.J., Funk, C.R., Mani, S.K., Hughes, A.R., Montgomery, C.A., et al. (1995) Mice lacking progesterone receptor exhibit pleiotropic reproductive abnormalities. *Genes & Development*. 9 (18), 2266–78.

[194]   Brisken, C., Heineman, A., Chavarria, T., Elenbaas, B., Tan, J., Dey, S.K., et al. (2000) Essential function of Wnt-4 in mammary gland development downstream of progesterone signaling. *Genes and Development*. 14 (6), 650–654.

[195]   Brisken, C., Park, S., Vass, T., Lydon, J.P., O'Malley, B.W., and Weinberg, R.A. (1998) A paracrine role for the epithelial progesterone receptor in mammary gland development. *Proceedings of the National Academy of Sciences of the United States of America*. 95 (9), 5076–5081.

[196]   Lee, H.J. and Ormandy, C.J. (2012) Interplay between progesterone and prolactin in mammary development and implications for breast cancer. *Molecular and Cellular Endocrinology*. 357 (1–2), 101–107.

[197]   Gonzalez-Suarez, E., Jacob, A.P., Jones, J., Miller, R., Roudier-Meyer, M.P., Erwert, R., et al. (2010) RANK ligand mediates progestin-induced mammary epithelial proliferation and carcinogenesis. *Nature*. 468 (7320), 103–107.

[198]   Cristea, S. and Polyak, K. (2018) Dissecting the mammary gland one cell at a time. *Nature Communications*. 9 (1), 2473.

[199]   Hanayama, R., Nagata, S., Geske, F., Lehman, L., Hanson, L., Neville, M., et al. (2005) Impaired involution of mammary glands in the absence of milk fat globule EGF factor 8. *Proceedings of the National Academy of Sciences*. 102 (46), 16886–16891.

[200]   Marti, A., Feng, Z., Altermatt, H.J., and Jaggi, R. (1997) Milk accumulation triggers apoptosis of mammary epithelial cells. *European Journal of Cell Biology*. 73 (2), 158–65.

[201]   Li, M., Liu, X., Robinson, G., Bar-Peled, U., Wagner, K.U., Young, W.S., et al. (1997) Mammary-derived signals activate programmed cell death during the first stage of mammary gland involution. *Proceedings of the National Academy of Sciences of the United States of America*. 94 (7), 3425–30.

[202]   Baxter, F.O., Neoh, K., and Tevendale, M.C. (2007) The Beginning of the End: Death Signaling in Early Involution. *Journal of Mammary Gland Biology and Neoplasia*. 12 (1), 3–13.

[203]   Furth, P.A. (1999) Mammary Gland Involution and Apoptosis of Mammary Epithelial Cells. *Journal of Mammary Gland Biology and Neoplasia*. 4 (2), 123–127.

[204]   Witty, J.P., Wright, J.H., and Matrisian, L.M. (1995) Matrix metalloproteinases are expressed during ductal and alveolar mammary morphogenesis, and misregulation of stromelysin-1 in transgenic mice induces unscheduled alveolar development. *Molecular Biology of the Cell*. 6 (10), 1287–303.

[205]   Wiseman, B.S., Sternlicht, M.D., Lund, L.R., Alexander, C.M., Mott, J., Bissell, M.J., et al. (2003) Site-specific inductive and inhibitory activities of MMP-2 and MMP-3 orchestrate mammary gland branching morphogenesis. *The Journal of Cell Biology*. 162 (6),.

[206]   (n.d.) Breast cancer statistics | Cancer Research UK.

[207]   (n.d.) Cancer.

[208]   (n.d.) U.K. Population (2020) - Worldometer.

[209]   McPherson, K. (2000) ABC of breast diseases: Breast cancer—epidemiology, risk factors, and genetics. *BMJ*. 321 (7270), 1198.

[210]   Boyle, P. and Howell, A. (2010) The globalisation of breast cancer. *Breast Cancer Research*. 12 (SUPPL. 4), S7.

[211]   Eccleston, A., Bentley, A., Dyer, M., Strydom, A., Vereecken, W., George, A., et al. (2017) A Cost-Effectiveness Evaluation of Germline BRCA1 and BRCA2 Testing in UK Women with Ovarian Cancer. *Value in Health*. 20 (4), 567–576.

[212]   Prakash, R., Zhang, Y., Feng, W., and Jasin, M. (2015) Homologous recombination and human health: The roles of BRCA1, BRCA2, and associated proteins. *Cold Spring Harbor Perspectives in Biology*. 7 (4), a016600.

[213] Narod, S.A. and Foulkes, W.D. (2004) BRCA1 and BRCA2: 1994 and beyond. *Nature Reviews Cancer*. 4 (9), 665–676.

[214] Hinck, L. and Näthke, I. (2014) Changes in cell and tissue organization in cancer of the breast and colon. *Current Opinion in Cell Biology*. 26 (1), 87–95.

[215] Weigelt, B., Geyer, F.C., and Reis-Filho, J.S. (2010) Histological types of breast cancer: How special are they? *Molecular Oncology*. 4 (3), 192–208.

[216] Althuis, M.D., Fergenbaum, J.H., Garcia-Closas, M., Brinton, L.A., Patricia Madigan, M., and Sherman, M.E. (2004) Etiology of Hormone Receptor-Defined Breast Cancer: A Systematic Review of the Literature. .

[217] Dai, X., Li, T., Bai, Z., Yang, Y., Liu, X., Zhan, J., et al. (2015) Breast cancer intrinsic subtype classification, clinical use and future trends. *American Journal of Cancer Research*. 5 (10), 2929–2943.

[218] Koh, J. and Kim, M.J. (2019) Introduction of a new staging system of breast cancer for radiologists: An emphasis on the prognostic stage. *Korean Journal of Radiology*. 20 (1), 69–82.

[219] Tang, P. and Tse, G.M. (2016) Immunohistochemical surrogates for molecular classification of breast carcinoma: A 2015 update. in: Arch. Pathol. Lab. Med., College of American Pathologists, pp. 806–814.

[220] Dai, X., Li, T., Bai, Z., Yang, Y., Liu, X., Zhan, J., et al. (2015) Breast cancer intrinsic subtype classification, clinical use and future trends. *American Journal of Cancer Research*. 5 (10), 2929–2943.

[221] Cheang, M.C.U., Chia, S.K., Voduc, D., Gao, D., Leung, S., Snider, J., et al. (2009) Ki67 Index, HER2 Status, and Prognosis of Patients With Luminal B Breast Cancer. *Articles | JNCI*. 101 736.

[222] Perou, C.M., Sørile, T., Eisen, M.B., Van De Rijn, M., Jeffrey, S.S., Ress, C.A., et al. (2000) Molecular portraits of human breast tumours. *Nature*. 406 (6797), 747–752.

[223] Sørlie, T., Perou, C.M., Tibshirani, R., Aas, T., Geisler, S., Johnsen, H., et al. (2001) Gene expression patterns of breast carcinomas distinguish tumor subclasses with clinical implications. *Proceedings of the National Academy of Sciences of the United States of America*. 98 (19), 10869–10874.

[224]   Howlader, N., Altekruse, S.F., Li, C.I., Chen, V.W., Clarke, C.A., Ries, L.A.G., et al. (2014) US incidence of Breast cancer Subtypes Defined by Joint Hormone receptor and Her2 Status.

[225]   Waks, A.G. and Winer, E.P. (2019) Breast Cancer Treatment A Review. *Clinical Review & Education JAMA | Review*. 321 (3), 288–300.

[226]   Dalmau, E., Armengol-Alonso, A., Muñoz, M., and Seguí-Palmer, M.Á. (2014) Current status of hormone therapy in patients with hormone receptor positive (HR+) advanced breast cancer. *Breast*. 23 (6), 710–720.

[227]   Smith, I.E. and Dowsett, M. (2003) Aromatase Inhibitors in Breast Cancer. *New England Journal of Medicine*. 348 (24), 2431–2442.

[228]   Scott, A.M., Wolchok, J.D., and Old, L.J. (2012) Antibody therapy of cancer. *Nature Reviews Cancer*. 12 (4), 278–287.

[229]   Lee, J.J.X., Loh, K., and Yap, Y.S. (2015) PI3K/Akt/mTOR inhibitors in breast cancer. *Cancer Biology and Medicine*. 12 (4), 342–354.

[230]   Agrawal, A., Gutteridge, E., Gee, J.M.W., Nicholson, R.I., and Robertson, J.F.R. (2005) Overview of tyrosine kinase inhibitors in clinical breast cancer. *Endocrine-Related Cancer*. 12 (Supplement_1), S135–S144.

[231]   Zimmer, A.S., Gillard, M., Lipkowitz, S., and Lee, J.M. (2018) Update on PARP Inhibitors in Breast Cancer. *Current Treatment Options in Oncology*. 19 (5), 21.

[232]   Spring, L.M., Wander, S.A., Zangardi, M., and Bardia, A. (2019) CDK 4/6 Inhibitors in Breast Cancer: Current Controversies and Future Directions. *Current Oncology Reports*. 21 (3), 25.

[233]   Maughan, K.L., Lutterbie, M.A., and Ham, P.S. (2010) Treatment of Breast Cancer. .

[234]   Lu, J., Wang, Q., Wang, B., Wang, F., and Wang, H. (2011) Developmental genes during placentation: Insights from mouse mutants. *Frontiers of Biology in China*. 6 (4), 300–311.

[235]   Hu, D. and Cross, J.C. (2010) Development and function of trophoblast giant cells in the rodent placenta. *International Journal of Developmental Biology*. 54 (2–3), 341–354.

[236]   Ander, S.E., Diamond, M.S., and Coyne, C.B. (2019) Immune responses at the maternal-fetal interface. *Science Immunology*. 4 (31), eaat6114.

[237]   Mori, M., Bogdan, A., Balassa, T., Csabai, T., and Szekeres-Bartho, J. (2016) The decidua—the maternal bed embracing the embryo—maintains the pregnancy. *Seminars in*

Immunopathology. 38 (6), 635–649.

[238]   Rossant, J. and Cross, J.C. (2001) Placental development: Lessons from mouse mutants. *Nature Reviews Genetics*. 2 (7), 538–548.

[239]   Woods, L., Perez-Garcia, V., and Hemberger, M. (2018) Regulation of Placental Development and Its Impact on Fetal Growth—New Insights From Mouse Models. *Frontiers in Endocrinology*. 9 570.

[240]   Watson, E.D. and Cross, J.C. (2005) Development of structures and transport functions in the mouse placenta. *Physiology*. 20 (3), 180–193.

[241]   Malassiné, A., Frendo, J.L., and Evain-Brion, D. (2003) A comparison of placental development and endocrine functions between the human and mouse model. *Human Reproduction Update*. 9 (6), 531–539.

[242]   Hemberger, M., Hanna, C.W., and Dean, W. (2020) Mechanisms of early placental development in mouse and humans. *Nature Reviews Genetics*. 21 (1), 27–43.

[243]   Krilleke, D., DeErkenez, A., Schubert, W., Giri, I., Robinson, G.S., Ng, Y.S., et al. (2007) Molecular mapping and functional characterization of the VEGF164 heparin-binding domain. *Journal of Biological Chemistry*. 282 (38), 28045–28056.

[244]   Claxton, S., Kostourou, V., Jadeja, S., Chambon, P., Hodivala-Dilke, K., and Fruttiger, M. (2008) Efficient, inducible Cre-recombinase activation in vascular endothelium. *Genesis*. 46 (2), 74–80.

[245]   Gu, C., Rodriguez, E.R., Reimert, D. V., Shu, T., Fritzsch, B., Richards, L.J., et al. (2003) Neuropilin-1 conveys semaphorin and VEGF signaling during neural and cardiovascular development. *Developmental Cell*. 5 (1), 45–57.

[246]   Morgan, E.A., Schneider, J.G., Baroni, T.E., Uluçkan, O., Heller, E., Hurchla, M.A., et al. (2010) Dissection of platelet and myeloid cell defects by conditional targeting of the beta3-integrin subunit. *FASEB Journal : Official Publication of the Federation of American Societies for Experimental Biology*. 24 (4), 1117–27.

[247]   Wu, T.J., Gibson, M.J., and Silverman, A.J. (1995) Gonadotropin-Releasing Hormone (GnRH) Neurons of the Developing Tectum of the Mouse. *Journal of Neuroendocrinology*. 7 (12), 899–902.

[248]   Tomayko, M.M. and Reynolds, C.P. (1989) Determination of subcutaneous tumor size in

athymic (nude) mice. *Cancer Chemotherapy and Pharmacology*. 24 (3), 148–154.

[249]   Reynolds, L.E. and Hodivala-Dilke, K.M. (2006) Primary mouse endothelial cell culture for assays of angiogenesis. *Methods in Molecular Medicine*. 120 503–509.

[250]   Brachtendorf, G., Kuhn, A., Samulowitz, U., Knorr, R., Gustafsson, E., Potocnik, A.J., et al. (2001) Early expression of endomucin on endothelium of the mouse embryo and on putative hematopoietic clusters in the dorsal aorta. *Developmental Dynamics*. 222 (3), 410–419.

[251]   Robinson, S.D., Reynolds, L.E., Kostourou, V., Reynolds, A.R., da Silva, R.G., Tavora, B., et al. (2009) αvβ3 integrin limits the contribution of neuropilin-1 to vascular endothelial growth factor-induced angiogenesis. *Journal of Biological Chemistry*. 284 (49), 33966–33981.

[252]   Schindelin, J., Arganda-Carreras, I., Frise, E., Kaynig, V., Longair, M., Pietzsch, T., et al. (2012) Fiji: An open-source platform for biological-image analysis. *Nature Methods*. 9 (7), 676–682.

[253]   De Clercq, K., Lopez-Tello, J., Vriens, J., and Sferruzzi-Perri, A.N. (2020) Double-label immunohistochemistry to assess labyrinth structure of the mouse placenta with stereology. *Placenta*. 94 44–47.

[254]   Ellison, T.S., Atkinson, S.J., Steri, V., Kirkup, B.M., Preedy, M.E.J., Johnson, R.T., et al. (2015) Suppression of β3-integrin in mice triggers a neuropilin-1- dependent change in focal adhesion remodelling that can be targeted to block pathological angiogenesis. *DMM Disease Models and Mechanisms*. 8 (9), 1105–1119.

[255]   Atkinson, S.J., Gontarczyk, A.M., Alghamdi, A.A., Ellison, T.S., Johnson, R.T., Fowler, W.J., et al. (2018) The β3-integrin endothelial adhesome regulates microtubule-dependent cell migration. *EMBO Reports*. 19 (7),.

[256]   Ray, M.K., Fagan, S.P., and Brunicardi, F.C. (2000) The Cre-loxP system: a versatile tool for targeting genes in a cell- and stage-specific manner. *Cell Transplantation*. 9 (6), 805–15.

[257]   Shaikh, A.C. and Sadowski, P.D. (1997) The Cre Recombinase Cleaves the lox Site in trans*. .

[258]   Kim, H., Kim, M., Im, S.-K., and Fang, S. (2018) Mouse Cre-LoxP system: general principles to determine tissue-specific roles of target genes. *Laboratory Animal Research*. 34 (4), 147.

[259]   Metzger, D. and Chambon, P. (2001) Site-and Time-Specific Gene Targeting in the Mouse. *METHODS*. 24 71–80.

[260]   Pfannkuche, K., Wunderlich, F.T., Doss, M.X., Spitkovsky, D., Reppel, M., Sachinidis, A., et al.

(2008) Generation of a double-fluorescent double-selectable Cre/loxP indicator vector for monitoring of intracellular recombination events. *Nature Protocols*. 3 (9), 1510–1526.

[261]   Hu, S., Liu, Z., Zhang, X., Zhang, G., Xie, Y., Ding, X., et al. (2016) "cre/loxP plus BAC": A strategy for direct cloning of large DNA fragment and its applications in Photorhabdus luminescens and Agrobacterium tumefaciens. *Scientific Reports*. 6 (1), 1–9.

[262]   Madisen, L., Zwingman, T.A., Sunkin, S.M., Oh, S.W., Zariwala, H.A., Gu, H., et al. (2010) A robust and high-throughput Cre reporting and characterization system for the whole mouse brain. *Nature Neuroscience*. 13 (1), 133–40.

[263]   Shehata, M., van Amerongen, R., Zeeman, A.L., Giraddi, R.R., and Stingl, J. (2014) The influence of tamoxifen on normal mouse mammary gland homeostasis. *Breast Cancer Research*. 16 (4), 411.

[264]   Daniel, C.W., Silberstein, G.B., Van Horn, K., Strickland, P., and Robinson, S. (1989) TGF-β1-induced inhibition of mouse mammary ductal growth: Developmental specificity and characterization. *Developmental Biology*. 135 (1), 20–30.

[265]   Langer, R. and Folkman, J. (1976) Polymers for the sustained release of proteins and other macromolecules. *Nature*. 263 (5580), 797–800.

[266]   Joza, S., Wang, J., Tseu, I., Ackerley, C., and Post, M. (n.d.) Fetal, but Not Postnatal, Deletion of Semaphorin-Neuropilin-1 Signaling Affects Murine Alveolar Development.

[267]   Kitsukawa, T., Shimizu, M., Sanbo, M., Hirata, T., Taniguchi, M., Bekku, Y., et al. (1997) Neuropilin-semaphorin III/D-mediated chemorepulsive signals play a crucial role in peripheral nerve projection in mice. *Neuron*. 19 (5), 995–1005.

[268]   Gu, C., Rodriguez, E.R., Reimert, D. V., Shu, T., Fritzsch, B., Richards, L.J., et al. (2003) Neuropilin-1 conveys semaphorin and VEGF signaling during neural and cardiovascular development. *Developmental Cell*. 5 (1), 45–57.

[269]   Takada, Y., Ye, X., and Simon, S. (2007) The integrins Gene organization and evolutionary history. *Genome Biology*. 8 215.

[270]   Hynes, R.O. (2002) Integrins: Bidirectional, allosteric signaling machines. *Cell*. 110 (6), 673–687.

[271]   Bronson, F.H. (2001) Puberty in Female Mice Is Not Associated with Increases in Either Body Fat or Leptin. *Endocrinology*. 142 (11), 4758–4761.

[272] Safranski, T., Lamberso, W.R., and Keisler, D.H. (1993) Correlations among Three Measures of Puberty in Mice and Relationships with Estradiol Concentration and Ovulation1. *Biology of Reproduction*. 48 (3), 669–673.

[273] Vá Zquez ‡ §, F., Carlos Rodríguez-Manzaneque, J., Lydon, J.P., Edwards, D.P., O'malley, B.W., and Luisa Iruela-Arispe, M. (1999) Progesterone Regulates Proliferation of Endothelial Cells*. .

[274] Ferraro, F., Lo Celso, C., and Scadden, D. (2010) Adult stem cells and their niches. *Advances in Experimental Medicine and Biology*. 695 155–168.

[275] Dalton$, S.L., Marcantoniosll, E.E., and Assoianll, R.K. (1992) THE JOURNAL OF BIOLOGICAL CHEMISTRY Cell Attachment Controls Fibronectin and a581 Levels in Fibroblasts IMPLICATIONS FOR ANCHORAGE-DEPENDENT AND-INDEPENDENT Integrin GROWTH*. .

[276] Kanda, H., Tanaka, T., Matsumoto, M., Umemoto, E., Ebisuno, Y., Kinoshita, M., et al. (2004) Endomucin, a sialomucin expressed in high endothelial venules, supports L-selectin-mediated rolling. *International Immunology*. 16 (9), 1265–1274.

[277] Brachtendorf, G., Kuhn, A., Samulowitz, U., Knorr, R., Gustafsson, E., Potocnik, A.J., et al. (2001) Early expression of endomucin on endothelium of the mouse embryo and on putative hematopoietic clusters in the dorsal aorta. *Developmental Dynamics*. 222 (3), 410–419.

[278] Liu, C., Shao, Z.-M., Zhang, L., Beatty, P., Sartippour, M., Lane, T., et al. (2001) Human Endomucin Is an Endothelial Marker.

[279] Kuhn, A., Brachtendorf, G., Kurth, F., Sonntag, M., Samulowitz, U., Metze, D., et al. (2002) Expression of Endomucin, a Novel Endothelial Sialomucin, in Normal and Diseased Human Skin. .

[280] Zuercher, J., Fritzsche, M., Feil, S., Mohn, L., and Berger, W. (n.d.) Norrin stimulates cell proliferation in the superficial retinal vascular plexus and is pivotal for the recruitment of mural cells.

[281] Keuschnigg, J., Karinen, S., Auvinen, K., Irjala, H., Mpindi, J.-P., Kallioniemi, O., et al. (2013) Plasticity of Blood-and Lymphatic Endothelial Cells and Marker Identification.

[282] Johnson, N.C., Dillard, M.E., Baluk, P., Mcdonald, D.M., Harvey, N.L., Frase, S.L., et al. (2008) Lymphatic endothelial cell identity is reversible and its maintenance requires Prox1 activity.

[283] Tavora, B., Batista, S., Reynolds, L.E., Jadeja, S., Robinson, S., Kostourou, V., et al. (2010)

Endothelial FAK is required for tumour angiogenesis. *EMBO Molecular Medicine*. 2 (12), 516–28.

[284]   Ni, C.W., Kumar, S., Ankeny, C.J., and Jo, H. (2014) Development of immortalized mouse aortic endothelial cell lines. *Vascular Cell*. 6 (1), 1–10.

[285]   Lertkiatmongkol, P., Liao, D., Mei, H., Hu, Y., and Newman, P.J. (2016) Endothelial functions of platelet/endothelial cell adhesion molecule-1 (CD31). *Current Opinion in Hematology*. 23 (3), 253–259.

[286]   Petzelbauer, P., Halama, T., and Gröger, M. (2000) Endothelial adherens junctions. in: J. Investig. Dermatology Symp. Proc., Blackwell Publishing Inc., pp. 10–13.

[287]   Greene, C., Hanley, N., and Campbell, M. (2019) Claudin-5: Gatekeeper of neurological function. *Fluids and Barriers of the CNS*. 16 (1), 1–15.

[288]   Yuan, L., Le Bras, A., Sacharidou, A., Itagaki, K., Zhan, Y., Kondo, M., et al. (2012) ETS-related gene (ERG) controls endothelial cell permeability via transcriptional regulation of the claudin 5 (CLDN5) gene. *Journal of Biological Chemistry*. 287 (9), 6582–6591.

[289]   Wigle, J.T., Harvey, N., Detmar, M., Lagutina, I., Grosveld, G., Gunn, M.D., et al. (2002) An essential role for Prox1 in the induction of the lymphatic endothelial cell phenotype. *EMBO Journal*. 21 (7), 1505–1513.

[290]   Jackson, D.G. (2004) Biology of the lymphatic marker LYVE-1 and applications in research into lymphatic trafficking and lymphangiogenesis. *APMIS*. 112 (7–8), 526–538.

[291]   Payne, S., De Val, S., and Neal, A. (2018) Endothelial-Specific Cre Mouse Models. *Arteriosclerosis, Thrombosis, and Vascular Biology*. 38 (11), 2550–2561.

[292]   Ulvmar, M.H., Martinez-Corral, I., Stanczuk, L., and Mäkinen, T. (2016) *Pdgfrb-Cre* targets lymphatic endothelial cells of both venous and non-venous origins. *Genesis*. 54 (6), 350–358.

[293]   Demoulin, J.-B. and Montano-Almendras, C.P. (2012) Platelet-derived growth factors and their receptors in normal and malignant hematopoiesis. *American Journal of Blood Research*. 2 (1), 44–56.

[294]   Kilani, B., Gourdou-Latyszenok, V., Guy, A., Bats, M., Peghaire, C., Parrens, M., et al. (2019) Comparison of endothelial promoter efficiency and specificity in mice reveals a subset of Pdgfb-positive hematopoietic cells. *Journal of Thrombosis and Haemostasis*. 17 (5), 827–840.

[295]   Yeh, H.J., Ruit, K.G., Wang, Y.X., Parks, W.C., Snider, W.D., and Deuel, T.F. (1991) PDGF A-chain gene is expressed by mammalian neurons during development and in maturity. *Cell*. 64 (1), 209–216.

[296]   Wilson, E., Mai, Q., Sudhir, K., Weiss, R.H., and Ives, H.E. (1993) Mechanical strain induces growth of vascular smooth muscle cells via autocrine action of PDGF. *Journal of Cell Biology*. 123 (3), 741–747.

[297]   Gouon-Evans, V. (2000) Leukocyte regulation of postnatal mammary gland. .

[298]   Alva, J.A., Zovein, A.C., Monvoisin, A., Murphy, T., Salazar, A., Harvey, N.L., et al. (2006) VE-Cadherin-Cre-recombinase transgenic mouse: A tool for lineage analysis and gene deletion in endothelial cells. *Developmental Dynamics*. 235 (3), 759–767.

[299]   Robinson, S.D., Reynolds, L.E., Kostourou, V., Reynolds, A.R., da Silva, R.G., Tavora, B., et al. (2009) αvβ3 integrin limits the contribution of neuropilin-1 to vascular endothelial growth factor-induced angiogenesis. *Journal of Biological Chemistry*. 284 (49), 33966–33981.

[300]   Tavora, B., Reynolds, L.E., Batista, S., Demircioglu, F., Fernandez, I., Lechertier, T., et al. (2015) Endothelial-cell FAK targeting sensitizes tumours to DNA-damaging therapy. *Nature*. 514 (7520), 112–116.

[301]   Mayhew, T.M. (2006) Allometric studies on growth and development of the human placenta: Growth of tissue compartments and diffusive conductances in relation to placental volume and fetal mass. *Journal of Anatomy*. 208 (6), 785–794.

[302]   Szasz, O., Vincze, G., Szigeti, G.P., Benyo, Z., and Szasz, A. (2018) An allometric approach of tumor-angiogenesis. *Medical Hypotheses*. 116 74–78.

[303]   Honvo-Houéto, E. and Truchet, S. (2015) Indirect immunofluorescence on frozen sections of mouse mammary gland. *Journal of Visualized Experiments*. 2015 (106),.

[304]   Paine, I.S. and Lewis, M.T. (2017) The Terminal End Bud: the Little Engine that Could. *Journal of Mammary Gland Biology and Neoplasia*. 22 (2), 93–108.

[305]   Hinck, L. and Silberstein, G.B. (2005) The mammary end bud as a motile organ. *Breast Cancer Research*. 7 (6), 245–251.

[306]   Macias, H. and Hinck, L. (2012) Mammary gland development. *Wiley Interdisciplinary Reviews: Developmental Biology*. 1 (4), 533–557.

[307]   Bray, K., Gillette, M., Young, J., Loughran, E., Hwang, M., Sears, J.C., et al. (2013) Cdc42

overexpression induces hyperbranching in the developing mammary gland by enhancing cell migration. *Breast Cancer Research*. 15 (5), 1–18.

[308]   Williams, J.M. and Daniel, C.W. (1983) Mammary ductal elongation: Differentiation of myoepithelium and basal lamina during branching morphogenesis. *Developmental Biology*. 97 (2), 274–290.

[309]   Tirziu, D. and Simons, M. (2009) Endothelium as master regulator of organ development and growth. *Vascular Pharmacology*. 50 (1–2), 1–7.

[310]   Stahl, A., Connor, K.M., Sapieha, P., Chen, J., Dennison, R.J., Krah, N.M., et al. (2010) The mouse retina as an angiogenesis model. *Investigative Ophthalmology and Visual Science*. 51 (6), 2813–2826.

[311]   Sherer, D.M. and Abulafia, O. (2001) Angiogenesis during implantation, and placental and early embryonic development. *Placenta*. 22 (1), 1–13.

[312]   Pasquier, J., Ghiabi, P., Chouchane, L., Razzouk, K., Rafii, S., and Rafii, A. (2020) Angiocrine endothelium: From physiology to cancer. *Journal of Translational Medicine*. 18 (1), 1–17.

[313]   Barry, D.M., McMillan, E.A., Kunar, B., Lis, R., Zhang, T., Lu, T., et al. (2019) Molecular determinants of nephron vascular specialization in the kidney. *Nature Communications*. 10 (1), 1–14.

[314]   Goddard, L.M., Murphy, T.J., Org, T., Enciso, J.M., Hashimoto-Partyka, M.K., Warren, C.M., et al. (2014) Progesterone receptor in the vascular endothelium triggers physiological uterine permeability preimplantation. *Cell*. 156 (3), 549–562.

[315]   Walter, L.M., Rogers, P.A.W., and Girling, J.E. (2005) The role of progesterone in endometrial angiogenesis in pregnant and ovariectomised mice. *Reproduction*. 129 (6), 765–777.

[316]   Heryanto, B. and Rogers, P.A.W. (2002) Regulation of endometrial endothelial cell proliferation by oestrogen and progesterone in the ovariectomized mouse. *Reproduction*. 123 (1), 107–113.

[317]   Perrot-Applanat, M., Cohen-Solal, K., Milgrom, E., and Finet, M. (1995) Progesterone Receptor Expression in Human Saphenous Veins. *Circulation*. 92 (10), 2975–2983.

[318]   Zheng, S., Huang, J., Zhou, K., Xiang, Q., Zhang, Y., Tan, Z., et al. (2012) Progesterone enhances vascular endothelial cell migration via activation of focal adhesion kinase. *Journal*

of Cellular and Molecular Medicine. 16 (2), 296–305.

[319]   Carlos Rodriguez-Manzaneque, J., Graubert, M., and Luisa Iruela-Arispe, M. (2000) Endothelial cell dysfunction following prolonged activation of progesterone receptor. .

[320]   MATSUMOTO, M., NISHINAKAGAWA, H., KUROHMARU, M., HAYASHI, Y., and OTSUKA, J. (1992) Pregnancy and Lactation Affect the Microvasculature of the Mammary Gland in Mice. *The Journal of Veterinary Medical Science*. 54 (5), 937–943.

[321]   Pepper, M.S., Baetens, D., Mandriota, S.J., Di Sanza, C., Oikemus, S., Lane, T.F., et al. (2000) Regulation of VEGF and VEGF receptor expression in the rodent mammary gland during pregnancy, lactation, and involution. *Developmental Dynamics*. 218 (3), 507–524.

[322]   Brisken, C. and Ataca, D. (2015) Endocrine hormones and local signals during the development of the mouse mammary gland. *Wiley Interdisciplinary Reviews: Developmental Biology*. 4 (3), 181–195.

[323]   Watson, C.J. and Khaled, W.T. (2008) Mammary development in the embryo and adult: a journey of morphogenesis and commitment. *Development*. 135 (6),.

[324]   Heyne, G.W., Plisch, E.H., Melberg, C.G., Sandgren, E.P., Peter, J.A., and Lipinski, R.J. (2015) A simple and reliable method for early pregnancy detection in inbred mice. *Journal of the American Association for Laboratory Animal Science*. 54 (4), 368–371.

[325]   Jansson, T. and Powell, T.L. (2007) Role of the placenta in fetal programming: underlying mechanisms and potential interventional approaches A B S T R A C T. *Clinical Science*. 113 1–13.

[326]   Tai-Nagara, I., Yoshikawa, Y., Numata, N., Ando, T., Okabe, K., Sugiura, Y., et al. (2017) Placental labyrinth formation in mice requires endothelial FLRT2/UNC5B signaling. *Ru ̈ Diger Klein*. 10 19.

[327]   Weber, E.M., Algers, B., Hultgren, J., and Olsson, I.A.S. (2013) Pup mortality in laboratory mice--infanticide or not? *Acta Veterinaria Scandinavica*. 55 (1), 83.

[328]   Weber, E.M., Hultgren, J., Algers, B., and Olsson, I.A.S. (2016) Do laboratory mouse females that lose their litters behave differently around parturition? *PLoS ONE*. 11 (8),.

[329]   FINN, C.A. (1963) REPRODUCTIVE CAPACITY AND LITTER SIZE IN MICE: EFFECT OF AGE AND. *Journal of Reproduction and Fertility*. 6 (2), 205–214.

[330]   BIGGERS, J.D., FINN, C.A., and McLAREN, A. (1962) LONG-TERM REPRODUCTIVE

PERFORMANCE OF FEMALE MICE. *Reproduction*. 3 (3), 313–330.

[331] PARSONS, P.A. (1964) PARENTAL AGE AND THE OFFSPRING. *The Quarterly Review of Biology*. 39 (3), 258–275.

[332] Girling, J.E., Lederman, F.L., Walter, L.M., and Rogers, P.A.W. (2007) Progesterone, But Not Estrogen, Stimulates Vessel Maturation in the Mouse Endometrium. *Endocrinology*. 148 (11), 5433–5441.

[333] Soares, M.J. (2004) The prolactin and growth hormone families: Pregnancy-specific hormones/cytokines at the maternal-fetal interface. *Reproductive Biology and Endocrinology*. 2 (1), 1–15.

[334] Ain, R., Canham, L.N., and Soares, M.J. (2003) Gestation stage-dependent intrauterine trophoblast cell invasion in the rat and mouse: Novel endocrine phenotype and regulation. *Developmental Biology*. 260 (1), 176–190.

[335] VIRGO, B.B. and BELLWARD, G.D. (1974) Serum Progesterone Levels in the Pregnant and Postpartum Laboratory Mouse. *Endocrinology*. 95 (5), 1486–1490.

[336] Kim, M., Park, H.J., Seol, J.W., Jang, J.Y., Cho, Y.S., Kim, K.R., et al. (2013) VEGF-A regulated by progesterone governs uterine angiogenesis and vascular remodelling during pregnancy. *EMBO Molecular Medicine*. 5 (9), 1415–1430.

[337] Yasugi1, T., Kaido2, T., and Uehara2, Y. (1989) Changes in Density and Architecture of Microvessels of the Rat Mammary Gland During Pregnancy and Lactation. .

[338] Tighe, M., Molassiotis, A., Morris, J., and Richardson, J. (2011) Coping, meaning and symptom experience: A narrative approach to the overwhelming impacts of breast cancer in the first year following diagnosis. *European Journal of Oncology Nursing*. 15 (3), 226–232.

[339] Sherwood, L.M., Parris, E.E., and Folkman, J. (1971) Tumor Angiogenesis: Therapeutic Implications. *New England Journal of Medicine*. 285 (21), 1182–1186.

[340] Muthakkaruppan, V.R., Kubai, L., and Auerbach, R. (1982) Tumor-induced neovascularization in the mouse eye. *Journal of the National Cancer Institute*. 69 (3), 699–708.

[341] Holmgren, L. and Folkman, U. (1995) Dormancy of micrometastases: Balanced proliferation and apoptosis in the presence of angiogenesis suppression. .

[342] Parangi, S., O'Reilly, M., Christofori, G., Holmgren, L., Grosfeld, J., Folkman, J., et al. (1996)

Antiangiogenic therapy of transgenic mice impairs de novo tumor growth. *Proceedings of the National Academy of Sciences of the United States of America*. 93 (5), 2002–2007.

[343]   Lampropoulou, A. and Ruhrberg, C. (2014) Neuropilin regulation of angiogenesis. *Biochemical Society Transactions*. 42 (6), 1623–1628.

[344]   Silva, R., D'Amico, G., Hodivala-Dilke, K.M., and Reynolds, L.E. (2008) Integrins: The keys to unlocking angiogenesis. *Arteriosclerosis, Thrombosis, and Vascular Biology*. 28 (10), 1703–1713.

[345]   Murphy, P.A., Begum, S., and Hynes, R.O. (2015) Tumor Angiogenesis in the Absence of Fibronectin or Its Cognate Integrin Receptors. *PLOS ONE*. 10 (3), e0120872.

[346]   Reynolds, L.E., Wyder, L., Lively, J.C., Taverna, D., Robinson, S.D., Huang, X., et al. (2002) Enhanced pathological angiogenesis in mice lacking β3 integrin or β3 and β5 integrins. *Nature Medicine*. 8 (1), 27–34.

[347]   Almokadem, S. and Belani, C.P. (2012) Volociximab in cancer. *Expert Opinion on Biological Therapy*. 12 (2), 251–257.

[348]   Alday-Parejo, B., Stupp, R., and Rüegg, C. (2019) Are integrins still practicable targets for anti-cancer therapy? *Cancers*. 11 (7),.

[349]   Jubb, A.M., Strickland, L.A., Liu, S.D., Mak, J., Schmidt, M., and Koeppen, H. (2012) Neuropilin-1 expression in cancer and development. *Journal of Pathology*. 226 (1), 50–60.

[350]   Mackey, J.R., Kerbel, R.S., Gelmon, K.A., McLeod, D.M., Chia, S.K., Rayson, D., et al. (2012) Controlling angiogenesis in breast cancer: A systematic review of anti-angiogenic trials. *Cancer Treatment Reviews*. 38 (6), 673–688.

[351]   Sandler, A., Gray, R., Perry, M.C., Brahmer, J., Schiller, J.H., Dowlati, A., et al. (2006) Paclitaxel–Carboplatin Alone or with Bevacizumab for Non–Small-Cell Lung Cancer. *New England Journal of Medicine*. 355 (24), 2542–2550.

[352]   Kerbel, R.S. (2008) Tumor angiogenesis. *New England Journal of Medicine*. 358 (19), 2039–2049.

[353]   Kerbel, R.S. (2012) Strategies for improving the clinical benefit of antiangiogenic drug based therapies for breast cancer. *Journal of Mammary Gland Biology and Neoplasia*. 17 (3–4), 229–239.

[354]   Fürstenberger, G., Von Moos, R., Lucas, R., Thürlimann, B., Senn, H.J., Hamacher, J., et al.

(2006) Circulating endothelial cells and angiogenic serum factors during neoadjuvant chemotherapy of primary breast cancer. *British Journal of Cancer*. 94 (4), 524–531.

[355]   Casanovas, O., Hicklin, D.J., Bergers, G., and Hanahan, D. (2005) Drug resistance by evasion of antiangiogenic targeting of VEGF signaling in late-stage pancreatic islet tumors. *Cancer Cell*. 8 (4), 299–309.

[356]   Shojaei, F., Lee, J.H., Simmons, B.H., Wong, A., Esparza, C.O., Plumlee, P.A., et al. (2010) HGF/c-Met acts as an alternative angiogenic pathway in sunitinib-resistant tumors. *Cancer Research*. 70 (24), 10090–10100.

[357]   Huang, D., Ding, Y., Zhou, M., Rini, B.I., Petillo, D., Qian, C.N., et al. (2010) Interleukin-8 mediates resistance to antiangiogenic agent sunitinib in renal cell carcinoma. *Cancer Research*. 70 (3), 1063–1071.

[358]   Hu, P., Zhang, W., Xin, H., and Deng, G. (2016) Single cell isolation and analysis. *Frontiers in Cell and Developmental Biology*. 4 (OCT), 116.

[359]   Eberhard, A., Kahlert, S., Goede, V., Hemmerlein, B., Plate, K.H., and Augustin, H.G. (2000) Heterogeneity of angiogenesis and blood vessel maturation in human tumors: Implications for antiangiogenic tumor therapies. *Cancer Research*. 60 (5), 1388–1393.

[360]   Herzog, B., Pellet-Many, C., Britton, G., Hartzoulakis, B., and Zachary, I.C. (2011) VEGF binding to NRP1 is essential for VEGF stimulation of endothelial cell migration, complex formation between NRP1 and VEGFR2, and signaling via FAK Tyr407 phosphorylation. *Molecular Biology of the Cell*. 22 (15), 2766–2776.

[361]   Somanath, P.R., Malinin, N.L., and Byzova, T. V. (2009) Cooperation between integrin αvβ3 and VEGFR2 in angiogenesis. *Angiogenesis*. 12 (2), 177–185.

[362]   Byzova, T. V., Goldman, C.K., Pampori, N., Thomas, K.A., Bett, A., Shattil, S.J., et al. (2000) A mechanism for modulation of cellular responses to VEGF: Activation of the integrins. *Molecular Cell*. 6 (4), 851–860.

[363]   Bruns, A.F., Herbert, S.P., Odell, A.F., Jopling, H.M., Hooper, N.M., Zachary, I.C., et al. (2010) Ligand-Stimulated VEGFR2 Signaling is Regulated by Co-Ordinated Trafficking and Proteolysis. *Traffic*. 11 (1), 161–174.

[364]   Smith, G.A., Fearnley, G.W., Abdul-Zani, I., Wheatcroft, S.B., Tomlinson, D.C., Harrison, M.A., et al. (2016) VEGFR2 Trafficking, Signaling and Proteolysis is Regulated by the Ubiquitin Isopeptidase USP8. *Traffic*. 17 (1), 53–65.

[365]   Yu, P., Zhang, Z., Li, S., Wen, X., Quan, W., Tian, Q., et al. (2016) Progesterone modulates endothelial progenitor cell (EPC) viability through the CXCL12/CXCR4/PI3K/Akt signalling pathway. *Cell Proliferation*. 49 (1), 48–57.

[366]   Soldi, R., Mitola, S., Strasly, M., Defilippi, P., Tarone, G., and Bussolino, F. (1999) Role of α(v)β3 integrin in the activation of vascular endothelial growth factor receptor-2. *EMBO Journal*. 18 (4), 882–892.

[367]   Masson-Gadais, B., Houle, F., Laferrière, J., and Huot, J. (2003) Integrin αvβ3 requirement for VEGFR2-mediated activation of SAPK2/p38 and for Hsp90-dependent phosphorylation of focal adhesion kinase in endothelial cells activated by VEGF. *Cell Stress & Chaperones*. 8 (1), 37.

[368]   Chen, T.T., Luque, A., Lee, S., Anderson, S.M., Segura, T., and Iruela-Arispe, M.L. (2010) Anchorage of VEGF to the extracellular matrix conveys differential signaling responses to endothelial cells. *Journal of Cell Biology*. 188 (4), 595–609.

[369]   Somanath, P.R., Razorenova, O. V., Chen, J., and Byzova, T. V. (2006) Akt1 in endothelial cell and angiogenesis. *Cell Cycle*. 5 (5), 512–518.

[370]   Roberts, M.S., Woods, A.J., Dale, T.C., Van Der Sluijs, P., and Norman, J.C. (2004) Protein Kinase B/Akt Acts via Glycogen Synthase Kinase 3 To Regulate Recycling of v3 and 51 Integrins. *MOLECULAR AND CELLULAR BIOLOGY*. 24 (4), 1505–1515.

[371]   Lund, N., Henrion, D., Tiede, P., Ziche, M., Schunkert, H., and Ito, W.D. (2010) Vimentin expression influences flow dependent VASP phosphorylation and regulates cell migration and proliferation. *Biochemical and Biophysical Research Communications*. 395 (3), 401–406.

[372]   Fantin, A., Lampropoulou, A., Senatore, V., Brash, J.T., Prahst, C., Lange, C.A., et al. (2017) VEGF165-induced vascular permeability requires NRP1 for ABL-mediated SRC family kinase activation. *Journal of Experimental Medicine*. 214 (4), 1049–1064.

[373]   Manning, B.D. and Toker, A. (2017) Leading Edge Review AKT/PKB Signaling: Navigating the Network.

[374]   Funa, K. and Sasahara, M. (2014) The roles of PDGF in development and during neurogenesis in the normal and diseased nervous system. *Journal of Neuroimmune Pharmacology*. 9 (2), 168–181.

[375]   Rafii, S., Butler, J.M., and Ding, B. Sen (2016) Angiocrine functions of organ-specific endothelial cells. *Nature*. 529 (7586), 316–325.

[376]   Iber, D. and Menshykau, D. (2013) The control of branching morphogenesis. *Open Biology*. 3 (SEP),.

[377]   Sohal, D.S., Nghiem, M., Crackower, M.A., Witt, S.A., Kimball, T.R., Tymitz, K.M., et al. (2001) Temporally Regulated and Tissue-Specific Gene Manipulations in the Adult and Embryonic Heart Using a Tamoxifen-Inducible Cre Protein. *Circulation Research*. 89 (1), 20–25.